Molecular Basis of Ligand Binding to the M_1 Muscarinic Acetylcholine Receptor: Focus on the Second Extracellular Loop.

Jason Alexander Goodwin

A thesis submitted in fulfilment of the requirements of The University of London for the degree of Doctor of Philosophy.

2006

National Institute for Medical Research
The Ridgeway,
Mill Hill
London NW7 1 AA

University College London
Gower Street
London WC1E 6BT

ProQuest LLC
789 East Eisenhower Parkway
P.O. Box 1346
Ann Arbor, MI 48106-1346

Abstract

The second extracellular loop (E2) of the M_1 muscarinic acetylcholine receptor (mAChR) links transmembrane (TM) helices 4 and 5 and is predicted to play a role in the acetylcholine (ACh) binding pocket. Potential ligand contact residues were selected using a rhodopsin homology model of the M_1 mAChR and mutated to alanine. Cys98, postulated to form a disulphide (S-S) anchor to Cys178, Asp99, possibly part of a ligand access channel, and Phe197 and Trp378, predicted to complete the floor of the binding pocket, were also mutated. The double cysteine mutant was also generated. Radioligand binding assays showed that COS-7 cells expressed mutants at near to wild-type (WT) levels except for Cys 98 Ala, Cys178Ala and Asp99Ala (10-20% of WT). The affinity of the antagonist (-)-N-methylscopolamine (NMS) was reduced by Cys98Ala (40-fold), Asp99Ala (22-fold), and Cys178Ala (16 fold). ACh affinity was reduced by Asp99Ala (11-fold), Cys98Ala (12-fold), Arg171Ala (7-fold), Cys178Ala (70-fold) and Ile180Ala (5-fold). The TM domain mutants Phe197Ala and Trp378Ala reduced NMS affinity 90 and 400-fold respectively but reduced ACh affinity only 2-fold and 13-fold. The mutants, supplemented with six E2 loop mutants from a previous study were able to activate the G_q-linked phosphoinositide signalling pathway. Cysteine mutations produced greater than 2500-fold reductions in ACh potency resulting in a 10-20-fold loss of signalling efficacy. Effects were also observed for other E2 loop mutants, most notably a 9-fold loss of efficacy for Ser184Ala. Dissociation rate constants for NMS and 3-Quinuclidinyl Benzilate (QNB) were increased by the majority of mutations, Arg171Ala, Cys178Ala and Trp378Ala being the most significant. The results imply that the E2 loop plays a more important role in the binding of ACh than NMS while NMS may bind deeper within the TM domain than ACh. Maintenance of the S-S bond was essential for receptor activation. Studies with additional ligands showed that pilocarpine, oxotremorine-M and oxotremorine followed an ACh-like binding pattern, whereas the atypical agonists McN-A-343 and AC-42 may bind outside the ACh binding pocket.

Table of Contents

List of Figures

Chapter 1

Chapter 2

Chapter 3

Chapter 4

Chapter 5

Chapter 6

List of Tables

List of Abbreviations

2-D	Two Dimensional
3-D	Three Dimensional
5-HT	5-Hydroxytryptamine
7-TM	7-Transmembrane
α-AR	α-Adrenergic Receptor
α-MEM	α-Minimal Essential Medium
^{3}H-NMS	(-)-[^{3}H]-N-methylscopolamine
^{3}H-QNB	(-)-[^{3}H]-Quinuclidinylbenzilate
AC	Adenyl Cyclase
ACh	Acetylcholine
AP-2	Adaptor Protein 2
ASM	Alanine Scanning Mutagenesis
BAI	Brain Specific Angiogenesis Inhibitory Receptors
β-AR	β-Adrenergic Receptors
β-ARK	β-Adrenergic Receptor Kinase
bp	Base Pair
BRET	Bioluminescence Resonance Energy Transfer
BSA	Bovine Serum Albumin
CAM	Constitutively Active Mutant
CASR	Calcium sensing Receptor
cAMP	Cyclic Adenosine Monophosphate
cGMP	Cyclic guanosine Monophosphate
CHO	Chinese Hamster Ovary cells
CNS	Central Nervous System
COS-7	African Green Monkey Kidney Cells
CRHR	Corticotropin Releasing Hormone Receptor
DAG	Diacylglycerol
DMSO	Dimethylsulfoxide
DNA	Deoxyribonucleic Acid
Dpm	Disintegrations Per Minute
dsDNA	Double Stranded DNA
e_A	Compound Efficacy
EC_{50}	Drug Concentration that Produces 50% of the Maximal Effect
ECACC	European Collection of Cell Cultures
EGF	Epidermal Growth Factor
E2 Loop	Second Extracellular Loop
E_{max}	Maximum Receptor Induced Signal
EDTA	Ethylenediaminetetraacetic Acid
E.coli	*Escherichia coli*
ER	Endoplasmic Reticulum
EMR	EGF-Like Modulating Receptor
ERK	Extracellular Regulated Kinase
FITC	Fluorescein Isothiocyanate
FRET	Fluorescent Resonance Energy Transfer
G-protein	Gaunine Nucleotide Binding Protein
GABA	γ-Amino-n-butyric Acid
GAIP	Gα-Interacting Protein
GAP	GTPase Activating Protein
GDP	Guanine 5'-Diphosphate
GFP	Green Fluorescent Protein

GI	Gastro Intestinal
GnRHR	Gonadotrophin Releasing Hormone Receptor
GPCR	G-protein Coupled Receptor
GRK	G-protein-coupled Receptor Kinase
GTP	Guanine 5'-Triphosphate
GTPase	Guanine 5'-Triphosphatase
HEPES	N-[2-hydroxyethyl]piperazine-N'-[2-ethanesulphonic acid]
IC_{50}	Drug Concentration that Inhibits the Maximum Response by 50%
IANBD	N, N' Dimethyl-N-[idoacetyl)-N'[7'Nitrobenzyl-2-oxa-1, 3 diazol-4-yl] ethylene diamine
IgG	Immunoglobulin G
I Loop	Intracellular Loop
IP_3	Inositol 1, 4, 5 Triphosphate
K_A	Association Constant
K_{app}	Measured Apparent Affinity Constant
K_{act}	Agonist Potency ($1/EC_{50}$)
K_{Bin}	ACh Binding Constant
K_D	Dissociation Constant
kDA	Kilo Daltons
KO	Knockout
LEC	Lectomedin Receptors
LNB-7TM	Long –N-Terminal Class B 7-TM
LTB_4	Leukotriene B4
LTP	Long Term Potentiation
mAChR	Muscarinic Acetylcholine Receptor
MCH	Melanin Concentrating Hormone
mGluR	Metabotropic Glutamate Receptor
MAP Kinase	Mitogen-activated Protein Kinase
Mc-N-A-343	[4-[[N-(3-Chlorophenyl)carbamoyl]oxy]-2-butynyl]-trimethylammonium
MOPS	3-[N-Morpholino]propane-1-sulfonic acid
mRNA	Messenger Ribonucleic Acid
MTS	Methanethiosulphonate
n	Number
ND	Not Determined
NSB	Non-Specific Binding
n_H	Hill Coefficient
NEM	N-Ethyl Maleimide
NK Receptor	Neurokinin Receptor
NIMR	National Institute for Medical Research
NMDA	N-Methyl D-Aspartate
NMR	Nuclear Magnetic Resonance
NMS	N-Methylscopolamine
OD	Optical Density
pX	-Log (X)
PBS	Phosphate Buffered Saline
PCR	Polymerase Chain Reaction
PI	Phosphoinositide
PIP_2	Phosphatidylinositol-4,5-Bisphosphate
PIP_3	Phosphatidylinositol-1,4,5-Triphosphate
PKA	Protein Kinase A
PKC	Protein Kinase C
PLC	Phospholipase C

PTHR	Parathyroid Hormone Recptor
RAMP	Receptor Activity Modifying Protein
RGS	Regulator of G-protein Signalling
Rpe	Retinal Pigment Epithelium
rpm	Revolutions Per Minute
R-SAT	Receptor Selection and Amplification Technology
SCAM	Substituted Cysteine Accessibility Method
SCTR	Secretin Receptor
SDS	Sodium Dodecyl Sulphate
S.E.M	Standard Error of the Mean
SV40	Simian Virus 40
TAE	Tris-acetate/EDTA Buffer
TCA	Trichloroacetic Acid
TM	Transmembrane
TMB-8	3,4,5 trimethoxybenzoic acid 8-(dimethylamino) octyl ester
UV	Ultraviolet
v/v	Volume for Volume
WT	Wild Type
w/v	Weight for Volume

Chapter 1.

Introduction

1.1. G-protein Coupled Receptors; Classification

Communication between cells in biological systems is a fundamental necessity for the growth and survival of organisms. Cell to cell communication is mediated by cell surface receptors that essentially act as sensors and interpreters of extracellular activity. Receptors co-ordinate the various communicative signals from chemical messengers received by a cell and initiate a signalling pathway within the cell that can have various outcomes on cellular processes such as gene transcription and/or alterations of calcium concentration for example. Neurotransmitter molecules such as acetylcholine, metal ions such as potassium or hormones such as epinephrine are the major entities of cell-cell chemical communications. Muscarinic acetylcholine receptors (mAChRs) belong to a super-family of receptors known as the G-protein coupled receptors (GPCRs). GPCRs are a vast and diverse set of membrane bound signalling molecules. Ubiquitous throughout the body, GPCRs perform essential roles as mediators of communication between the extra-cellular environment and the intra-cellular space and are important for many physiological processes including, regulation of neuronal excitability, cognition, metabolism, behaviour, reproduction and development. It is therefore no surprise that approximately half of all modern pharmaceuticals are directed at G-protein coupled receptors, the top selling ones treat diseases such as asthma, migraines hyper-tension schizophrenia, peptic ulcers and numerous allergies (Wise et al., 2002). However, the number of drugs that are available target only a tiny minority of GPCRs and successfully treat only a fraction of GPCR-related diseases. It is evident therefore that there is still huge potential for the development of GPCR-targeted pharmaceuticals, although identifying which GPCRs require modulation for treatment requires an enormous and multi-disciplined effort.

A recent and comprehensive reverse transcription-polymerase chain reaction study (Vassilatis et al., 2003) reported that a total of 750 GPCRs are expressed in human tissues. Of these 367 bind endogenous ligands (endoGPCRs); endoGPCR ligands include peptides, amino acids, small neurotransmitter molecules and nucleotides the remainder (283 human) are olfactory chemosensory receptors, binding ligands from the external environment such as pheromones and tastes. Another study of 2003 (Fredriksson et al., 2003) using a phylogenetic approach put the total of human GPCRs at closer to 800, of which 342 were functional non-olfactory receptors and 458 olfactory receptors, and account for ~2% of the human genome. Classification of such a large and important family of proteins is complex and the existence of pseudogenes and repeats in the naming of GPCRs only adds to the complexity. Thus, for the purposes of this study I will refer to the classification system described by Fredriksson et al (Fredriksson et al., 2003) known as the GRAFS system. Here GPCRs are classed phylogenetically into five main families: Glutamate (15 members), Rhodopsin, (701 members the largest group), Adhesion (24 members), Frizzled/taste (24 members) and Secretin (15 members). The families are further sub-divided according to the type of ligand that they bind. There is practically no sequence homology between the major family groups. However, this large super-family of proteins shares the same basic structural architecture. They all contain 7-Transmembrane (7-TM) helical domains that span the cell membrane and are connected by 3 intra and 3 extra-cellular loops with the N-terminus positioned extracellularly and the C-terminus in the cytoplasm. Variability among GPCR structures occurs in all areas of the sequence. Sequence variation is least in the transmembrane domains and greatest at the N & C-Termini. For a full and current review of GPCR structure (Stenkamp et al., 2005)

A short synopsis of each of the main groups in the GRAFs system will be given. Figure 1.1 illustrates the GRAFS classification system as described by Fredriksson. The

Secretin family (named after the first receptor cloned in this class) bind large polypeptides that share well-conserved amino acid sequences that act in a paracrine fashion. In the classical A-F classification system secretin and adhesion receptors were grouped in the same category (Class B) but recent genomic analysis of the adhesion receptors by Bjarnadottir et al place adhesion and secretin receptors in two distinct families of receptor (Bjarnadottir et al., 2004) The secretin receptors share a typical 7-TM structure but are distinguished by a 60-80 amino acid N-terminus, containing a sequence rich in cysteine residues that form conserved disulphide bonds which are particularly important for the binding of peptide ligands. This group consists of the hormone binding receptors such as the parathyroid hormone receptors (PTHR), the corticotrophin-releasing hormone receptors (CRHRs) and the secretin receptor itself (SCTR). Also belonging to this group are the calcitonin family of receptors and the calcitonin-like receptor, CGRP (calcitonin gene related peptide). CGRP is an unusual receptor because it requires the co-expression of RAMPs (receptor activity modifying proteins) in order for cell trafficking and ligand interaction to occur (Conner et al., 2006). RAMPs have three biological functions they transport co-expressed calcitonin like receptors to the cell surface, define its pharmacology and dictate its state of glycosylation (Foord and Marshall, 1999).

All members of this family have been shown to regulate intracellular cyclic AMP via adenylyl cyclase coupling upon stimulation of the G_s class of G-proteins and some of the members of this class can also activate phospholipase C (PLC) (Harmar, 2001) The adhesion receptors are a relatively new but unique category of GPCRs (Fredriksson et al., 2003). These receptors have been previously termed LNB-7TM receptors (Long N-Terminal class B -7TMs) and have large and complex functional domains in their N-Terminal regions. These include multiple epidermal growth factor-like (EGF) domains, conserved cysteine motifs. As the name might suggest these receptors are thought to

Figure 1.1.The GRAFS Sytem of GPCR Classification

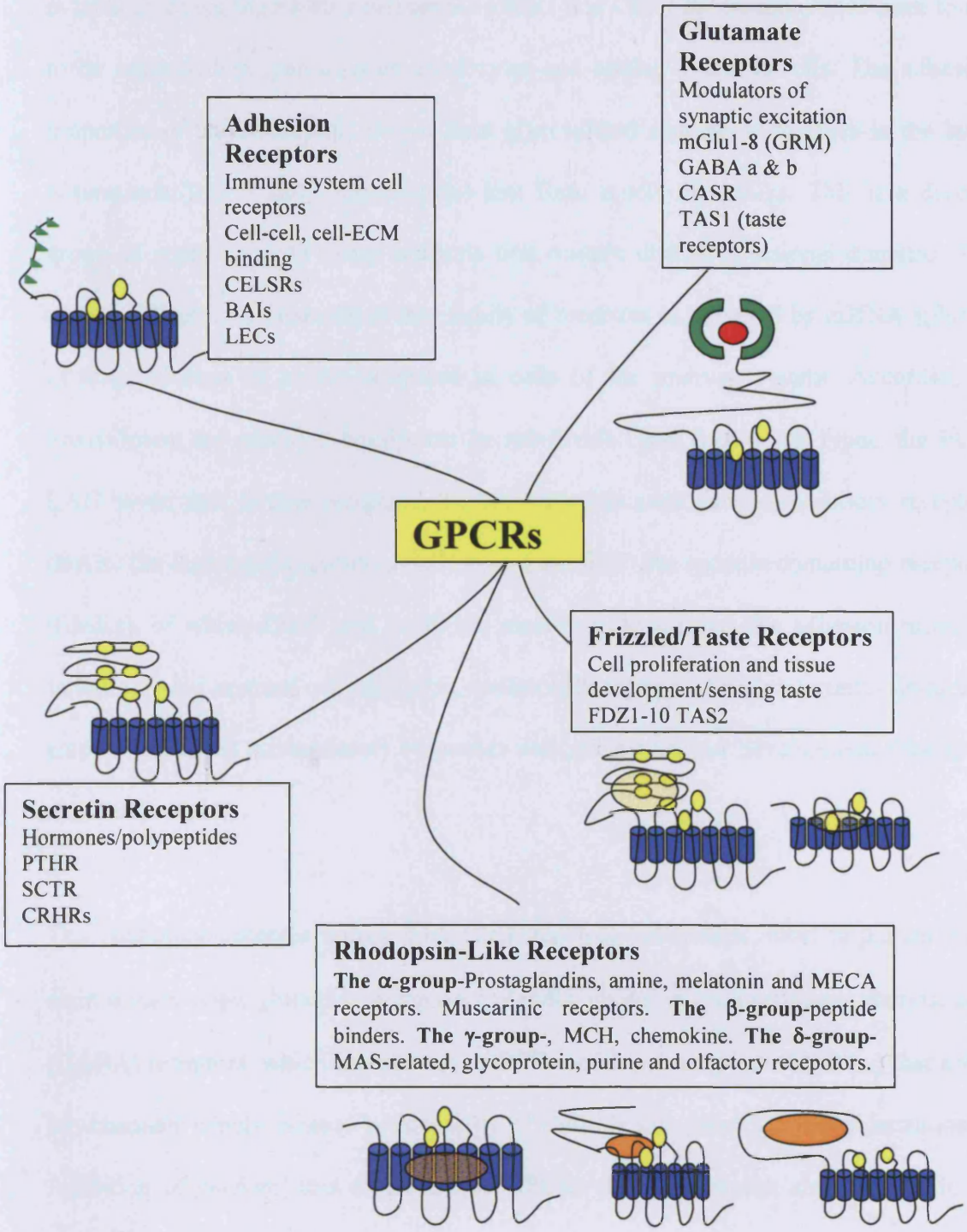

Overview of the classification of G-protein Coupled Receptors based on the GRAFS system as described by Fredriksson et al 2003. Blue cylinders represent TM-helices, orange ovals ligand binding domains, yellow circles conserved disulphide bonded cysteine residues, green triangles EGF-like motifs and green semicircles N-terminal lobes of the Glutamate receptor class. The M_1 mAChR belongs to the Rhodopsin-Like Receptors. Developed from (Fredriksson et al., 2003) and (Bockaert and Pin 1999).

participate in cell adhesion and are highly expressed in the immune system, specifically in leukocytes e.g the F4/80 molecule but EMR1 and CD97 for example have been found to be expressed in granulocytes, monocytes and resting T and B-cells. The adhesion properties of these receptors derive from glycosylated asparagine residues in the large N-terminus (200 – 2800 amino acids) that form mucin-like stalks. This is a diverse group of receptors with many isoforms that contain distinct functional domains. The variety of isoforms produced in this family of receptors is provided by mRNA splicing of large clusters of exons expressed in cells of the immune system. According to Freidriksson the adhesion family can be sub-divided into 3 or 4 sub types, the EGF-LAG seven pass G-type receptors, the brain-specific angiogenesis-inhibitory receptors (BAIs) the lectomedin receptors (LECs) and the EGF-like module containing receptors (EMRs), of which CD97 and F4/80 are members. As a group the adhesion receptors function to aid immune cell migration, anchor cells to the extracellular matrix, induce or amplify localised inflammatory responses and guide neuronal development (Stacey et al., 2000)

The Glutamate receptor family is divided into four sub-groups, most importantly the eight metabotropic glutamate receptors (mGluR), mGlu1-8 and two γ-aminobutyric acid (GABA) receptors, which include non- GPCR ionotropic receptors ($GABA_A$) that act as ion channels which increase permeability of chloride ions causing hyperpolarization or inhibition of neurons; and metabotropic GPCRs ($GABA_B$) which are involved in K^+ efflux from neurons. The principal effect of $GABA_B$ agonism is muscle relaxation. There is also the single calcium-sensing receptor and five receptors proposed as taste receptors. The ligand binding sites for these receptors reside within the large extracellular domains that characterize this group of receptors. The metabotropic glutamate receptors are divided into three groups dependant upon their G-protein coupling, binding of selective ligands and effector activation. mGlu1 and 5 couple to G_q

and activate PLC, whereas mGlu 4, 6, 7 and 8 couple to G_i and G_o and inhibit adenylyl cyclase. mGlu2 couples to Gi and Go and also inhibits adenylyl cyclase but binds a different set of selective agonists and antagonists. Sharing the typical 7-TM spanning helical domains of the GPCR super-family the glutamate receptors are distinguished by their characteristic N-terminal domain. The N-terminal domain consists of two lobes that form a glutamate-binding cavity, which is often referred to, as the "venus fly trap" domain due to the closure of the two lobes around the bound glutamate molecule, leading to the activation of the receptor. Glutamate is an important neurotransmitter and glutamate receptors are widely distributed at pre and post-synaptic locations throughout the central nervous system where, in general they modulate mechanisms of neuronal excitability. Glutamate receptors are implicated in many psychiatric and neurological disorders of the central nervous system, prompting a sustained effort to regulate glutamate receptor activity via pharmacological means. Glutamate is the major neuro-excitatory transmitter molecule of the mammalian nervous system. $GABA_B$ acting via $GABA_A$ ionotropic receptors is the major inhibitors of synaptic transmission. Knockout mice studies have shown that the metabotropic glutamate receptors play key roles in motor learning and spatial memory (mGlu1), retention of spatial learning and fear contextualisation (mGlu5), motor function and seizure states (mGlu4), processing of visual stimulation (mGlu6) and amygdala dependent learning and epilepsy etiology (mGlu7) (Schoepp, 2001). Both mGlu and GABA receptors have ionotropic receptor counterparts that are less closely related to each other than their 7-TM namesakes and function as transmitters of excitatory or inhibitory action potentials. Thus the roles of the $GABA_B$ and mGlu receptors are more modulatory in the control of synaptic inhibition/excitation, monitoring excess or a deficit of neurotransmitter in the synaptic cleft.

The Frizzled/Taste2 receptors cluster together in the same group due to a few consensus sequences in TM2 (IFL), TM5 (SFLL) and TM7 (SxKTL) (Fredriksson et al., 2003). The N-terminal of the Tas2 receptors is very short (unlike Tas1 of the glutamate family) and unlikely to contain a ligand binding domain whereas the Frizzled receptors have a 200 amino acid N-terminal with a conserved set of cysteine residues that harbours a Wnt binding domain, known as the fz motif. The fz motif is found in many other non-GPCR proteins, for example it is found in the collagen VVIIIa1 protein and in some receptor tyrosine kinases (Rehn et al., 1998). In the body these two classes of receptor perform entirely different functions. Surprisingly, the Tas2 receptors are dissimilar enough from the Tas1 receptors found in the Glutamate group to warrant placing them in a group of their own. Expressed in the tongue and palate epithelium taste receptors provide valuable information about the quality of food. Tas1 R2 receptors have been indicated to form heteromeric complexes with Tas1 R1 and Tas1 R3 receptors of the Glutamate group that can bind various taste related amino acids. For example a Tas1 R2 and a Tas1 R1 complex can detect the artificial sweetness of aspartate (Nelson et al.). However, as a homomeric complex Tas2 receptors have been shown, by expressing Tas2 genes in "sweet cells" in the mouse, to detect only bitter tastes. Many of the natural ligand/taste molecules that bind to taste receptors are unidentified but candidates for the Tas2R16 in humans include salicin and related compounds (Mueller et al., 2005).

The Wnts are a group of 20 or more, vertebrate genes that express secreted glycoproteins that act as the ligands for members of the Frizzled group of GPCR's, of which there are 10 members so far described (FZD1-10). These ligands and the Frizzled receptors are essential for the early development of mammalian cells and tissues, regulating cell proliferation, apoptosis and cellular polarity. Frizzled receptors were shown to trigger a G-protein induced phosphatidylinositol response by Slusarski et al

(Slusarski et al., 1997) leading to the expression of an extensive array of gene products essential for embryonic development including for example, transcription factors, Ras related proteins, chaperone related proteins, kinases, apoptotic proteins and proteins important for chromosomal separation (Li et al., 2004)

The rhodopsin family of receptors, comprising 241 non-olfactory out of 701 receptors, are the largest group in the 7-TM family. However, the number of reported receptors in this group seems to vary quite considerably throughout the literature and many receptors of this group remain "orphans" with no known ligand that can be assigned to them. Using the GRAFS system of classification the rhodopsin family of GPCRs can be sub-divided into four separate groups, the α-group, includes the prostaglandins (15 members), the amine receptors (40 members), the melatonin receptors (3 members). The β-group has no branches and comprises 35 peptide binding receptors. The γ-group includes, the melanin-concentrating hormone (MCH) (2 members) and the chemokine (42 members) cluster of receptors. The δ-group has four main clusters, the MAS-related receptors (8 members), the glycoprotein receptors (8 members) the purine receptors (42 members) and the olfactory receptors (~460 members). Due to the huge and diverse nature of the rhodopsin group of receptors detailed descriptions of all the members is beyond the scope of this chapter. Instead focus will be given to two members of the amine group of receptors, the dopamine and serotonin receptors which are of direct relevance to this study, since the muscarinic acetylcholine receptors, the focus of this study, belong to this group and share similar structural and activity characteristics. Rhodopsin itself will be covered in more detail in a following section when a more detailed description of the 7-TM receptor structure will be given.

Included in the rhodopsin family of receptors is the peptide binding neurokinin receptors 1, 2 and 3 (NK-1 NK-2 and NK-3) which bind the mammalian tackykinins,

substance P, neurokinin A and B respectively. Although these receptors are homologous they display a different pharmacology (Gether, 2000). This is due to multiple epitopes found throughout these receptors which contribute to the sub-type selectivity of tackykinin peptides. Substitution of the extracellular loops of NK-1 and NK-3 for example suggested that the first extracellular loop and two residues of the second extracellular loop were involved in the binding of tackykinin peptides (Fong et al., 1992). Other studies involving chimeric receptors (Gether et al., 1993) suggested that neurokinin A may partially enter the transmembrane binding crevice. This indicates that there are differences in the binding modes of homologous peptides. Other rhodopsin-like peptide binding receptors such as the V2 vasopressin receptor are also likely to have this ligand binding selectivity determined by key residues in the extracellular loop regions and residues at the top of the transmembrane domains (Cotte et al., 1998). There is evidence that that the extracellular loops are also involved in the binding of peptide ligands for the angiotensin (Hjorth et al., 1994), somatostatin (Liapakis et al., 1996) and opioid (Wang et al., 1995) receptors.

The biogenic amine receptors all share similar structural architecture of the classic GPCRs with seven membrane spanning helical regions linked by 3 intra and 3 extra cellular loop regions with the N-terminus on the extracellular side and the C-terminal on the intra cellular side of the plasma membrane. A conserved disulphide bond linking the top of TM 3 to the second extra cellular loop is a conserved feature of all the amine receptor sub-types although in general overall sequence homology is variable among the different classes. Dopamine receptors, serotonin or 5-HT (5-hydroxytryptamine) receptors, histamine receptors, adrenergic receptors, trace amine receptors and muscarinic receptors all bind structurally related small biogenic amines that act as neurotransmitter molecules in the central and peripheral nervous system and perform a vast array of functions and are implicated in the etiology of many disease states. It is

therefore of little surprise to know that the pharmacological control of these receptors potentially offers enormous therapeutic benefits and as such discovery of selective ligands is currently of paramount importance to both the academic and pharmaceutical industries.

Dopamine, the major catecholamine of the brain and the endogenous agonist of dopamine receptors serves to regulate a plethora of functions in the mammalian brain and is implicated in such diseases as Parkinsons, schizophrenia and Tourettes syndrome. Dopamine receptors fall into five distinctive sub-types (D_1-D_5). The D_1 and D_5 receptors positively stimulate adenyly cyclase generating a signal transduction cascade via the cAMP second messenger system, differentiating them from D_2, D_3 and D_4 which inhibit adenylyl cyclase activity. The D_1 and D_5 receptors share a high degree of conservation in their transmembrane regions as do D_2, D_3 and D_4 and therefore not surprisingly a similar pharmacological distinction is made between the sub-types, so that D_1 and D_2 like receptors bind agonists such as apomorphine and antagonists such as chlorpromazine with variable shifts in affinity. The D_1 receptor is the most widespread of the dopamine receptors in both the central and peripheral nervous systems. Activation of D_1, D_2 and D_3 receptors in the ventral striatum for example controls forward locomotion, whereas in the nucleus accumbens agonist binding to D_3 receptors inhibits locomotor activity (Diaz et al., 1995). For full reviews of dopamine receptor functions see (Jackson and Westlind-Danielsson, 1994). Another important role for dopamine receptors is their role in reinforcing properties of drug (especially cocaine) self administration, where D_2 receptors stimulate drug reinforcement and stimulate cocaine seeking behaviour (Self et al., 1996). Other functions of dopamine receptors in the brain include cognition and emotive responses. In the peripheral nervous system dopamine receptors are located in blood vessels, adrenal glands, kidneys, and the heart and are responsible for inhibition of norepinephrine and vasodilation, inhibition of

aldosterone secretion, increase of renal filtration rates and stimulation of rennin secretion, respectively. For a comprehensive review of dopamine receptors and a full set of references see (Missale et al., 1998).

Serotonin or 5-HT receptors are perhaps the most complex group of neurotransmitters found in the central and peripheral nervous system. They comprise of at least 14 members (5-HT1-7), including multiple splice variants and 3 sub-types belonging to the ligand-gated ion channel group of receptors. Expressed from an intron-less gene (Chanda et al., 1993) 5-HT-receptors bind the endogenous and intrinsically fluorescent neurotransmitter serotonin, which is secreted at numerous sites throughout the central and peripheral nervous system. The primary function of 5-HT receptors upon activation by serotonin is to inhibit adenylyl cyclase reducing intra-cellular levels of cAMP. This action is mediated predominantly via the $G\alpha_{i/o}$ class of G-proteins, although studies have shown that 5-HT receptors can interact with a range of G-protein a-sub-units with differing affinities, in mammalian cells the heirachy is $G\alpha_{i3} > G\alpha_{i2} > G\alpha_{i1} >> G\alpha_{o} >> G\alpha_{2} >> G\alpha_{z}$. (Garnovskaya et al., 1997) and (Raymond et al.). Messenger RNA for 5-HT receptors has been found in the gut, muscle, kidneys and lymphatic tissue, but is predominant in the limbic forebrain, i.e. hippocampus, raphe nuclei, amygdala, hypothalamus and the cortex. Here they are involved in maintaining circadian rhythms, thermoregulation, mood, pain, addictions, libido, and locomotor activity. Other evidence has shown 5-HT receptor involvement in obsessive compulsive disorder, asthma and heart conditions. For detailed reviews of 5-HT receptors see (Pucadyil et al., 2005) and (Hoyer et al., 2002).

1.2. Structure of 7-TM Receptors Based on the Rhodopsin X-Ray Crystallographic Structure.

The first attempts by Hibert et al (Hibert et al., 1991) in 1991 to reveal the general structure of GPCRs using computer generated three dimensional homology models based on the structure of bacteriorhodopsin, gave clear insight to the existence of seven transmembrane spanning helices. These authors also tried to define the ligand binding sites for the dopamine D_2, $5HT_2$, α_2 and β_2 adrenergic receptors and the M_2 mAChR. Although their details were a little inaccurate, they did provide a good working model upon which further experiments could be designed to further refine those missing details. An alpha carbon template for the 7-TM helices in the rhodopsin family of GPCRs was created by Baldwin et al (Baldwin et al., 1997). Taking sequence information from ~500 GPCR sequences and using frog rhodopsin as a template they generated data that provided more precise information on the structures orientations, locations and lengths of the TM helices. The authors also suggested the possible orientation of the chromophore binding site although they could not describe it in detail. This provides a basis for further experiments including for example, site directed mutagenesis (Han et al., 1996a; Han et al., 1996b), substituted cysteine accessibility methods (SCAM) (Javitch et al., 1994., Javitch et al., 1995.), creation of metal binding sites (Elling et al.,1995 Thirstrup et al., 1996) and site-directed spin labelling studies (Farahbakhsh et al., 1993; Farahbakhsh et al., 1995.) Although Baldwin et al. created a template for GPCR structure compatible with the combined data, the over simplification of using straight helical segments meant that helix axes parameters needed more refining. The race to create a true atomic high resolution X-ray crystallographic structure was on.

Finally, in 2000 the X-ray crystallographic structure of the photoreceptor rhodopsin was solved at 2.8 Angstroms resolution. To date, Rhodopsin is the only GPCR for which a

high-resolution structure has been determined (Palczewski et al., 2000; Teller et al., 2001). Consequently, the structure solved by Palczewski and colleagues has been widely employed as a model for other GPCRs and has superseded earlier models based on electron crystallography (Baldwin et al., 1997). Palczewski's structure has remained the basis for the interpretation of structure-activity relationships for a wealth of mutagenesis and affinity labelling studies for related 7-TM receptors, see (Hulme and Lu, 1998; Hulme et al., 2003; Lu et al., 2001; Savarese et al., 1992). The general secondary (see figure 1.2) and tertiary structure (figure1.3) of 7-TM receptors comprises a typical extracellular glycosylated N-terminal domain leading to seven membrane spanning α-helices (TM domains), connected by 3 alternating extracellular loop regions and 3 intracellular loop regions terminating in a shorter eighth α-helix anchored parallel to the lipid membrane via palmitoylated cysteines at the C-terminal region. Two highly conserved cysteine residues form a disulphide bond connecting the top of TM3 and the second extracellular loop (E2 Loop) in all but a small minority of GPCRs. This disulphide bond appears to be crucial for correct expression and maintenance of the structural stability of the receptor and is a general feature with the cysteine pair conserved in virtually all GPCRs (Davidson et al., 1994; Savarese et al., 1992).

The transmembrane α-helices vary from between 20-30 amino acids in length, somewhat longer than predicted by hydrophobicity plots (Trumpp-Kallmeyer et al., 1992). This was due to the complex dielectric nature of the membrane and the failure of the hydrophobicity plot method to identify helices that contained polar residues on both sides of that helix. Surprisingly nearly 40% of the transmembrane domain interacts with the phospholipid head groups (Ballesteros et al., 2001) rather than the hydrophobic core as may be expected. For amine receptors, residues at the cytoplasmic boundaries are rich in basic amino acids, such as lysine and arginine and provide an overall positive charge complementing the negative charge of the phospholipids head groups. This

allows the correct orientation of the receptor into the membrane and is referred to as the "positive inside rule". The cytoplasmic ends of the TM helices can be determined by the presence of regions rich in basic residues.

Figure 1.2. Secondary Structure of 7-TM Receptors

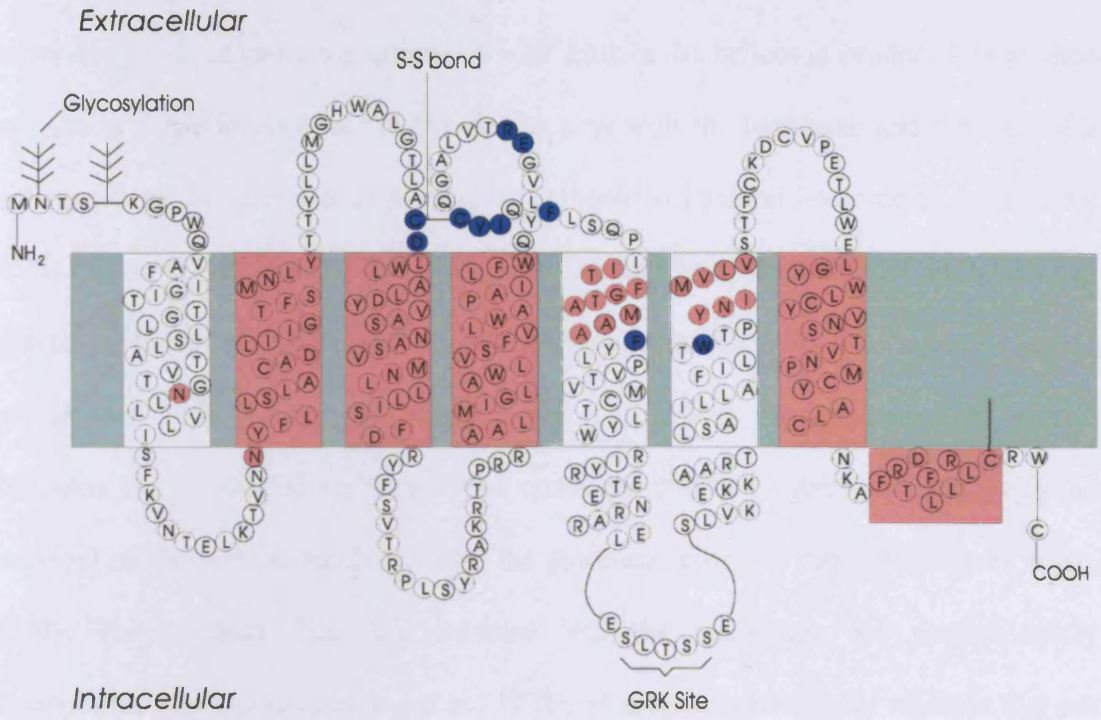

The general secondary structure of 7-TM receptors is represented here in the form of a snake diagram of the M_1 mAChR based on Baldwin et al. structure (Baldwin et al., 1997). The residues of the M_1 mAChR are shown in circles. Blue circles indicate residues that have been mutated to alanine in this study. Helical domains coloured pink have been previously mutated by this laboratory. Counting from the N-terminus there are seven transmembrane helices connected by 3 extracellular loops and 3 intracellular loops. An eighth helix lies parallel to the membrane anchored by a palmitoylated cysteine residue at its C-Terminus. Also shown are the two highly conserved cysteine residues that form a disulphide link between the top of TM3 and the E2 loop. At the N-Terminal end there are two asparagine residues that allow glycosylation of the receptor. The large third intracellular loop incorporates a G-protein receptor kinase (GRK) binding domain and in this model some residues have been omitted from the I3 loop and the C-terminus for the sake of clarity.

1.2.1. The Transmembrane Helices

High resolution structural data revealed that the TM helices contains numerous kinks twists and bends at various positions. A ~26° kink in the helices is produced by proline residues. The steric clash of the pyrrolidine ring with the backbone and the loss of a hydrogen bond between the amide and the carbonyl at position i-4 result in the kinking of the TM helix (Barlow and Thornton, 1988; Sansom and Weinstein, 2000). Kinks can also be produced by glycine residues that can impart flexible hinge-like regions (Kumar and Bansal, 1998).Twists and bends in the TM helices can be caused by serine, threonine and asparagine residues which retain the ability to hydrogen bond with the carbonyl of the protein backbone from the preceding a-helical turn (Ballesteros et al., 2000). The residues that face outward into the membrane are predominantly hydrophobic (Trumpp-Kallmeyer et al., 1992), as may be expected for residues that are in contact with the lipid bilayer. Residues at the cytoplasmic end of the TM helices are involved in the coupling of the heterotrimeric G-proteins (see sections 1.3 and 1.5). Since rhodopsin is still the only GPCR whose structure has been solved the following descriptions of the TM helices all relate to the rhodopsin template and similar structures are assumed for other GPCRs in the rhodopsin class and differences are indicated where evidence exists. The following will refer to residues according to the nomenclature of Ballesteros and Weinstein (Ballesteros, 1995), whereby the helix number is followed by a number indicating its relative position to the most conserved residue of the helix, which is assigned the number .50. Eg 3.50 refers to the most conserved residue (Arginine) in helix three and 3.49 indicates the residue that precedes it. The following structural information can be found in more detail in refs (Ballesteros et al., 2001b; Teller et al., 2001)

TM1 is 44 Å long and contains 30 residues starting at Trp 1.30 and ending with Gln 1.59. It has an angle to the membrane normal of 25° and the helix itself has a slight 12°

of bend due to a proline at position 1.49. Although proline is conserved in the opsin group of receptors most amine receptors have a glycine–asparagine sequence that generates a similar kink angle. In fact Gly 1.49 is highly conserved in the amine receptors.

TM2 also has 30 residues and in rhodopsin the N-terminal of the helix is kinked at an angle of 24° to the membrane normal and the C-terminal of the helix at a 33° angle to the membrane normal. The TM2 helix starts at Pro2.38 at the cytoplasmic end and ends at His 2.67 at the extracellular end. In bovine rhodopsin the kink occurs at the Gly-Gly-X-Thr-Thr sequence. Although this sequence is not fully conserved in the M_1 mAChR there are two threonine residues at an analogous position. As in rhodopsin these threonine residues may cause the kink by the formation of hydrogen bonds with the carbonyl oxygen of the proceeding helical turn, thus stabilising the bend. The D_2 Dopamine receptor, another cationic receptor which does retain proline residues at similar locations (Pro-X-Thr) may also have a similar bend. It is likely that differently located proline residues may be feature in the structural diversity of GPCRs. An example occurs in TM2 of the chemokine CCR5 receptor where a Thr-X-Pro motif has been identified (Govaerts et al., 2001).

TM3, the longest helix (48 Å) with 33 residues from Pro 3.22 at the top end to Val 3.54 at the cytoplasmic end has a tilt angle of 33° to the membrane normal. This 33° tilt positions this helix so that it bisects the helical bundle bringing it into contact with TM2, TM4, TM5 and TM7. This has important implications for the maintenance of ground state and activated state interactions between residues of these helices. The cytoplasmic end of TM3 contains the particularly well conserved E(D)RY motif important for G-protein interaction. In rhodopsin there are a number of subtle bends creating a ~12° kink, caused by a series of serine, threonine and cysteine residues that

are ~50% conserved in other GPCRs, but essentially this helix is nearly straight. In the M_1 mAChR 4 serine residues could potentially produce the same subtle kink and it is likely that it is a feature of most 7-TM receptors. To support this it has been shown that if the D_2 receptor TM3 domain is modelled as an ideal α-helix then it clashes sterically with TM4 (Ballesteros et al., 2001).

TM4 is the shortest helix at only 23 amino acids in length from Asn 4.46 to Val 4.62. Apart from the 24° kink at the very end of the helix provided by two proline residues 4.59 and 4.60, the helix is straight. Only one proline is found at this position in M_1 mAChRs and D_2 dopamine receptors. A similar kink as that found in rhodopsin was discovered in the D_2 receptor by Javitch et al. (Javitch et al., 2000) by the use of the substituted cysteine accessibility method. TM4 it has been hypothesised, serves as a stabilising support for the inactive ground state of the receptor, or it may be involved in receptor dimerisation involving an outward facing Trp 4.50 residue.

TM5 at 26 residues in length runs from Asn 5.35 to Gln 5.60. At 35Å long it has two internal kinks of 25° and 15°. The actual helix domain of TM5 extends for just 3 helical turns (12-residues) and is possibly a dynamic structure. The kink at the highly conserved proline 5.50 results in an unusual bulge at His 5.46 suggested to be caused by it hydrogen bonding with Glu 3.37 of TM3. However, this hydrogen bond does not appear to be conserved in other 7-TM receptors, although other sequences may provide a similar distortion, a series of threonine residues in M_1 mAChR for example. In the D_2 receptor it was predicted that the serine residue 5.42 made direct contact with the ligand in the binding pocket, but when a standard proline link was modelled, this residue faced away from the binding site. Thus it was concluded that the unusual kink and distortion may be necessary for a proper ligand contact to be made and that the helix may need to rotate to achieve this (Allman et al., 2000; Liapakis et al., 2000).

TM6 is the second longest of the helical bundle at 31 amino acids and the most kinked, with a bend of 36°. Proposed to be critically involved in the activation mechanism of the 7-TM receptors it is unlikely that the structure of TM6 shows too much variability between the different classes of receptors. It is the highly conserved proline 6.50 that provides the universal kink predicted in this helix in nearly all GPCRs. TM6 forms van-der Waals interactions and a water mediated hydrogen bonding network with TM2, TM3 TM5 and TM7. The highly conserved tryptophan 265 in rhodopsin (Trp 378 M_1 mAChR) is a key residue in this h-bond netwok because it is involved in both the binding of ligand and the activational state of the receptor.

TM7 is the shortest helix with only 21 residues spanning from Ile7.33 to Tyr 7.53. TM7 is elongated and distorted around the retinal attachment residue Lys 269 where the helix differs from an α-helical structure to a tighter 3_{10}- helix (Riek et al., 2001). This has the effect of constricting the binding cleft in which the retinal is attached. Rhodopsin is the only TM receptor that has its ligand covalently bound. It therefore seems unlikely that a similar unusual structural architecture exists in other GPCRs. A kink at this position was discredited by double revertant mutagenesis study conducted on the $5HT_2$ receptors (Sealfon et al., 1995). However, SCAM studies of the D_2 receptor did predicted a large degree of twisting at position Ser 7.46 similar to that seen for rhodopsin (Fu et al., 1996). Since methylsulfonate reagents could not bind to a cysteine at this position it was deemed unlikely that a normal proline kink was present. This evidence suggests that a similar twisting effect occurs in most 7-TM receptors at this point. The tighter 3_{10}-Helix is continues until Val 7.45/Ala 7.46 where an acute 41° bend is produced (Riek et al., 2001) tilting the helix away from the central cleft. Beyond this point the helix reverts to an α-helical formation for one turn before a conserved proline 7.50 kinks the helix again. This proline is part of the conserved NPXXY motif a signature sequence found in

nearly all GPCRs. At the cytoplasmic end of TM7 there is a short four residue linker region that connects the cytoplasmic helix to the main TM helical bundle.

Helix 8 of rhodopsin is 10 residues in length and starts at Lys 311. Helix 8 is anchored, perpendicular to the plane of the membrane aqueous interface, by buried side chain contact residues at the cytoplasmic end of TM1 eg Phe 58 and Val 61 and TM7 Phe 313 and Met 317. These contacts are required for proper folding of rhodopsin receptor. In bovine rhodopsin helix 8 is further secured to the lipid membrane via two palmitoylation sites at a conserved cysteine residue, Cys 322 and at Cys 323 (Langen, 1999). A single cysteine at position 457 was shown using alanine scanining mutagenesis to be the palmitoylation site of the M_2 mAChR (Hayashi, 1997), analogous to Cys 435 in the M_1 mAChR. Helix 8 may be responsible for the correct orientation of the receptor in the membrane as well as being involved with G_t α-sub-unit interactions. The **C-terminal** region prceeding helix 8 is just 4 residues long from residue 334 to 338 and is likely to be a flexible and mobile entity with no apparent conformation.

Figure 1.3. 3D-Homology Model of the M_1 mAChR Receptor: Lateral View

The figure shows the rhodopsin homology model of the M_1 mAChRs seen from the lateral, membrane spanning view. The model shows the various twists, kinks and bends that are a feature of the seven transmembrane helices due to proline, serine or threonine residues (see text for details). To produce the homology model, 20 models created by threading the M_1 amino acid sequence on to the rhodopsin model were energy minimised using molecular dynamics software (Lu, 2001). The arrangement of the transmembrane helices and their conformational kinks are easily distinguished in this view. The binding pocket for exogenous ligands such as acetylcholine is indicated by the inclusion of an ACh molecule at the approximate position of the central binding site. The binding site lies approximately one third of the way down the inner surface of the transmembrane helices.

1.2.2. The Intra and Extra Cellular Domains

It is very likely that the cytoplasmic (intracellular) loops are flexible and mobile and this is reflected in their poor resolution in the X-ray crystallographic structure of rhodopsin (Palczewski et al., 2000; Teller et al., 2001). Thus their structures are not well defined due to several different conformations observed especially for the I3 loop. Nevertheless, a general outward projection of the intracellular loops into the cytoplasm is consistent with a canopy structure that enables interaction with all three G-protein sub-units in the membrane. In a later study of rhodopsin structure (Li et al 2004.) using a molecular replacement strategy from the 2.8Å model, the details of the extracellular loop domains become clearer. The **I1 loop** is short in length, just 5 residues in rhodopsin and comprises mainly basic and hydrophobic residues that are 97% conserved in the opsin family. Two residues, Leu 68 and Arg 69 are inwardly facing and make van der Waals and H-bonding interactions with TM1, TM2 and Helix 8. The importance of the first intracellular loop to receptor activation is still a matter for debate with few studies providing direct evidence of its critical involvement. Nevertheless, the length of the I1 loop is conserved among GPCRs, suggesting a structural role. Studies by Moro et al. on the M_1 receptor (Moro et al., 1994) and Amatruda et al. on Formyl peptide receptors (Amatruda et al., 1995) have shown that maintenance of the I1 loop structure is necessary for efficient ligand dependent G-protein coupling. The debate is whether or not residues of the I1 loop make direct contact with the G-protein or whether loss of function in mutagenesis studies is due to structural perturbations.

The **I2 loop** contains, at its N-terminus region, the highly conserved Asp-Arg-Tyr motif and the middle Arg residue occurs in 99% of all GPCRs in the rhodopsin class of receptors (Baldwin et al., 1997). In fact the N-terminus of I2 forms a cytoplasmic 3-turn helical extension of TM3. The Asp-Arg-Tyr (DRY) motif has been the focus of many reports that show that the mutation of the Arg residue in the middle of the motif causes

drastic reductions in the efficiency of G-protein coupling. (Jones et al., 1995; Prossnitz et al., 1995; Scheer et al., 1995) and so has been proposed as the switch that enables G-protein interactions (Burstein et al., 1998). In fact these authors also suggested that it is the entire I2 loop that acts as the switch responsible for G-protein activation. The Jones et al study (Jones et al., 1995) also showed that the charge preserving Arg-Lys mutation retained the ability for the M_1 receptor to couple to the G-protein. Li et al (Li et al. 2004) report that the I2 loop is L-shaped and lies parallel to the membrane. In the conserved E(D)RY motif Glu 134 (E instead of D in rhodopsin) is negatively charged and forms a salt bridge with Arg 135. Arg 135 also forms van der Waals contacts with hydrophobic residues of TM6. The protonation of Glu 134 is required for the activation of transducin (Gt), possibly emphasising the importance of the motif in the GPCR signalling processes. However, there is an argument that the DRY sequence is not required for G-protein activation. A study by Rosenkilde et al. (Rosenkilde et al., 2005) showed that the conversion of the DRY sequence to DTW in open reading frame 7 of a rhodopsin-like 7-TM receptor encoded by the equine herpervirus signalled as effectively as wild type. The tyrosine residue of the motif is less well conserved and a different amino acid occurs at this position in ~20% of GPCRs in the rhodopsin class (Baldwin et al., 1997). Though not essential for G-protein coupling this residue when mutated, often leads to large reductions in expression (Lu et al., 1997), indicative of a role in stabilising the functional conformation.

The **I3 loop** is a less well conserved structure in the rhodopsin class of GPCRs, showing considerable variability in sequence length. In rhodopsin itself the I3 loop contains just 35 residues, whereas in the M_1 receptor the I3 loop extends for more than 150 residues. Furthermore, deletion of 129 amino acids from the middle of the I3 loop sequence produces some loss of function and decreased efficacy yet G-protein coupling is still viable (Lu et al, 1997). This shows that it is the N-terminal and C-terminal domains of

the I3 loop that are critical for activation of the G-protein, although selectivity is conferred by the specific residues of different classes of GPCRs. In the muscarinic receptors M_1-M_5, mutagenesis studies (Hill-Eubanks et al., 1996) identified a limited number of uncharged hydrophobic residues in the N-terminus that can determine G-protein selectivity. In a site directed spin labelling study these residues mapped to an amphiphilic α-helix in rhodopsin that are believed to form a surface conducive to G-protein coupling (Altenbach et al., 1996). Similarly, 4 hydrophobic residues at the C-terminus of the I3 loop in M_3 receptors (Ala488, Ala489, Leu492 and Ser493) are also involved in the recognition of G-proteins. These residues are conserved in M_1 but are different in M_2 and M_4. Residues of this region have been studied extensively in mutagenesis studies and are reviewed by Wess et al (Wess, 1996). An overview of the intracellular loops is illustrated in figure 1.4 below.

Figure 1.4. 3D-Homology Model of the M_1 mAChR Receptor: Cytoplasmic View

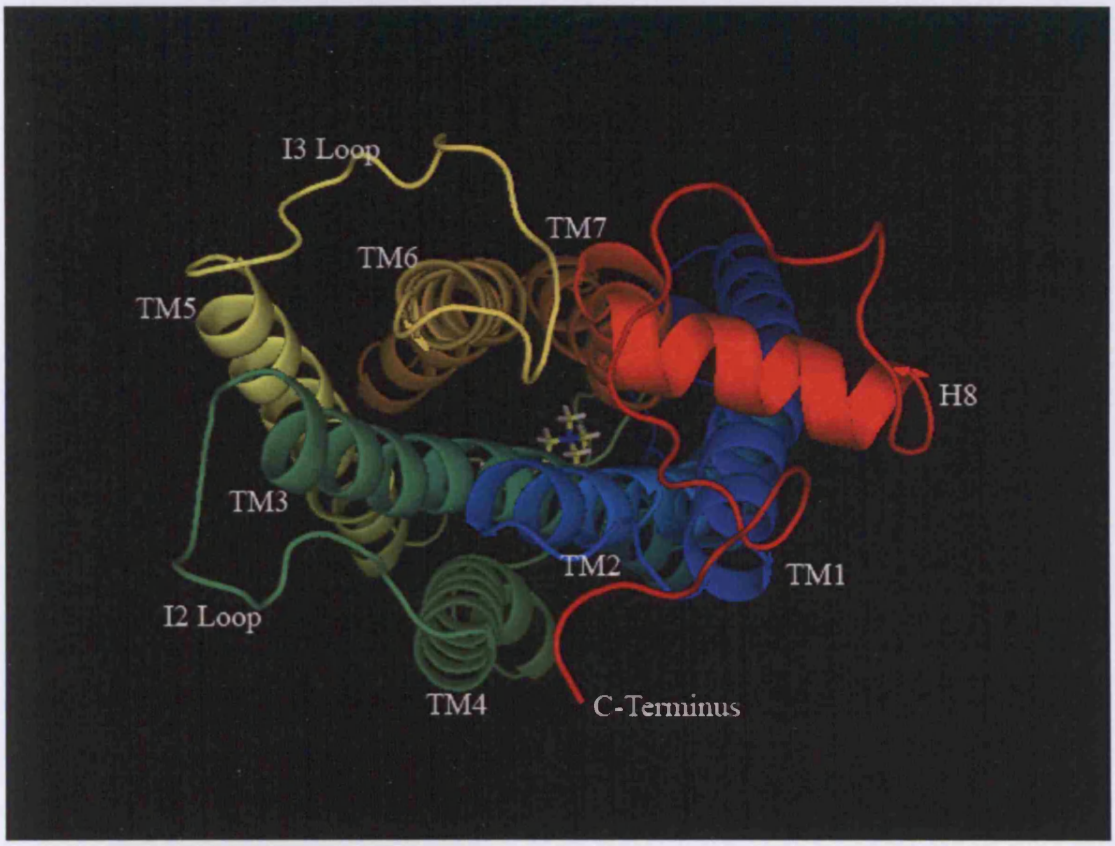

The figure shows the view of the M_1 homology model from the cytoplasmic surface. Residues at the cytoplasmic surface provide contacts for activation of G-proteins. The highly conserved DRY sequence occurs at the N-terminus of the I2 loop at the cytoplasmic end of TM3 and may be a key motif involved in the binding of G-protein. Selectivity for G-protein interaction is determined by sequence variation in the N-terminus and C-terminus of the I3 loop domain (se below for further details)

The **N-terminal domain** varies enormously between GPCR families. The glutamate, frizzled, taste and the peptide-binding rhodopsin-like receptors for example have large N-terminal domains involved in the binding of larger peptide ligands, although perhaps not exclusively so. The N-terminal domain of the V1a Vassopressin receptor, for example, has been shown to bind only peptide agonists but not peptide or non-peptide antagonists (Hawtin et al., 2000) and this also seems to be true of other neurohypophysical hormone receptors, such as the oxytocin receptor (OTR) (Postina et al., 1996), although it was shown that the extracellular loops of the OTR were also involved in agonist binding. In rhodopsin the N-terminus has a globular structure comprising 33 amino acids and is glycosylated at Asn 2 and at Asn 15 with a $Man_3GlcNAc_3$ carbohydrate moiety (Teller et al., 2001). The N-terminus and the E2 loop are cross-linked by water mediated H-bonds between the β1-β2 hairpin and the β3-β-4 hairpin and the whole structure has been described a s forming a 'plug' over the retinal binding pocket

Relatively little is known about the function of the **E1 loop** in the rhodopsin class of receptors, but it has been shown to be important for the binding of peptide ligand in the mouse Corticotrophin Realeasing Factor receptor 2_β (Grace et al 2004) and a conserved aspartate is important for the binding of vasoactive intestinal peptide (VIP) to to the VIP receptor as shown by mutagenesis studies (Du et al. 1997). In the Matsui study of the M_1 mAChR (Matsui et al., 1995) the Trp 91 to Ala mutation reduced ACh affinity by ~40-fold and affected the affinity of several antagonists and Trp 91 was proposed to be one of the residues that line the ligand access channel. The E1 loop is presumed to have a more structural and stabilising role in the rhodopsin class of receptors and may be critical to the correct folding of the nascent peptide. It may also be important for the binding of allosteric and selective ligands as proposed by Spalding et al. and Matsui et al. (Matsui et al., 1995; Spalding et al., 2002).

The **E2 loop** of the M_1 mAChR is the focus of this study and is discussed extensively throughout the study. See below for a description of the E2 loop.

The **E3 loop** is a short sequence of just nine (rhodopsin) or seven (mAChRs) amino acids and there is no sequence homology between the GPCRs in the rhodopsin class. Although there has been little interest in the E3 loop in terms of endogenous ligand activation it has been shown in the M_2 receptor that it is important for allosteric ligand interactions. The authors of a recent study using mAChR E3 loop chimeras (Jakubik et al., 2005) showed the importance of a three amino acid sequence (Asn-Val-Thr) in positive co-operativity of strychnine-like allosteric modulators. Another mutagenesis study (Huang et al., 1999) showed that gallamine and W84 (allosteric modulators) share a binding epitope on the E2 loop and near the junction of the E3 loop and TM7 on the M_2 mAChR. The extracellular loops of a version of the M_1 mAChR homology model are depicted in figure 1.5 below.

Figure 1.5. 3D-Homology Model of the M_1 mAChR: Extracellular View

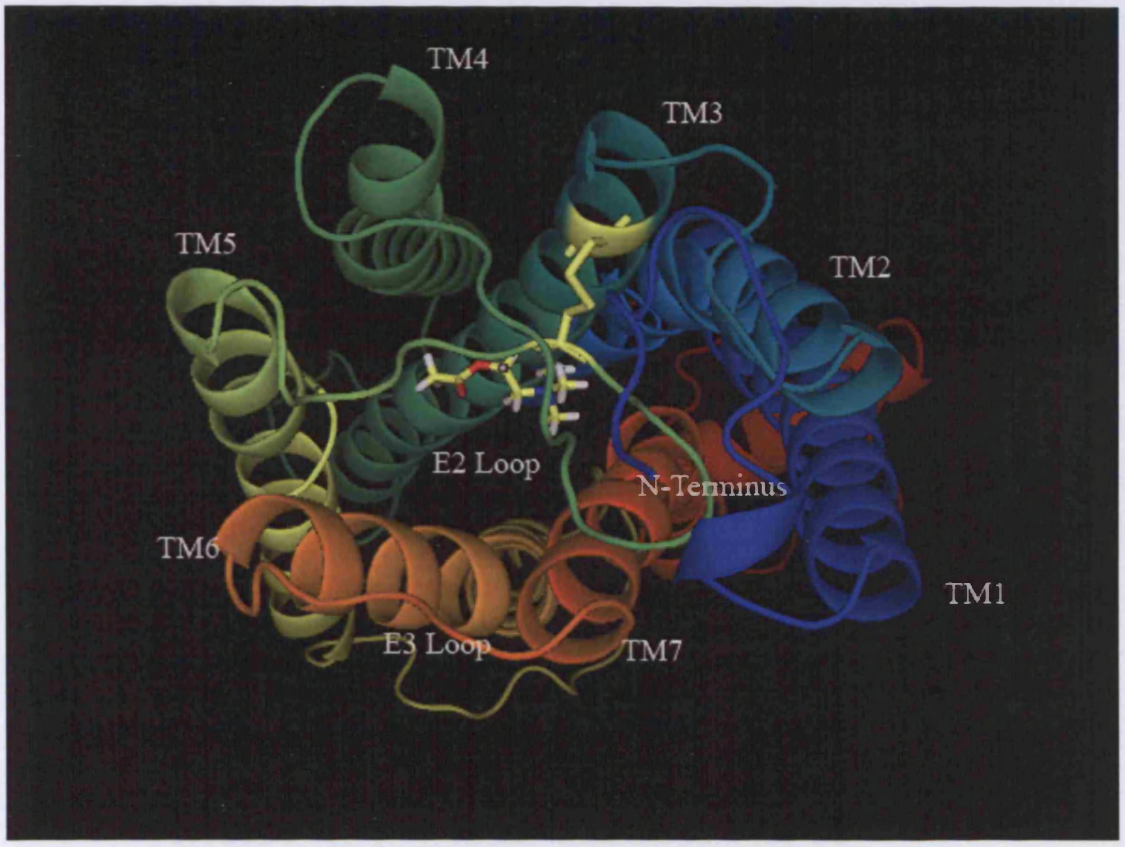

The extracellular view shows the anti-clockwise order of the seven transmembrane helices as viewed from the extracellular surface. The position of the Cys-Cys disulphide bond that links the top of TM3 with the E2 loop is highlighted as yellow sticks The E2 loop (shown in green) doubles back on itself and the residues flanking the S-S bond protrude towards the ligand-binding pocket. The central binding pocket is indicated by the inclusion of an ACh molecule in the core of the molecule. Whether or not residues of the E2 loop are directly involved in ligand contact is one of the issues to be investigated in this study. NB. The full N-terminal domain is not shown in this model.

1.3. General Principles of G-protein Coupled Receptor Activation.

GPCRs exist in multiple states, minimally an inactive state (R) stabilised by antagonists and an active conformation (R*) stabilised by agonists. The binding of agonists at the exofacial side activates a selection of specific hetero-trimeric G-proteins on the cytoplasmic side of the receptor catalysing GDP release from the α-sub-unit of the G-protein heterotrimer and its replacement by GTP. The major, larger component of heterotrimeric G-proteins the α-domain (~39-45 KDa) is tightly bound to both the β-sub-unit (35-39 KDa) and the γ–sub-unit (6-8KDa) to form a complete and functional complex. To date there have been 28 distinct α-sub-units described divided into 4 families as determined by their sequence homology, G_s, G_i, G_q and G_{12} and these interact with the β and γ sub-units of which there are 5 and 12 different variants respectively (Cabrera-Vera et al., 2003). Although not all combinations are favoured, the diversity of sub-unit interactions provides the specificity required for the subtleties of GPCR signal transduction. Even so, the βγ sub-units always remain associated.

The mechanisms for heterotrimeric G-protein coupling are common to all membrane bound GPCRs. The binding of G-protein transfers a reversible and specific signal into the cell. The binding of the nucleotide GDP to the α-sub-unit allows the βγ sub-units to bind also, this greatly increases the association of the Gα sub-unit with the receptor. Although the α sub-unit of the G-protein can bind to the receptor in the absence of the βγ sub-units, their binding to the GDP associated α-sub-unit significantly enhances receptor binding. The binding of an agonist in the central binding pocket activates the receptor by causing a conformational change which favours the binding of a heterotrimeric G-protein complex. On binding to the receptor the α sub-unit rapidly replaces the bound GDP with GTP. The binding of GTP destabilises the tight interaction between the α and βγ sub-units of the G-protein and the complex is

predicted to dissociate, although this is a matter of debate. Bunemann et al. have shown using a FRET approach that YFP labelled $G\alpha_i$ and CFP labelled $G\beta\gamma$ sub-units did not dissociate upon noradrenaline activation of α_{2A} adrenergic receptors in living cells (Bunemann et al., 2003). Assuming dissociation of the sub-units does occur then the α and $\beta\gamma$ sub-units can then activate numerous membrane associated effector proteins depending on the sub-type specificity of the G-protein sub-units, which in turn initiate further downstream signalling cascades. Examples of downstream effectors are, adenylyl cyclase, phospolipase $C_{\beta 1\text{-}4}$, phospholipase A_2, tyrosine kinases, ion channels and mitogen activated protein kinases. For example activation of the M_1 mAChR inhibits the M-current potassium channel leading to an increase in neuronal firing rates. Some of these effectors could be activated or indeed be inhibited by G-protein sub-units, or could be activated/inhibited via second messenger molecules further down the signalling pathway. Initially, signal cascades may result in alteration of intra-cellular calcium ion or cAMP levels. As a further consequence of GPCR activation, a multitude of intermediary signal transduction pathways can be initiated, potentially leading to gene transcription. The signal is terminated by the intrinsic GTPase activity of the α-sub-unit that hydrolyses GTP to GDP and the cycle can begin again. See figure 1.6 for the heterotrimeric G-protein structure and figure 1.7 for an overview of the G-protein activation cycle.

Figure 1.6. Structure of Heterotrimeric G-protein Complex

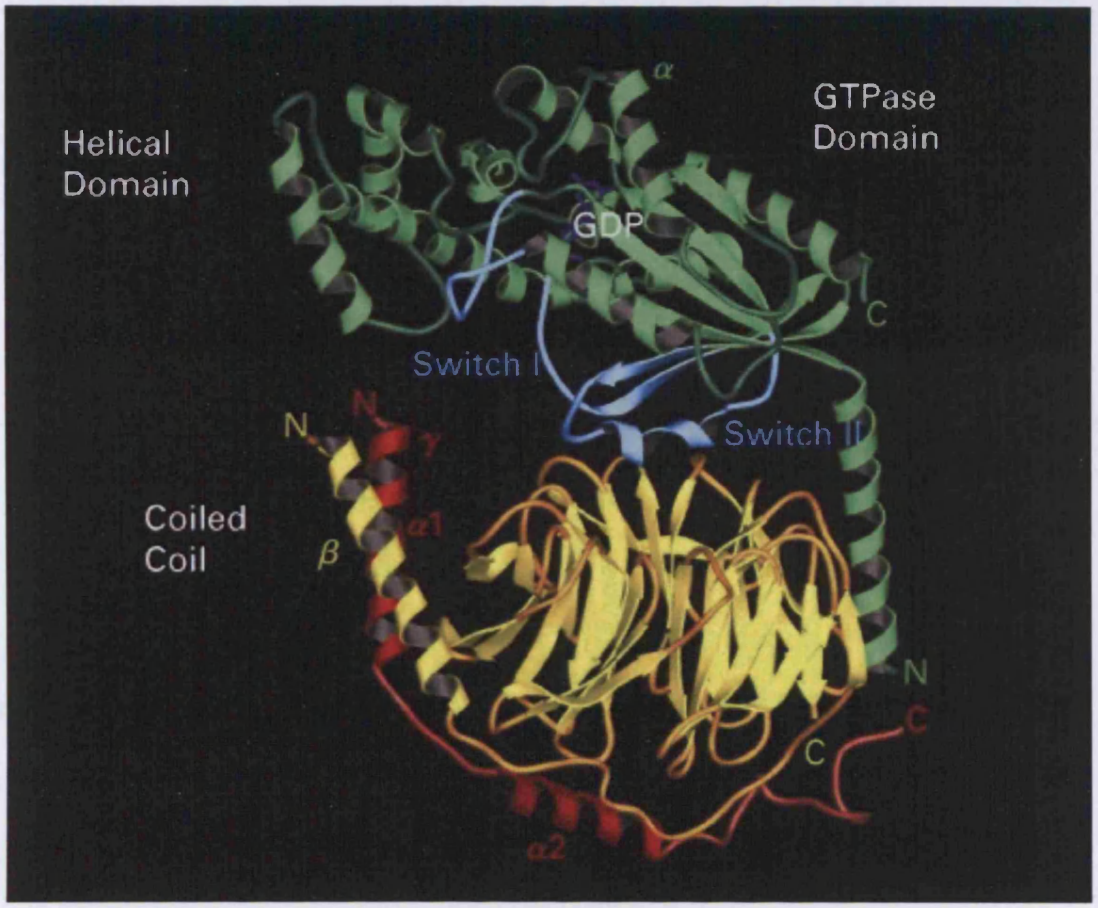

Ref darwin.bio.uci.edu/~bardwell/231B_2004_Sig1.ppt

Basic tertiary structure of a heterotrimeric G-protein complex. The α sub-unit is shown in green, in yellow the β sub-unit is shown and in red the smaller γ sub-unit. GTP displaces GDP and binds to the α sub-unit upon activation of the receptor, resulting in the release of the α and βγ sub-units from the receptor-G-protein complex to initiate a signal transduction cascade via downstream effector proteins. The α sub-unit, which has intrinsic GTPase cap-ability, hydrolyses GTP into GDP and the cycle of activation can begin again.

In most signal transduction systems G-proteins are present in the cell in 10-100 molar excess compared to receptors at ~100,000 copies per cell, with one receptor having the potential to activate up to 100 G-proteins before desentisation events remove the receptor from the cell surface (Alousi et al., 1991). Recent evidence suggests that the coupling of G-proteins to receptors may not always occur by the classic diffusion and collision model, but rather that homodimers of receptors are pre-coupled to the G-protein trimer creating a pentameric complex poised to initiate a signal cascade (Nobles et al., 2005). Evidence of this has also been provided by Baneres et al (Baneres and Parello, 2003). Using a MALDI-TOF mass spectrometry cross-linking strategy and neutron scattering in solution, they showed, in-vitro, that the human leukotriene B_4 receptor exists as homodimer pre-coupled to a single heterotrimeric G-protein complex, with the agonist having a significantly (>10-fold) higher affinity for the pentameric complex than for the monomeric or dimeric receptor alone. Evidence contradicting pre-coupling is provided by Hein et al. (Hein Peter, 2005). Using another FRET based study these authors could not find any evidence of receptor G-protein pre-coupling but that coupling of the $\alpha 2_A$ adrenergic receptor to $G\alpha i$ and $\beta\gamma$ sub-units occurred via the classical collision model. It would appear that both mechanisms are possible depending upon the nature of the signal to be transmitted. If the signal is required to be transduced at high speed, then pre-coupling of receptor and G-protein complexes would be favoured. However if amplification of the signal is required then it may be more favourable to for collision coupling to occur.

The coupling of receptors to G-proteins and their subsequent activation is described by the ternary complex model. The model (figure 1.7b) shows that the binding of an agonist is distinct from the binding of G-protein to the receptor. It is assumed that the association of receptor and a GDP ligated G-protein complex is reversible and has an affinity constant described by the term K_G. The second assumption is that it is the

receptor-G-protein complex (RG) that is responsible for the activation process to occur. The activation of the G-protein is realised upon the catalysis of GDP dissociation and the rapid association of GTP from the cytosol. This process is described by the catalytic rate constant k_{cat}. An agonist, when bound to the receptor, can affect the rate of this catalytic exchange because agonist binding can change the αK parameter, the fraction of receptors in the activated state. The effect of ligand binding can be expressed in terms of a cooperativity factor α, which for agonists is greater than 1 and for antagonists and inverse agonists is less than 1. The same cooperativity factor applies to the affinity of the ligand for free receptor relative to the G-protein-receptor complex. This means that the binding of an agonist can enhance G-protein coupling and that agonist can bind with a higher affinity to receptors that are precoupled to G-protein complexes than they can to free receptor. Conversely, the binding of inverse agonists or antagonists reduces the likelihood of a receptor G-protein complex being formed and may bind with lower affinity to pre-coupled RG complex.

Hydrolysis of bound GTP via the GTPase activity of the G-protein inactivates the G-protein and is governed by the rate constant k_h. The rate at which inactivation of the G-protein occurs can be increased by accessory RGS proteins (regulators of G-protein signalling). RGS proteins are best described as GTPase activating protein (GAPs) which bind to the activated form of Gα accelerating GTPase activity, thus promoting a rapid termination of G-protein signalling. For the M_1 mAChR, RGS2 is responsible for termination of signalling and was found to bind directly to the third intracellular loop to effect $G_{q/11}$ α signalling (Bernstein et al., 2004). It is the conformation of the I3 loop that determines the selectivity of RGS proteins and not the class of the Gα sub-unit. Phospholipase C β1 is also believed to interact with the RG complex and modulate activation (Biddlecome et al., 1996).

T Figure 1.7. An Overview of the G-protein Activation Cycle.

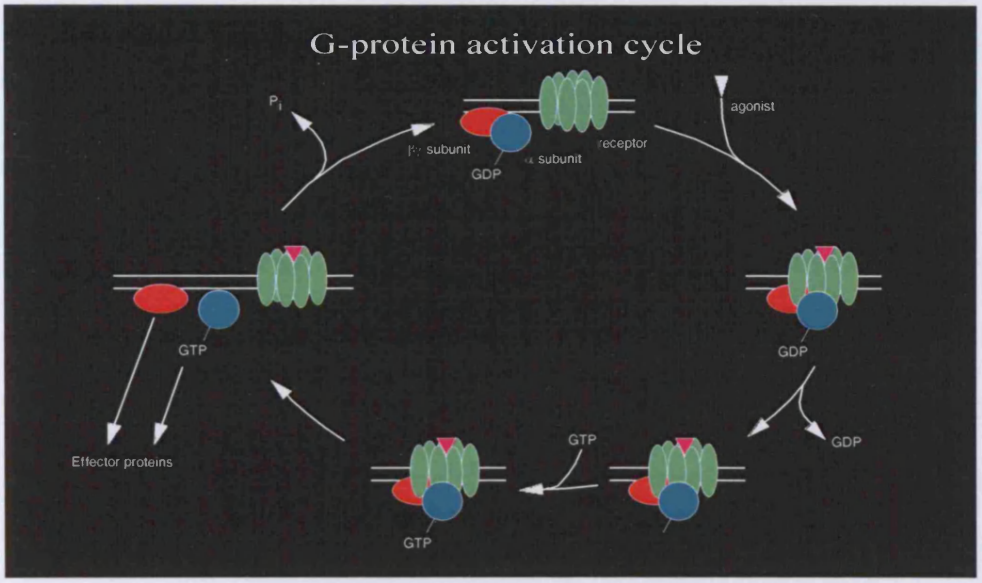

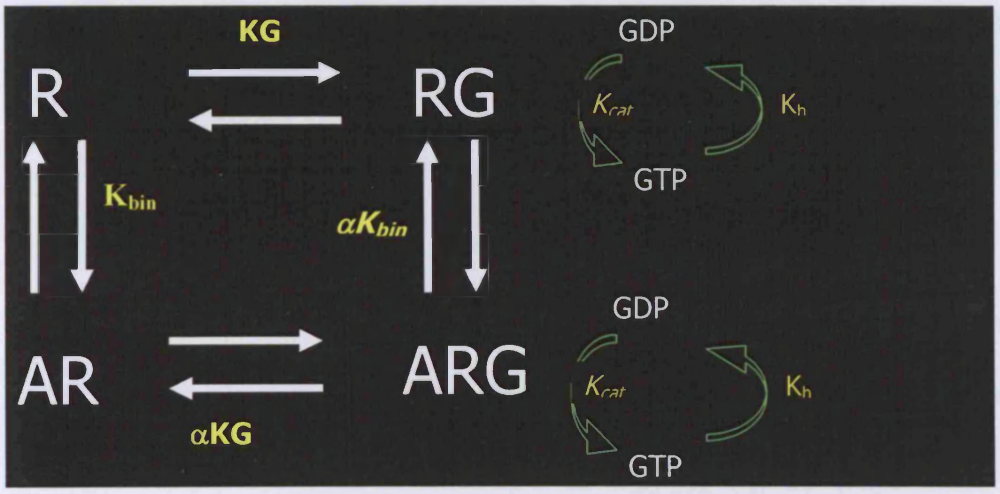

Binding of an agonist to the exofacial side of a G-protein coupled receptor causes a conformational change that opens a G-protein binding pocket on the cytoplasmic side of the receptor. Binding of the G-protein to the activated receptor catalyses the release of GDP and the binding of GTP to the α-sub-unit of the G-protein complex. Bound GTP then allows the partial or complete dissociation of the α-sub-unit from the βγ sub-unit. The mobilised sub-units are then free to initiate multiple downstream signalling cascades via interaction with effector proteins such as phospholipase C (PLC). The process is terminated by the inherent GTPase activity of the α sub-unit which may be accelerated by G-protein activating proteins (GAPs) such as RGS proteins. The release of inorganic phosphate allows re-coupling of the α and βγ sub-units.

NB. K_{bin} = Ach affinity constant. KG = G-protein affinity constant.

Although the simple ternary complex model successfully describes the binding of agonist and the consequent activation of the receptor, it provides no insight into the mechanistic origin of the cooperativity factor α. By incorporating the cooperativity factor into the two-state model of receptor activation some progress can be made. The so-called extended ternary complex model (below) shows that it is the activated state of the receptor which must bind and activate the G-protein. This model shows that there is a background or basal concentration of activated receptor (R*) which can activate the G-protein independently of agonist binding. This basal level of signalling is governed by the conformational constant K. The effect of ligand binding can be seen by the degree to which the conformational constant changes and becomes αK in the ligated state of the receptor and the ligand binding constant K_A becomes αK_A. Experimentally measured binding constants can now be determined by a combination of parameters. $K_{bin} = K_A(1+\alpha K) / (1+K)$. Basal signalling and ligand induced signalling efficacy are (K / 1+K) KG and αK / (1+αK) KG. Variations in the fraction of receptors in the activated state when fully occupied lead to differences in ligand efficacy. Variations in receptor signalling such as those induced by mutations can effect any of the parameters of the system and so lead to characteristic phenotypes.

The Extended Ternary Complex Model

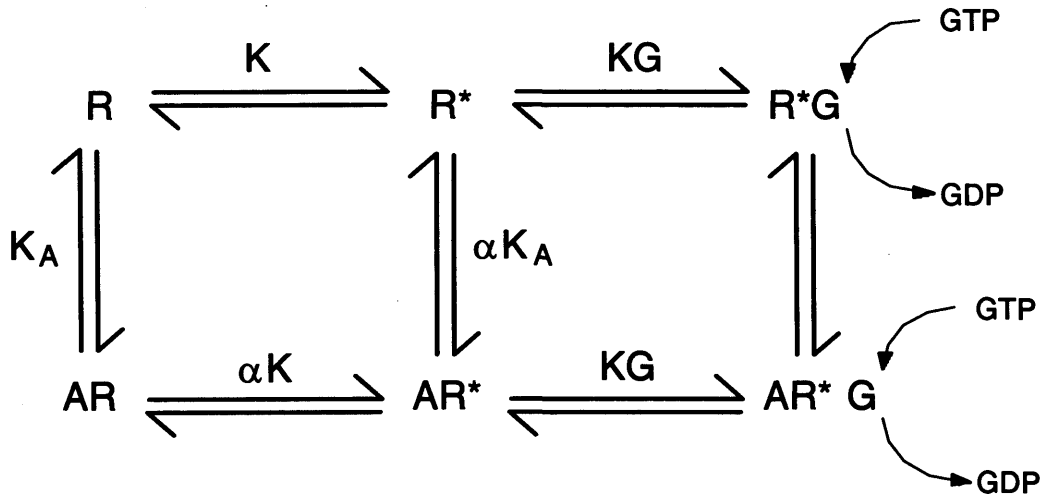

1.3.1 Desensitisation of GPCRs

Activation of G-protein signalling pathways is not a constant process and steps must be taken by the cell to guard against over stimulation. High activation of a receptor can lead to a reduced ability to signal in the future. This is known as desensitisation and is the opposite of sensitisation where under stimulation can lead to an increased ability for the receptor to be stimulated. Receptors can become desensitized in two ways. Firstly by controlling the number of receptors on the cell surface and secondly by regulating the signalling efficacy of cell surface receptors. Receptors are in equilibrium between cell surface activity and synthesis and endosomal degradation. Agonist dependent stimulation of the same receptor often leads to internalisation of the receptor into endosomes where upon they are either re-cycled (sensitisation) or degraded in endosomes. A major mechanism for controlling the activity of GPCRs is the activation-dependent regulation of receptors, known as homologous desensitisation. This mechanism of desensitisation is based on the fact that the activated state of the GPCR acts as a substrate for protein phosphorylation by a family of GPCR kinases (GRKs). GRKs can distinguish between the activated and the ground state of receptors as they are catalytically activated by stimulated receptors. There have been 7 GRKs described (Willets et al., 2003). The GRK 1 & 7 family is found predominantly in visual systems GRK4 is found primarily in the testes, meaning that GRKs3,5 and 6 are responsible for the regulation of the majority of GPCRs. GRKs share a N-terminal domain structure similar to RGS proteins a central kinase domain and a variable C-terminal (Pitcher et al., 1998).

In order for GRKs to participate in homologous desensitisation they must be able to phosphorylate the target receptor and be localised to the membrane in the vicinity of the activated receptor. GRKs are located to the membrane via their carboxyl terminal domains which are modified with a farnesyl or geranylgeranyl group. Unprenylated

GRKs are unlikely to associate with membranes and thus are rendered inactive. Once an activated receptor is phosphorylated by a GRK another family of proteins, the arrestins, bind to the receptor. Recognising both the GRK phophorylated site and the activated receptor bound arrestins prevent further activation of the receptor by prevention of GDP-GTP exchange (Perry and Lefkowitz, 2002). Arrestins are bi-lobed proteins with a mainly β-sheet structure, containing a large phosphoprotein binding pocket. The GRK and arrestin desensitisation mechanism is also involved in the internalisation of inactivated receptors and the recycling of receptors back to the cell surface.

GRKs involvement in the internalisation process is simply due to their recruitment of arrestins to the activated receptor. Once localised at the activated receptor the arrestin proteins bind to both AP2, a clathrin adaptor protein, and to clatharin itself. The binding of clathrin then facilitates the entry of the desensitised receptors into clatharin coated pits which are subsequently internalised by endocytosis. Clathrin-mediated endocytosis of receptors depends on motifs that have been described as being on the C-terminal domains of receptors. However, a common endocytic motif has yet to be identified. GRKs and arrestins can recruit a variety of other proteins that can further regulate or transduce downstream signalling. For example GRKs have been reported to bind PI3-kinases which are involved in receptor trafficking and initiating further receptor dependent signalling. Arrestins also serve as adaptor molecules that can ferry a range of signalling proteins to activated receptors.

1.4 Oligomerisation of GPCRs

Until the early 1980s it was presumed that GPCRs functioned as monomeric entities forming complexes with G-proteins upon ligand activation. It was Agnati et al. (Agnati LF, 1982) who proposed that GPCRs may actually form oligomeric complexes in a manner analogous to other membrane receptors, such as tyrosine kinase receptors. Evidence that GPCRs could actually form homodimeric or higher oligomeric complexes was first gained over a decade later by the use of coimmunoprecipitation techniques. Hebert et al (Hebert et al., 1996) using differential epitope tagging (HA and Myc) of the β_2 Adrenergic receptor showed that the β_2 AR homodimer was resistant to SDS treatment and that the homodimer stabilised the active state. They also showed that inverse agonists favoured the monomeric state and that this had implications for the biological activity of the receptor. Similar studies also revealed the existence of homodimerisation of the D_2 dopamine receptor (Ng et al., 1996), the metabotropic glutamate receptor 5 (Romano et al., 1996) and the M_3 mAChR (Zeng and Wess, 1999). One of the problems of interpreting such data is the possibility that the over expression of hydrophobic receptors in in-vitro systems may cause artifactual aggregations of receptors due to misfolding or incomplete solubilisation of the receptors. Despite methods used to improve solubility and stabilise dimers other methods were needed to demonstrate conclusively that GPCR dimerisation occurred in living cells.

The development of fluorescence resonance energy transfer techniques enabled researchers to observe receptor/receptor interactions in living cells without disturbing the cellular environment. The principle of resonance energy transfer is based on the transfer of nonradiative energy between the electromagnetic dipoles of an energy donor and an acceptor. Overlap of the emission and excitation spectra for the donor and the acceptor allows the energy transfer between fluorophores attached to two molecules to be measured and this provides an indication of the relative closeness of one molecule to

another. There are two types of experiment, bioluminescence resonance energy transfer (BRET) and fluorescent resonance energy transfer (FRET). The difference is that for FRET assays both the donor and the acceptor are fluorescent, whereas with the BRET system the donor has an intrinsic bioluminescence as a result of catalytic enzyme activity (Hovius et al., 2000). By genetically linking either green fluorescent protein (GFP) or Renilla luciferasec to the C-terminus of the human β_2 adrenergic receptor and co-expressing them in the same cells, Angers et al (Angers et al., 2000) were able to show colocalisation consistent with the formation of constitutive homodimers in living cells for the first time. Stimulating these cells with the selective β_2 AR agonist isoproterenol increased the BRET signal and suggests that activation of the receptor either increases dimerisation or that conformational changes induced by activation bring the GFP and the luciferase moieties into even closer proximity.

A more recent study by Liang et al. (Liang et al., 2003) provided visual evidence, using atomic force microscopy (AFM), of the higher order organisation of rhodopsin and opsin receptors in their native environment. These authors revealed that rhodopsin and opsin form structural dimers spatially arranged in paracrystalline arrays in rod outer segment (ROS) disk membranes from Rpe65-/- mutant mice (retinal pigment epithelium deficient mice) (see figure 1.8). The specialized nature of ROS cells and the high density of photoreceptors in their membranes is unusual for GPCRs. The sheer number of receptors expressed in the membrane may force the formation of oligomeric complexes. As a caveat, this problem may also arise when over-expressing receptors in cell based systems. Over-expression of receptors may lead to aggregations of receptors, through hydrophobic interactions and thus may be falsely interpreted as receptor oligomerisation. One of the interesting debates about receptor oligomerisation is whether or not dimers are pre-formed during biosynthesis and export through the ER and Golgi apparatus or whether ligand induced activation causes monomeric receptors

to couple to proximal receptors. One study on a non-GPCR, has shown that the erythropoitin receptor is preformed as a dimer and that hormone activation promotes a conformational change of the dimer rather than forming a dimeric complex (Livnah et al., 1999; Remy et al., 1999). The use of coimmunoprecipitation, western blot analysis and energy transfer techniques have all revealed three basic scenarios for GPCR dimerisation: i) the amount of stable preformed dimers is not altered upon treatment with ligand. eg the δ-opioid receptor (McVey et al., 2001); ii) addition of ligand can alter the amount of dimers eg. β_2 adrenergic receptors (Hebert et al., 1996); iii) dimerisation is only possible by pre-treatment with ligand eg. the somatostatin 5 receptor (Rocheville et al., 2000).

Is dimerisation necessary for activation? Hebert et al. (Hebert et al., 1996) also showed in their study that perturbation of β_2 adrenergic receptor dimers with an inhibitory peptide derived from TM6 reduced signalling activity by ~10-fold. Recent evidence from Guo et al. (Guo et al., 2005) has shown, using crosslinking of substituted cysteines, the extensive and dynamic contribution of TM4 in forming dimers of the D_2 dopamine receptor and that conformational changes at the TM4 and TM5 interfaces are important for receptor activation. Differences in conformation were observed, by changes in cross-linking of substituted cysteine residues in the dimeric complexes when receptors were induced by either an inverse agonist or an agonist. This suggested that the structure of the two protomers (each receptor in a dimer is termed the protomer) at the interface was related to the conformation of the binding site. Mesnier et al. (Mesnier and Baneres, 2004) provided evidence for the idea that the binding of ligand to just one binding site in the dimer was sufficient to promote the active conformation in the other protomer. Using purified leukotriene B_4 receptor heterodimers where one protomer has a lower affinity for the agonist LTB_4 they showed using FRET and GTPγS binding assays that agonist induced activation of one of the monomers in the dimeric complex

specifically altered the conformation of the unliganded monomer. This strengthened the observations of Percherancier et al. (Percherancier et al., 2005) who, using a sensitive BRET methodology, also found that conformational changes were induced in both protomers of the CXCR4 and CCR2 Chemokine receptor homo and hetero dimers upon agonist binding to just one of the protomers.

As well as being able to form dimers and perhaps higher order oligomeric complexes with a receptor of the same species (homodimers) growing evidence has revealed that receptors are also able to form alternative functioning oligomers with other types of receptor (heterodimers) that are able to activate a variety of signalling pathways. The list of GPCR heterodimers is growing and is of immense clinical significance. For a full review of GPCRs that have been found to heterodimerize see Prinster et al. (Prinster et al., 2005). To give just one relevant example, Maggio et al (Maggio et al., 1999) demonstrated, using tripitramine and pirenzepine competition binding experiments with chimeric constructs from M_2 and M_3 mACh receptors, that interaction or 'crosstalk' between the two sub-types was possible. Co-transfection of an M_2 mutant (N404S) that was unable to bind antagonist, with the WT M_3 receptor showed that two entire receptors were able to interact to form a small subpopulation that can bind the M_2 selective antagonist tripitramine. These pharmacologically based experiments demonstrated that heterodimerization of muscarinic receptors is possible, but these authors could offer no insight to the clinical significance of their findings. If it is validated that heterodimerization of GPCRs is a common phenomenon that occurs in vivo, then the challenge facing drug discovery programs and the implications for GPCR regulation are enormous and mind boggling. The identification of dimer interfaces by studies such as Guo et al. (Guo et al., 2005) and assessing their stability and ligand induced or constitutive activation properties may lead to the development of novel compounds to regulate GPCR functions.

Figure 1.8 Arrangement of Rhodopsin and Opsin Dimers

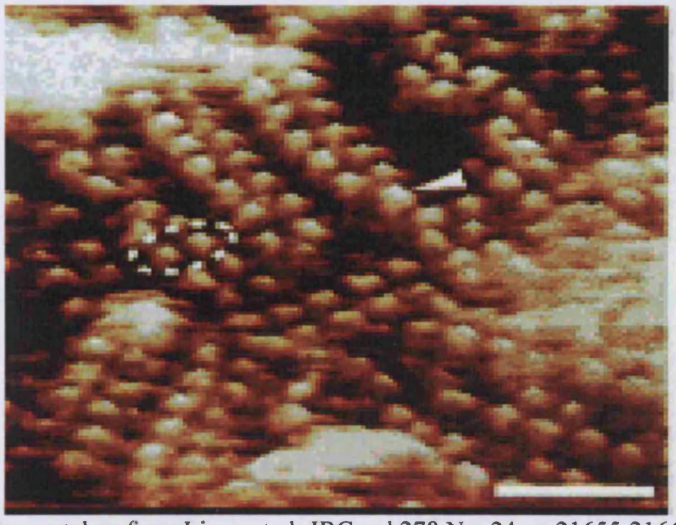

Image taken from Liang et al. JBC vol 278 No. 24 pp 21655-21662

The figure shows rows of rhodopsin and opsin dimers in disk membranes taken from Rpe65-/- mutant mice and visualised using atomic force microscopy. The dimers are spatially arranged in a paracystalline lattice. An occasional monomer is indicated by an arrowhead. The scale bar represents 15nm and the vertical brightness is 2.0nm.

1.5 Muscarinic Acetylcholine Receptors Sub-Types (M_1-M_5)

Sir Henry Dale first described two distinct acetylcholine receptors in 1914. One was activated by nicotine (the nicotinic receptors) and the other was activated by muscarine (Dale, 1914). Muscarine is the pharmacologically active ingredient derivative of the fly agaric mushroom, *Amanita muscaria.* As members of the Rhodopsin class of receptors they are amongst the most studied receptors of the GPCR superfamily of membrane proteins. Muscarinic receptors mediate the metabotropic effects of acetylcholine in the central and peripheral nervous systems. Pharmacological studies initially suggested the existence of more than one muscarinic receptor sub-type (Hammer RBC et al., 1980). Numa and colleagues (Kubo et al, 1986) and Peralta and colleagues (Peralta EG et al., 1987) revealed the genetic identification of the M_1 and M_2 sub-types. A further 3 types, M_3, M_4 and M_5 were discovered a year later by Bonner, Buckley and co-workers. (Bonner TI et al., 1987; Hulme et al., 1990). The chromosomal locations of the five sub-types are based on further work by Bonner et al. are reported to be: - **M_1**-11q12-13, **M_2** - 7q35-36, **M_3** -1q43-44, **M_4** -11p12-11.2 and **M_5** -15q26 (Caulfield and Birdsall, 1998). A line up of their individual sequences is shown below (table 1.1). The five muscarinic acetylcholine receptor sub-types are highly homologous in the transmembrane helical domains, but the N & C terminals and the loop domains show greater variability. As in other members of the rhodopsin-like family, highly conserved residues Asp-Arg-Tyr (DRY) are found at the cytoplasmic end of Transmembrane 3 (TM 3) (Jones et al., 1995; Lu et al., 1997a) and two conserved cysteine residues form a stabilising disulphide bond between the 1st and the 2nd extracellular loops (Kurtenbach, 1990; Kurtenbach et al., 1990; Savarese et al., 1992). Careful sequence analysis has revealed differences in the five subtypes that are related to the ability of the sub-types to bind a different class of G-protein (see previous section).

Table 1.1 Amino Acid Sequence Alignment of the Five Rat mAChR Subtypes

The sequence below compares the amino acid sequences of all five rat muscarinic acetylcholine receptor sub-types. Highlighted in green are the transmembrane domains 1-7 for the M_1 mAChR and in yellow the location and sequence of the M_1 mAChR E2 loop.

```
   1                  50

ACM1_RAT  .......... .......... .......... .........M NTSVPPA.VS
ACM2_RAT  .......... .......... .......... ......MNNS T....NSSNN
ACM4_RAT  .......... .......... .......... ......MXNF TPVNGSSANQ
ACM3_RAT  MTLHSNSTTS PLFPNISSSW VHSPSEAGLP LGTVTQLGSY NISQETGNFS
ACM5_RAT  .......... .......... .......... .........ME GESYNESTVN

          51                                                  100
ACM1_RAT  PNITVLAP.. GKGPWQVAFI GITTGLLSLA TVTGNLLVLI SFKVNTELKT
ACM2_RAT  GL....AITS PYKTFEVVFI VLVAGSLSLV TIIGNILVMV SIKVSRHLQT
ACM4_RAT  SVRLVTAAHN HLETVEMVFI ATVTGSLSLV TVVGNILVML SIKVNRQLQT
ACM3_RAT  SNDTSSDPLG GHTIWQVVFI AFLTGFLALV TIIGNILVIV AFKVNKQLKT
ACM5_RAT  GTPVNHQALE RHGLWEVITI AVVTAVVSLM TIVGNVLVMI SFKVNSQLKT

          101                                                 150
ACM1_RAT  VNNYFLLSLA CADLIIGTFS MNLYTTYLLM GHWALGTLAC DLWLALDYVA
ACM2_RAT  VNNYFLFSLA CADLIIGVFS MNLYTLYTVI GYWPLGPVVC DLWLALDYVV
ACM4_RAT  VNNYFLFSLG CADLIIGAFS MNLYTLYIIK GYWPLGAVVC DLWLALDYVV
ACM3_RAT  VNNYFLLSLA CADLIIGVIS MNLFTTYIIM NRWALGNLAC DLWLSIDYVA
ACM5_RAT  VNNYYLLSLA CADLIIGIFS MNLYTTYILM GRWVLGSLAC DLWLALDYVA

          151                                                 200
ACM1_RAT  SNASVMNLLL ISFDRYFSVT RPLSYRAKRT PRRAALMIGL AWLVSFVLWA
ACM2_RAT  SNASVMNLLI ISFDRYFCVT KPLTYPVKRT TKMAGMMIAA AWVLSFILWA
ACM4_RAT  SNASVMNLLI ISFDRYFCVT KPLTYPARRT TKMAGLMIAA AWVLSFVLWA
ACM3_RAT  SNASVMNLLV ISFDRYFSIT RPLTYRAKRT TKRAGVMIGL AWVISFVLWA
ACM5_RAT  SNASVMNLLV ISFDRYFSIT RPLTYRAKRT PKRAGIMIGL AWLVSFILWA

          201                                                 250
ACM1_RAT  PAILFWQYLV GERTVLAGQC YIQFLSQPII TFGTAMAAFY LPVTVMCTLY
ACM2_RAT  PAILFWQFIV GVRTVEDGEC YIQFFSNAAV TFGTAIAAFY LPVIIMTVLY
ACM4_RAT  PAILFWQFVV GKRTVPDNQC FIQFLSNPAV TFGTAIAAFY LPVVIMTVLY
ACM3_RAT  PAILFWQYFV GKRTVPPGEC FIQFLSEPTI TFGTAIAAFY MPVTIMTILY
ACM5_RAT  PAILCWQYLV GKRTVPPDEC QIQFLSEPTI TFGTAIAAFY IPVSVMTILY

          251                                                 300
ACM1_RAT  WRIYRETENR ARELAALQGS ET........ .PGKGGGSSS SSERSQPGAE
ACM2_RAT  WHISRASKSR IK........ ......KEKK EPVANQDPVS PSLVQGRIVK
ACM4_RAT  IHISLASRSR VH........ ......KHRP EGPKEKKAKT LAFLKSPLMK
ACM3_RAT  WRIYKETEKR TKELAGLQAS GTEAEAENFV HPTGSSRSCS SYELQQQGVK
ACM5_RAT  CRIYRETEKR TKDLADLQGS DSVAEAKK.R EPAQRTLLRS FFSCPRPSLA

          301                                                 350
ACM1_RAT  GSPESPPGRC .......CRC CRAPRLLQAY SWKE..EEEE DEGSMESLTS
ACM2_RAT  PNNNNMPGGD GGLEHNKIQN GK...APRDG VTETCVQGEE KESSNDSTSS
ACM4_RAT  PSIKKPPPGG ASREE..LRN GKLEEAPPPA LPPPPRPVPD KDTSNESSSG
ACM3_RAT  RSSRRKYGRC HFWFTTKSWK PSAEQMDQDH SSSDSWNNND AAASLENSAS
ACM5_RAT  QRERNQASWS SSRRST.... STTGKTTQAT DLSADWEKAE QVTTCSSYPS

          351                                                 400
ACM1_RAT  SEGEEPGSE. .....VVIKM P......... .......... ......MVDS
```

```
ACM2_RAT  AAV..... .......... ........AS NMRDDEITQD ENTVSTSLDH
ACM4_RAT  SATQNTKERP .......... ........PT ELSTAEATTP ALPAPTLQPR
ACM3_RAT  SDEEDIGSET RAIYSIVLKL PGHSSILNST KLPSSDNLQV SNEDLGTVDV
ACM5_RAT  SEDEAK.PTT DPVFQMVYK. .......SEA KESPGKESNT QETKETVVNT

          401                                                450
ACM1_RAT  EAQAPTKQPP KS.....SPN TVKRPTK... .........K GRDRGGKGQK
ACM2_RAT  SRDDNSKQTC IKIVTKAQKG DVYTPTSTTV ELVGSSGQSG DEKQNVVARK
ACM4_RAT  TLNPASKWSK IQIVTKQTGN ECVTA....I EIVPATPAGM RPAAN.VARK
ACM3_RAT  ERNAHKLQAQ KSM..GDGDN CQKDFTKLPI QLESAVDTGK TSDTNSSADK
ACM5_RAT  RTENSDYDTP KYFLSPAAAH RLKSQKCVAY KFRLVVKADG TQETNNGCRK

          451                                                500
ACM1_RAT  P......... .......... .RGKEQLAKR KTFSLVKEKK AARTLSAILL
ACM2_RAT  I......... .......... VKMPKQPAKK KPP.PSREKK VTRTILAILL
ACM4_RAT  F......... .......... ASIARNQVRK KRQMAARERK VTRTIFAILL
ACM3_RAT  TTATL.PLSF KEATLAKRFA LKTRSQITKR KRMSLIKEKK AAQTLSAILL
ACM5_RAT  VKIMPCSFPV SKDPSTKGPD PNLSHQMTKR KRMVLVKERK AAQTLSAILL

          501                                                550
ACM1_RAT  AFILTWTPYN IMVLVSTFCK DCVPETLWEL GYWLCYVNST VNPMCYALCN
ACM2_RAT  AFIITWAPYN VMVLINTFCA PCIPNTVWTI GYWLCYINST INPACYALCN
ACM4_RAT  AFILTWTPYN VMVLVNTFCQ SCIPERVWSI GYWLCYVNST INPACYALCN
ACM3_RAT  AFIITWTPYN IMVLVNTFCD SCIPKTYWNL GYWLCYINST VNPVCYALCN
ACM5_RAT  AFIITWTPYN IMVLVSTFCD KCVPVTLWHL GYWLCYVNST INPICYALCN

          551                                          592
ACM1_RAT  KAFRDTFRLL LLCRWDKRRW RK...IPKRP GSVHRTPSRQ C.
ACM2_RAT  ATFKKTFKHL LMCHYKNIGA TR......... .......... ..
ACM4_RAT  ATFKKTFRHL LLCQYRNIGT AR......... .......... ..
ACM3_RAT  KTFRTTFKTL LLCQCDKRKR RKQQYQQRQS VIFHKRVPEQ AL
ACM5_RAT  RTFRKTFKLL LLCRWKKKKV EEKLYWQGNS KLP....... ..
```

The location and biochemistry of each sub-type determines its physiology and its function (Bymaster et al., 2003b). **M_1** mAChRs are found predominantly and are the most abundantly expressed muscarinic receptors in all the major regions of the forebrain, particularly the cerebral cortex, hippocampus and the striatum (Levey, 1993). At these locations the M_1 mAChRs are involved in higher cognitive processes such as learning and memory. M_1 receptors mediate most of the Ach-stimulated PIP_2 breakdown and MAP kinase activation in the hippocampus and cerebral cortex (Hamilton and Nathanson, 2001) and activate ion channels underlying prolonged oscillations in the hippocampus (Fisahn et al., 2002). Muscarinic acetylcholine receptors also have the ability to stimulate shedding of cell surface growth factors and amyloid precursor proteins, which has important implications for the progress of Alzheimers disease. The first mAChR gene to be knocked out in mice was the M_1 sub-type. Hamiliton and coworkers (Hamilton et al., 1997) found that M_1 KO mice did not exhibit epileptic seizures when treated with pilocarpine, unlike the WT controls or the other four sub –type knockouts (Bymaster et al., 2003b). Therefore, M_1 is strongly implicated in the pathophysiology of some forms of epilepsy. Behavioural studies of M_1 knockout mice (Gerber et al., 2001; Miyakawa et al., 2001) showed that although M_1 KO did not produce phenotypes deficient in motor co-ordination, nocioception or anxiety-related behaviour, they did show increased locomotor activity. The authors attributed this to increases in dopamine release and proposed that the M_1 mAChR have some regulatory effect on the release of dopamine in the neurons of the substantia nigra. If this is the case, then selective M_1 agonists may help alleviate symptoms of Parkinsons disease, which is associated with reduced striatal dopamine release. The discovery of selective M_1 ligands may also impact on the treatment of schizophrenia, another disease where inappropriate M_1 regulation of dopamine release in the forebrain is suspected (Gerber et al., 2001). Hamiliton and Nathanson (Hamilton and Nathanson, 2001) demonstrated the lack of a MAPK signalling pathway in primary cortical cultures of M_1-deficient mice

and a later study, by Berkley et al. (Berkeley et al., 2001) confirmed this by showing that the MAPK pathway remained intact in the CA1 hippocampal neurons of M_2-M_5 KO mice. Since the MAPK signalling pathway is implicit in neuronal plasticity and neuronal cell differentiation it is possible that deficiencies in M_1 mAChR expression or function could be behind specific developmental, physiological or behavioural abnormalities.

M_2 and **M_4** receptors both selectively couple to the Gi/o class of G-proteins and have very similar ligand binding profiles. M_2 receptors are expressed throughout the central nervous system and in the periphery, especially in smooth muscle and tissues of the heart, whereas M_4 receptors are found predominantly in the CNS, particularly the regions of the forebrain. In the heart M_2 receptors are involved in the regulation of heart beat. Stimulation of the parasympathetic nervous system releases ACh from vagal nerve endings, which binds to (predominantly) M_2 mAChRs in the sinotrial node reducing heart beat frequency. M_2 mAChRs appear to be solely responsible for the regulatory effect despite the presence of the other mAChR sub-types in heart cardiac muscle (Caulfield and Birdsall, 1998). M_2 may be involved in shivering responses as oxotremorine-induced tremors were ablated in M_2 KO mice and furthermore, M_2 receptors found in the hypothalamus have also been implicated in the regulation of body temperature (Gomeza et al., 1999). Evidence of another role for M_2 receptors found at nocioceptors in skin tissues has been demonstrated by Bernardini et al (Bernardini et al., 2001). These authors also showed M_2 KO mice had reduced sensitivity to intrathecal and intra cerebral ventricular oxotremorine. In hot plate tests M_2 deficient mice did not show muscarine induced desentisization of pain impulses as opposed to M_4 deficient mice (Bernardini et al.). Stimulation of autoreceptors at cholinergic nerve endings allows acetylcholine to control its own release. Zhang et al (Zhang et al., 2002a) showed that M_2 receptors were responsible for the auto-inhibition of ACh in the mouse

hippocampus and cerebral cortex regions of the brain. Regulation of ACh release is fundamental to processes such as cognition and locomotor control and as such this information is of great clinical importance and has relevance to Alzheimers and Parkinsons disease.

M_3 receptors are also located in various regions of the brain and peripheral organs and tissues that are innervated by the parasympathetic nervous system. They perform actions associated with glandular function and regulation of smooth muscle contraction, particularly in the gut. A striking feature of M_3-deficient mice, observed by Yamada et al (Yamada et al., 2001b) was their significant loss of body mass accompanied by reductions in serum leptin and insulin levels as a result of reduced food intake. Expressed at relatively high levels in the hypothalamus, M_3 receptors may be responsible, in part, for the regulation of appetite. Regulation of salivary secretion has also been attributed to M_3 receptors found in the salivary glands. Although Yamada et al. (Yamada et al., 2001b) found that pilocarpine induced salivation was only significantly (50%) reduced at the middle concentration of three different dose strengths. Other studies have implicated M_1, M_4 (Bymaster et al., 2003a) and M_5 (Takeuchi et al., 2002) as contributing to mAChR mediated salivation.

M_4 receptors are preferentially expressed in the CNS forebrain (Levey, 1993) and are believed to regulate striatal dopamine release through action on the cell bodies of striatal GABAergic projection neurons (Zhang et al., 2002b). M_4-deficient mice show statistically significant increases in basal locomotor activity and suggest a regulatory role of M_4 receptors on Dopamine D_1 receptor locomotor activity. This highlights the fact that functional interactions of the cholinergic and dopaminergic pathways are important for striatal function and as such its control is relevant to the treatment of Parkinsons disease.

M_5 receptors the last mAChR to be cloned is found in both neuronal and non-neuronal cells are expressed at low levels and until recently little was known about their physiological functions. The discovery of M_5 receptors in peripheral and cerebral blood vessel endothelium, has implicated M_5 receptors as being able to mediate ACh –induced dilation of arteries and arterioles. The vaso-relaxing affect of ACh effects only cerebral blood vessels and not the carotoid or coronary arteries via M_5 mediated dilation, as shown by Yamada et al. (Yamada et al., 2001a). The implications for cerebrovascular disorders are many and as such M_5 receptors are an attractive target for novel therapeutic strategies. M_5 Knockout mice have been shown to change drug seeking behaviours. The conditioned place preference test showed that effects of morphine and opioids were significantly reduced in M_5-deficient mice (Basile et al., 2002). The expression of M_5 receptors in the substantia nigra and the nucleus accumbens is consistent with their role as modulators of dopamine release in the mid-brain and their involvement in the rewarding effects of drug abuse. However the complex neuronal pathways that are involved these modulatory effects remain to be discovered.

In the greater scheme of behavioural mechanisms mAChRs are important biochemically active modulators of synaptic plasticity, cognition, potentiation, pathogenesis and psychosis and further discoveries of their physiological roles in the CNS and peripheral nervous system are likely. For a brief summary of mAChR sub-type localisation and function see table 1.2. The muscarinic receptors are clinically important targets for treatment of schizophrenia (M_4), Alzheimers (M_1 and M_2) and Parkinsons (M_4) disease as well as chronic obstructive pulmonary disease (COPD) (M_1, M_2 and M_3), glaucoma (M_3), urinary incontinence and gastrointestinal mobility (M_2 and M_3) and have also been implicated as being involved in the control of appetite (M_3)

Table 1.2. Summary of Muscarinic Receptor Sub-Types $M_1 - M_5$.

MAChR Sub-Type	M_1	M_2	M_3	M_4	M_5
Predominant Localisation	***BRAIN:*** cortex hippocampus striatum hypothalamus dentate gyrus. ***PERIPHERY:*** sympathetic ganglion salivary glands	***BRAIN*** : Brain stem cerebellum forebrain olfactory bulb amygdala ***PERIPHERY:*** heart, smooth and cardiac muscle	***BRAIN*** : cortex hippocampus . ***PERIPHERY:*** Exocrine and endocrine glands, smooth muscle	***BRAIN*** : basal forebrain striatum hippocampus ***PERIPHERY:*** smooth muscle, vascular endothelia	***BRAIN*** : substantia nigra. striatum. ***PERIPHERY:*** peripheral blood vessels
G-protein coupling	$G_{q/11}$	$G_{i/0}$	$G_{q/11}$	$G_{i/0}$	$G_{q/11}$
Functional Response	M-current inhibition Stimulation of sympathetic ganglia Activation of MAP kinase Mediation of hippocampal oscillations	Activates K^+ channels Inhibition of Ca^{2+} channels reduces cytosolic cAMP decreased heart rate. decrease neuro-transmitter release (pre-synaptic)	Smooth muscle contraction. Glandular secretion. Decrease neuro-transmitter release (pre and post synaptic).	Activation of K^+ channels Inhibition of Ca^{2+} channels Reduction of cytosolic cAMP Inhibition of neurotrans-mitter release.	Facilitating dopamine release. Reduction of addictive effect of morphine. Mediates ACh-induced dilation of cerebral arteries
Effectors & Second Messengers	PLC IP_3 DAG Ca^{2+} / PKC	Adenylyl Cyclase cAMP(-) Ion Channels K^+ Channels	PLC IP_3 DAG Ca^{2+} / PKC Ion Channels	Adenylyl Cyclase cAMP(-)	PLC IP_3 DAG Ca^{2+} / PKC
Chromosomal Localisation	11q12-13	7q35-36	1q43-44	11p12-11.2	15q26
No. Amino Acids in Protein Humans/Rat	460/460	466/466	590/589	479/478	532/531

Legend: ***PLC*** (Phospholipase C), ***IP_3*** (Inositol 1, 4, 5 triphosphate) ***DAG*** (Diacyl glycerol), ***PKC*** (Protein Kinase C)

1.6 Muscarinic Acetylcholine Receotor Activation

M_1, M_3 and M_5 mAChR subtypes activate the G_q/G_{11}, class of G-proteins stimulating phospholipase C_β isoforms to break down inositol 4,5 bisphosphate (PIP_2). Breakdown of PIP_2 liberates inositol triphosphate (IP_3) that mobilises intracellular calcium and diacylglycerol that in turn stimulates protein kinase C, leading to effects including modulating slow potassium and calcium conductances. Depletion of PIP_2 inhibits the KCNQ/M (Kv7) potassium channel that modulates the M-current leading to increases in repetitive action potential discharges. M_2 and M_4 mAChRs couple primarily to G-proteins of the G_i and G_o class distinguishing the even numbered mAChRs from the odd numbered sub-types. The activation of αG_i inhibits adenylyl cyclase (Nasman et al., 2002). The β and γ sub-units activate fast inward rectifier potassium channels and inhibit voltage sensitive calcium channels. Active mAChRs are phosphorylated by specific kinases, promoting the binding of arrestins, thus nucleating complexes which themselves can activate multiple kinase cascades (Hamilton et al., 1997). Some of the effector proteins and the inositol phosphate signalling cascade can be seen in figure 1.9.

Current theory suggests that the inactive ground state of mAChRs is dependent upon specific interhelical interactions. The residues L116 (TM3), F374 (TM6) and N414 (TM7) supported by S120 (TM3) and Y418 (TM7) have been proposed as providing a network of Van der Waals and hydrogen bond interactions that help to selectively stabilise the ground state of the M_1 mAChR. The mutation to alanine of these residues decreases receptor stability, increases agonist affinity and induces agonist-independent basal signalling activity especially for the L116A mutant. (Lu and Hulme, 2000). Mutations that produce constitutively active mAChRs have also been reported by Spalding (Spalding and Burstein, 2001) and Schmidt (Schmidt et al.2003). The binding of the agonist is predicted to disrupt these interhelical interactions creating a new set of interactions that stabilize the activated conformation of the receptor. It is believed that it is the closure of a series of binding site aromatic residues (see below figure 1.11)

around the tetramethylammonium head group of acetylcholine that transduces binding energy into the energy required to rearrange the ground state network of H-bonds. Closure of the aromatic cage around the ACh head group is predicted to precipitate the re-alignment of TM6 and TM7 relative to TM3 into the active conformation (Hulme et al., 2003). The disruption to ground state interactions caused by closure of aromatic residues around ACh is likely to result in the movement of TM6 and TM3. This mobilisation may precipitate outward movements of the surrounding helices leading to the appearance of buried residues that are able to associate with a G-protein heterotrimer. This is a possible mechanism to describe the conformational switch that converts the inactive receptor into an activated state with increased affinity for G-protein (Hulme et al., 2001).

Structural studies of rhodopsin (Li et al., 2004 ; Okada et al., 2002) have highlighted the importance of a water mediated hydrogen bonding network connecting TM2, TM3, TM6 and TM7 that is re-organised to produce the active conformation of the receptor. It has also been shown using alanine scanning mutagenesis (Hulme et al., 2003; Lu et al., 2001) that central to the activation of muscarinic receptors is the rearrangement of a H-bond network involving Asp71 that links TM2 to TM1 via Asn 43. Although these residues are important for stabilisation of the ground state they appear to have a dual role because they are also important for activation of the receptor. It is probable that the highly conserved NSXXNPXXY motif in TM7 is centrally involved in the conformational change that allows for a rearrangement of contacts to stabilise the activated state. The re-orientation of Tyr 418 may transmit the activated conformation of the receptor to helix 8 which lies perpendicular to the lipid bi-layer and is involved in the coupling of the activated receptor to a G-protein. Another residue critical for receptor signalling is Arg 123, again a highly conserved residue in the 'DRY' sequence in the I2 loop of the rhodopsin family of receptors, forms a charge-stabilised hydrogen

bond with Glu360 (conserved in monoamine receptors and rhodopsin). Mutation of the Glu360 residue produces constitutively active receptors, highlighting the constraining nature of this interaction in the native receptor (Högger et al., 1995).

Using electron paramagnetic resonance measurements, Farahbakhsh and Klein-Seetharaman and co-workers (Farahbakhsh et al., 1995; Klein-Seetharaman et al., 1999) studied the spin-spin interactions of nitroxide spin labels that were attached to the cytoplasmic loops and helix termini of rhodopsin. Their studies revealed that activation of the receptor causes a clockwise rotation of TM6, relative to the cytoplasmic end of the receptor and an outward movement relative to TM3. Dunham and Farrens (Dunham and Farrens, 1999), using a fluorescence spectroscopic approach in conjunction with PyMPO-maleimide cysteine mutant reactivity experiments, provided further evidence that a conformational change at TM6 is characteristic of rhodopsin activation. A fluorescence spectroscopy study by Jensen et al on the β_2 Adrenergic receptor (Jensen et al., 2001) added further evidence that an outward movement of the cytoplasmic region of TM6 follows agonist induced activation. Upon activation, helix 8, lying parallel to the lipid membrane and perpendicular to the transmembrane helices, also undergoes a conformational movement. Movement of helix 8 of the rhodopsin receptor uncovers a crevice between TM7 and H8 that only becomes accessible to a monoclonal antibody upon light induced activation (Abdulaev and Ridge, 1998). The monoclonal Ab binds to an epitope that includes Tyr 418 part of the highly conserved NPXXY motif, characteristic of rhodopsin-like GPCRs, believed to be critical for G-protein activation. For a graphical description of the relative movements associated with receptor activation (see figure 1.10. panel a).

G-protein contact residues are located at the cytoplasmic end of TM3 TM5, TM6 and TM7 where they face inwards, away from the membrane. The intra-cellular loops I2 and I3 and Helix 8 also harbour G-protein contact residues. An alanine scanning

mutagenesis study (Lee et al., 1996) found that a series of conserved positively charged residues located in the I3 loop of the M_1 mAChR, ($K^{361}K^{362}AAR^{365}$) were important for maximal agonist activity. Another study of M_2 receptor mutants co-expressed with the M_1, M_3 and M_5 specific $G\alpha_q$ sub-units (Kostenis et al., 1997) identified the same region as conferring selectivity to the coupling of either $G\alpha_{q/11}$ to M_1,M_3 and M_5 mAChRs or $G\alpha_i$ to M_2 and M_4 receptors. The selective coupling of either $G\alpha_{q/11}$ or $G\alpha_i$-proteins to mAChR's seems to be determined by the sequence in the I3 loop and TM5 as shown below highlighted in yellow.

	I3 LOOP ***TM5***	
M_4	–E R K V T R T I F A I L-	} Couple to $G\alpha_i$
M_2	-E K K V T R T I L A I L -	
M_1	–E K K A A R T L S A I L	} Couple to $G\alpha_{q/11}$
M_3	-E K K A A R T L S A I L	
M_5	- E K K A A R T L S A I L	
Rho	-E K E V T R M V I I M V	Couples to Transducin

Interestingly the specific interaction of $G\alpha_{q/11}$ with M_1,M_3 and M_5 mAChRs and $G\alpha_i$ with M_2 and M_4 receptors can be reversed by switching just three amino acids at the C-terminus of the G-protein (Conklin et al., 1993) including a glycine residue that is thought to be important for specifying G-protein coupling interactions. Later mutagenesis studies of α-transducin (Onrust et al., 1997) and a yeast Gα sub-unit (Kallal and Kurjan, 1997) predicted that a 45-amino acid sequence in the C-terminal of the Gα sub-unit form a surface that interacts with cytoplasmic domains of the receptor. Once the 2 angstrom resolution X-ray crystallographic structure of a G-protein heterotrimer was solved (Lambright et al., 1996) these residues mapped to the α4-β6 loop, the β6 strand and the α5 helix of the C-terminal region of the Gα sub-unit (see figure 1.10 panel b). In addition to these key contact sites other receptor-G-protein interactions are important to anchor the G-protein to the receptor. For example another

study using an environmentally sensitive fluorophore identified helix 8 as interacting with the βγ sub-units of transducin (Phillips and Cerione, 1992; Phillips et al., 1992) which also appear to enhance membrane binding of the α sub-units (Clapham and Neer, 1997). The binding site for Helix 8 may lay between blades 1 and 2 of the so-called β-propellor proximal to the farnesylated C-terminus of the γ sub-unit and the N-terminal helix of the α sub-unit. The more structurally diverse βγ sub-units may confer added selectivity to receptor/G-protein coupling. For full reviews of G-protein-receptor coupling see (Clapham and Neer, 1997; Wess, 1998).

In summary, activation of muscarinic receptors may occur by the rupture of Wan der Waals contacts and re-arrangement of a specific hydrogen bonding network caused by the closing of the aromatic cage around the ACh head group. This could lead to mobilisation of the TM helices, in particular TM3 TM6 and TM7, resulting in the exposure of epitopes required for G-protein interaction. Specific residues in the I3 loop appear to confer the selective characteristic epitope that can discriminate which class of G-protein binds to which receptor. Structural elements of the G-protein provide a surface that allows both specific interaction and anchoring points that enables the receptor in the activated state to relay an agonist induced signal into an activated G-protein.

Figure 1.9 Calcium Ion Release via the Activation of Muscarinic Receptors

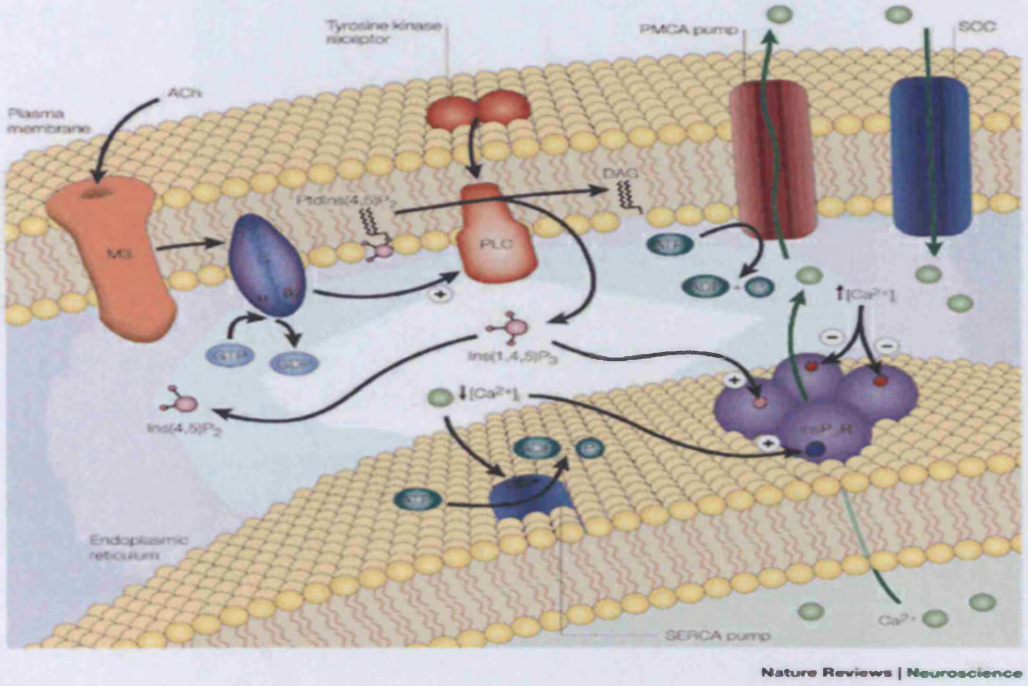

The figure shows some of the signalling pathways initiated by the activation of muscarinic receptors. The receptor depicted in the figure is the M_3 sub-type, but the pathway for M_1 and M_5 sub-types is analogous. Upon activation the release of the G-protein sub-units stimulates phospholipase C that in turn catalyses the breakdown of PIP_2 into IP_3 and diacylglycerol (DAG). IP_3 stimulates the release of calcium ions from the intracellular store in the endoplasmic reticulum and influx through the cell membrane. *Image taken from Nature reviews neuroscience vol 2 p 387-396* (Clapham, 2001)

1.10. Receptor G-protein Interactions

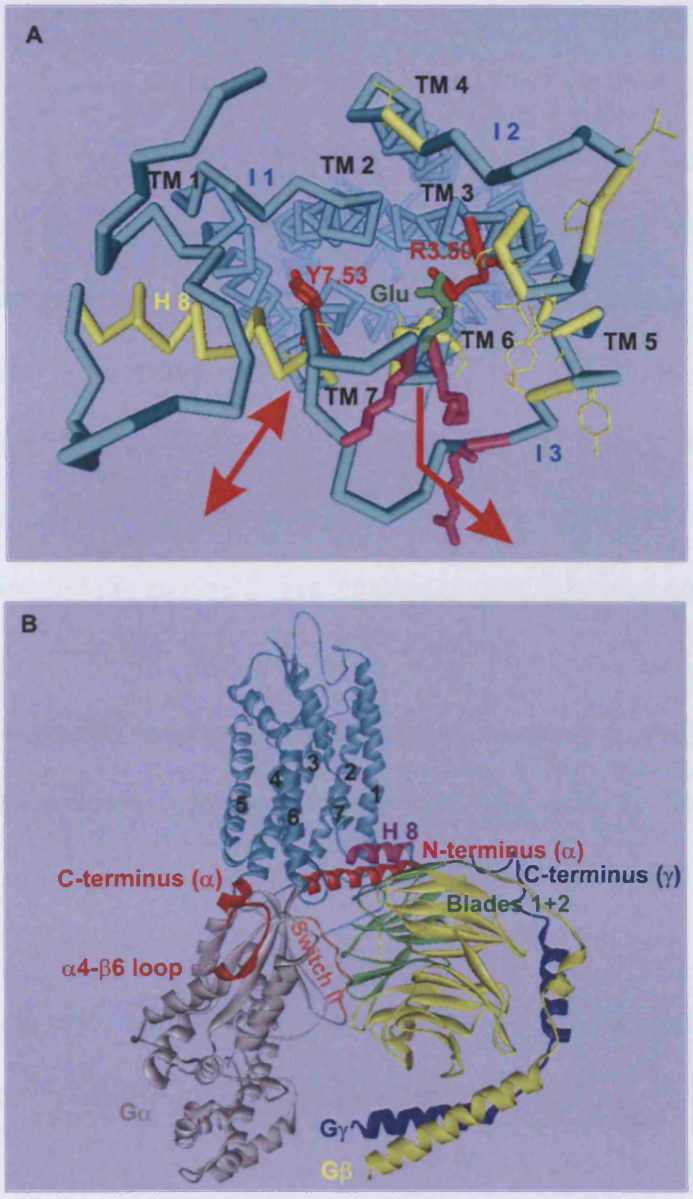

a) G-protein recognition sites on the M_1 mAChR viewed from the cytoplasmic surface. Residues with a positive charge on the I3 loop are shown in magenta and correspond to residues involved in G-protein coupling. Potential G-protein contact residues are highlighted in yellow. The completely conserved Arg at 3.50 (R123 in M_1) is idicated in red. Arrows indicate the relative outward movement of helices 6, 7 and 8 upon receptor activation. **b)** A theoretical model of the rhodopsin-transducin(G-protein) complex. Contact with the recptor is believed to be through the N and C-terminus of the Gα sub-unit.(shown in grey) between the α4-β6 loop. The Gγ (blue) and Gβ (yellow) sub-units of the transducin trimeric complex are also shown. Figure courtesy of Lu et al. (Lu et al., 2002).

1.7. The M_1 mAChR Transmembrane Binding Site

In rhodopsin, the ligand 11-cis-retinal, which acts as an inverse agonist, is covalently immobilised in the binding pocket. Photoisomeration of this molecule to the trans-form activates the receptor. By contrast, it is the binding of an exogenous ligand to a binding pocket which activates or inhibits the other receptors in the same class. The natural agonist for muscarinic receptors is acetylcholine. ACh is a ubiquitous neurotransmitter molecule, secreted from nerve terminals in the CNS and parasympathetic post-ganglionic neurons. Affinity labelling and alanine scanning mutagenesis studies {Lu, 2001; Hulme. E.C, 2003 #183; Kurtenbach, 1990) have revealed the binding site for N-methylscopolamine (NMS) and ACh. The binding pocket is located approximately one third of the way down the transmembrane helical domains. The most important residues, whose mutation gave greater than 30-fold reduction in ACh affinity in the ground state of the receptor, have been shown to be:- Asp 105, Tyr 106, Tyr 381, Tyr 404 and Tyr 408 of TM's 3, 6 & 7 respectively (see figure 1.11 a).

Many of the amino acids participating in the binding site for the synthetic muscarinic antagonist N-methylscopolamine (NMS) have been established. The important side chains for NMS binding were revealed to be those of; Asp 105, Tyr 106, Tyr 381, Asn 382, Tyr 404 and Tyr 408 (See figure 1.11 b). The polar head group of the NMS molecule is believed to fit into a charge-stabilised aromatic cage. Mutagenesis studies suggest that the positively charged head group of ACh binds in a similar manner to that of NMS but that the side chain of ACh does not extend as deeply into the TM region. In fact alanine substitution of Val 113 and Phe 374, located further down the TM helices, reduced the binding affinity of NMS more than 10-fold, not only did not reduced but actually increased the binding affinity of ACh (Hulme E.C, 2003). Residues homologous to those involved in ACh and NMS binding are found in other cationic amine receptor family members (Shi and Javitch, 2002) supporting the view that

particular sequence positions are critical for ligand binding and consequent receptor activation. There may be other aspects of ligand binding that must also be considered. Some residues may form part of an entrance channel into the binding pocket. In this study Asp 99 is hypothesised to be just such a residue. Residues of the 2nd extracellular loop of mAChRs may also be involved in ligand contact, by analogy with residues of the rhodopsin E2 loop.

Work in this laboratory has so far concentrated on the TM domains of the M_1 mAChR. However the X-ray crystallographic structure of rhodopsin reveals that the extracellular domains are folded into a compact structure. A key element of this is the 2nd extracellular loop (E2 loop) which folds into a β-hairpin and penetrates into the binding pocket, located in the TM domains, where it is stabilised by the conserved disulphide bond. The analogy commonly used is that the E2 loop caps the binding pocket, acting as a lid to hold in the bound ligand. In rhodopsin residues of the E2 loop form part of the retinal binding site. The question is:- are the homologous residues in the muscarinic receptors also functioning as part of the binding site?

Residues involved in the binding of NMS are in very similar positions in the TM regions of the M_1 mAChR as the residues of rhodopsin, which bind 11-cis-retinal. However this may not be true for all muscarinic ligands. Despite the similarity of their pharmacological actions different ligands may have different modes of binding. For example the antagonist 3-quinuclidnyl-benzilate (QNB) has a chemical structure analogous to NMS (see figure 2.1), but the binding affinity of QNB is not affected by replacement of Tyr 381 with alanine (Ward et al., 1999a). In contrast the replacement of this residue greatly reduces the affinity of NMS for M_1 receptors.

Figure 1.11. M_1 Muscarinic Receptor Model Showing Predicted Ligand Binding Sites for Acetylcholine & N-Methylscopolamine

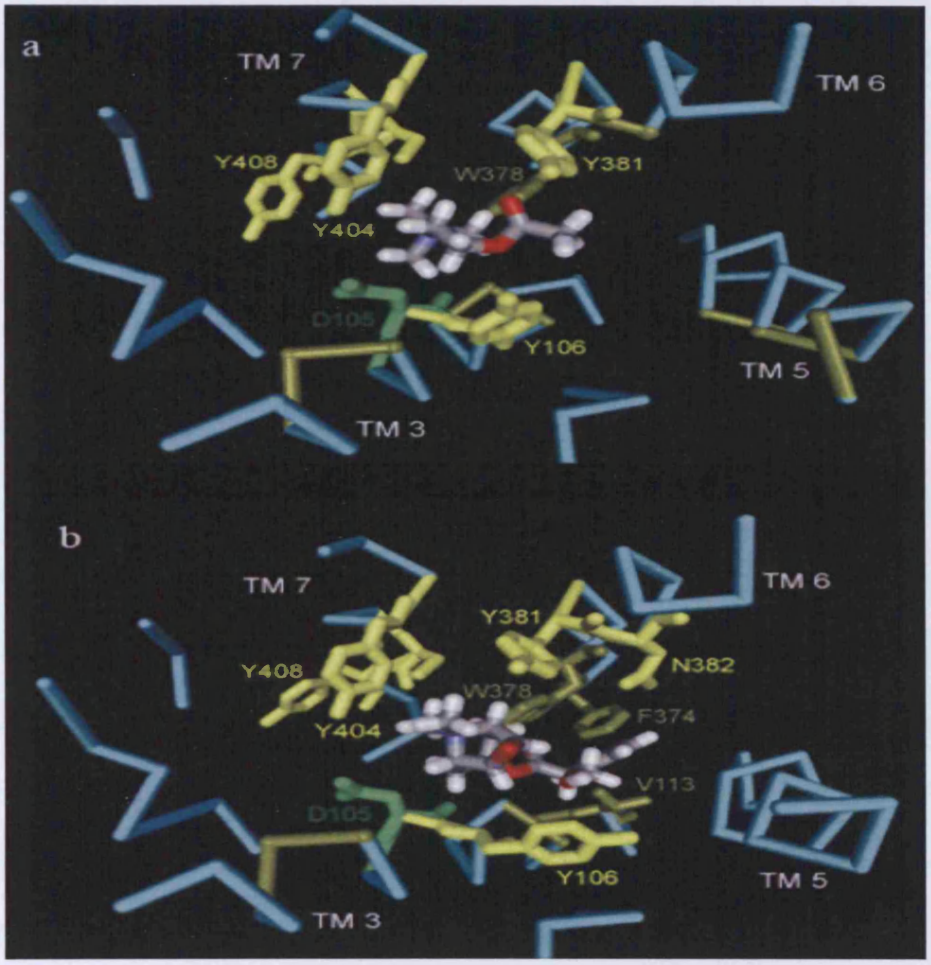

Alanine scanning mutagenesis (ASM) studies have suggested many of the residues in the transmembrane domain involved in the binding of acetylcholine **a)** and N-Methylscopolamine **b)** Residues involved in the binding of the two molecules show some overlap. The positively charged head groups of both ACh and NMS are stabilised in an aromatic cage within the binding pocket. ACh has a shorter side chain which appears not to extend as deeply into the binding pocket as does the bulkier side chain of NMS. The phenyl ring of NMS is predicted to lie close to Asn 110, Val 113 and Phe 374 as the substitution of these residues in ASM studies reduced the affinity of the receptor for NMS by approximately 10-fold (Hulme et al., 2003; Lu and Hulme, 1999; Lu et al., 2001)

1.8. The Second Extracellular Loop

One of the most striking features of the second extracellular loop (E2 loop) modelled on the structure of rhodopsin is that it dives down into the transmembrane domains forming two beta strands (β3 & β4). The sequence alignment for the E2 loop in both rhodopsin and the five mAChR sub-types are illustrated in table 1.3 and shows the position of the β_3 & β_4 strands in relation to the rest of the loop. In bovine rhodopsin one of these strands contacts retinal (Palczewski et al., 2000). It may be the case that the E2 loop is involved in agonist and/or antagonist recognition in small molecule aminergic receptors such as those of the muscarinic class. Evidence for a direct role for the E2 loop of mAChRs in ligand binding and receptor activation is sketchy. There is however evidence that the E2 loop of the dopamine D2 receptor (another small molecule aminergic receptor) does indeed line the binding site crevice and plays a role in ligand binding specificity (Shi and Javitch, 2004). Whereas the residues involved in ligand binding in the TM domains of rhodopsin-like GPCRs are relatively well conserved, the extracellular loops exhibit greater variation. This leads to the hypothesis that the E2 loop in particular may offer a greater variety of ligand contacts, thus providing innate ligand specificity for receptor subtypes.

Further evidence for the involvement of the E2 extracellular loop in ligand contact has been provided by Wurch and colleagues (Wurch et al., 1998) using chimeric human 5-hydroxytryptamine receptors (5-HT_{1D} & 5-HT-_{1B}). Interchanging the E2 loops of one subtype with another exchanged the specificity for ketanserin (a 5-HT selective antagonist), implicating the E2 loop in the binding of ketaserin. In a very similar study, three adjacent residues, G196, V197 and T198 of the 2nd EC loop in β_1-Adrenergic Receptors were determined to significantly change antagonist binding profiles (Zhao et al., 1996). These authors hypothesise that large antagonists bind to the surface of the β

$_1$-adrenergic Receptor via the E2 loop and extracellular TM 5 residues, in contrast to smaller agonist molecules that bind within the TM binding pocket.

Leppik et al. have explored the possibility that larger allosteric antagonist molecules, such as gallamine, bind to the surface of mAChRs via the extracellular loops (Leppik et al., 1994). Gallamine allosterically modulates the binding of classical muscarinic ligands, showing selective binding with greater affinity at M_2 mAChRs than at M_1. Substituting the acidic EDGE sequence in the E2 loop of the M_2 subtype with the homologous uncharged LAGQ sequence of the M_1 subtype led to an 8-fold reduction in affinity for gallamine. Inserting the EDGE sequence into the M_1 subtype gave an increase in gallamine affinity. This implicates the E2 loop, specifically the acidic residues, in the binding of the allosteric antagonist gallamine to the M_2 mAChR.

Only one study has been performed that looked extensively at the 2nd extracellular loop of the M_1 mAChR subtype. Matsui et al conducted agonist (ACh) and antagonist (NMS) affinity binding studies on alanine substitution mutants of eight residues in the E2 loop of the M_1 mAChR. These were: - Trp 164, Gln 165, Gly 169, Arg 171, Thr 172, Gln 181, Phe182 and Ser 184. The charged and polar aromatic residues, which are conserved in the different sub-types, formed part of a larger set that were potential candidates for the binding of allosteric ligands. NB from this point on when talking about residues or mutations used in this study the single lettetr amino acid code will be used for the sake of simplicity.

Overall these mutations had little effect on the expression of the receptor or on the affinity of agonist or antagonist binding. A small decrease in affinity was observed for acetylcholine for the W164A mutant, while Q181A showed a small increase in affinity for acetylcholine. Similarly, the binding of gallamine was largely unaffected to either

occupied (with ligand) or unoccupied mutated receptors. In contrast, mutations W91A and W101 in the E1 loop and W400A and Y404A of the E3 loop had a much greater impact on the affinities of both acetylcholine and N-methylscopolamine and also on the allosteric kinetics involved in gallamine binding (Matsui et al., 1995).

The E2 loop of the M_1 mAChR contains 22 amino acids and 12 of the 22 residues are conserved throughout the muscarinic family of receptors. There are two residues fewer in the E2 loop of rhodopsin at the position of E170 and R171 in the M_1 mAChR. Based on the rhodopsin homology model there may also exist a β3 and β4 strand formed by residues N-terminal and C-terminal to the conserved cysteine at position 178 (see table 1.3). As in nearly all GPCRs there is a disulphide bond anchoring the E2 loop to the TM helices. In the case of the M_1 receptor this S-S bond is formed between C98 at the top of Helix 3 and C178 in the E2 loop. The precise nature of the E2 loop structure in the mAChRs is still in doubt and investigations of its role in ligand binding and function is the purpose of this study and as such is discussed in much more detail in the introduction, discussion and conclusion sections of the results chapters presented below. A homology model of the E2 loop showing the relative positions of the residues to be analysed in this study is shown below in figure 1.12

Figure 1.12 E2 Loop Residues of the M_1 mAChR

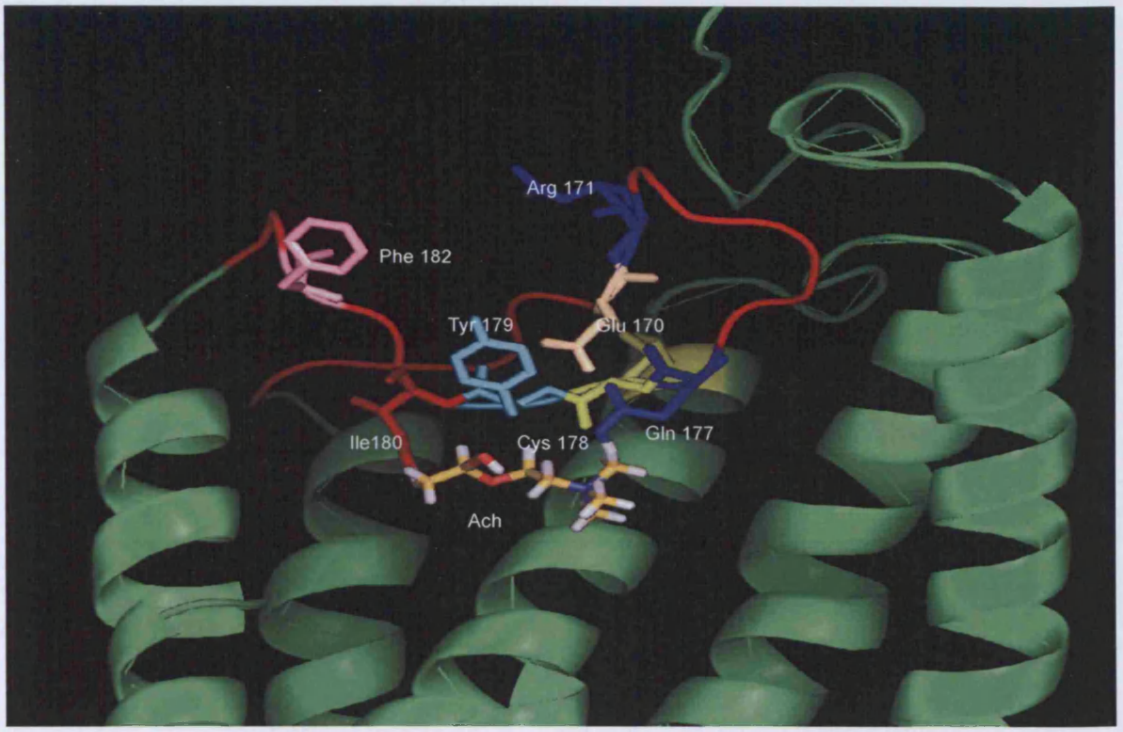

The figure highlights the residues of the E2 loop of the M_1 mAChR mutated to alanine in the present study. Acetylcholine is placed in a position approximating its true location in the ligand binding pocket. The E2 loop residues were positioned based on the rhodopsin homology model and then energy minimised to allow for the different properties of the individual amino acids. The figure serves to illustrate the potential for ligand contact residues being present in the E2 loop. However, this model may require refinement subsequent to the experimental data presented below.

Table 1.3. Sequence Alignment for the E2 Loop in Rhodopsin and Muscarinic Acetylcholine Receptors

The table shows the sequence alignment of the five muscarinic sub-types compared to the E2 loop sequence from bovine rhodopsin, stretching between two highly conserved proline residues (green) at the tops of TM4 and TM5, from which the muscarinic homology models are derived. Highlighted with blue arrows are the residues that form the β3 and β4 strands. Residues highlighted in red indicate residues mutated to alanine in this study. The highly conserved cysteine residue that forms the disulphide bond is shown in yellow. Compared to rhodopsin the muscarinic receptors have extra two residues in the E2 loop, in M_1 they are Glu and Arg, in M_2 Val and Arg and in M_3, M_4 & M_5 Lys and Arg. These extra residues form a distinctive bulge in the E2 loop that is not present in the rhodopsin loop.

	β_3 strand →		β_4 strand →		
Bovine Rhodopsin	PPLVGWSRYI	PE--GMQCSC	GIDYYTPHEETNNES	FVIYMFVVHFI	IPLI
M_1_RAT	PAILFWQYLV	GERTVLAGQC	YIQFLSQ-----PII	TFGTAMAAFY	LPVTVMCT
M_2_RAT	PAILFWQFIV-	GVRTVEDGEC	YIQFFSN-----AAV	TFGTAIAAFY	LPVIIMTV
M_3_RAT	PAILFWQYFV	GKRTVPPGEC	FIQFLSE-----PTI	TFGTAIAAFY	MPVTIMTI
M_4_RAT	PAILFWQFVV	GKRTVPDNQC	FIQFLSN-----PAV	TFGTAIAAFY	LPVVIMTV
M_5_RAT	PAILCWQYLV	GKRTVPPDEC	QIQFLSE-----PTI	TFGTAIAAFY	IPVSVMTI

1.9 Project Aims-

Overall, the role of the 2nd extracellular loop of the M_1 mAChR is still to be conclusively determined. Studies on other small molecule aminergic receptors seem to suggest that the E2 loop does indeed function to add selectivity and provide contact residues for the binding of ligands. This study will attempt to provide further evidence to ascertain the function of the 2nd extracellular loop of the M_1 muscarinic receptor and by association the other 5 subtypes, by attempting to answer the following questions

1). Are there any residues in the E2 loop that are critical to, or involved in, the binding of various agonists, antagonists or allosteric modulators, either internally or exofacially to the receptor?

2). Does the E2 loop function as a 'cap' over the ligand binding pocket, by making contacts with the bound ligand?

3). Do the cysteine residues that form the disulphide link between the E1 and the E2 loop contribute in any way to the binding of ligands?

4). Are there any residues of the E2 loop that are important in the activation of the receptor or maintaining the receptor in the deactivated state?

5). What residues, if any, might be involved in the binding of truly M_1 selective ligands?

6). Can we refine the M_1 mAChR model of the E2 loop based on the results produced in this study?

The main approach to understanding the role of the E2 loop in M_1 mAChRs in this study, is to use the technique of alanine scanning mutagenesis, effectively replacing individual residues of the E2 loop with alanine and observing the affect of the mutations on receptor expression, ligand binding, ligand dissociation and receptor activation. As with all mutagenesis studies the effect of a mutation on binding a ligand is open to interpretation. Does the mutation affect the binding of the ligand directly, or is the difference in affinity observed due to an indirect conformational change? Therefore the experimentalist must draw on a range of information and structural insights when interpreting the results. For instance, a large (>100-fold) reduction in the affinity of an antagonist molecule may be compatible with a direct (first shell) interaction of the mutant side chain with the ligand molecule. A smaller effect may indicate a conformational perturbation (second shell effect). Nevertheless, without a definitive structure of the M_1 receptor, alanine scanning mutagenesis provides the best method to understand the structural characteristics of the E2 loop and its function in the wild type receptor.

In addition to the selected E2 loop amino acids, mutations of three other non-E2 loop mutations will be analysed. They are: - D99A, a residue believed to be important for the channelling of ligands into the binding pocket and F197A and W378A believed to be important for the binding of NMS. These last two residues are located at the base of the binding pocket but their significance for antagonist and agonist binding needs to be confirmed. In our study I hope to clarify how all of these residues function in the structure and activation of the M_1 mAChR. In the previous study by Matsui et al (Matsui et al., 1995) a complimentary group of residues of the E2 loop were mutated to alanine and general ligand binding characteristics were assessed. However no functional data was collected in that study. To redress this omission PI assays were performed on seven of the Matsui E2 loop mutants in this study to provide a more comprehensive

analysis of the role of E2 loop residues in receptor function. In the bigger picture this research aims to provide information that may be useful in the design of M_1 selective ligands that in the future may alleviate certain diseases associated with the muscarinic cholinergic system, such as Alzheimers, epilepsy, chronic pain and smooth muscle disorders.

Chapter 2.

Materials And Methods

2.1 Materials

The pCD expression vector containing the entire coding sequence for the rat M_1 mAChR was originally a gift from Dr. NJ. Buckley (Bonner et al. 1987), formerly of NIMR. The construct was further modified in this laboratory by the insertion of unique restriction sites and is now denoted pCDE The QuikChange™ double-stranded site-directed mutagenesis kit was supplied by Stratagene. The Big Dye™ Terminator v1.1 Cycle sequencing kit was purchased from Applied Biosystems and Long Ranger gel solution was supplied by Flowgen. Pellet Paint™ co-precipitant was provided by Novagen. Plasmid mini and maxi preps were supplied by Qiagen, as were gel extraction and min elute gel extraction kits. Restriction endonucleases *Nhe I* & *Sac I* were provided by Roche. The Fast-Link™ ligation kit was supplied by Epicentre Technologies. SEA KEM Gold™ agarose gel was supplied by FMC Bioproducts. Bacterial growth media were supplied by media dept at NIMR. All other chemicals used were supplied by Sigma Aldrich, unless otherwise stated.

COS-7 cells (African green monkey kidney cells) came from The European Collection of Cell Cultures (E.C.A.C.C.). Tissue culture reagents were from GIBCO BRL Laboratories. Atropine, [^{3}H]-(-)-N-methyl scopolamine 84 Ci.mmol^{-1} and (-)-Quinuclidinyl-[phenyl-^{3}H]-Benzilate 48 Ci.mmol^{-1} were from Amersham Biosciences. National Diagnostics supplied liquid scintillation solution. All other reagents were purchased either from Sigma Aldrich or Promega. AC-42 was a gift from Accadia Pharmaceuticals inc. Oligonucleotides were manufactured and supplied by Sigma Genosys.

Figure 2.1 Structures of Compounds Used for Radioligand Binding Studies

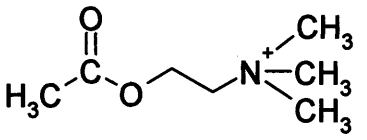

Acetylcholine (ACh)

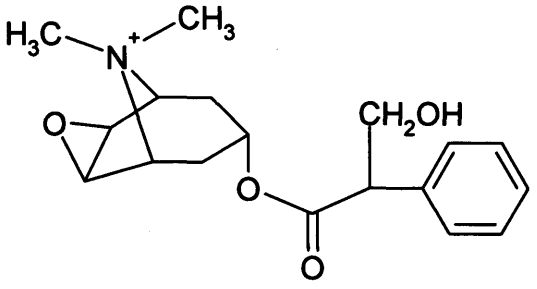

N-Methylscopolamine (NMS)

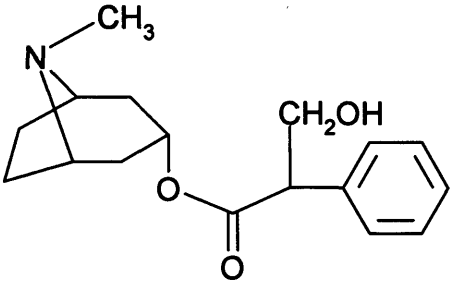

Atropine

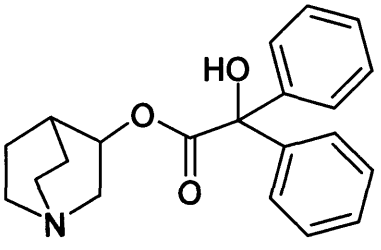

QNB

2.2 PCDE Expression Vector

The entire coding sequence of the rat M_1 mAChR is contained within the pCDE construct (figure 2.2). The coding sequence is under the control of a Simian virus (SV) 40 promoter and polyadenylation sequence, which allows high copy number of replication of the plasmid in COS-7 cells that express the SV40 large T-antigen. The plasmid also carries a pBR322 origin and ampicillin resistance genes as a selective marker and to allow propagation in a culture of *E. coli* cells. The mutations of the E2 loop, TM3 and TM5 used in this study lie between *Sac* I and *Nhe* I unique restriction sites, a relative distance of 950bp.

2.3 Site Directed Mutagenesis

The mutations of the E2 loop and the single mutations in TM3, 5 & 6 were introduced into the pCDE vector using the QuikChange™ mutagenesis Kit. Simply, two oligonucleotides, one forward, one reverse, containing the desired codon change for each individual mutation (see table 2.1) were annealed to the denatured double stranded wild type rM_1 sequence of the plasmid at 55°C, then extended using *Pfu* Turbo DNA polymerase. The syntheses of mutant strands were performed using the cycling conditions shown below.

Process	No. Cycles	Temp°C	Time
Initial Denaturing	1	95	30 secs
Denaturing	12	95	30secs
Primer Annealing	12	55	1 min
Extension	12	68	4.48mins

This creates mutated complimentary strands containing staggered nicks. After temperature cycling the complimentary strands were digested with 1 µL *Dpn* I endonuclease for 1 hour at 37°C, which selectively digests parental, methylated DNA, enriching the mutated complimentary DNA strands ready for transformation of competent *E. coli* which is described below.

2.4 Preparation of Competent *E. coli*

Competent DH5α cells were prepared by a modified version of the Hanahan method (Hanahan, 1983). DH5α stock was streaked onto a L-agar plate and grown overnight at 37°C. A single colony was selected and used to inoculate 100mL of L-Broth and grown to an O.D. of 0.25. The culture was cooled and spun at 4,000rpm, 4°C for 10 min. The pellet was gently re-suspended in 40mL of transformation buffer (30mM KOAc, 100mM RbCl, 10mM $CaCl_2$, 15% (v/v) glycerol), pH 5.8 (acetic acid), filter sterilised) and cooled on ice for 10min. The suspension was re-centrifuged 4,000rpm for 10 min and the pellet re-suspended in 2mL ice cold transformation buffer II (10mM MOPS, 75mM $CaCl_2$, 10mM RbCl, 15% (v/v) glycerol, pH 6.5 (KOH),filter sterilised). 100μL aliquots in Eppendorf tubes were snap frozen on dry ice and stored at –80°C.

2.5 Transformation of Competent Cells

1μL of DNA from the ligation procedure was added to 50μL of competent *E. coli* DH5α cells (thawed on ice), incubated on ice for 30 min, and then heat shocked at 42°C for exactly 45 seconds in Falcon tubes. Then, 500μL of SOC medium (SOB medium containing 1% 2.2M glucose) was added to the cells, which were then incubated at 37°C for 1 hour to allow expression of the ampicillin resistance gene. The culture was then plated out on 50μg/mL ampicillin agar plates and grown overnight at 37°C. Single colonies were picked for sequence analysis between the *Sac* I and *Nhe* I restriction sites to check for the desired mutation and any errors that may have been incorporated into the DNA.

2.6 Preparation of Plasmid DNA

Mini and Maxi scale preparations of the mutant plasmids were performed using the Qiagen Mini and Maxi prep kits. Both kits work using the same principles, only the scale differs. *E. coli* transformed with the mutant plasmids were cultured overnight at

37°C in L-Broth supplemented with 50μg/mL ampicillin. The following day the cells were pelleted and lysed in 0.1M NaOH, 1% sodium dodecyl sulphate (SDS) in the presence of RNAase. RNA was digested and plasmid & chromosomal DNA denatured. Neutralization was performed by addition of KOAc, precipitating chromosomal DNA and cell debris and SDS. Then, ~800μL of sample was loaded onto anion-exchange columns to bind the plasmid DNA in low salt buffer. Chromosomal DNA and cell debris was cleared from the column with a medium salt wash. The plasmid was then washed from the column with a high salt buffer. A sample of the recovered plasmid was run on a 1% agarose gel to check size and efficiency of recovery. For maxi-prepped plasmids purity and concentration were checked spectrophotometrically at 260nm/280nm. A ratio value of 1.8 confirmed that the plasmid was uncontaminated with protein.

2.7 Sub-cloning of Mutant DNA

To circumvent the need to sequence the entire plasmid containing the mutation it was preferable to excise the region containing the insert and re-ligate it back into a correspondingly cut wild type vector. A 950 base pair region containing the mutated sequence was cleaved from the mutated plasmid DNA using the restriction endonucleases *Sac* I and *Nhe* I. The cleaved fragment was purified and identified on a 1% Agarose gel. The gel slice was extracted and the insert recovered and purified using the Qiagen Min Elute™ kit. The gel was dissolved in guanidine thiocyanate (buffer QG) at 55°C to release the insert. The solution was loaded onto an anion exchange column binding the insert. Then a series of washes removed any trace of agarose and finally the insert was eluted in a high salt buffer. The *Sac* I – *Nhe* I region of a wild type plasmid was excised using the same restriction endonucleases and then the vector was gel purified and recovered using the Qiagen Gel Extraction Kit in a method analogous to the recovery of the insert DNA. Then, ~1μg of the mutated insert DNA was ligated to ~0.5μg of the cut vector using the Epicentre Fast-Link Ligation kit. The ligation

reaction was performed at room temperature for 2 hours using T4 DNA ligase and 10mM ATP. Competent DH5α cells were then transformed with 1μL of the ligation reaction mix.

2.8 Sequencing of Mutants

Plasmids from resulting clones containing the desired mutation were identified using the Sanger dideoxy nucleotide sequencing method (Sanger et al., 1977) using Big DyeTM Terminators v1.1. Sample for sequencing were prepared as shown in the table below.

Step	**Action**	
	Reagent	**Qunatity**
1	Terminator ready reaction mix	8μL
	Template DNA	200-500ng (1μL)
	*Sequencing Primers	9.6pmol (1μL)
	ddH_2O	10μL
2	Mix well and spin	
3	Place in Therrmal Cycler	

* Sequencing primers
Forward 5'-GGCCTCCTGTCTCTAGCTACAG-3' (T_m 63.2°C)
Reverse 5'-CCCCTGGCTGTGACCTCTCTCTGAGC-3'(T_m 75.1°C)

Once prepared, samples were transferred to a MWG Biotech Primus 96+ thermal cycler and run as follows. Samples were run for 25 cycles:- 1) rapid thermal ramp to 96°C; 2) 96°C for 10 secs; 3) Rapid thermal ramp to 50°C; 4) 50°C for 5 secs; 5) rapid thermal ramp to 60°C; 6) 60°C for 4 minutes. Samples were then spun briefly. Then 2μL of 2M NaAc and 50mL of 96% ethanol were added to each sequencing reaction and incubated on ice for 20-30 minutes to precipitate DNA. Samples were then spun at high speed (14,000 rpm) for 15-30 minutes to pellet DNA. Supernatent was then aspirated and the pellet was washed with 70% ethanol and re-spun for 15-30 minutes and washed again and allowed to dry for ~30mins befor addition of 4mL of loading buffer (5:1 ration of formamide and 25mM EDTA (pH8.0) blue dextran). Samples were loaded onto and run on a 6 % polyacrylamide gel using the automated ABI 377 DNA sequencing system. Resultant sequences were analysed using DNA Star software, to confirm the presence of

the correct mutated codon and to verify that no aberrant mutations had occurred. Below is an example of sequencing data for the I180A mutant. Highlighted in yellow is the region of mutation. The WT rM_1 sequence (2nd row) shows the I180 codon as ATC and the mutant sequences below are I180A showing the change of codon to GCC.

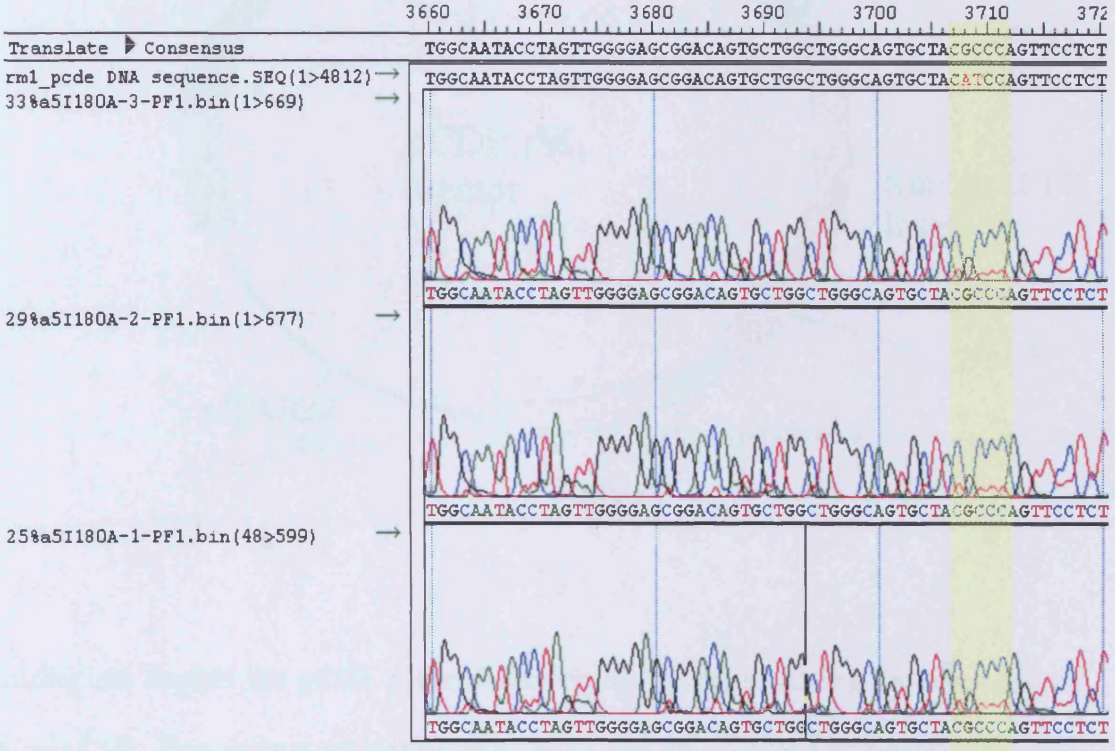

Figure 2.2 The pCDE Expression Vector Containing the rat M_1 mAChR Gene

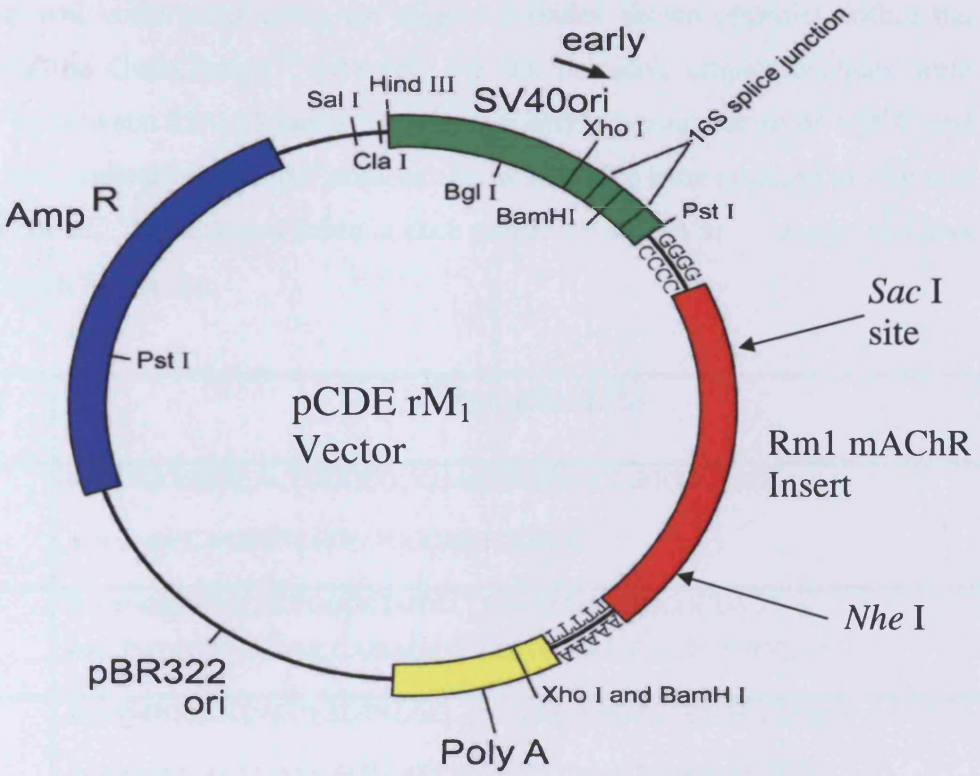

The diagram depicts the pCDE plasmid containing the entire coding sequence for the rM_1 mAChR. Two unique restriction sites *Sac* I and *Nhe* I in the coding region allow cloning procedures without disturbing the expression and consequent function of the translated protein. The ampicillin resistance gene facilitates selection and replication within *E.coli* cells. A high level of expression of the M_1 mAChR in COS-7 cells is driven by the SV40 promoter through interaction with the large T-antigen present in the cell line.

Table 2.1 Mutant Oligonucleotides used for QuikChange Site Directed Mutagenesis Procedure

Each mutant was constructed using the oligonucleotides shown opposite within the parameters of the QuikChange™ protocol. For the protocol, oligonucleotides were required to be between 25 – 45 bases long, have a melting temperature of >75°C and generally a G-C content of 40%. All primers/oligonucleotides were required to start and end with a G or a C. The changed bases in each primer are shown in red and in all cases denote the codon for alanine.

Mutant	Olignucleotide
C98A	For-5'-GGGCACACTGGCCGCCGACCTCTGGCTGGCCCTG-3' Rev-5'-GCCAAGGTCGGCGGCCAGTGTGCCC-3'
D99A	For-5'-GGGCACACTGGCCTGTGCCCTCTGGCTGGCCCTG-3' Rev-5'-CAGGGCCAGCCAGAGAGGGCACAGGCCAGTGTGCCC-3'
E170A	For-5'-GGCAATACCTAGTTGGGGCGCGGACAGTGCTGGCTGGG-3' Rev-5'-CCCAGCCAGCACTGTCCGCGCCCCAACTAGGTATTG-3'
R171A	For-5'-GGCAATACCTAGTTGGGGAGGCGACAGTGCTGGCTGGG-3' Rev-5'-CCCAGCCAGCACTGTCGCCGCCCCAACTAGGTATTG-3'
Q177A	For-5'-CGGACAGTGCTGGCTGGGGGCGTGCTACATCCAGTTCCTCTCC-3' Rev-5''-GGAGAGGAACTGGATGTAGCACGCCCCAGCCAGCACTGTCCGC-3'
C178A	For-5'-CGGACAGTGCTGGCTGGGGCAGGCCTACATCCAGTTCCTCTCC-3' Rev-5''-GGAGAGGAACTGGATGTAGGCGTCCCCAGCCAGCACTGTCCGC-3'
C178N	5'- GCTGGGGCAGAACTACATCCAGTTCCTCTCC-3' 5'-GGAACTGGATGTAGTTCTGCCCAGCCAGC-3'
C98A/C178A	*C98A Mutant vector was mutated again using the **C178A** Oligo*
Y179A	For-5'-GCTGGCTGGGCAGTGCGCCATCCAGTTCCTCTTCC-3' Rev-5'-GGAGAGGAACTGGATGGCGCACTGCCCAGCCAGC-3'
I180A	For-5'-GGCTGGGCAGTGCTACGCCCAGTTCCTCTCCCAACCC-3' Rev-5'-GGGTTGGGAGAGGAACTGGGCGTAGCACTGCCCAGCC-3'

F182A	For-5'-GGGCAGTGCTACATCCAGGCCCTCTCCCAACCC-3' Rev-5'-GGGTTGGGAGAGGGCCTGGATGTAGCACTGCCC-3'
F197A	For-5'-GGCACAGCCATGGCCGCCGCCTACCTCCCTGTCACGG-3' Rev-5'-CCGTGACAGGGAGGTAGGCGGCGGCCATGGCTGTGCC-3'

2.9 Electroporation of COS-7 Cells

COS-7 cells were grown in 30 mL of MEM alpha media supplemented with 10% heat inactivated New Born Calf Serum and 1% Glutamate in 175cm^2 culture flasks at 37°C in 5% CO_2 until confluent. Cells were washed twice in Phosphate Buffered Saline (PBS) buffer then dislodged from the flask using a 5 min treatment with 3.5mL trypsin versene and then transferred in 5mL supplemented media (as above) to a 50mL corning tube and the volume was made up to 50mL. For each mutant transfection 1.5 flasks of cells were pooled. i.e. for the transfection of 4 mutant plasmids 6 flasks of COS-7 cells were pooled. Once collected, cells were spun at 3,000rpm for 3 min at 4°C to pellet. Cells were re-suspended in 50mL serum free media (ice cold, no supplements) then re-spun as previously. Cells were then re-suspended in 0.8mL of ice-cold serum free media and added to a cold cuvette containing 15μg mutant DNA plasmid. The cells (approx 3 x 10^7 per cuvette) were then electroporated using a BioRad Gene Pulser at the optimised setting of 260 volts, 960 microfarads and left to recover for at least 5 min. The cells were then re-suspended in 30mL warm supplemented media and plated onto 10cm diameter culture dishes. Cells were incubated at 37°C for 72 hours in 5% CO_2 in a humidified incubator.

2.10 Preparation of COS-7 Cell Membranes

After incubation, transfected COS-7 cells were washed twice in PBS. 1mL of harvesting buffer (20mM HEPES, 10mM EDTA, pH 7.5) was added to each dish and incubated at 5°C for ≥15min. Cells were then scraped off the surface of the dish using a Teflon scraper and transferred to a glass or a mechanical homogeniser. After approx 20 strokes or 15 secs in the homogeniser cell membranes were transferred to 50mL polypropylene centrifuge bottles and spun at 17,000rpm in a Beckman J-17 rotor to pellet membranes. Membranes were then re-suspended in storage buffer (20mM HEPES, 1mM EDTA, pH 7.5) and further homogenised using a Polytron PT3100 at setting 10-12 for 30 secs.

1mL aliquots were taken then snap frozen on dry ice and stored at –75°C. The protein concentration of each sample was determine by the BCA method (Smith et al., 1985) using 25μL of sample in a 96-well plate format

2.11 N-Methylscopolamine and Quinuclidinyl Benzilate Saturation Binding Assays

For binding assays membranes were prepared as follows. A 1mL aliquot of a membrane preparation was spun at 14,000rpm in an Eppendorf 5415C centrifuge for 10-15 mins. Pelleted membranes were re-suspended in 50mL binding buffer (0.1M NaCl, 20mM NaHEPES, 1mM $MgCl_2$ pH 7.5) to a final concentration of total protein of 10-30μg / mL. The membranes were homogenised at Polytron PT3 100 setting 10-12 for 30 secs. For ^{3}H-NMS saturation binding assays 8 concentrations of ^{3}H-NMS were prepared in binding buffer, to give final assay concentrations (FAC) from 1 x 10^{-11}M – 3 x 10^{-9}M. For ^{3}H-QNB saturation binding assays 8 concentrations of ^{3}H-QNB were prepared in binding buffer to give FACs from 1 x 10^{-12}-3 x 10^{-10}M. 10μL of ^{3}H-NMS or ^{3}H-QNB which were pipetted into polystyrene tubes and 1mL of membrane preparation added. A 1μM atropine sample was prepared to determine non-specific binding. After mixing assays were incubated at 30°C for 2 hours (^{3}H-NMS) or 4 hours (^{3}H-QNB) in order for ligand association with receptors to reach equilibrium. Binding was rapidly terminated by vacuum filtration, using a Brandel cell Harvester, on to Whatman GF/B filter mats. Mats were pre-treated with 0.1%v/v polyethyleneimine for 30 min before use. Filtermats were washed three times with ~4mL ice-cold ddH_2O. Individual filters were punched into 5mL scintillation vials and mixed with 4mL liquid scintillation fluid. The vials were left overnight in a dark cupboard to allow the radioactivity to be extracted. The following day radioactivity was measured using a Wallac 1490 counter. Samples were counted for 5-60 minutes depending on the quality of the data. All ^{3}H-NMS and ^{3}H-QNB saturation-binding assays were repeated at least 3 times, unless otherwise stated. This method was later developed by using the faster cleaner cheaper Tom-tec

method. In principle the assay is the same, except that the binding reactions are conducted in deep 96-well plates. Membranes are harvested onto a 96-sample filtermat which were dried at 50°C for 30min. Instead of using liquid scintillation fluid, a solid scintillation product (meltilex) was then melted onto the filtermat containing the harvested membranes. Radioactivity was counted on a 1450 Microbeta Trilux counter. The counter was pre calibrated by comparison of three binding assays performed on the Brandell and the same assays read on the trilux. The difference between the two sets of repeated data was used to calculate the efficiency of the Microbeta counter.

2.12 Competition Binding Assays

Membranes were prepared as previously described in preceding paragraph. For acetylcholine competition assays a fixed FAC of ^{3}H-NMS of between 3 x 10^{-10}M and 3 x 10^{-9}M was used depending on the measured ^{3}H-NMS affinities of the mutants. A series of dilutions of acetylcholine bromide or other agonist was prepared in binding buffer from stocks made up in binding buffer or DMSO to yield a FAC of 3 x 10^{-8}M up to 3 x 10^{-1}M. Total and non-specific binding (of ^{3}H-NMS) were determined using buffer alone and 1μM atropine respectively. Each acetylcholine or other agonist concentration was performed in quadruplicate. Samples were incubated for 2 hours at 30°C or 4 hours for ^{3}H-QNB. Assays for each mutant were performed in triplicate unless otherwise stated. Procedure for ^{3}H-QNB competition assays performed in the sam way except that [^{3}H-QNB] ranged between 3 x 10^{-11}M and 3 x 10^{-10}M dependant upon particular mutant.

2.13 Atropine Rescue of Poorly Expressing Mutants

In order to enhance expression levels of some mutants (e.g. F197A), which were expressed at low levels in COS-7 cells an atropine rescue procedure was used (Lu and Hulme, 1999). Simply, cells were grown for 24 hours in supplemented α-MEM media. After this the medium was changed to supplemented α-MEM media containing 1μM

atropine. Cells were then further incubated for 48 hours at 37°C. Membranes were prepared in the usual way except an extra three washes were done to ensure complete removal of excess atropine and binding assays performed as previously described.

2.14 Phosphoinositide Turnover Assays

Transfected cells were grown in 12-well plates at 37°C, 5% CO_2 and labelled with 1μCi/mL *myo*-D-^{3}H-inositol after 24 hours. The cells were grown for a further 48 hours allowing incorporation of the *myo*-D-^{3}H-inositol into inositol 4,5 bisphosphate (PIP_2) within the cell. The medium containing the *myo*-D-^{3}H-inositol was removed and the cells were incubated for 30 min in warm Krebs-bicarbonate solution (120mM NaCl, 3.1mM KCl, 1.2mM $MgSO_4$, 2.6mM $CaCl_2$, 10mM Glucose and 25mM $NaHCO_3$, pH 7.4) containing 10mM LiCl (to inhibit inositol phosphatase enzyme), that had been pre-incubated for ~18 hours at 37°C and 5% CO_2 to ensure correct pH. The cells were incubated in this solution for 30 minutes at 37°C 5%CO_2. After incubation adding a series of increasing concentrations of acetylcholine, made up in the Krebs-bicarbonate solution, stimulated the cells to activate. The stimulation of PI hydrolysis was terminated by removal of the agonist containing medium, the addition of 5% ice-cold perchloric acid and incubation at 4°C for 20 minutes. 0.4mL of the lysate was then added to 0.1mL of 10mM EDTA and 0.5mL of a 1:1 ratio (v/v) of tri-n-octylamine and 1,1, 2 trichlorotrifluoroethane (freon) solution. The samples were then vortexed and centrifuged at 4,000rpm for 10 minutes in a Heraeus Megafuge to separate aqeous phase containing phosphoinositides from the non-aqueous phase. Then, 0.3mL of the aqueous upper phase was added to columns containing Dowex AG 1 x 8 resin (formate form dry mesh size 100-200). The columns were washed with 10mL dH_2O, then 25mM NH_4COOH, and finally the ^{3}H- inositol phosphates were eluted with 1M NH_4COOH, 0.1M HCOOH. 1mL of the eluted sample was collected and 10mL Liquiscint scintillation fluid was added. Samples were counted on a Wallac 1409 counter for 10min per sample.

2.15 Dissociation Kinetics

Assays were performed on COS-7 cell membranes, prepared as described above, in deep, 1.2mL 96-well polypropylene plates (Receptor Technologies). 450µL of membranes in binding buffer (0.1M NaCl, 20mM NaHEPES, 1mM $MgCl_2$ pH 7.5) containing mutant or WT receptors were pre-incubated with 10µL of 2 x 10^{-9}M ^{3}H-NMS or 2 x 10^{-9}M ^{3}H-QNB for either 2 or 4 hours respectively in a water bath at 30°C. A reverse time course of dissociation was then performed, by addition of 440µL dissociation mix (pre-prepared in binding buffer) containing a FAC of 2 x 10^{-6}M atropine for dissociation of ^{3}H-NMS or 10^{-5}M unlabelled NMS for dissociation of QNB. Samples were returned to a water bath at 30°C until the addition, at the appropriate time point, of the next volume of dissociation mix. At the final time point reactions were stopped by harvesting the membranes on to a 96-well filter mat, the filtermats were dried at 50°C for ~30mins before the addition of meltilex scintillation wax. Radioactivity was counted on a 1450 Microbeta Trilux counter.

2.16 Data Analysis

Data produced from binding assays was analysed using SigmaPlot™ for windows (Jandel Scientific). Data points were fitted to models using non-linear least square fitting using inverse standard error weighting.

2.16.1. Saturation Binding Data Analysis: The one site model of binding.

Data produced from ^{3}H-NMS saturation binding assays was fitted to a one-site model of binding.

$$A + R \underset{k_2}{\overset{k_1}{\rightleftharpoons}} AR$$

Where R = receptor, A = ligand, k_1 = rate of association constant of the forward rection and k_2 = the rate constant of dissociation for the reverse reaction where the affinity constant is given as

$$K_A = k_1 / k_2$$

$$K_D = k_2 / k_1$$

$$[AR] = K[A][R];$$

where K is the affinity constant governing the binding of the ligand to the receptor.

The concentration of free receptor [R] may be calculated from the equation :

$$[R_t] = [R] + [AR]$$

Where [Rt] = total receptor concentration.

Rearrangement gives:

$$[R] = \frac{[Rt]}{1 + K[A]} \quad (1)$$

And hence:

$$[AR] = \frac{[Rt]K[A]}{1 + K[A]} \quad (2)$$

Data fitted to this model generates estimates of the affinity constant, K and concentration of the binding sites [R_t]. During fitting, ligand concentrations and affinity constants were expressed in the form $10^{\log[A]}$ or $10^{\log K}$ respectively. In saturation binding experiments the analysis program used fitted non-specific and specific binding simultaneously (described by Hulme and Birdsall 1992). This method also takes into account ligand depletion (when a significant proportion of labelled ligand becomes bound to the receptor). In these experiments however, ligand depletion was minimal at <2%. A figure of <10% ligand depletion is acceptable. Values any greater than this might have distorting effects on the fitted data

2.16.2. Competition Binding Assay Data Analysis.

Competition assay data was fitted using the model for the Hill equation:

$$\frac{[AR]}{[Rt]} = \frac{(K_{app}[A])^{n_H}}{1+(K_{app}[A])^{n_H}}$$

R = Receptor, A = Ligand [Rt] = Total receptor concentration,

K_{app} = Apparent affinity constant of the competing ligand;

$^{n}_{H}$ = Hill coefficient.

The Hill equation above shows the direct saturation form of the equation. Data was actually fitted in sigma plot using the following equation, where f = the predicted fit in dpm for y values and produces an inhibition or competition binding curve.

$$f = (bmax\text{-}bns)/(1+10^{(nh(pk+x))})+bns$$

The Hill coefficient is an indicator of how the ligand binds to the receptor. If the value is equal to 1 the competition curve is consistent with the ligands binding to a homogenous set of binding sites. If the value is greater than 1, then there maybe positive co-operativity of ligand binding. Conversely, if the value is significantly less than 1, then negative co-operativity may be occurring or the ligand could be binding to a heterogeneous population of receptors. The apparent affinity constant obtained from competition binding assays using the Hill equation or one site model were corrected to take into account the receptors affinity for the radioligand. This was achieved by using the Cheng Prusoff correction factor (Cheng and Prusoff, 1973). Thus:

$$\text{Log } K = \text{Log } K_{app} + \text{Log } (1+K_{NMS}[NMS])$$

K = Corrected affinity constant of competing ligand.(K_{BIN})

K_{app} = measured apparent affinity constant of competing ligand

K_{NMS} = Affinity constant of [^{3}H]-NMS

[NMS] = Concentration of [^{3}H]NMS radioligand used in the assay.

Competition assay data was fitted to the Hill equation.

2.16.3. Competition Binding Data – Two-Site Model of Binding

Where appropriate data was analysed using a two site model of binding as described by Hulme & Birdsall 1992. The model generates two fractions of binding site, one having high affinity the other having low affinity for the ligand.

$$f = (B\max - BNS)\left(\frac{Fr_H}{1+K_H[A]} + \frac{1-Fr_H}{1+K_L[A]}\right) + BNS$$

[L*] is the concentration of radioligand and Fr_H and Fr_L represent the high and low affinity fraction of affinity states with K_H and K_L being their equivalent affinity constants. The binding constants were corrected for the Cheng Prusoff shift.

2.16.4. The Four Parameter Logistic Function: Analysis of Phosphoinositide Turnover Data

Data from phosphoinositide turnover assays was fitted using a four parameter logistic function based on the Hill equation. (Wells, 1992) and fitted to the following equation.

$$dpm = (dpm_{total} - basal)\frac{(K[A])^{n_H}}{1+(K[A])^{n_H}} + basal$$

where; dpm_{total} = total dpm; basal = basal level of PI hydrolysis; K= apparent association constant; n_H = Hill coefficient

2.16.5. Functional Analysis: Efficacy Calculation

An estimate of the efficacy of agonist to induce a signalling response was calculated using the following equation.

$$e_A = \left(\frac{K_{act}}{K_{bin}(1-basal)} - 1 \right) / \underline{R}_T \quad \text{when Emax ~1}$$

Alternatively when Emax is significantly less than 1 e.g. for a partial agonist or a mutation that reduces maximum signalling the following equation is used to determine efficacy.

$$e_A = \left(\frac{E\max}{1 - E\max} \right) \frac{1}{\underline{R}_T}$$

Where:- e_A = Agonist signaling efficacy parameter; K_{act} = Measured 1 / EC_{50} value for individual mutant or WT sample in each P.I. Assay; K_{Bin} = Previously measured and corrected Acetylcholine affinity constant for individual mutant or wild type; $\underline{R}_T$ = estimate of the effective ratio of total receptor concentration to receptor-accessible G-protein $[R_T]/[RG]$ and for WT over-expression in COS-7 cellsthis ratio has been estimated as 20 i.e. 20 receptors for every G-protein (Lu et al 1997). For mutations, this value was scaled in proportion to the level of expression measured by radioligand saturation assays

2.16.6 Statistical analysis of data.

Experimental data was treated in two ways. In the first instance ligand binding data and functional dose response data for new mutations was compared to well-established control values for NMS, QNB and ACh. Quinn and Keogh (2002) recommend that there "should be no adjustment for multiple testing if the tests represent clearly-defined and separate hypotheses". Wild-type controls were included in virtually all experiments, and gave values not significantly different to previously measured values. Since each new mutant essentially represented an independent comparison, it was considered reasonable

to analyse these results with standard paired t-tests against the matched control values using Excel. For each mutant, the means and SEMs are calculated for the whole group of measurements. The significance levels are given as $P<0.05$, or $P<0.01$. In fact a 1-way ANOVA (Excel) followed by Dunnett's post-hoc test confirmed the significance values.

In the second group of experiments, a series of compounds were compared with one another using a selected set of previously-characterised mutant receptors including E2 loop, transmembrane mutants, and the wild-type receptor. The compounds included novel and unconventional ligands as well as classical antagonists, agonists and partial agonists. In this case the null hypothesis is that the binding of each compound is not affected by the set of mutations, so a 1-way ANOVA was performed in each case. These were followed up with two-tailed t-tests to give an indication of the significance of individual differences to wild-type values. These are given as $P<0.05$, or $P<0.01$.

More data is required in some instances to give a final picture.

2.16.7 Receptor Modelling : Analysis of Mutants

All M_1 mAChR models were produced in house and are designated with the file names. M1Model042001.pdb, AChmodel.pdb, NMSdock042001.pdb and AChdock1104.pdb. Stuctures and models in this thesis were created using pyMOL vers. 0.98 and analysis of H-bond formation (Chapter 7) was performed using the modelling programme Web Viewer-Lite, with the detection threshold set at 2.2Å±0.5 (min) and 2.7Å±0.5 (max).

Figure 2.3. The Extended Ternary Complex Model and Parameters Obtained from Binding and Functional Studies

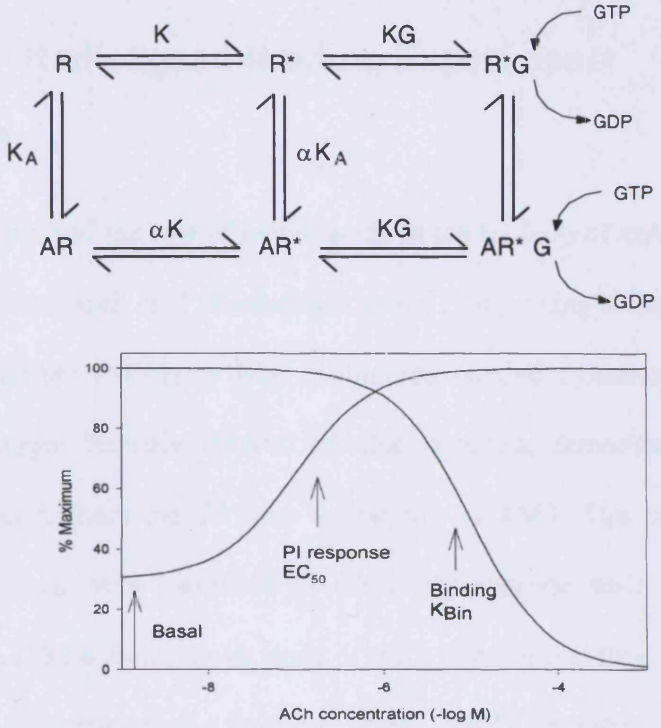

Antagonist affinity constant K_{NMS}

Receptor expression level $\underline{R}_T$

ACh affinity constant K_{Bin} ($=K_A(1+\alpha K)$)

Basal PI signal ($= K\underline{K}\underline{G}R_T/(1+K\underline{K}\underline{G}R_T)$)
ACh potency K_{Act} ($=1/EC_{50}$)

ACh signalling efficacy $\underline{K}\underline{G}.\alpha K/(1+\alpha K) = (K_{Act}/K_{Bin}(1\text{-Basal}) -1)/\underline{R}_T$

Ratio of functional R to G is ca. 20 for wild-type receptor in COS-7 cells.

The model describes algebraically the parameters that can be obtained from binding experiments on wild type and mutant receptors after expression in COS-7 cells. The extended ternary complex model describes the various states of the receptor and its ligand and G-protein complexes. The model describes how the parameters measured after expression of a mutant receptor in COS-7 cells relate to the underlying binding constants, and how they may be combined to give a measure of its signalling efficacy.

Chapter 3.

Radioligand Binding Experiments

3.1. Introduction -

Few studies have examined the role of amino acids in the E2 loop of mAChRs. One of the earliest studies by Kurtenbach et al (Kurtenbach et al., 1990), using selective incorporation of ^{3}H-N-ethyl maleimide (NEM) to label disulphide bonded cysteines and subsequent sequencing of cyanogen bromide cleaved labelled peptides, demonstrated the putative disulphide bond that anchors the E2 loop to the top of TM3. The conserved cysteine residues C98 and C178 were identified as the likely cysteine residues that form the disulphide bond. In 1992 a mutagenesis study of the 9 cysteine residues of the M_1 mAChR was performed by Savarese et al (Savarese et al., 1992). Included in the study, the disulphide bonded cysteine residues C98 (TM3) and C178 (E2 loop) were mutated to serine and characterised for ^{3}H-QNB binding and function using the agonist carbachol. These workers showed that point mutants of C98 and C178 to serine lacked ^{3}H-QNB binding and failed to mediate carbachol-stimulated phosphoinositides hydrolysis. The authors concluded that the disulphide bond formed between C98 and C178 is critical for formation of the ligand binding domain and for correct folding of the receptor

A comprehensive study by Wess et al (Zeng et al., 1999) underlined the importance of the homologous cysteine residues C140 & C220 in the M_3 mAChR for proper cell surface localisation and ^{3}H-NMS and carbachol binding. Using ELISA and radioligand binding techniques expression levels of the cysteine mutants were shown to be reduced 10-20-fold and drastic reductions in binding affinities for ^{3}H-NMS at all three cysteine to alanine mutants (C140A ~140-fold, C220A ~860-fold, and C140A/C220A ~50-fold) and carbachol

(>100-fold) binding affinities were recorded. Despite losses in expression and ligand binding affinities these authors were surprised to find that two mutants C220 and C140/C220 were able to mediate agonist-dependent PI hydrolysis, although with a huge decrease in potency (10,000-fold) compared to WT. So, despite improper folding, cysteine mutant M_3 receptors that were present on the cell surface were able to elicit a functional response, albeit at greatly increased agonist concentrations. This report emphasised the importance of the conserved disulphide bond thought to be present in nearly all GPCRs. Zeng and Wess (Zeng and Wess, 2000) have also proposed the possible formation of oligomeric muscarinic receptors via cross linking between conserved cysteines. The formation of muscarinic receptor aggregates, they suggest, precedes inter-molecular disulphide cross-linking.

Two studies have looked specifically at the LAGQ sequence in the E2 loop (see figure 3.1.) of the M_1 mAChR and the corresponding EDGE sequence in the E2 loop of the M_2 mAChR (Gnagey et al., 1999; Leppik et al., 1994) to determine their role in the binding of the allosteric ligand gallamine. In both studies replacing the EDGE sequence of M_2 with the LAGQ sequence derived from M_1, gave an 8-fold reduction in gallamine affinity at the unoccupied receptor and a 4-fold reduction in gallamine affinity at the NMS occupied receptor for the mutant M_2 receptor. In the complementary experiment, gallamine affinity was significantly increased by replacing the LAGQ sequence of the M_1 mAChR with the M_2 EDGE sequence (Gnagey et al., 1999). Reductions in ^{3}H-NMS affinity were also reported by Leppik et al. for the LAGQ-EDGE M_1 mutant (Kd WT = 52pM compared to Kd mutant = 107pM). These complementary studies highlight the potential for the E2 loop to bind ligands ectopically and influence the affinity of ligand binding to the orthosteric binding site by allosteric mechanisms, as well as to reduce the affinity of orthosteric ligands. Although no conclusions can be drawn about the role of the E2 loop in the

orthosteric binding pocket these results do suggest that the E2 loop is important for the binding of some allosteric ligands.

The study on the structure of rhodopsin and in particular the role and the structure of the E2 loop of rhodopsin, highlighting the proximity of the E2 loop to the orthosteric binding site (Li et al., 2004 ; Palczewski et al., 2000) is of particular relevance to the present study. M_1 mAChR E2 loop residues homologous to residues within rhodopsin that interact with the chromophore 11 cis retinal were chosen for mutation to alanine (see table 3.1 and figure 3.1). The E2 loop of rhodopsin folds back into the membrane embedded domain of the 11 cis retinal binding pocket and in particular the carboxylic side chain of Glu181 (E170 in M_1) points into the centre of the retinal polyene chain (Yan et al., 2002) affecting the retinylidene Schiff base in the meta-II rhodopsin state. Other E2 loop residues of rhodopsin have also been shown to participate structurally in the retinal binding pocket (Li et al. 2004). The β3-β4 sheet, a feature of the E2 loop in rhodopsin, forms a "plug" at the top of the binding pocket which is secured to main chain atoms of Y10 in β2 of the β1-β2 sheet. Additional, water mediated H-bonds via G182, Q184 and Y192 of the β3-β4 sheet further secure the loop to the β1-β2 sheet and the transmembrane domain. A key rationale of the present study is to determine if the E2 loop of the M_1 mAChR has similar structural properties to that of rhodopsin. Although Shi and Javitch (Shi and Javitch, 2002; Shi and Javitch, 2004), using substituted cysteine accessibility methods (SCAM), worked on the dopamine D2 receptor, their work seems to mirror the structural studies on rhodopsin (Li et al.2004), suggesting that the region C-terminal to the cysteine S-S bond of the E2 loop lies deeper within the transmembrane binding site.....(continued on page 105)

Figure 3.1 Alanine Mutations of Residues in the E2 Loop of the M_1 mAChR

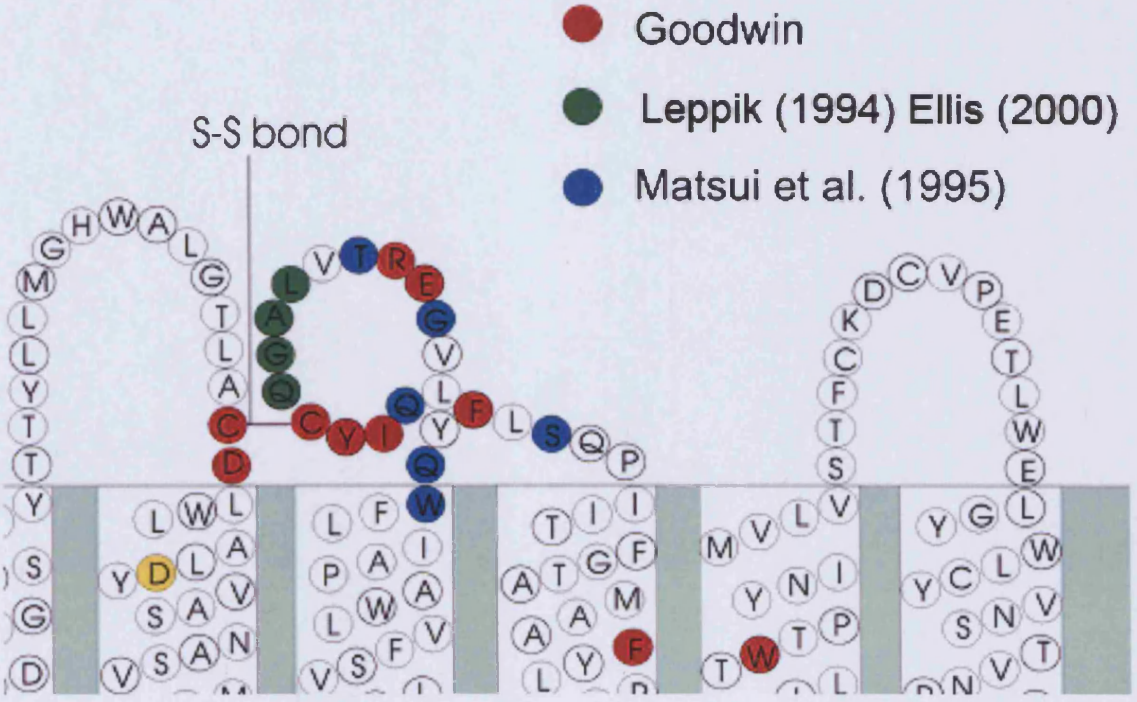

Snake diagram depicting E2 Loop amino acid sequence and secondary structure topology of the M_1 mAChR, highlighting residues from this and previous E2 loop studies that have been mutated to alanine. C98 at the top of TM3 is disulphide bonded to C178 in the E2 loop. Also highlighted in yellow in TM3 is the critical ACh contact residue D105 and is shown to indicate the approximate depth of the ACh binding site. Residues F197 TM5 and W378 TM 6 are also depicted. NB some mutations overlap between the three studies, e.g. F182A was analysed by Matsui et al and is also one of the subjects of the present study.

Table 3.1. Comparison of Rhodopsin and M_1 mAChR Binding Site Residues

Residues of the Rhodopsin binding site as reported by Jade Li et al (2004) are compared with M_1 mAChR binding site residues taken from this study and previous work from this laboratory (Hulme and Lu, 1998; Kurtenbach et al., 1990; Lu et al., 2001) TM residues (yellow) and E2 loop residues (green) were mutated to alanine in this study. *Non-highlighted residues have been studied by alanine substitution in previous studies

Retinal Binding site Residues	*Corresponding Residues in M_1 mAChR
W265	W378
Y268	Y381
T118	Y106
E122	W110
M207	T192
F212	F197
A117	D105
K296	Y408
C187	C178
F261	F374
A269	N382
F208	A193
A292	Y404
Y191	F182
G121	S109
H211	A196
G188	Y179
C167	L156
I189	I180
E181	E170
S186	Q177
A272	V385

crevice then the N-terminal region. The N-terminal residues of the E2 loop, they suggest, are located so as to protrude into the extracellular space. They concluded that it is the residues C-terminal to the conserved cysteine residue that are likely to contribute to ligand binding. Variations in the length of the E2 loop between different GPCRs probably reflect the variation in size of endogenous ligands. A larger ligand requires the E2 loop to be longer to accommodate it while a smaller ligand requires the geometrical constraint of a shorter E2 loop. The amino acid sequence of the E2 loop shows considerable variation across the class of rhodopsin-like GPCRs, however, the sequence C-terminal to the conserved cysteine is more highly conserved amongst functionally related receptors. Residues I180, Q181, F182 and S184 of the M_1 mAChR at this position are completely conserved in the corresponding positions in all five of the mAChRs sub-types. In addition, the residue C-terminal and adjacent to the C178 residue, is an aromatic amino acid in M_1-M_4 receptors; only M_5 has a charged polar side chain (Glu) at this position.

In another study (Klco et al. 2005), evidence was provided that the E2 loop is essential for the activation of the complement factor 5a receptor (C5a). The authors demonstrated using random saturation mutagenesis that the E2 loop of the C5a receptor acted, unexpectedly, as a negative regulator of C5a activation. Furthermore, the authors found that the E2 loop of the C5a receptor tolerated amino acid substitutions extremely well; in fact many mutations resulted in a gain of function phenotype. Interestingly, the conserved cysteine residue C188 (homologous to C178 in the M_1 mAChR) only tolerated a single substitution (C188M) in the 29 receptors they generated by random saturation mutagenesis. These authors proposed that the E2 loop of the C5a and perhaps other GPCRs stabilizes the inactive ground state of the receptor, but could not suggest the molecular mechanism involved. There are a range of studies that focus on the role of the E2 loop in other GPCRs which are reviewed systematically by Shi and Javitch (Shi and Javitch, 2002). In summary, it appears that the

role of the E2 loop in ligand entry and binding and in allosteric modulation may differ between different GPCRs. For example, the variation in the length and amino acid sequence of the E2 loop between different GPCRs is likely to significantly alter the role the E2 loop has to play in specific receptor-ligand interactions. In short, more detailed high resolution structural analysis and experimentation are required to reveal the role of the E2 loop for specific GPCRs.

In this study, seven potential ligand contact residues of the second extracellular loop were identified using the rhodopsin homology model (Palczewski et al., 2000) of mAChRs (see figure 3.1 and table 3.1). The selected residues of the E2 loop of the M_1 mAChR homologous to the retinal contact residues were chosen for mutation to alanine. They included the structurally important disulphide bonded cysteine 178. In addition to the seven E2 loop residues mutated in this study, six other residues of the E2 loop, previously characterized by Matsui et al (Matsui et al., 1995) have been included in this study for analysis of their function in receptor stimulation (results in Chapter 4). It is hoped that these data will provide a more complete understanding of the role of the E2 loop in M_1 mAChR ligand binding and stimulation. A double cysteine mutant (C98A/C178A) and a C178N mutant were also constructed, in order to better understand the individual binding and functional characteristics of the two cysteine residues. Mutation of C178 to N replaces the polarisable sulphur-containing side chain with a polar residue. Other mutations of C178 were planned, C178V for example, was chosen because it has a bulky hydrophobic non-polarisable side chain, to gain a better insight into the contribution C178 makes to the binding of ligands. Unfortunately, however, after several attempts at mutating C178 to other amino acids only the C178A and the C178N mutants were successful and viable. Four residues in the TM domain were also chosen for mutation to alanine. F197 (TM5) and W378 (TM6) help complete the picture of ligand contact residues within the defined

binding pocket. D99 has been proposed to act as a ligand docking residue in mAChRs and other 7-TM receptors (Jakubik et al., 2000). C98 was also mutated to alanine because it is the other cysteine involved in the disulphide bond.

3.2 Results

3.2.1. Effects of mutations on ^{3}H-NMS and ^{3}H-QNB Binding: Characteristics; Technical Issues.

The binding of increasing concentrations of ^{3}H-NMS or ^{3}H-QNB to M_1 mAChRs transiently expressed in COS-7 cell membranes exhibits a saturable and a non-saturable component. The saturable component can be suppressed by the inclusion of a sufficient amount of unlabelled competing ligand, such as atropine. Atropine therefore provides the non-specific binding values. Analysis of saturation curves using a simple 1 site model for binding yields estimates of total concentration of binding sites (Bmax) for the tritiated ligand and of its affinity constants. Certain mutations cause receptors to be expressed at very low levels, C178A for example, making characterisation extremely problematic. Three methods were employed to rescue poorly expressed mutant receptors. Firstly, atropine was added to the culture media 48 hours prior to harvesting. Atropine, a high affinity inverse agonist, is similar in structure to NMS, except that it contains a tertiary amine head group instead of a quaternary group. This allows atropine to access the cytoplasm where it is believed to act like a molecular chaperone (Lu and Hulme, 1999). Binding to and stabilizing the nascent receptor on its journey through the endoplasmic reticulum and the Golgi network, it allows poorly-expressing mutants to reach the plasma membrane. Once in the membrane the mutant receptors can be harvested and characterized. Indirect saturation binding curves provided a second approach to overcome poor expression of mutants or mutants with significantly reduced affinity compared to WT. In this instance unlabelled NMS is used to compete with the tritiated ligand (^{3}H-NMS), in hot-v-cold assays. This allows us to determine Kd values for poorly expressing and low affinity mutants. If a mutant has an extremely low affinity for a particular ligand then it is possible that the native residue in question participates in the binding of that particular ligand.

A third approach to characterising low expressing mutants was the use of a second radioligand, ^{3}H-QNB. This ligand has a 3-fold higher affinity than ^{3}H-NMS for the wild type mAChR and potentially binds to a different set of contact binding residues. That is, a specific mutation may reduce the affinity of NMS but not QNB. In addition, the antagonist ^{3}H-QNB, like atropine is also able to penetrate lipid membranes, allowing it to enter vesicles, which can be formed when preparing membranes for analysis. Receptors can become trapped within these vesicles, effectively eliminating the entry of hydrophilic quaternary amines such as NMS. Hence the use of ^{3}H-QNB instead of NMS can overcome some of the problems caused by poor expression and low affinity.

Summaries of expression levels and binding affinities of NMS and QNB binding sites of mutants compared to wild type can be seen in table 3.2 and an example of mutant expression before and after atropine treatment can be seen in figure 3.2.

Table 3.2. Summary of NMS and QNB Affinity Constants and Expression Levels: All Mutants

	NMS			QNB		
E2 Loop Mutants	**n**	**Expression %WT**	**pKd -log M**	**n**	**Expression %WT**	**pKd -log M**
WT	17	100±5.3	9.87±0.04	9	100±9.7	10.63±0.04
C98A/C178A*§	7	53.3±7.8	8.37±0.1[a]	3	26.3±9.6	8.80±0.1[a]
E170A	5	46.6±24.4	9.75±0.1	3	39.9±3.3	10.83±0.1
R171A	4	45.2±27.7	9.25±0.03[a]	3	40.8±2.2	10.45±0.1
Q177A	4	51.3±31.3	9.82±0.03	3	57.6±0.43	10.57±0.2
C178A*§	8	43.1±7.1	8.77±0.1[a]	3	48.5±19.0	9.27±0.04[a]
C178A†	3	4.8±0.5	ND	ND	ND	ND
C178N*§	5	45.9±8.4	8.56±0.1[a]	3	49.8±4.2	9.45±0.1[a]
Y179A	3	60.3±6.7	9.44±0.1[a]	3	81.6±6.4	10.39±0.1
I180A	3	67.35±8.4	9.46±0.03[a]	3	72.1±7.5	10.53±0.3
F182A	3	56.5±9.1	9.37±0.04[a]	3	70.5±15.0	10.94±0.2
TM Domain Mutants						
C98A*§	6	16.1±3.1	8.28±0.1[a]	3	19.6±4.5	9.16±0.1[a]
D99A*§	4	9.6±1.7	8.81±0.1[a]	3	15.0±11.2	10.10±0.1[b]
D99A†	2	4.3±1.2	ND	ND	ND	ND
F197A*§	3	66.3±10.0	7.89±0.1[a]	3	16.1±7.2	10.35±0.2
F197A†	3	4.3±3.0	ND	ND	ND	ND
W378A‡	3	N.D	7.25±0.1[a]	4	125.4±12.5	9.62±0.1[a]

*Denotes poorly expressing atropine Rescued Mutants
† Indicates Non-atropine treated values
§ pKd Values Determined by Hot-v-cold Experiments
‡ Denotes pKd Value determined by ^{3}H-QNB-v-NMS competition experiments
Statistical Significance (t-test) [a]$p<0.01$ and [b]$p<0.05$ wrt WT values.

Figure 3.2. Atropine Treatment of Growth Media Rescues Poorly Expressing C178A Mutant.

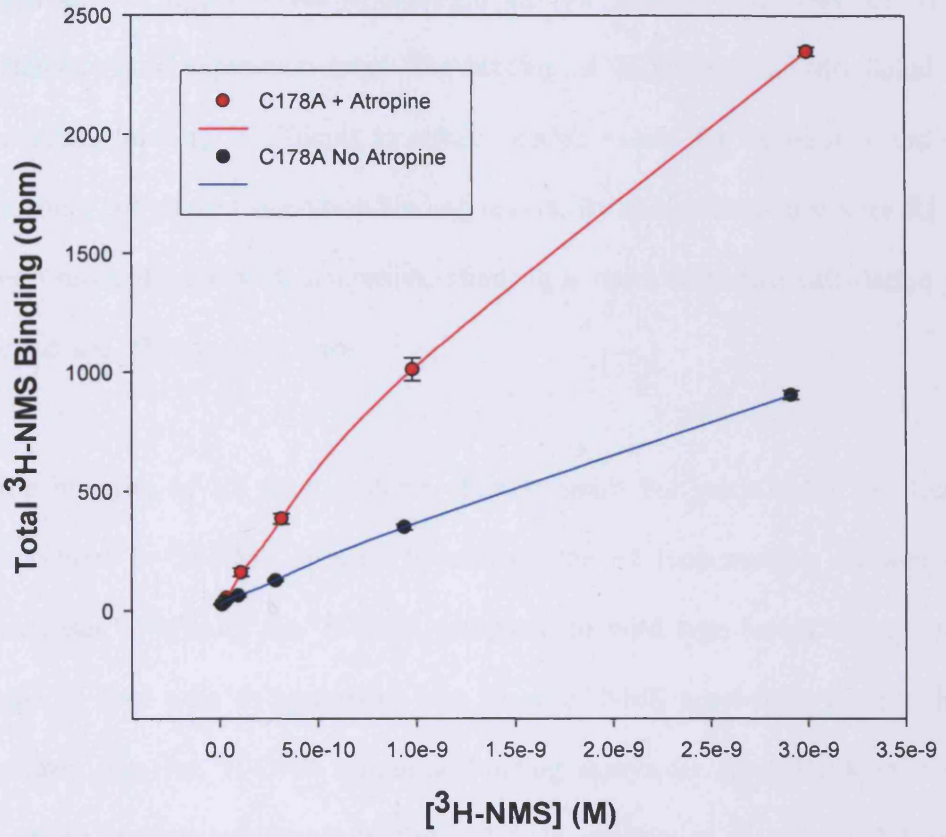

Representative ^{3}H-NMS saturation binding assay on COS-7 cell membrane preparations transiently expressing the poorly expressed C178A mutant with or without 10^{-6}M atropine added to the growth media. It can be seen that cells treated with atropine improve radioligand binding to the C178A mutant receptor. The data is representative of at least three independent experiments and all data points are the mean of quadruplicate assays ±S.E.M.

3.2.2 Determination of NMS and QNB Affinity Constants

In the Top Panel of figure 3.3 representative ^{3}H-NMS saturation curves from primary data are shown for wild type, R171A and C178A. The curves show mean total and non specific binding. The figure serves to highlight the low affinity of C178A for ^{3}H-NMS and its relatively poor expression level. The binding of ^{3}H-NMS to C178A failed to reach 50% saturation making it difficult to obtain precise values for expression and affinity using standard radioligand saturation binding assays. By comparison curves for R171A of the E2 loop reached over 80% saturation, allowing a more confident calculation of expression levels and affinity, to be made.

The majority of E2 loop mutants showed small but statistically significant (2-4-fold) reductions in ^{3}H-NMS affinity. In contrast the E2 loop mutants showed no significant decreases in affinity for ^{3}H-QNB compared to wild type levels of expression of QNB binding sites were in agreement with those of NMS apart from C178A. Representative primary data for ^{3}H-QNB saturation binding assays for some E2 loop mutants and the cysteine mutants are shown in figure 3.5. In contrast to the other E2 loop mutants the cysteine mutants showed large decreases in binding affinity for both NMS and QNB as determined by hot-v-cold competition binding assays (figure 3.4). C98A showed ~40-fold reduction in NMS affinity and ~30-fold reduction in QNB affinity. C178A showed ~10-fold reduction in NMS affinity and ~20-fold reduction in QNB affinity. C178N gave comparable reductions in both NMS and QNB affinity (to that of C178A). The double cysteine mutant, C98A/C178A showed ~30-fold reduction in NMS affinity and ~70-fold reduction in QNB affinity, three times the reduction in QNB affinity shown for C178A ($p<0.05$). Cysteine mutant affinity constants are also summarised in table 3.2.

Figure 3.3 Representative ^{3}H-NMS Radioligand Binding Curves for E2 Loop Mutants

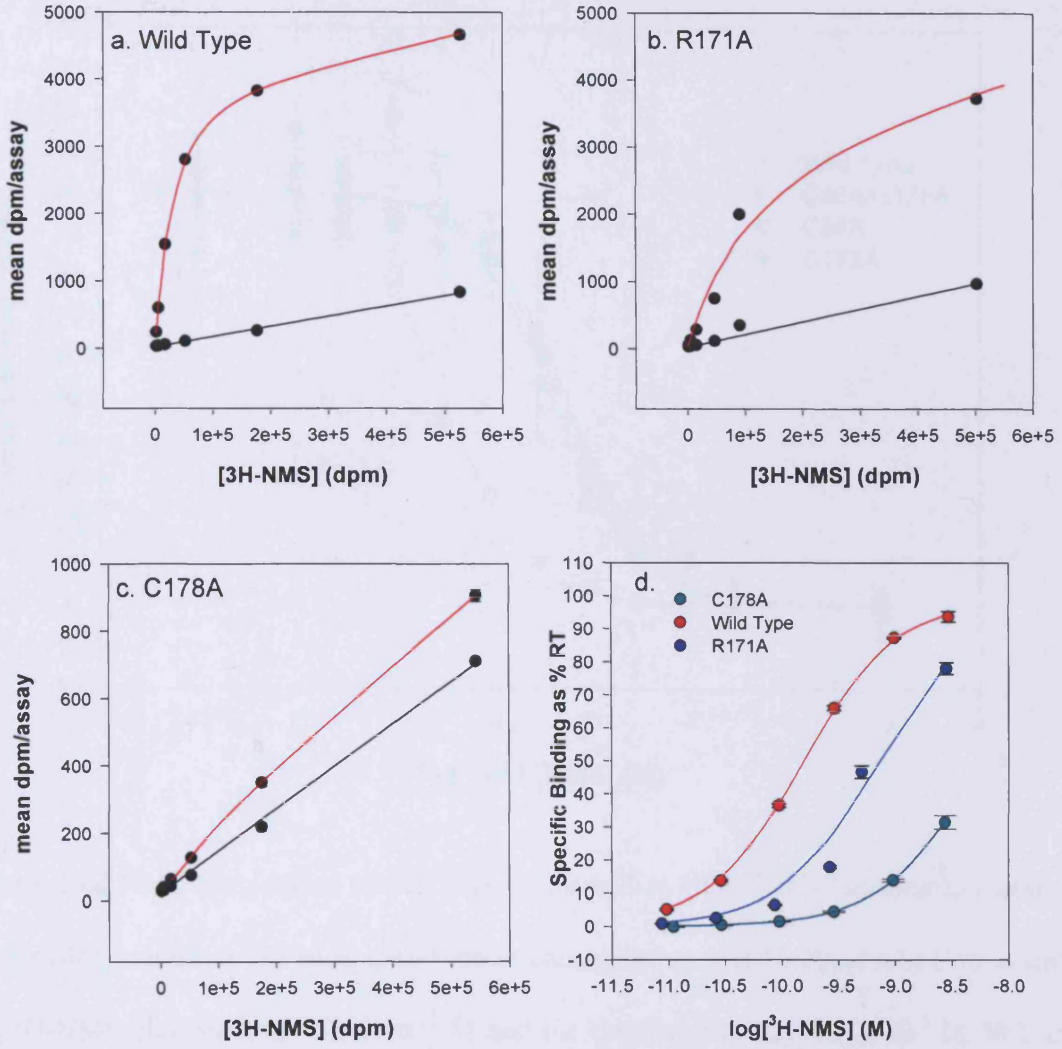

^{3}H-NMS saturation binding assays were performed on membrane preparations of receptors transiently expressed in COS-7 cells. Protein concentration was 10-30 µgmL . **a-c** represent total and non-specific binding plotted against increasing ^{3}H-NMS concentration. Values are the mean of quadruplicate points ± S.E.M. Full binding curves show the fits to a 1-site model of binding

a. WT pKd = 9.85±0.01 **b. R171A** pKd = 9.15±0.14. **c. C178A** pKd = 8.22±0.16 **d.** Curves from **a,b & c** plotted on log concentration (M) scale in relation to the estimated receptor occupancy

Figure 3.4. Representative Hot-v-Cold NMS Competition Binding Curves to Determine NMS pKd for Cysteine Mutants.

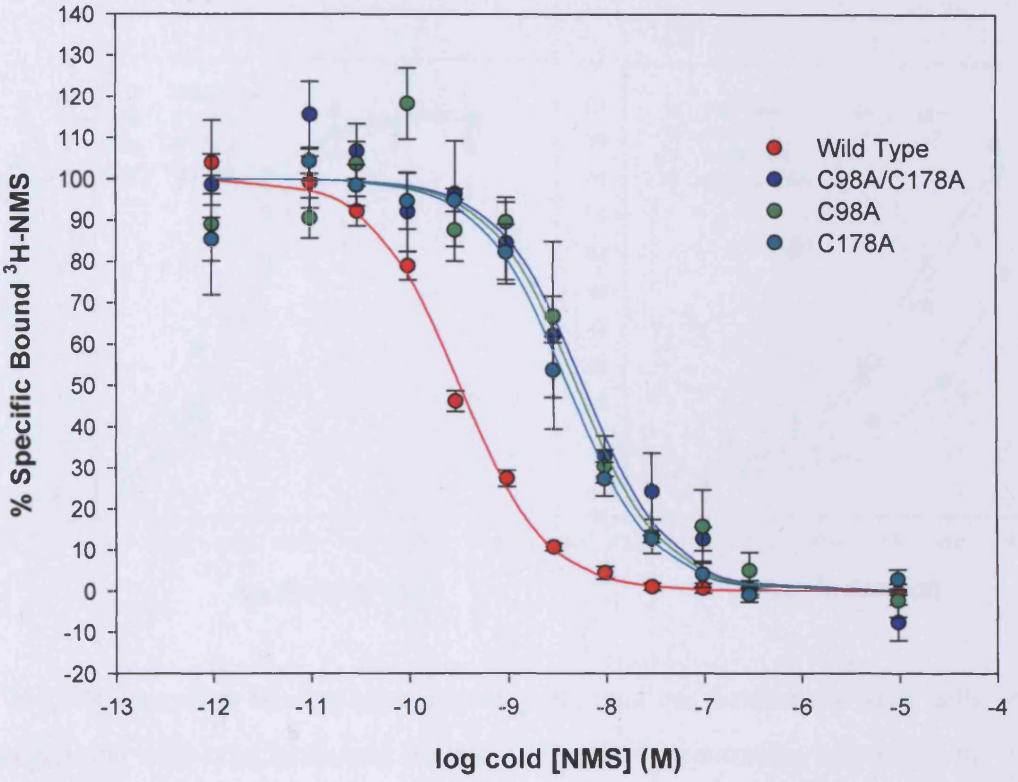

Hot-v-cold NMS competition curves were performed on COS-7 cell membranes transiently expressing mutant or WT receptors. Protein concentration was 10-20µg/mL. Concentration of ^{3}H-NMS used for WT = 3 x 10^{-11} M and for cysteine mutants = 3 x 10^{-9} M. **WT** (red) pKd = 9.5±0.04; **C98A** (green) pKd = 8.30±0.07; **C178A** pKd = 8.40±0.05 and **C98A/C178A** pKd = 8.23±0.09. Points are mean of quadruplicate assays and are shown ± S.E.M. All points were fitted to a 1-site model of binding and corrected using the Cheng Prusoff correction factor. Data is representative of at least three independent experiments.

Figure 3.5. Representative ^{3}H-QNB Binding Curves for E2 loop and Cysteine Mutants

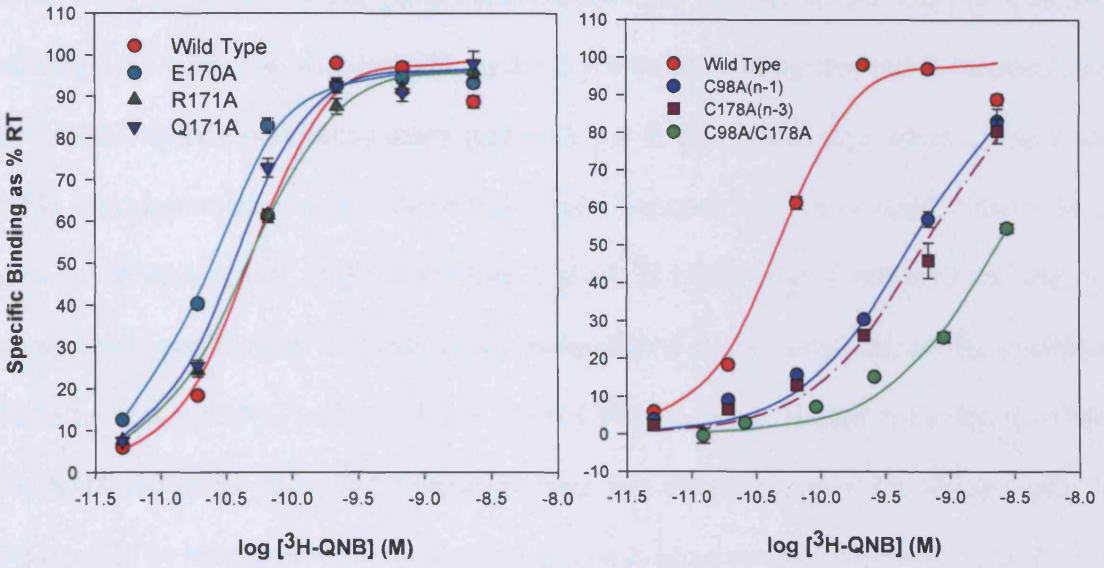

^{3}H-QNB saturation binding assays were performed on membranes from cells transiently expressing wild type or mutant receptors. Protein concentration was 10-30 µg/mL. **a.** E2 loop mutants. **WT** pKd = 10.82±0.09; **E170A** pKd = 10.98±0.03; **R171A** pKd = 10.54±0.03; **Q177A** pKd = 10.86±0.07. **b.** Cysteine mutants. **WT** pKd = 10.82±0.09; **C98A** pKd = 9.31±0.06; **C178A** pKd = 9.22±0.08; **C98A/C178A** pKd = 8.60±0.13. All points are the mean of quadruplicate assays ± S.E.M and are representative of at least three independent experiments.

The TM domain mutants D99A, F197A and W378A had a significantly greater effect on the affinity of NMS than QNB. Figure 3.6 shows representative data used to accurately determine pKd values for the TM domain mutants that showed severe reductions in NMS affinity. D99A has just sufficient affinity for NMS for its binding constant to be determined by an NMS saturation binding assay (panel a). For F197A (panel b) a series of hot-v-cold NMS experiments were able to determine a more accurate measure of NMS affinity. In the case of W378A (panel c) the >400-fold loss of ^{3}H-NMS affinity required the use of a competition assay using ^{3}H-QNB as the radio ligand to be competed off by unlabelled NMS to determine NMS affinity for W378A. D99A showed ~10-fold reduction in affinity for NMS and of the three TM domain mutants was the only mutant for which a pKd for NMS could be measured using standard saturation binding assays. Interestingly, D99A only reduced QNB affinity by 3-fold. F197A reduced NMS affinity ~100-fold but for QNB only 2-fold. W378A reduced QNB affinity by 10-fold compared to wild type.

In summary, R171A, Y179A, I180A and F182A caused relatively small but significant reductions in the binding constant for ^{3}H-NMS, without having the corresponding effect on the binding of ^{3}H-QNB. The cysteine mutants produced larger and significant reductions in both ^{3}H-NMS and ^{3}H-QNB affinity. Both F197A and W378A significantly reduced ^{3}H-NMS binding affinity, but only W378A significantly affected the binding of ^{3}H-QNB

3.2.3. Determination of Expression Levels

Once reliable pKd values had been obtained for those mutants with low expression and low NMS affinity, specifically the Cys mutants, F197A and W378A, it was possible to calculate a more precise estimate of the total number of NMS binding sites. This was achieved by re-analysing the original ^{3}H-NMS saturation binding data using constrained pKd values which were obtained by indirect means (hot-v-cold NMS assays and ^{3}H-QNB-v-NMS competition

assays). This was not possible for W378A because of the ~500-fold reduction in NMS affinity. Thus, expression levels for this particular mutant could only be calculated using ^{3}H-QNB saturation binding assays. Low expression levels and low affinity for NMS meant that for the mutant F197A in particular calculation of meaningful expression levels were difficult. Indeed, reliable estimates of Bmax for all mutants are reliant on sufficient binding affinity of the tracer ligand and the ability of the receptor to locate correctly in the membrane. Calculating the expression level for F197A by extracting the Bmax value by constraining data from Hot-v-cold NMS experiments inevitably led to a somewhat skewed Bmax value (~66% of WT expression). Data for F197A QNB binding was more accurate since QNB affinity was not affected by this particular mutant. Therefore the levels of expression of QNB binding sites was slightly more accurate (~16% of WT with a range of 7% - 46%) since Bmax could be measured by direct ^{3}H-QNB saturation binding assays.

In general it was shown that the E2 Loop mutants expressed at levels greater than 50% of WT, the exception being C178A which expressed at ~25%, even after atropine rescue. For the TM domain mutants, expression was more variable, probably due to the need for atropine rescue. For example, C98A (12% of WT) and D99A (~8% of WT) were the lowest expressing mutants of all those analysed. Interestingly the C178N mutant expressed both NMS and QNB binding sites at ~50% of WT values. The biggest surprise was that the double cysteine mutant C98A/C178A expressed NMS binding sites at higher levels (~50% of WT) than either of the single cysteine mutants. This was in contrast to QNB binding sites which were shown to express at only ~25% of WT levels for the C98A/C178A mutant but at similar levels for the single cysteine mutants. Another surprise was that W378A showed expression levels of QNB binding sites greater than wild type levels (125%). All expression levels, along with summary affinity data for NMS and QNB are shown in table 3.2. The comparisons of Bmax values for all mutants obtained from NMS and QNB

binding experiments (where possible) are in relatively good agreement with the exceptions of C98A/C178A and W378A.

Figure 3.6. Representative Binding Curves for Determination of NMS Affinity Constants for TM Domain Mutants

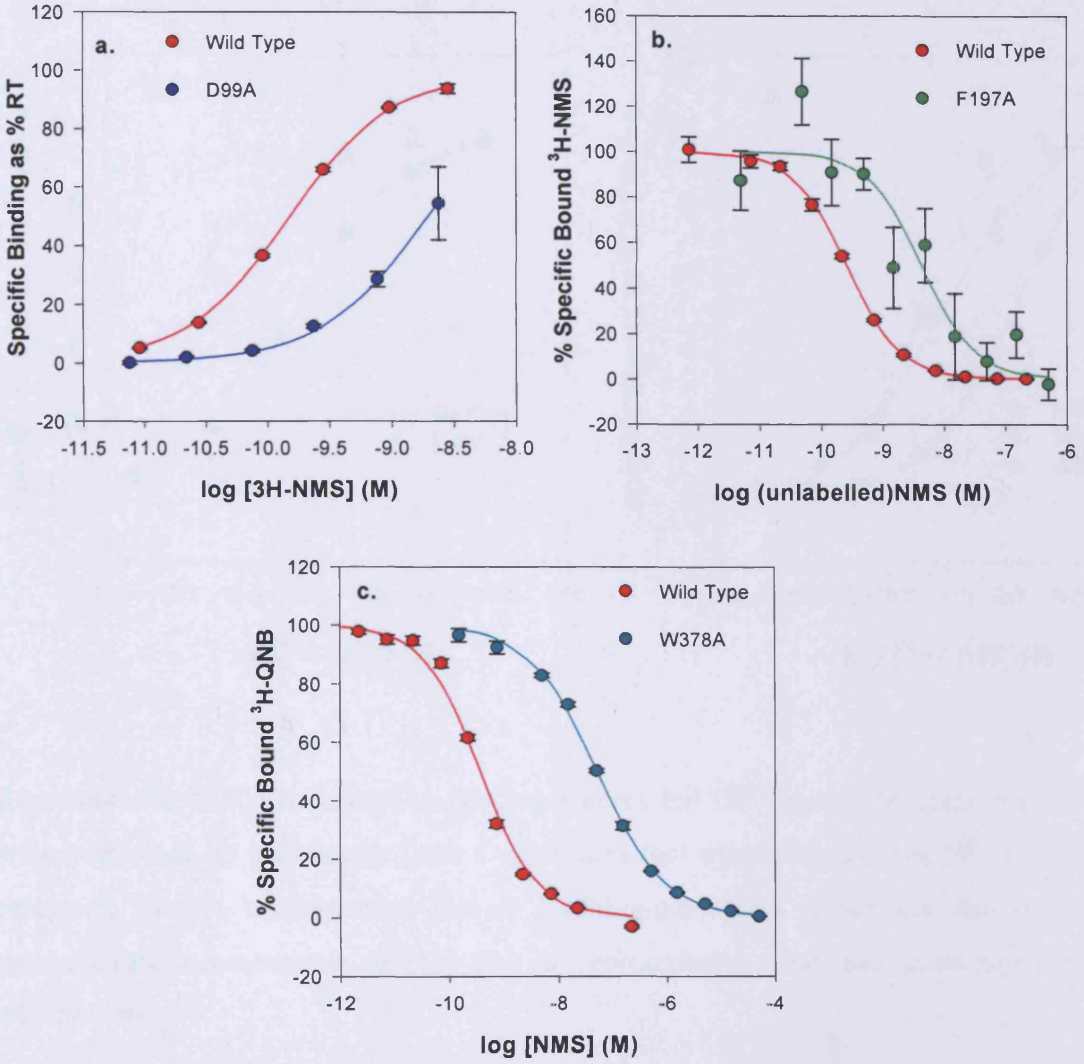

All assays were performed on COS-7 cell membranes transiently expressing WT or mutant receptors. Total protein = 10-30 μg/mL **a.** NMS saturation assay. pKd **WT** = 9.86±0.02, Bmax = 21.9fmol/mL; pKd **D99A** = 9.03±0.05; Bmax = 4.4fmol/mL. **b.** Hot-v-cold NMS competition assay; pKd **WT** = 9.60±0.02; **F197A pKd** = 8.08±0.20; **c.** ^{3}H-QNB-v-NMS competition assay; **WT** pKd = 9.43±0.02; **W378A** pKd = 7.20±0.02. Data points are mean of quadruplicate measurements and are shown ±S.E.M and are representative of at least three independent experiments and are corrected using the Cheng Prussof Correction Factor. Data is representative of at least 3 independent experiments.

Figure 3.7. Representative [^{3}H]-QNB Saturation Binding Curves for TM Domain Mutants

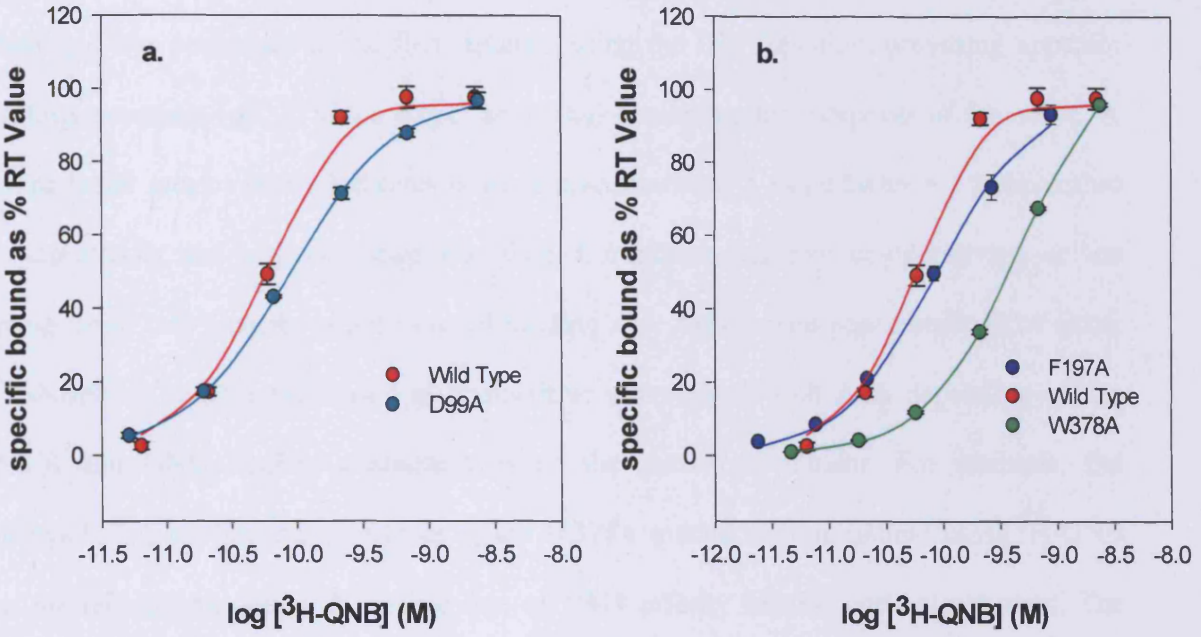

Representative ^{3}H-QNB Saturation Binding Curves for TM Domain Mutants. All assays were performed on membranes from COS-7 cells that transiently express WT or mutant receptors. Protein concentration was = 10-30µg/mL. Data points are the mean of quadruplicate measurements ±S.E.M and are representative of at least three independent experiments.

a. WT pKd = 10.60±0.11; Bmax = 59.8fmol/mL **D99A** pKd = 10.10±0.02; Bmax = 15.3fmol/mL (with atropine rescue).

b. F197A pKd 10.08±0.04; Bmax = 3.9fmol/mL (with atropine rescue) **W378A** pKd = 9.77±0.11; Bmax = 59.5fmol/mL. Data is representative of at least 3 independent experiments.

3.3. Acetylcholine Competition Binding Experiments

Competition assays were designed to analyse the binding of ACh to mutant M_1 mAChRs. Analysis was performed in the first instance using the Hill Equation, providing apparent affinity constants (pIC_{50}) and a slope factor (n_H) describing the steepness of the curve. A slope factor greater than 1 indicates positive co-operativity, a slope factor = 1 indicates no co-operativity and a slope factor less than 1 indicates negative co-operativity, or the presence of two separate populations of binding site. Appropriate concentrations of either ^{3}H-NMS or ^{3}H-QNB were used in competitive experiments with ACh depending on the NMS and QNB binding characteristics of the individual mutant. For example, the acetylcholine binding characteristics of the W378A mutant were measured using ^{3}H-QNB as the radioligand due to the severe loss of NMS affinity for this particular mutant. The radioligand used in competition assays is clearly stated in the following representative figures. Again atropine was used to provide the non-specific component for the analysis. The model for analysing acetylcholine affinity differs from the simple 1-site model in that the Hill equation allows for the slope of a curve to be greater or less than 1. Representative curves for E2 loop mutants are presented first, followed by illustative data for the cysteine mutants and TM domain mutants.

3.3.1. E2 Loop Mutants-ACh Binding

The acetylcholine competition binding curve for wild type gave a pK value = 5.00 with a mean slope factor of 0.84±0.03 and ACh reduced the percentage of specific binding of ^{3}H-NMS to zero at ~1mM ACh. Two of the E2 loop mutants showed significant reductions in acetylcholine affinity, namely R171A (~7-fold) and I180A(~5-fold). The majority of E2 loop mutants returned pIC_{50} values approximating wild type values. Example ACh

competition data is shown in figure 3.8 and mean pIC_{50} and Hill coefficient values for wild type and all mutants are given in table 3.3.

Table 3.3 Summary Data of ACh Affinity Constants: All Mutants.

	n	Mean IC_{50}+/- S.E.M	Hill coefficient
Wild Type	24	5.00±0.05	0.84±0.03
E2 Loop Mutant			
C98A/C178A	6	3.10±0.10[a]	0.95±0.22
E170A	4	5.19±0.18	0.75±0.04
R171A	4	4.17±0.15[a]	0.93±0.21
Q177A	4	5.14±0.10	0.88±0.04
C178A	6	3.18±0.14[a]	1.25±0.15
C178N	5	2.94±0.07[a]	0.80±0.14
Y179A	3	4.75±0.18	0.74±0.11
I180A	3	4.35±0.18[b]	0.85±0.03
F182A	4	5.08±0.06	0.80±0.07
TM Domain Mutants			
C98A	6	3.90±0.18	0.47±0.06[a]
D99A	4	3.65±0.12[a]	0.77±0.11
F197A	4	4.76±0.24	0.72±0.37
W378A§	7	3.86±0.09[a]	1.34±0.09[a]

‡ Atropine Rescued Mutants

Statistical Significance (2-tailed t-test) [a]$p<0.01$ and [b]$p<0.05$ with respect to WT values

§ pKa values obtained using ^{3}H-QNB as competing radioligand.

Figure 3.8. Representative ACh Competition Curves for E2 Loop Mutants.

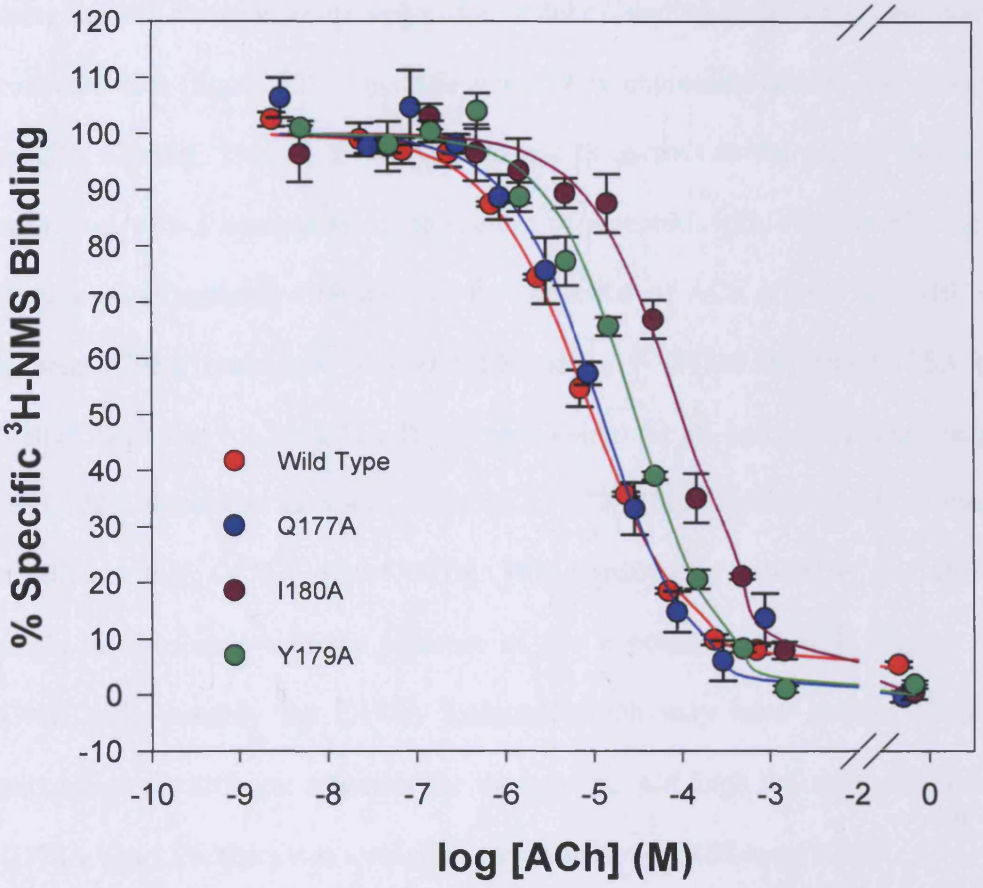

Assays were performed on COS-7 cell membranes transiently expressing WT or Mutant receptors. Protein concentration was 10-30μg/mL. Data points are the mean of quadruplicate measurements ±S.E.M and curves were fitted using the Hill equation. Binding curves have been subject to Cheng Prusoff correction. 10^{-6}M Atropine used for non-specific controls [^{3}H-NMS] used for WT = 10^{-10}M and for Mutants = 3 x 10^{-10}M. **WT** pIC_{50}= 5.06±0.03, n_H = 0.9; **Q177A** pIC_{50} = 4.91±0.01, n_H = 0.89; **I180A** pIC_{50}= 4.00±0.03, n_H = 0.87; **Y179A** pIC_{50}= 4.52±0.03, n_H = 0.93.

3.3.2. Cysteine Mutants-ACh Binding

The ACh binding data from individual experiments for the cysteine mutants when analysed using the Hill equation and a single site model of binding showed apparent poor fits to the collected data (figure 3.9). This was due to low expression levels, low affinity and low specific binding. That is, the curves did not fit as well to the plotted data as would be consistent with a homogeneous population of receptors with a single binding site. Also, there was an apparent difference in the reduction of ACh affinity and Hill coefficients between C98A (mean pK = 3.90±0.18 and n_H = 0.47±0.06) and C178A (mean pK= 3.18±0.14 and n_H = 1.25±0.15). These mean values for pK and n_H indicate a larger effect of the C178A rather than the C98A mutation on ACh affinity and C98A has a lower mean Hill coefficient than C178A of 0.47±0.06. This significantly ($p<<0.01$) low Hill coefficient might be consistent with the presence of two populations of ACh binding sites for the C98A (and possibly the C178A mutants) which may have similar affinities for the antagonist but different affinities for the agonist. Although the mean Hill coefficient for C178A was 1.25, there was a range of values from n_H =0.58 to n_H = 1.77

To provide a better insight to the possibility that the C98A mutant gave rise to two distinct populations of receptors ACh competition data for C98A was pooled and analysed using a 2-site model of binding and is presented in figure 3.10. Data was pooled and normalised by taking the ratio of mean dpm minus non-specific binding to mean dpm for total specific binding for each ACh concentration and calculating a mean value for the whole data set. Analysis of the pooled data showed that C98A gave a larger fraction of high affinity sites at 60% than low affinity sites at 40% of the total population. The mean pK_H (affinity constant of the high affinity sites) was 4.33±0.22 and the mean pK_L (affinity constant of the low affinity sites) was 2.58±0.21.

To further analyse the C98A mutant a more detailed experiment was performed using a wider range of ACh concentrations and to provide different radioligand occupancies of the two populations of sites (see figure 3.11). This data was then analysed by using a 1-site model and a 2-site model of binding and compared. The wild type competition data was consistent with the results reported in table 3.3. The data for C98A did not fit well to the 1-site model (figure 3.9) but better fitted the 2-site model (shown in figure 3.11). C98A shows a population of receptors with a mean pK_H = 5.13±0.03, and a mean pK_L= 2.27±0.03, in roughly equal proportions (~50%) and the residuals in this analysis were randomly distributed (data not shown). The possibility of that the C178A mutant also produces two populations of binding site requires further investigation.

3.3.3. Transmembrane Domain Mutants-ACh Binding

Of the TM domain mutants D99A displayed the largest effect on acetylcholine binding with a ~20-fold reduction in affinity but with an n_H value (0.77±0.11) close to wild type (0.84±0.03). An example of an ACh-v-^{3}H-NMS competition assay for D99A is shown in figure 3.12 (panel a). The reduction in ACh affinity for D99A was twice the reduction in affinity noted for NMS for this mutant. For F197A and W378A ^{3}H-QNB was used as the radioligand for ACh competition assays, see figure 3.12 (panel b) for representative data. F197A only had a very minor (<2-fold) effect on the affinity of ACh, in contrast to the ~14 fold reduction observed for W378A The mean slope factor for F197A was unchanged. A Hill coefficient greater than 1 was consistently observed for W378A in ACh competition assays and the mean n_H value was 1.34, hinting at the possibility that this mutant may display co-operativity for ACh binding.

Figure 3.9. Representative Acetylcholine Competition Binding Curves for Cysteine Mutants

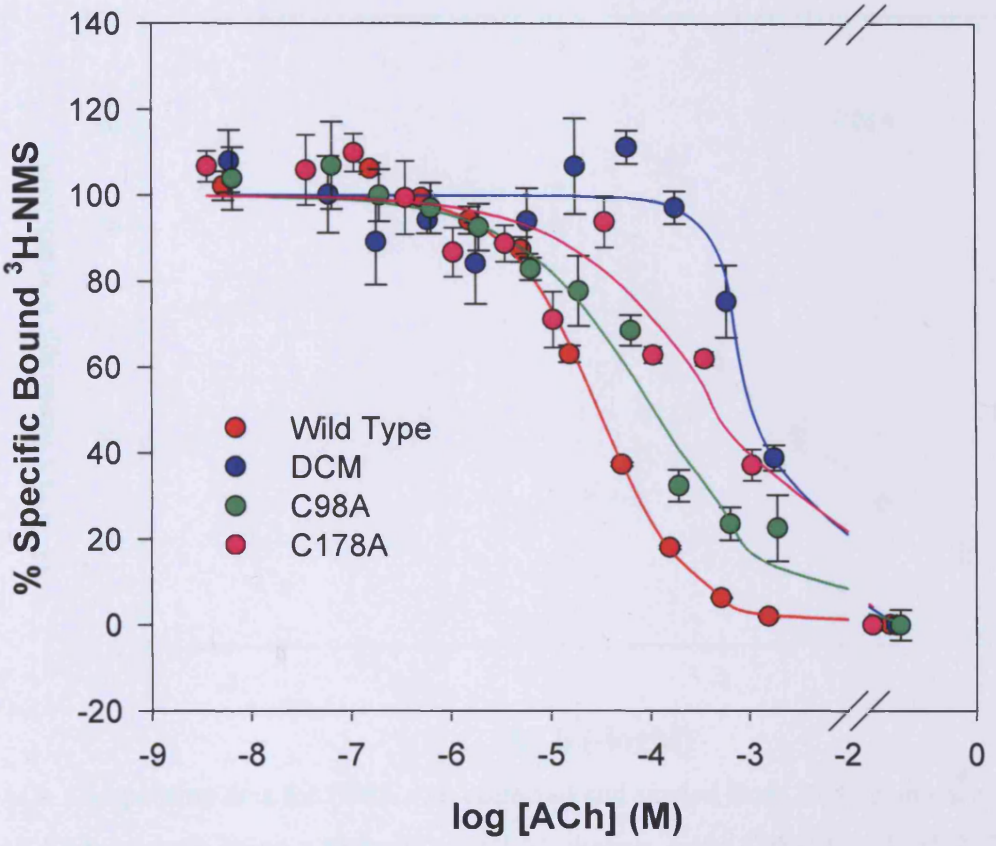

Assays were performed on COS-7 cell membranes transiently expressing WT or Mutant receptors. Protein concentration was 10-30μg/mL. Data points are the mean of quadruplicate measurements ±S.E.M and represent at least three independent experiments. Curves are fitted using the Hill equation. Binding curves have been subject to Cheng Prussof correction. 10^{-6}M Atropine used for non-specific controls. [^{3}H-NMS] used for WT = 10^{-10}M and for Mutants = 3 x 10^{-9}M . **WT** pIC_{50}= 4.51±0.01, n_H = 0.95; **C98A/C178A** pIC_{50} = 2.90±0.04, n_H = 1.73; **C98A** pIC_{50}= 3.96±0.10, n_H = 0.65; **C178A** pIC_{50}= 3.29±0.08, n_H = 0.65.

Figure 3.10. Analysis of Pooled Data for C98A ACh Competition Binding Experiments (2-site model).

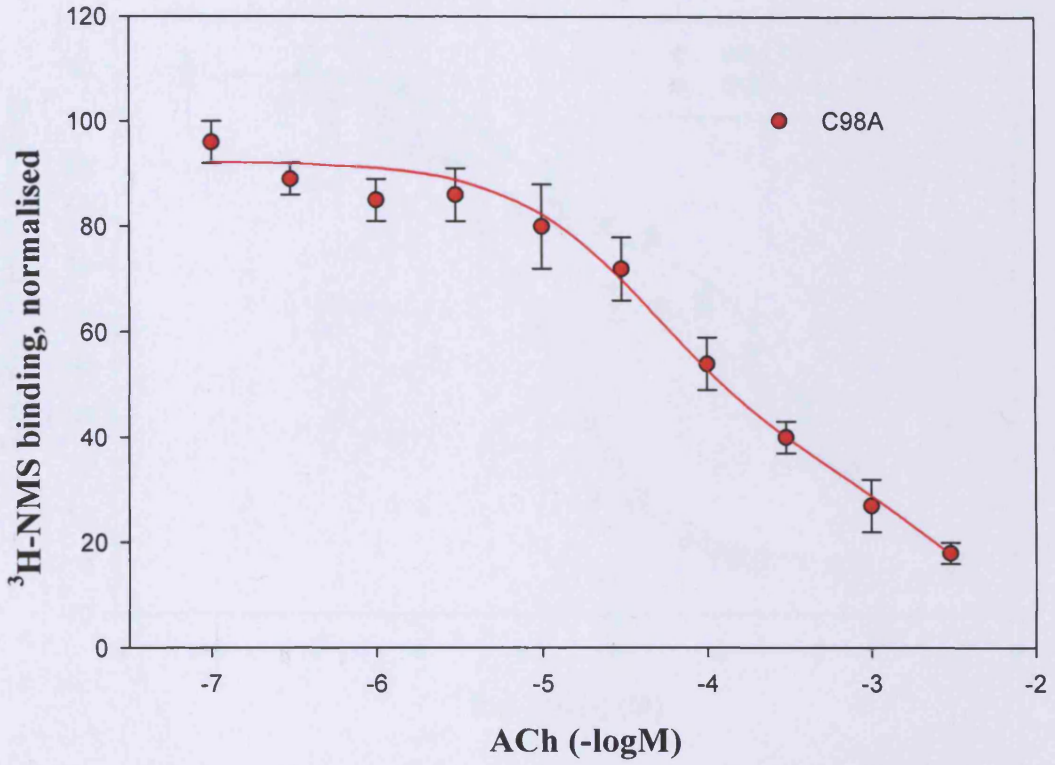

ACh Competition data for C98A was collected and pooled from 8 independent experiments ±S.E.M Analysis using a two site model of binding gave: **C98A** Fr (H) 60.7±9.1 pKH = 4.33±0.22 pKL =2.58±0.21. Data was pooled and normalised using the percentage of the ratio of mean dpm minus non-specific binding and the mean dpm for specific binding for all ACh competition data. i.e. (mean dpm – B_{NS}) / (B_{TOT} – B_{NS}) x 100

Figure 3.11. Detailed ACh Competition Binding Experiment to Further Characterise the C98A Mutant Using a 2-Site Model of Binding

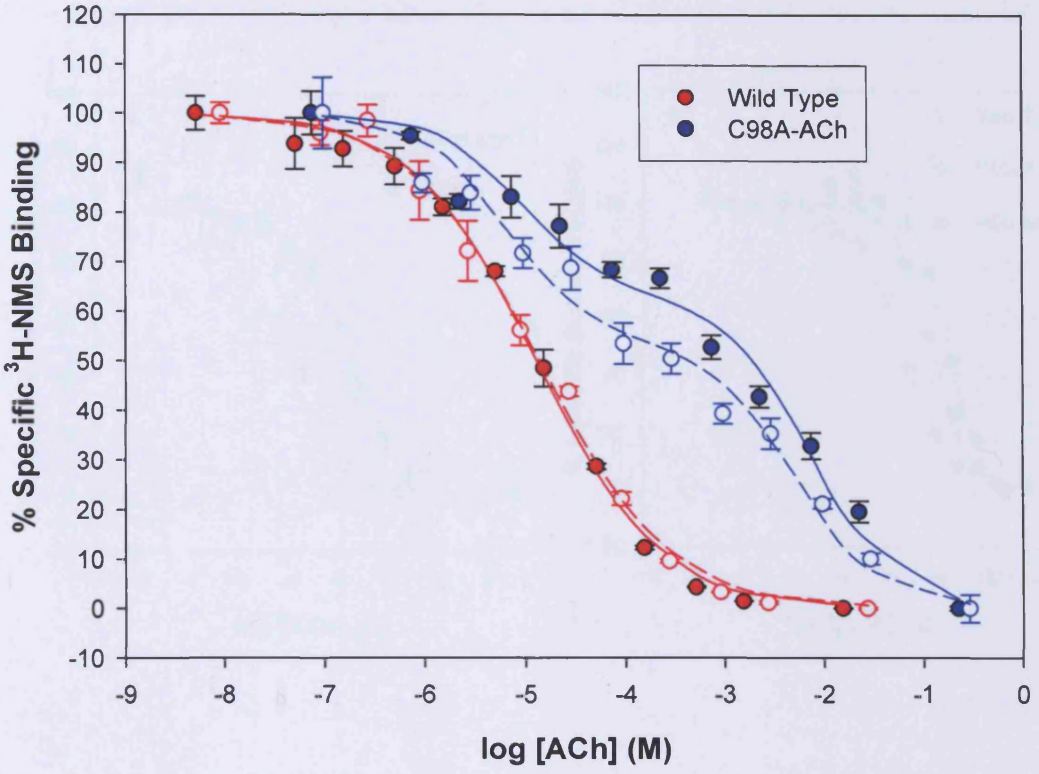

2-site analysis of competition binding curve for C98A and WT control. Assays were performed on COS-7 cell membranes transiently expressing WT or mutant receptors. Protein concentration was = 10-30μg/mL. Samples counted for 60 min. Data points are the mean of quadruplicate measurements ±S.E.M and curves are fitted using a 2-site model of binding, where Fr(H) = fraction of high affinity sites. Two ^{3}H-NMS concentrations were used for WT = 10^{-11}M, for A high [^{3}H-NMS](solid blue points and line) = 2 x 10^{-9} M and a low [^{3}H-NMS] = 2 x 10^{-10}M (dark blue dashed line) **WT high [^{3}H-NMS]** pIC_{50} = 4.88±0.06,nH = 0.71±0.06, **WT low [^{3}H-NMS]** pIC_{50} = 4.85±0.07; n_H = 0.70±0.06; **C98A high [^{3}H-NMS]**, FrH = 0.37±0.01; high affinity site pIC_{50} = 5.11±0.002 pKL= 2.23±0.002; **C98A low [^{3}H-NMS]** Fr(H)=0.48±0.03, pKH = 5.17±0.03, pKL = 2.30±0.03.

Figure 3.12. Representative Acetylcholine Competition Binding Curves for TM Domain Mutants.

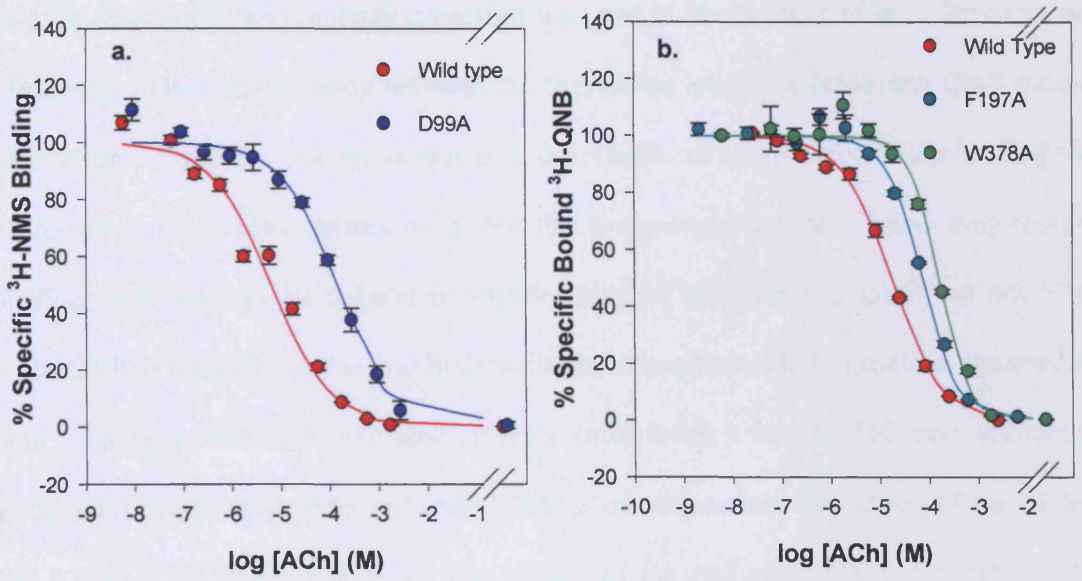

Representative acetylcholine competition binding curves for TM domain mutants. Assays were performed on COS-7 cell membranes from cells transiently expressing WT or mutant receptors. Total [protein] 10-30 µg/mL. Data points are the mean of quadruplicate measurements ±S.E.M and curves are fitted using the Hill equation. pIC_{50} values are corrected using the Cheng Prusoff correction factor. Curves are representative of at least 3 independent experiments.

a. WT IC_{50} = 5.21±0.02, n_H =0.84±0.01; **D99A** IC_{50} = 3.85±0.03. n_H =0.86±0.02.

b. WT IC_{50} = 4.70±0.01, n_H =0.83±0.02; **F197A** IC_{50} = 4.11±0.01, n_H =1.19±0.03; **W378A** IC_{50} = 3.68±0.02, n_H =1.44±0.04

3.4 – Discussion and Conclusions

A graphical summary of the effects of mutations in the E2 loop on NMS affinity is presented in figure 3.13. and compared with the effects on ACh affinity In general the E2 loop (excepting C178A) mutants expressed well and at levels close to wild Bmax values. There was a slight discrepancy between the expression levels for NMS and QNB binding sites for some mutants. The Bmax relates to the number of complete or viable binding sites expressed at the receptor surface or at least that are accessable to the ligand. Any receptor binding sites that may be trapped in vesicles may be accessable to QNB but not NMS. Since QNB is a tertiary amine and hydrophilic it is therefore able to penetrate vesicles and bind to receptors that have their binding site located inside a vesicle. This may account for the small differences in NMS and QNB binding site expression. Mutations of the E2 loop had a limited (< 10-fold) effect on the affinity of the antagonist NMS. Collectively this suggests that E2 loop residues have limited role in the binding of NMS and are unlikely to make highly specific direct contacts with the antagonist. They may be similar to certain residues found in the second shell of the M_1 mAChR centrally located transmembrane binding site (Lu et al., 2001), for example, mutations of residues L102 and A103 of TM3, I161 and L162 of TM4 and V409 and S411, all in close proximity to the binding site, but whose mutation to alanine reduced NMS affinity less than 10-fold. The data presented in this thesis supplements the previous study of Matsui et al (1995) which showed the effects of other E2 loop mutations on ACh and NMS binding affinity. Mutation of cysteine 178 to alanine did show a ~10-fold reduction in affinity for NMS, but this is much less than that reported for the homologous mutation in the M_3 mAChR (Zeng et al., 1999) where a 866-fold reduction in NMS affinity was observed for the analogous mutant. It must be noted there were differences in the buffering conditions used for this study and that of Zeng et al. That is the buffer used by Zeng et al contained 25mM sodium phosphate, 5mM $MgCl_2$ and

no HEPES unlike the binding buffer used in this study (see methods section 2.11). This affected the free ion concentrations and consequently affected binding affinities. Mutation of the conserved C98 residue significantly reduced the affinity (~40-fold) of NMS again, less than reported by Zheng et al (Zeng et al., 1999) in the analogous C140A mutant. The results of the present study are consistent with the role of the S-S bond in maintaining receptor stability and therefore stability of the binding site, as mutation to alanine severely reduced receptor expression and effected a significant loss of affinity for NMS, QNB and ACh, although these effects are not necessarily related.

Consistent with Savarese et al and Zeng et al (Savarese et al., 1992. Zeng et al., 1999) the maintenance of the S-S bond is critical for correct folding of the protein In our study even after atropine rescue C98A and C178A expressed NMS & QNB binding sites at only ~40% of WT levels. The paradox here is the somewhat better expression of the double cysteine mutant C98A/C178A which expressed at ~70% of WT levels (when the growth media was supplemented with atropine). The implication is that without either C98 or C178 the receptor is able reach the plasma membrane in the correct orientation more often than if one or other of the S-S bonded cysteine is singularly present. There is the possibility that the single cysteine, becoming randomly bonded to other proteins in the endoplasmic reticulum by a process described as thiol dependent retention (Reddy and Corley, 1998), negates receptors ever reaching the cell surface, instead remaining trapped in the intracellular milieu. Hence, without either cysteine present as in the C98A/C178A mutant, the opportunity for thiol dependent retention is prevented, allowing a greater ratio of atropine rescued double cysteine mutant receptors to correctly fold and reach the membrane surface properly orientated. Nevertheless, it was expected, having rescued expression of the S-S bond mutants, that the disruption of the S-S bond would have a more pronounced effect on

the binding of NMS because of the large reductions in NMS affinity witnessed by Zeng et al (Zeng et al., 1999) for the analogous mutations of the M_3 receptor.

Figure. 3.13. Effects of E2 Loop Mutations on NMS and ACh Affinity

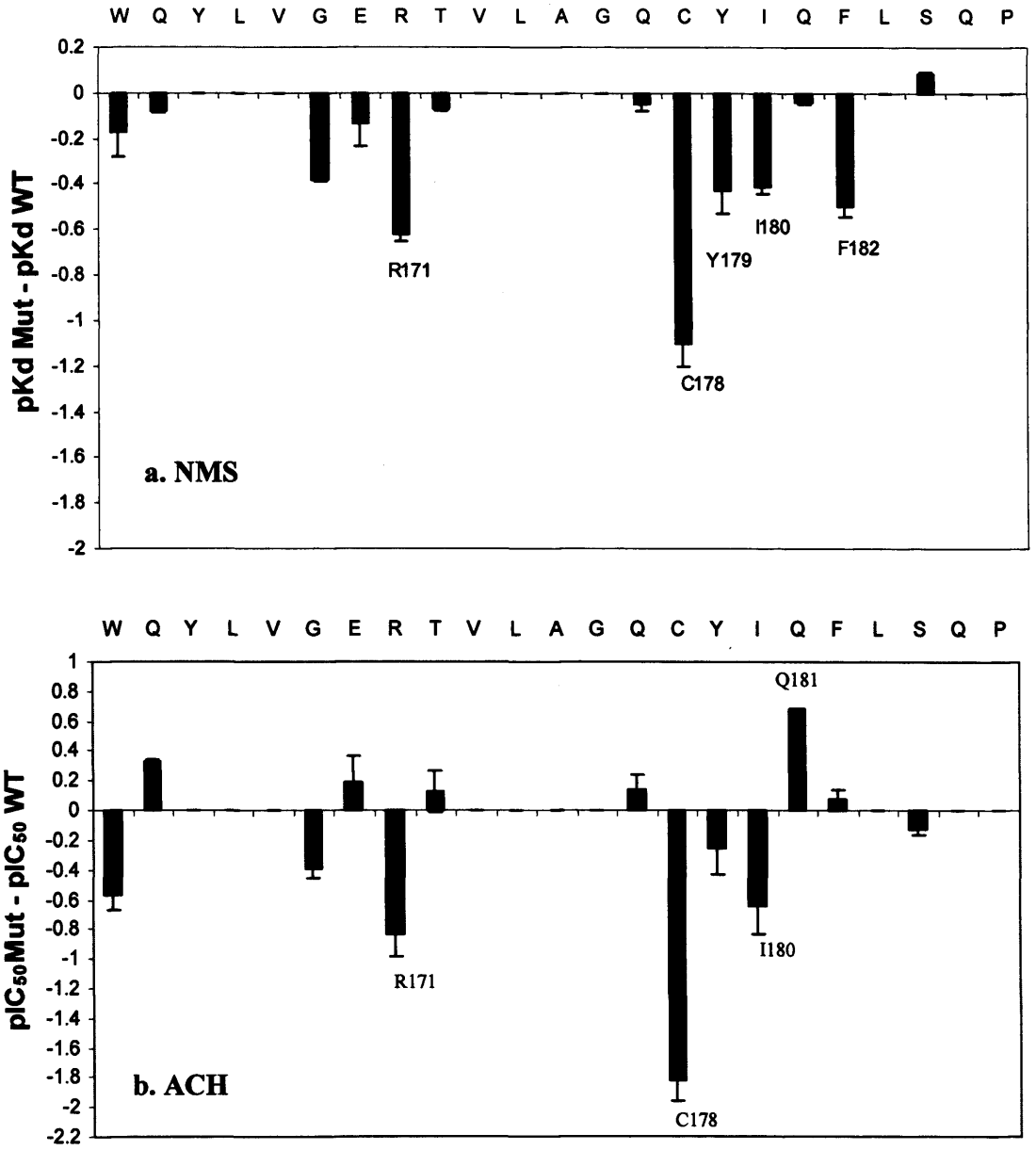

Effects of Mutations of E2 loop residues of M_1 mAChR on the binding affinities of NMS and ACh. Results are mean ±S.E of at least three determinations. Bars represent log difference in binding affinity compared to WT and includes data from Matsui et al(Matsui et al., 1995). E2 Loop residues on the X-axis are represented with the single letter code. Both decreases and increases are shown. **a.** Effects of mutations on the affinity of NMS, mean pKd of NMS at WT receptors = 9.87±0.05. **b.** effects of mutations on the affinity of ACh, mean pIC_{50} of ACh at WT receptors = 5.00±0.04.

The double cysteine mutant C98A/C178A showed a similar reduction in NMS affinity to C98A and slightly greater than that of the C178A and C178N mutant. The fact that the binding affinity of NMS was not as strongly reduced by C178A, suggests that the integrity of the TM domain residues (D105, Y106, F197, N382, Y381, W378) (Hulme and Lu, 1998) is more critical for NMS binding than is the maintenance of the S-S bond. The ~3-fold reduction in affinity found for R171A, I180A, F182A (all conserved in the mAChR sub-types) and Y179A, provides evidence that these residues may play a secondary role in forming and augmenting the environment for the NMS binding site. In general, these observations may be consistent with the role of homologous E2 loop residues that are in close proximity to the retinal binding pocket of rhodopsin (Li et al.2004). The E2 loop may form a second shell of contacts that help maintain the correct conformation of the binding site required for the agonist to fit most efficiently.

The much larger effect of F197A (>100-fold) and W378A (>400-fold) mutations on NMS affinity are consistent with the theory that the NMS side chain penetrates and binds deep inside the transmembrane domain. According to the homology model both F197 and W378 (both highly conserved residues in the rhodopsin family of GPCRs) lie at the base of the binding pocket, where they may participate in Pi-Pi bond interactions with the phenyl ring of the NMS side chain. Looking at the relative positions of the benzene ring of NMS in relation to the phenyl ring of F197 and the indole ring of W378 in the M_1 homology model, it is possible that a T-shaped benzene-phenol dimer interaction is possible with F197 and a sandwich benzene dimer pi-pi bond is possible with W378 (Sinnokrot and Sherrill, 2004). The T-shaped dimer is thought to have a lower binding energy than the sandwich dimer and the results of the present study support this in that mutation of W378 caused a greater loss of NMS affinity than did F197A. This finding is consistent with the W378F mutation studied by Wess et al (Wess et al., 1993) which gave less than 10-fold reduction in the

affinity of NMS, thus confirming the importance of the presence of an aromatic residue at this critical position in the transmembrane domains of the rhodopsin-family of GPCRs. Interestingly, F197A and W378A had much smaller effects (2-fold and 10-fold respectively) on QNB binding as previously reported for other mutations of certain TM domain residues, Y381A, Y404A, C407A and Y408A (Lu et al., 2001) (Ward et al., 1999a). This highlights the different modes of binding of NMS and QNB and reflects their differing molecular structures. A graphical summary of antagonist binding data for TM domain mutants is presented in figure 3.14.

Apart from the effect of removing the S-S bond via the cysteine mutants, point mutations of the E2 loop had virtually no effect on the binding of QNB with all E2 loop residues showing less than 3-fold reduction in affinity for QNB. Evidence provided by this study supports the theory of different modes of binding of NMS and QNB. In addition D99A reduced the affinity of NMS more than 10-fold, whereas the reduction in QNB affinity was only ~3-fold. This finding may suggest an alternative mode of entry into the binding site for the hydrophobic QNB molecule, perhaps via the lipid membrane region through the TM domains. This idea is based on the proposal that D99 is part of an initial ligand docking mechanism (Jakubik et al., 2000) for hydrophilic ligands such as NMS. Therefore it is very unlikely that any residues of the E2 loop make pivotal binding contacts with QNB. Mutation of central binding site residues D105, Y106 (TM3) (Lu and Hulme, 1999a) and N382 (TM6) (Ward et al., 1999a) all caused large reductions in ^{3}H-QNB affinity, suggesting that QNB also binds in the central binding cavity of the M_1 mAChR. C98A and C178A reduced QNB affinity ~30-fold, C178N 15-fold and the C98A/C178A mutant ~60-fold. Although significant reductions in affinity were seen for C98A, C178A and C178N and C98A/C178A, it is suggested that this loss of affinity is symptomatic of the perturbation of the integrity of the central binding site, effectively "taking the lid off" the

M_1 mAChR binding pocket perturbs the binding of QNB. Since mutation of F197 and W378 at the base of the binding cavity cause only minor reductions in affinity, but the disruption of the E2 loop structure caused greater reductions in affinity, it may be supposed that QNB binds more superficially in the binding pocket than NMS. This is further supported by the finding of the present study, where the reductions in QNB affinity were greater than that of NMS for the cysteine mutants This implies that maintenance of the overall E2 loop structure, rather than individual amino acid side chains, is somewhat more important for the binding of QNB than for NMS. Figures 3.13 and 3.14 summarise the NMS, ACh and QNB binding data for C98A and C178A.

The effects of E2 loop point mutations on ACh affinity were comparable to those mutations of "second shell" residues of the TM domains, L103, S109 and L386 for instance. Significant reductions in ACh affinity were recorded for R171A (~7-fold) and I180A (~5-fold). figure 3.13 (panel b) summarises the effects of mutations of E2 loop residues on ACh affinity and includes the data collected previously by Matsui et al (1995). Looking at figure 3.13 it appears that that mutation of E2 loop residues produce both selective increases and decreases in ACh affinity. It is interesting to note that none of the E2 loop mutations caused an increase in NMS affinity whereas alternation between increased and decreased affinity was observed for ACh, most significantly by the Q181A mutant from the Matsui study which increased ACh affinity 5-fold. Although minor, the slight increases and decreases in affinity noted for the E2 loop mutants may .....*continued on page 138*

Figure 3.14. Summary Binding Data for TM Domain Mutants

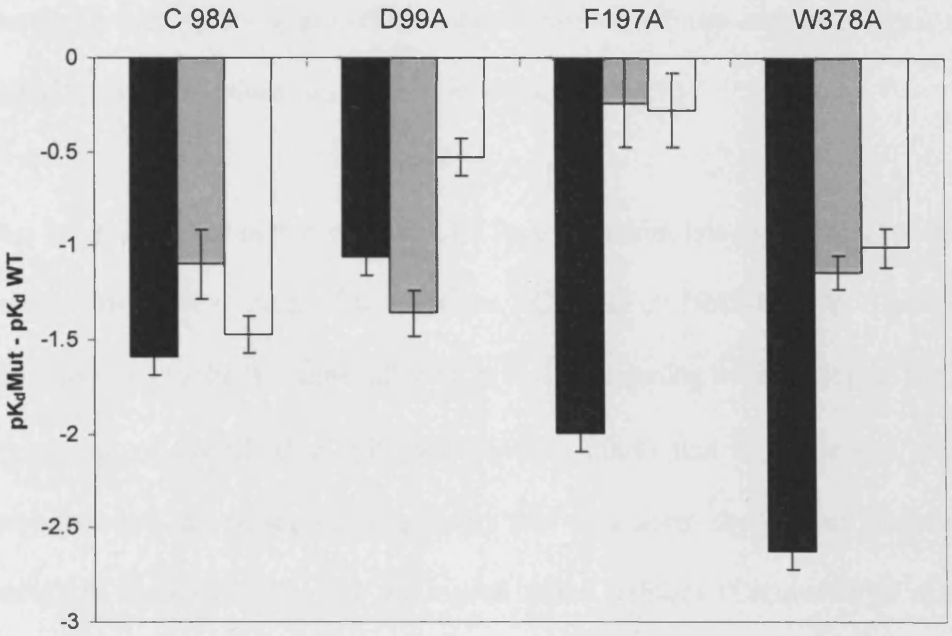

Effects of C98A, D99A, F197A and W378A mutations on NMS (black bar). ACh (grey bar) and QNB (white bar) binding affinity. Results shown are the mean ±S.E. of at least three determinations. Bars represent the log difference in binding affinity relative to WT binding affinity constants, where, WT- pKd NMS = 9.87±0.04, pIC_{50} ACh = 5.00±0.05 and pKd QNB = 10.68±0.04

be consistent with a tertiary structure similar to that of rhodopsin. This pattern of affinity changes might be consistent with a β-strand structure for the residues C-terminal to C178 whereby inwardly facing mutations cause a loss of affinity and in contrast mutation of outwardly facing residues cause minor increases in affinity.

It has been suggested in this study that E2 loop mutations lying C-terminal to the conserved cysteine residue have more of an effect on ACh than on NMS binding. These residues are predicted to form the β-4 sheet alluded to at the beginning of this chapter and support the conclusions of Javitch et al (Shi and Javitch, 2004) that it is the β-4 sheet structure protruding into the central binding cavity that may assist the correct binding of ligands. Indeed, in rhodopsin it is the analogous polar residues (Carravetta et al., 2004) and associated water molecules (Okada et al., 2002) of the E2 loop, folding into the retinal binding crevice that assist the rapid photoisomerisation of the retinylidene chromophore. Residues of the E2 loop of rhodopsin (in both β3and β4) achieve this by stabilising the developing partial positive charge at the centre of the polyene chain by solvation via a functional water molecule hydrogen bonded to the binding pocket via E2 loop residues (Carravetta et al., 2004). Although some reductions in affinity for both ACh and NMS (but not QNB) were observed for the analogous residues in the β-3 and β-4 sheet of the M_1 mAChR, the reductions were not of an order of magnitude that would suggest critical roles in ligand binding for the E2 loop in the central binding site. However a significantly different role is played by the Glu 181 residue of rhodopsin than that of the apparently redundant analogous M_1 mAChR residue, E170. In rhodopsin the Glu181 residue is central to the environment of the retinylidene Schiff base in the active metarhodopsin II photoproduct (Yan et al., 2002).

The cysteine mutants, C178A, C178N and C98A/C178A reduced ACh affinity ~70-fold, ~100-fold and ~80-fold respectively. Disruption of the S-S bond reduced the binding affinity of the agonist significantly and these effects are comparable with the mutation of the binding site residues Y106 and Y381. What still remains to be resolved however, is the question of whether or not the sulphur atom of the cysteine at position 178 in The M_1 receptor is itself involved in the binding of acetylcholine, or whether it is the global destabilising effect of the removal of the S-S bond on the transmembrane domain that accounts for the loss in ACh affinity. The fact that the C178A mutation reduces ACh affinity~70-fold, compared to only a ~10-15-fold loss in NMS affinity supports the idea that C178 is a more important residue for the binding of ACh than NMS. The alternative scenario is that C178A destabilises the ACh binding conformation to a greater extent than the NMS binding site without actually making any critical contact with ACh itself.

As the data suggested in the results section (figure 3.10 and 3.11), the C98A and mutant may express both a high and low affinity site for the binding of ACh. Further evidence for two populations of binding sites for the C98A mutant are seen in the consistently low Hill coefficients (mean n_H = 0.47±0.06) for this mutant. As has been shown by Avlani et al (Avlani, 2005), unusual intramolecular disulphide bonding may be possible between the cysteine of the E2 loop and either of the two cysteines in the E3 loop. It is possible therefore to imagine that for the C98A mutant where the C178 residue is free to form a non-native disulphide bond with either C391 or C394 of the E3 loop that multiple populations of receptors with different binding sites may exist. The data suggests that two populations of binding sites do exist, one of high affinity with pK = 4.7 and a low affinity site with pK = 2.5. The other possible explanation of the low Hill coefficient seen for C98A is that of negative co-operativity, possibly as a consequence of intermolecular S-S bond formation with an adjacent free C178 residue, effectively forming a dimeric receptor

complex. Due to the length of the E2 loop, it is more likely that an intramolecular S-S bond creates the two binding site phenotype of the C98A mutant. Data for the double cysteine mutant suggests that without either cysteine, no unusual disulphide bonds could be made, since the double cysteine mutant did not require analysis by a 2-site model of binding. This adds more weight to the existence of unusual S-S bond formation for the single cysteine mutants and the consequent generation of two seperate populations of receptors with two distinct binding sites.

The hypothesis that ACh binds more superficially in the binding pocket, than NMS, is borne out by the finding that neither F197A nor W378A caused a dramatic loss of affinity seen for NMS. This is analogous to the N382A mutation (Ward et al., 1999a) which caused ~4000-fold loss of NMS affinity but only a 5-fold reduction in ACh affinity. The conclusion to be drawn from this is that neither F197 nor W378 are critical for the binding of ACh, although W378 may play a more important role as part of the aromatic cage. The mutation of D99A caused a larger effect on the affinity of ACh (>20-fold) than NMS (10-fold). These effects are larger than reported for the analogous mutation from aspartate to the uncharged polar asparagine residue in the M_1 or M_2 receptor (Fraser et al., 1989; Vogel et al., 1999) and are consistent with the proposition that D99 may act as a primary ligand docking residue. From the homology model it appears that D99 lies too far from the internal aromatic cage residues of the core ligand binding site to have any direct contact with bound ligand. To account for the losses in ACh and NMS affinity seen for D99A in this study, it would be reasonable to imagine that D99 participates in the initial binding of ligands prior to their displacement to the central binding pocket. W157 (conserved in all mAChR subtypes), another residue proposed to act in conjunction with D99, is also postulated as a primary docking residue (Lu et al., 2001) and displays large reductions in ACh and NMS affinity (~100-fold) (Lu et al., 2001). A mechanism for the mandatory

docking step was proposed by Lu et al. (Lu et al., 2001) and expounded by Heitz et al. (Heitz et al., 1999), whereby an indirect conformational switch provided by P159 interfacing with the ligand leads to the contribution of W157 to high affinity binding and receptor activation. Our results suggest that D99 may also participate, although to a lesser extent, in a similar mechanism of ligand docking whereby the negatively charged polar side chain of D99A stabilises acetylcholine as it binds with high affinity to W157 before the ligand is transferred into the core binding pocket. It may now be appropriate to revise the M_1 mAChR homology model to incorporate the new evidence and that reflect the binding energies documented here. The E2 loop may pack against the upper regions of the transmembrane domains, helping to complete the environment of the agonist and antagonist binding site. The differences in binding energies, caused by alanine substitution of the E2 loop apply to the ground state of the receptor only. It is likely that these interactions might well be different in the activated state of the receptor

.

Chapter 4.

Functional Studies

4.1. Introduction.

G-protein coupled receptors can exist in multiple states, minimally in an inactive state that can be stabilised by the binding of antagonists and an active state stabilised by the binding of agonists. A network of van der Waals contacts and hydrogen bonds between the transmembrane helices, often between conserved residues, is responsible for the maintenance of the inactive state. These links are described in the rhodopsin model (Palczewski et al., 2000) and the M_1 homology model (Hulme et al., 2003). An active conformation can be promoted by the binding of agonists that disrupt this system of inter-helical interactions, creating a revised system of interactions that promote the stabilisation of an active conformation of the receptor. More specifically, it has been suggested by mutational studies (Lu and Hulme, 2000) and disulphide cross-linking studies (Sheikh et al.,1996; Han et al., 2005) that it is the agonist-induced relative movement of TM3, TM6 and TM7 that characterises the active conformation of GPCRs. Recently, it has also been proposed that conformational changes at the interface of dimeric receptor also plays an important role in receptor activation (Guo et al., 2005). However, the details of the mechanistic process remain to be elucidated.

The binding of an agonist, such as acetylcholine, at the exo-facial side of the receptor activates the selection of specific classes of hetero-trimeric G-proteins on the cytoplasmic surface of the receptor. Conformational rearrangements following agonist binding expose residues on the intracellular surface that promote dynamic and selective interaction with a set of G-proteins. In particular, intracellular loops I2 and I3 determine the specific interactions that determine which G-proteins are activated. These interactions are extensively reviewed by Wess et al (Wess et al., 1996; Wess et al.,

1998). Furthermore, which class of G-protein is activated may depend on the activating agonist Akam and colleagues (Akam et al. 2001) demonstrated, using ^{35}S-GTPγS binding studies that M_3 receptors preferentially selected $G_{i\alpha}$ over $G_{q/11}$ when stimulated with pilocarpine as opposed to methacholine. The binding of G-protein to the cytoplasmic surface of the receptor catalyses the release of GDP from the G-protein, enabling the binding of GTP which in turn promotes the release of the G-protein from the receptor. The activated G-protein then continues the signalling pathway via effector proteins, located in the membrane, specific to the receptor and G-protein sub-types.

The endogenous activation of the mAChR class of GPCRs is mediated by the small neurotransmitter molecule acetylcholine. ACh consists of an acetoxy side chain and a trimethylammonium head group (see figure 2.2 in Chapter 2 Methods). Site-directed mutagenesis studies in this lab (Hulme and Lu, 1998; Lu et al., 2002) have suggested that an aromatic cage consisting of residues Y106A, Y381, W378, Y404 and Y408 is critical for the binding of ACh and consequent activation of the receptor. Close proximity of the trimethylammonium head group of a bound ACh molecule to the residues of the aromatic cage suggest the potential mechanism for activation. It is believed that it is the tightening of the aromatic cage around the trimethylammonium head group that disrupts the hydrogen bond and van der Waals network that stabilises the inactive ground state, leading to conformational re-alignment of the inter-helical contacts into the activated state capable of G-protein interaction (Han et al., 1996a; Han et al., 2005).

The extended ternary complex model of receptor activation (see Materials and Methods figure 2.2) is a useful model to help us understand the effect of point mutations on receptor-G-protein interactions. In the basic scenario, assuming a predefined conformational equilibrium is in operation, agonists bind with greater affinity to the

activated state than the inactive ground state. This gives two conformational states, a low affinity state, and a high affinity state, the switch from one state to the other is determined by the product of the conformational constant K and the cooperativity factor for agonist binding, α. G-proteins couple selectively to the activated state of the receptor, with an affinity constant K_G Accepting that the bound G-protein is in the GDP-bound state, the exchange of GDP-GTP is governed by the rate constant K_{cat}

Using an evolutionary trace approach and correlation of published mutational studies Madabushi et al (Madabushi et al., 2004) identified commonly important residues in a diverse set of GPCRs. They showed that there may be generally conserved mechanisms for GPCR signal transduction. The binding of a ligand to the receptor induces conformation changes, leading to G-protein coupling and activation. The mechanism of activation is mediated by 3 main regions of the receptor, described (Madabushi et al., 2004) as trigger, linking core and coupling regions. Residues in the region of the ligand binding pocket, on binding ligand, tend to act as triggers of ligand induced conformational change. Mutation of these residues mainly reduces the affinity of ligands. Residues of the linking core region lie in between the binding site and the G-protein binding surface. Reductions in activation, expression and incorrect folding are associated with mutants found in this region because these residues tend to make interactions between the TM Helices. The coupling region found at the cytoplasmic interface is important for G-protein interactions and many mutations in this region can create constitutively active mutants.

The substitution of a particular amino acid with a methyl group-containing alanine residue effectively removes the side chain of the native residue effectively leaving an inert stub or hole. This can have, basically, four possible consequences (Hulme et al., 1999) (summarised in figure 4.1). Firstly the mutation can have no effect. This suggests

that the substituted residue is inconsequential in terms of receptor structure and may be described as a *filler* residue. The second possible outcome is that the mutation destabilises the active and inactive conformations of the receptor, without actually reducing the signalling capacity of those receptors that were properly expressed. In this case it is implied that the substituted residue makes an important contact necessary for the structural stability of the receptor, and it may be described as-a *stabiliser* residue. Subsets of this category are the *ligand anchor* residues that reduce ligand binding affinity without affecting signal efficacy. The implication is that, although the ligand has a lower affinity for the receptor, the ligand contact residue is not selectively important for the signalling conformation. Thirdly, mutated residues that selectively destabilise the ground state while simultaneously increasing ligand affinity, basal activity and signalling efficacy fall into the category of *constraining* residues. The characteristics of this type of residue suggest that they are involved in intra-molecular bonding networks that maintain stability of the ground state but are broken or attenuated in the activated state. In the fourth category mutations of *activator* residues cause loss of signalling efficacy, but do not affect levels of expression or stability. There is potential for this type of residue to fall into three different sub-groups of activator residues: i) the *intra-molecular activator* residues that make contacts that stabilise the active state at the expense of the inactive ground state; ii) The *ligand transducer*, whereby the residue only forms an inter-molecular contact with the ligand in the active state; iii) The *G-protein transducer* residue, which forms inter-molecular contacts with the G-protein in the activated state. In addition to the types of residues mentioned it is also possible to imagine residues that fulfil dual roles. For example a residue may exert a constraining function stabilising the ground state but alter roles when the receptor is activated, turning into a residue important for G-protein binding or signal transduction, for example.

The M_1, M_3 and M_5 mAChR subtypes activate the $G_{q/11}$ class of G-proteins stimulating phospholipase C_β isoforms to break down inositol 4, 5 bisphosphate (PIP_2). Breakdown of PIP_2 liberates two second messengers, diacylglycerol leading to activation of protein kinase C and inositol triphosphate (IP_3) that acts to mobilise intracellular stores of calcium modulating slow potassium and calcium conductances. IP_3 is then sequentially degraded by a series of phosphatase enzymes back into inositol which is then re-incorporated back into phosphatidylinositol in the membrane to begin the process anew. It is the turnover of phosphoinositides that can be measured to gain insight into the functional characteristics of mutant receptors. The PI assay, developed by Berridge et al. (Berridge et al.1983) is a robust method of measuring the accumulation of total ^{3}H-inositol labelled phosphoinositides. Essentially, by blocking phosphatase enzymes with lithium chloride, phosphoinositides produced upon acetylcholine stimulation of the receptor, are prevented from being recycled and can be collected and counted after elution from an anion exchange column (see Methods section 2.14).

Figure 4.1. Possible Outcomes of Alanine Scanning Mutagenesis on Receptor Function.

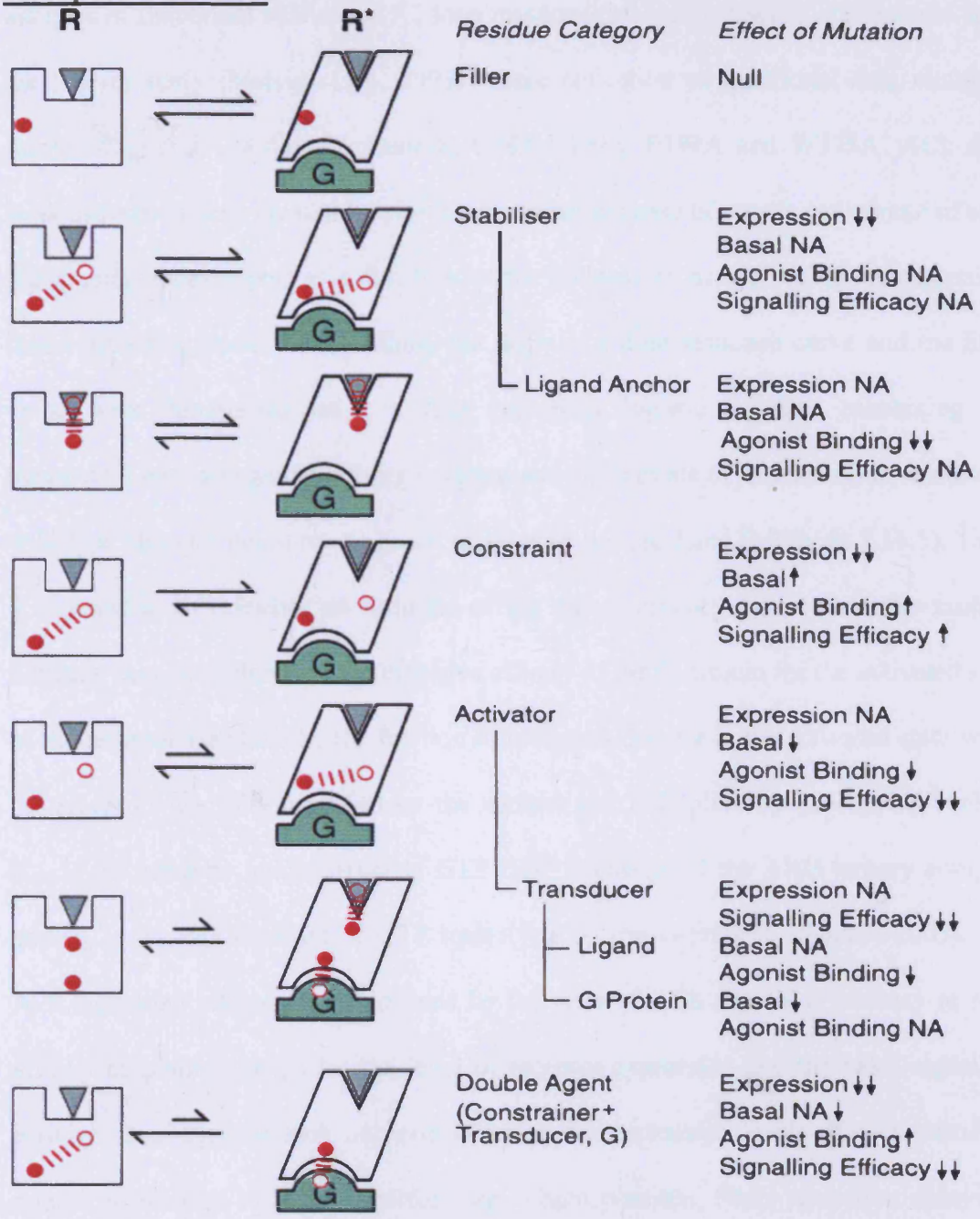

Classification of the function of amino acid side chains in GPCR activation by alanine scanning mutagenesis. The four main categories being, *filler, stabilising, constraining* and *activating*.Taken from (Hulme et al., 1999). See text for more detailed explanation.

Presented in the this chapter are representative data, complete tabulated results and analysis of functional studies for E2 loop mutants, (including a set of six mutants from the Matsui study (Matsui et al., 1995) where collection of functional data remained outstanding) and TM domain mutants, C98A, D99A, F197A and W378A. ACh dose response curves were created by plotting the mean increase of counts per minute of total phosphoinositides (dpm) as a function of the increase in acetylcholine concentration. Basal signalling, maximal signalling, the slope of a dose response curve and the EC_{50} value were determined using a four parameter logistic function combining the parameters with an agonist affinity constant and an estimate of expression in relation to wild type allows a measure of agonist efficacy to be calculated (Methods 2.16.5). Thus, it is possible to calculate an estimate of the signal efficacy for a particular mutant. Efficacy may be defined as "the effective affinity of the G-protein for the activated state of the receptor weighted by the fraction of receptors that are in the activated state when the receptors are fully occupied by the agonist and multiplied by $(1+K_{cat}/K_h)$" where K_{cat} is the catalytic rate constant of GTP-GDP exchange of the ARG ternary complex and K_h is the rate constant of GTP hydrolysis by the G-protein. (Hulme, 2005). The ACh signalling efficacy is determined by the ratio of ACh signalling potency to ACh affinity constant adjusted for the level of receptor expression and the basal signalling activity. Data analysis took into consideration the expression levels of each particular mutant in relation to WT by performing, where possible, NMS saturation assays on residual transfected cell membranes to obtain Bmax values from which the level of functional expression can be calculated for use in the calculation of efficacy. Where NMS saturation assays were impractical levels of expression were derived from previously performed QNB saturation assays, for example, for the W378A mutant.

4.2. Results

4.2.1. Basal and Maximum Signalling and Potency

Initially an assay was performed using plasmid DNA encoding WT M_1 mAChR to determine the optimal amount of plasmid DNA required for transfection into COS-7 cells to maximise the signalling response. For comparison with mutant DNA, where expression of mutant receptors required atropine rescue, the experiment was performed on cells grown to confluence in media alone or media containing atropine (10^{-6}M). The atropine was carefully washed off the cells by at least four changes of PBS before conducting the PI turnover assay. The data presented in figure 4.2 emphasises that optimising the plasmid concentration for transfection of cells was necessary. It can be seen that 30μg of DNA actually reduced the maximum PI signal of wild type receptors by ~1500dpm (~40%-50%) compared to transfection with 7.5μg DNA plasmid. Furthermore it was shown that wild type basal activity could be inhibited by subjecting receptor expressing cells to a dose of 10^{-6}M atropine. This reduced dpm by ~20%-40% of background signalling for the whole range of DNA concentrations. This experiment also illustrates that basal signalling of WT could be quite high. Throughout the course of the PI turnover assays there were occasions when the basal activity of wild type receptors was unexpectedly high, although, not consistently so. Overall, mean basal activity of wild type was 682.7±107.4 dpm and mean ACh stimulated maximum response was 3150±451 (n= 29) Null transfections were used to determine the background signal. Mean dpm for null transfections were 250±23.1 (n=3). Corrected for the null background, the basal signalling activity of the WT receptor was 432 dpm and the mean ACh stimulated maximum signalling activity was 2984 dpm.

Figure 4.2. Optimisation of DNA Plasmid Concentration for Transfection of COS-7 Cells for PI Turnover Assays

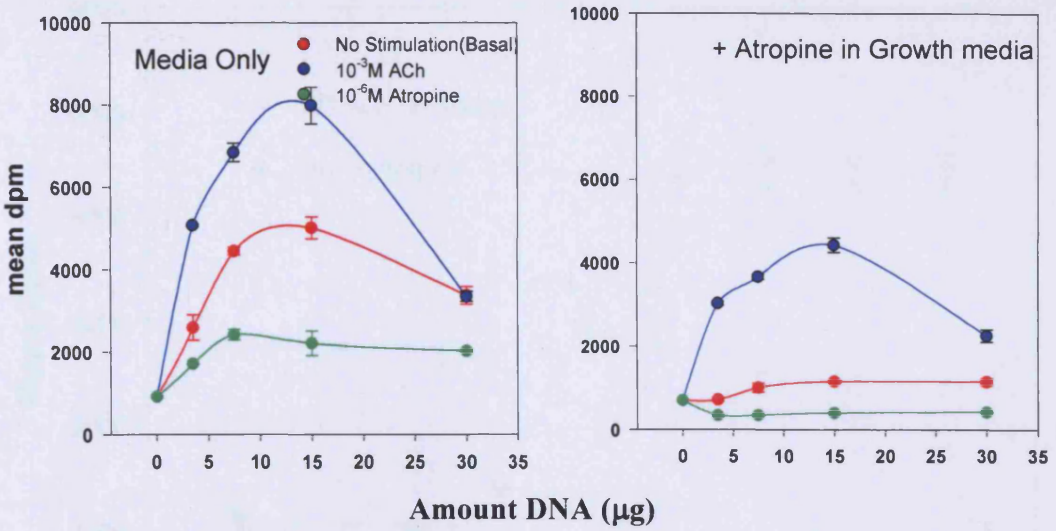

Determination of optimum concentration of plasmid for transfection into COS-7 cells for PI assays. The PI Assay was performed on live COS-7 cells grown in media alone or containing 10^{-6}M atropine as described in methods 2.13 Amounts of plasmid DNA used were, 0µg (null transfection), 3.5µg, 7.5µg, 15µg and 30µg of plasmid. Levels of basal signalling (red points), maximal signalling using 10^{-3}M ACh (blue points) and 10^{-6}M atropine inhibited signalling (green points) were recorded. All points are the mean of quadruplicate measurements.

Figure 4.3. Example of Wild Type Basal and Maximal Signalling

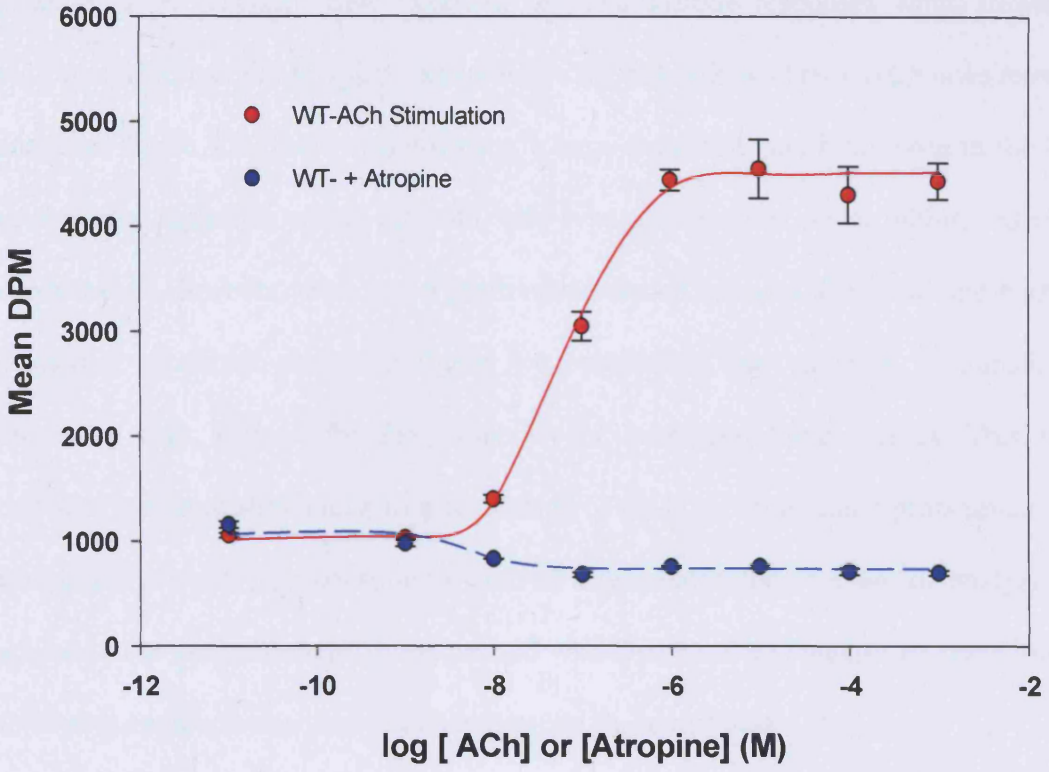

Example of a typical ACh stimulated dose response curve for WT M_1 mAChR showing maximal and basal signalling. Assays were performed on viable COS-7 cells grown in media alone and PI assay was conducted according to the protocol in methods 2.14. **WT** ACh stimulated Emax = 4452±47.8 dpm, Basal = 1144±17.3 dpm,. pEC_{50} = 7.20±0.05, n_H = 1.10±0.09. Basal signalling activity was inhibited by increasing concentrations of atropine. Basal signalling was reduced from 1176±39.2 dpm to 761.8±5.3 dpm, pIC_{50} = 8.25±0.02. All points are the mean of quadruplicate measurements and are shown ±S.E.M

The established laboratory protocol uses 15μg of DNA. The experiment shown in figure 4.2 is in reasonable agreement with this. COS-7 cells transfected with WT M_1 mAChR plasmid DNA generally gave excellent phosphoinositide responses when stimulated with acetylcholine. For a typical example of a M_1 mAChR wild type ACh dose response curve see figure 4.3. There was however, a large degree of variability seen in the basal to maximal signalling ratios for both wild type and mutants, even within individual experiments. However, there was a positive correlation between WT basal and maximal signalling values as shown in figure 4.4, suggesting that variation in transfection efficiency may account for the variability of basal and Emax values. This made calculating mutant stimulation as a percentage of wild type stimulation problematic. The variability of wild type constitutive activity exacerbated the problem of analysis. To address these inconsistencies in mutant and wild type basal and maximum signalling the following approach was used to better interpret the actual data.

Mutant Basal and Emax values were determined as ratios to contemporaneous wild type control values, where RB = ratio of basal values and RE = ratio of Emax values

Thus;

$$R_B = \frac{Basal_{Mut}}{Basal_{WT}} \quad \text{and} \quad R_E = \frac{E\max_{Mut}}{E\max_{WT}}$$

Taking the mean of individual separately determined values

Values were then corrected to account for the null signalling background

Thus, for example

$$R_B = \frac{Basal^*_{Mut} + Null}{Basal^*_{WT} + Null} \qquad R_E = \frac{E\max^*_{Mut} + Null}{E\max^*_{WT} + Null}$$

where Basal* Mut and Basal*WT are the intrinsic signalling activity of the mutant and wild type receptors.

So, it is easy to show that;

$$\frac{Basal^{*}_{Mut}}{Basal^{*}_{WT}} = RB(1+\frac{Null}{Basal^{*}_{WT}}) - \frac{Null}{Basal^{*}_{WT}}$$

Since,

$$\frac{Null}{Basal^{*}_{WT}} = 0.58$$

$$\frac{Basal^{*}_{Mut}}{Basal^{*}_{WT}} = 1.58R_B - 0.58$$

As an example for W164A

$$R_B = \frac{Basal_{Mut}}{Basal_{WT}} \qquad R_E = \frac{E\max_{Mut}}{E\max_{WT}}$$

Mean RB from 4 separate experiments = 0.481

Mean RE from 4 separate experiments = 0.883

$$\frac{Basal^{*}_{Mut}}{Basal^{*}_{WT}} = 1.58x0.481 - 0.58 = 0.18$$

$$\frac{E\max^{*}_{Mut}}{E\max^{*}_{WT}} = 1.084x0.883 - 0.084 = 0.873$$

Thus W164 basal activity ratio relative to WT = 0.18±0.20 (virtually no basal activity)

And a maximum signalling activity ratio relative to WT = 0.87±0.

Basal and Emax values for all mutants are shown in table 4.1.

Table 4.1 Summary of Phosphoinositide Signalling Parameters: All Mutants

Mutant	n	pEC_{50}	§ $\frac{E\max_{Mut}}{E\max_{WT}}$	§ $\frac{Basal_{Mut}}{Basal_{WT}}$
Wild Type	29	7.03±0.1	1.0	1.0
E2 Loop Muts				
W164A	4	5.61±0.04[a]	0.87±0.5	0.18±0.2*
Q165A	3	6.53±0.20[b]	1.60±0.4	0.43±0.3
G169A	3	6.49±0.02[a]	1.30±0.2	0.30±0.03*
E170A	3	6.99±0.20	1.08±0.4	0.89±0.04
R171A	6	6.31±0.10[a]	0.91±0.4	0.69±0.1
T172A	3	6.71±0.05[b]	1.33±0.3	0.64±0.08
Q177A	5	6.32±0.10[a]	0.96±0.30	0.65±0.10
Y179A	3	6.39±0.20	1.23±0.40	0.75±0.10
I180A	3	6.29±0.05[a]	1.39±0.60	0.44±0.10*
Q181A	3	6.86±0.20	1.24±0.40	1.41±0.50
F182A	4	6.90±0.04	1.22±0.30	1.06±0.30
S184A	3	5.84±0.20	0.86±0.20	0.07±0.10*
Cys Muts				
C98A	3	3.56±0.10[a]	0.40±0.06†	0.00*
C178A	4	3.51±0.03[a]	0.57±0.02†	0.73±0.40
C178N	3	3.62±0.10[a]	0.41±0.05†	0.00*
C98A/C178A	3	3.54±0.10[a]	0.65±0.02†	0.22±0.10*
TM Muts				
D99A	8	5.13±0.01	1.09±0.10	1.01±0.06
F197A	3	5.54±0.10[a]	1.67±0.50	1.70±0.30
W378A	3	4.51±0.10[a]	0.78±0.10	0.078±0.10*

§,See Text for details and example calculations
pEC_{50} statistical significance [a]$p<0.01$, [b]$p<0.05$ with respect to WT values
* Basal levels of signalling clearly reduced relative to WT in all comparisons ($p<0.05$)
†Emax clearly reduced relative to WT in all comparisons ($p<0.05$)

Figure 4.4.. Correlation of Wild Type Basal and Emax Values

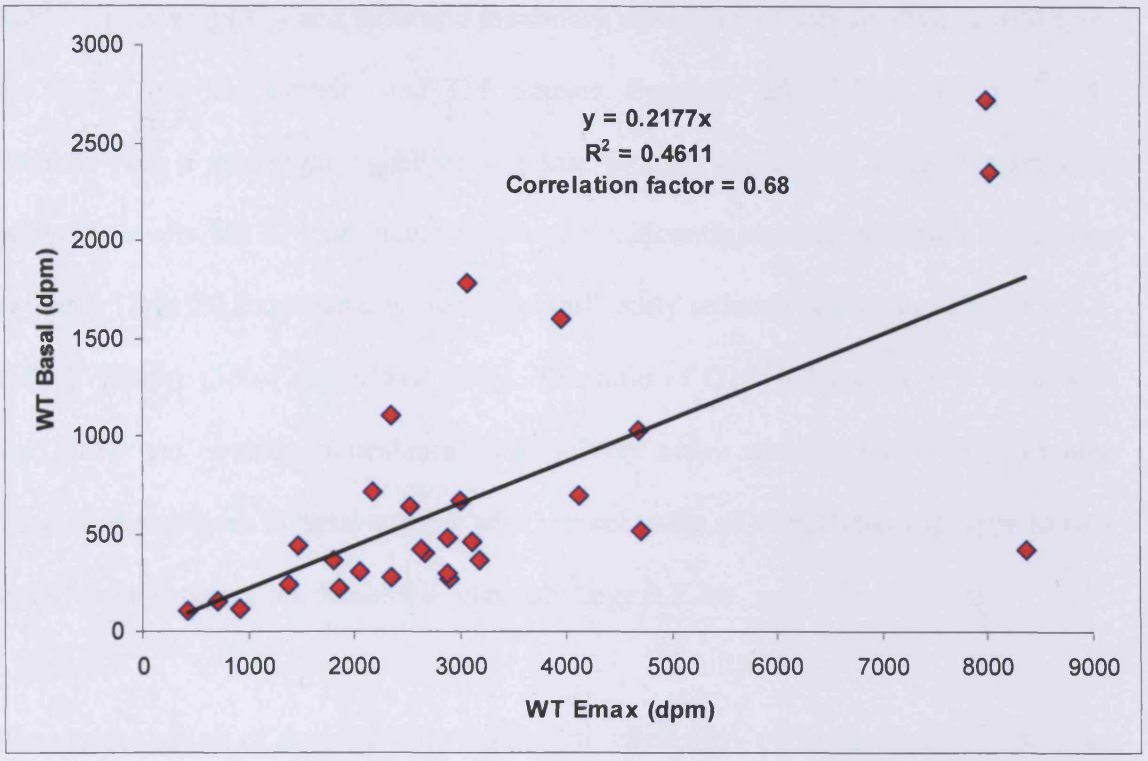

The graph correlates all 29 recorded Basal and Emax signalling activity values for the wild type M_1 mAChR The trendline is fitted to the equation y = 0.2177x which gives an R^2 value = 0.4611. Correlation of Basal and Emax values could be explained by the variation in plasmid transfection. A correlation between Basal and Emax signalling activity would support this and the graph shows a correlation factor of 0.68, suggesting that there is a correlation between Basal and Emax signalling activity.

4.2.2. E2 Loop Mutants-Signalling

Table 4.1 shows pEC_{50} and basal and maximum signalling activity relative to wild type for all E2 loop and cysteine and TM mutants. Generally all E2 loop (except C178) mutants gave a maximum signalling response to ACh stimulation close to maximum wild type levels. No E2 loop mutants showed significantly reduced maximum signalling activity. Three E2 loop mutants showed significantly reduced basal signalling W164A (18%), G169A (30%) and S184A (7%). The ratio of Q181A basal to WT basal was 1.41±0.50 and possibly indicates a constitutively active mutant. The Q181A mutant gave large increases in basal activity with respect to the co-transfected wild type in two out of three experiments, hence the relatively large S.E.M

The concentration of acetylcholine required to elicit 50% of the maximal signal from the wild type receptor was 93μM (pEC_{50} 7.03). Broadly speaking, pEC_{50} values for the E2 loop mutants were between 6.0 and 7.0 with a couple of exceptions. W164A gave a pEC_{50} value of 5.61 and S184A gave a pEC_{50} of 5.84 which is a 20-30 fold reduction in potency relative to WT values. Other mutations which significantly reduced pEC_{50} values were R171A, Q177A and I180A which all reduced ACh signalling potency by ~6-fold relative to WT. G169A and Q165A also showed significantly reduced pEC_{50} values of 4-fold relative to WT ($p<0.05$). Representative signalling data for E2 loop mutants is shown in figure 4.5

4.2.3. Cysteine Mutants-Signalling

All cysteine mutants showed consistent and statistically significant reductions in maximum signalling activity ratios compared to wild type. Generally, maximum signalling of the cysteine mutants was half that of WT receptors. Apart from C178A where inconsistency was observed, basal signalling of the cysteine mutants was also reduced to background signalling levels. Although in all experiments for C178A basal signalling values were low, corresponding wild type basal values were also unusually

low in two out of three experiments. Since all basal levels for C178A were at or below null transfection dpm values it is assumed that no basal signalling was apparent for C178A. All cysteine mutants produced pEC_{50} values >2500-fold reduced from WT pEC_{50} values that is, pEC_{50} values for C98A = 3.56, for C178A =3.51, C178N = 3.62 and C98A/C178A = 3.54. Representative signalling data for cysteine mutants is shown in figure 4.6 (b).

4.2.4. TM Domain Mutants-Signalling

Maximum signalling activity ratios compared to wild type were not reduced by D99A, F197A or W378A mutants The apparent increase in basal signalling activity for F197A (basal ratio to WT = 1.70±0.30) is a reflection of the unusually low WT basal signalling in three experiments and in reality the basal signalling of F197A is not believed to be significantly different from WT levels. However, W378A did reduce basal signalling activity to null background levels and basal activity was statistically different from wild type for this mutant. In general, pEC_{50} values were reduced more dramatically than for the E2 loop mutants. D99A reduced the pEC_{50} for ACh to 5.13, a 90-fold reduction in potency from WT. F197A reduced the pEC_{50} for ACh to 5.54, a 34-fold reduction and W378 reduced pEC_{50} for ACh to 4.51, a 370-fold reduction from wild type values. Representative signalling data for TM domain mutants is shown in figure 4.6 (a).

4.2.5 Comparison of Mutant Signalling Profiles

Figure 4.7 below highlight four mutations that have shown different ACh signalling profiles during the present study and indicate which mutations do or do not have a deleterious effect on signalling efficacy. E170A is an example of a mutation that does not reduce potency or ACh affinity compared to wild type. I180A is a mutation that reduced both agonist affinity (~8-fold) and as a consequence signalling potency (~6-fold). Q177A is an example of a mutation that did not significantly reduce ACh affinity

compared to WT but did show a significant ($p<<0.01$) reduction in potency (5-fold) and indicates that this mutation may also show a reduction in efficacy. C178A is an example of a mutation that significantly reduced both agonist affinity (~60-fold) and caused very large reductions in ACh signalling potency (~3000-fold). The next section evaluates the efficacy of ACh signalling for all mutants.

Figure 4.5. Representative Phosphinositide Dose Response Curves for E2 Loop Mutants

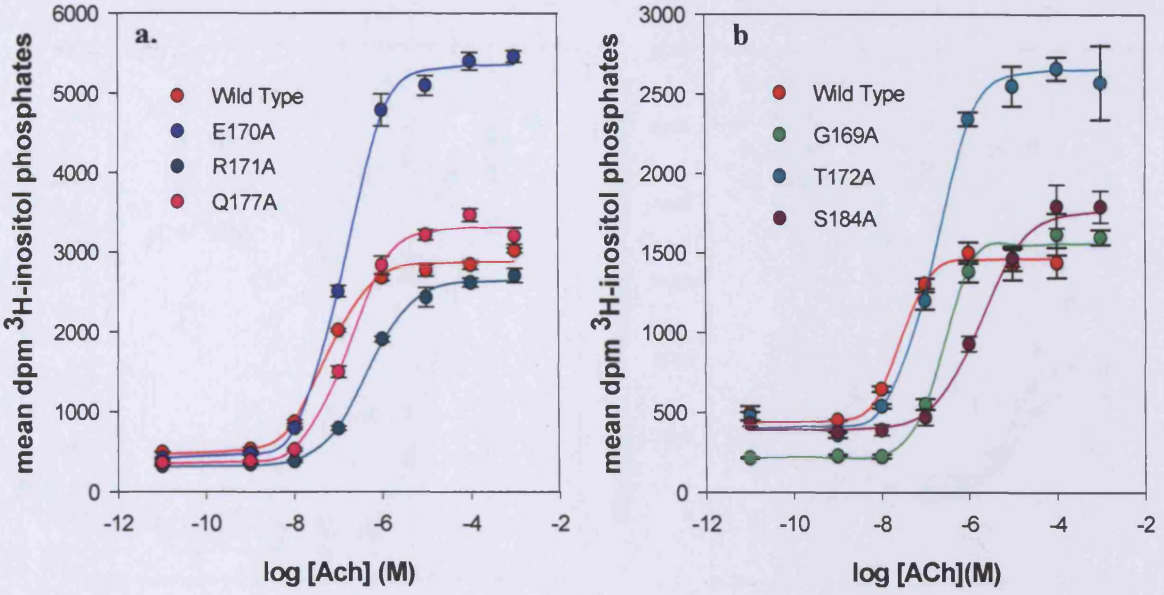

Representative acetylcholine dose response curves for E2 Loop mutants. COS-7 cells were transfected with 15μg of WT or mutant plasmid DNA and stimulated with increasing concentration of acetylcholine. Data points are mean of quadruplicate readings ±S.E.M and represent data from at least three independent experiments. Atropine at 10^{-6}M provided background counts.

a. Transfected using rat M_1 containing plasmid **WT** pEC_{50} = 7.26±0.04, Emax = 2882, Basal = 474.9; **E170A** pEC_{50} = 6.86±0.05, Emax = 5364, Basal = 428.8; **R171A** pEC_{50} = 6.35±0.05, Emax = 2652, Basal = 319.8; **Q177A** pEC_{50} = 6.77±0.07, Emax = 3319, Basal = 357.4.

b. Transfected using human M_1 containing plasmid **WT** pEC_{50} = 7.55±0.07, Rmax = 2882, Basal = 474.9; **G169A** pEC_{50} = 6.65±0.07, Emax = 1563, Basal = 217.0; **T172A** pEC_{50} = 6.77±0.05, Emax = 2661, Basal = 400.3; **S184A** pEC_{50} = 5.73±0.07, Emax = 1770, Basal = 389.8. Full curves are fitted to the four parameter logistic function. All Slope values ≈ 1

Figure 4.6. Representative Phosphoinositide Dose Response Curves for Cysteine and TM Domain Mutants

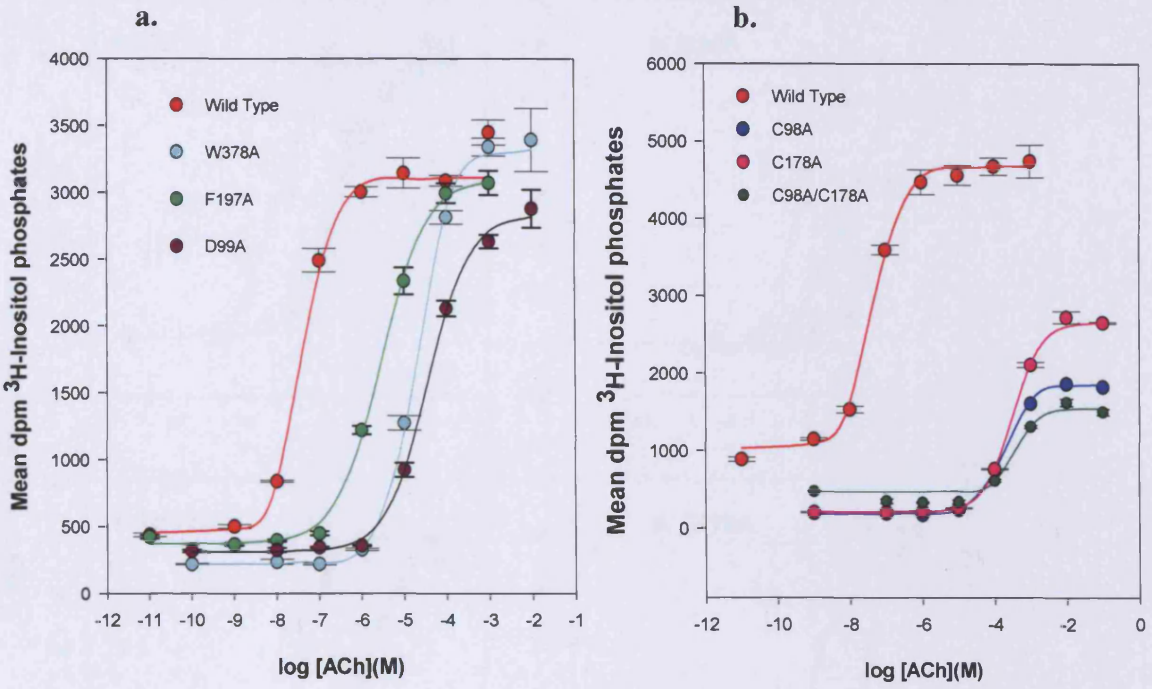

Representative acetylcholine dose response curves for E2 Loop mutants. COS-7 cells were transfected with 15µg of WT or mutant plasmid DNA and stimulated with increasing concentration of acetylcholine. Data points are mean of quadruplicate readings ±S.E.M and represent data from at least three independent experiments. Atropine at 10^{-6}M provided background counts.

a. TM Domain mutants **WT(rM$_1$)** pEC$_{50}$ = 7.36±0.04, Emax = 3111, Basal = 452.9; **D99A** pEC$_{50}$ = 4.44±0.05, Emax = 2835, Basal = 309.1; **F197A** pEC$_{50}$ = 5.53±0.05, Emax = 3106, Basal = 369.1; **W378A** pEC$_{50}$ = 4.70±0.04, Emax = 3324, Basal = 217.2.

b. Cysteine Mutants **WT(rM$_1$)** pEC$_{50}$ = 7.30±0.03, Emax = 4678, Basal = 1031; **C98A** pEC$_{50}$ = 3.75±0.02, Emax = 1859, Basal = 182.9; **C178A** pEC$_{50}$ = 3.51±0.01, Emax = 2657, Basal = 208.4; **C98A/C178A** pEC$_{50}$ = 3.40±0.07, Emax = 1549, Basal = 470.2. Full curves are fitted to the four parameter logistic function. All Slope values ≈ 1

Figure 4.7. Comparison of Acetylcholine Binding Curves and Dose Response Curves for E2 Loop Mutants

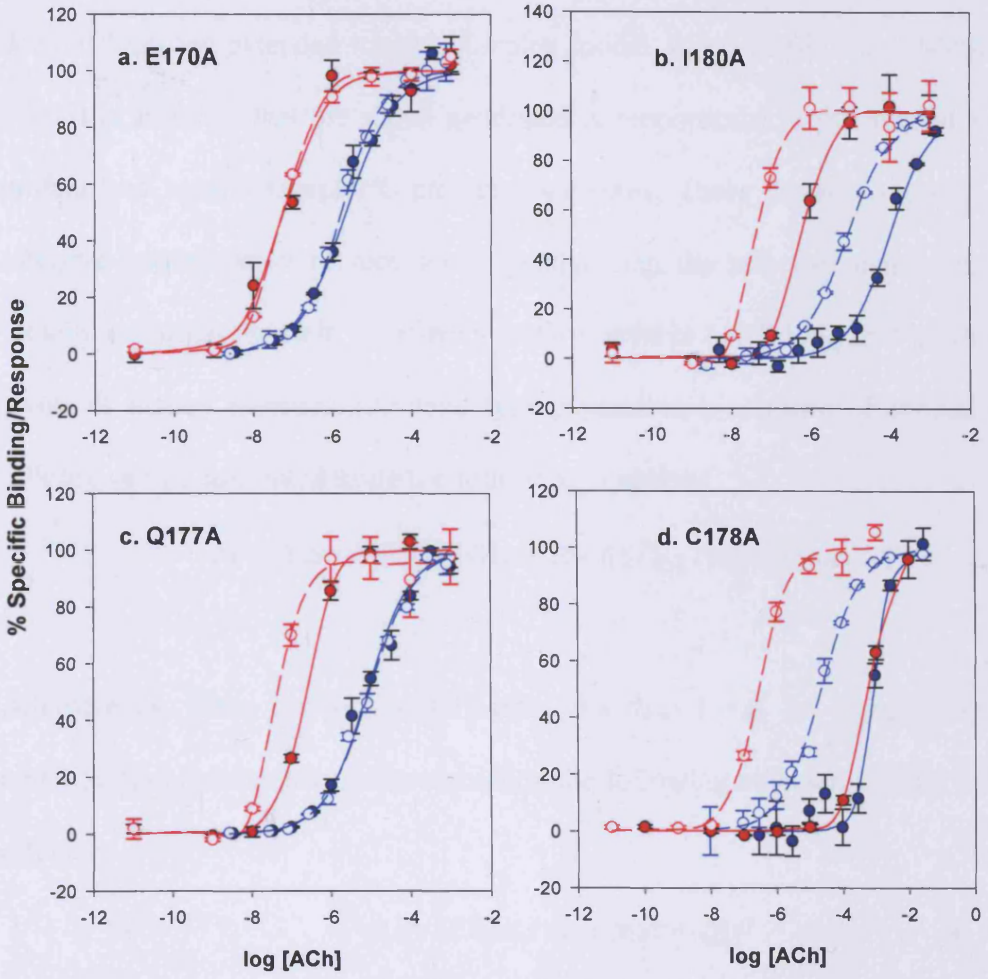

ACh binding and PI Assays performed as described in Methods 2.12 and 2.14 respectively. ACh binding curves (blue) are compared with ACh dose response curves (red) for WT controls (dashed line) and mutants (solid line).

a. E170A is an example of a mutation that changes neither the ACh affinity constant or the potency of the receptor compared to WT. **b.** I180A is an example of a mutantion that reduces both the affinity of ACh and as a consequence reduces ACh signalling potency. **c.** Q177A is an example of a mutation that does not reduce ACh affinity but does reduce the potency of the receptor compared to WT, indicative of a reduction in efficacy. **d.** C178A is an example of a mutation that reduces both ACh affinity and ACh potency relative to WT.

4.2.6. Calculations of signalling efficacy

Effects of mutations on agonist signalling efficacy can be estimated by using equations derived from the extended ternary complex model. (see Materials and Methods figure 2.3). It is assumed that the signal generated is proportional to the sum of receptor/G-protein and agonist/receptor/G-protein complexes. These equations apply when the effective concentration of receptor is greater than the effective concentration of G-protein. i.e. when the ratio of receptor to G-protein is >1. Taking into account relative levels of mutant expression to wild type expression a measure of agonist signalling efficacy can be calculated using the following equation

$$e_A = (Kact / (Kbin(1-Basal)) - 1) / \underline{R}_T \text{ (when Emax } \sim 1)$$

Alternatively, when Emax is significantly less than 1 e.g. for a partial agonist or a mutation that reduces maximum signalling the following equation is used to determine efficacy.

$$e_A = (Emax / (1- Emax)) \ / \underline{R}_T$$

Where Kact is equal to the $1/EC_{50}$ value. i.e. the effective potency of an agonist at a particular receptor and Kbin is equal to the affinity constant of the agonist at the same receptor. The values of $\underline{R}_T$ in this equation are the estimated functional ratios of receptor:G-protein. Experiments in which this ratio has been deduced by blockade of the receptor with the irreversible antagonist PrBCM (Lu et al., 1997b) have allowed us to estimate $\underline{R}_T = 20$ for the wild type receptor which is over expressed in COS-7 cells. Simply, efficacy values (e_A) are a measure of how effectively agonist occupied receptor assemblies can promote G-protein binding to form a ternary complex that subsequently catalyses GDP-GTP (measured by the rate constant K_{cat}) exchange to elicit a transducable signal.

Efficacy values obtained for all mutants in this study are shown in table 4.2 below. A good indication of a mutant that reduces agonist efficacy is one that reduces the pEC_{50} of an agonist but does not significantly reduce the agonist affinity constant as seen for the Q177A mutant.

4.2.7. E2 Loop Mutants-Efficacy

Most of the E2 loop mutants signalled with an efficacy comparable to wild type. Notable reductions in efficacy (<10-fold) were observed for W164A (7-fold) and Q177A (5-fold). Larger reductions in efficacy were seen for Q181A (11-fold) and S184A (17-fold). Q181A is a particularly interesting mutant since it increases ACh affinity (5-fold), does not significantly affect signalling potency but does reduce ACh signalling efficacy.

4.2.8. Cysteine Mutants-Effiacy

Substituting the cysteine side chains with alanine had greater effects on efficacy. The double cysteine mutation C98A/C178A reduced efficacy 48-fold whereas the single cysteine mutant C178A reduced efficacy of G-protein coupling by 8-fold. The C178N mutant reduced efficacy by 15-fold. Only one site (low affinity site) could account for the signalling efficacy of the C98A mutant. However, taking into account reduced expression and reduced ACh affinity at the low affinity site, C98A showed a signalling efficacy close to the WT value i.e. log $e_A$mut / $e_A$wt was 0.21. The efficacy value for C98A is open to question since it does not obey the equation shown above, because the recorded K_{bin} value is greater than the K_{act} value for the high affinity site. Thus, it is not possible in terms of the ternary complex model to estimate an efficacy value for the high affinity site proposed to exist for the population of C98A mutant receptors. If the alternative equation used for measuring signal efficacy, based on the Emax of C98A, is applied, then C98A reduces signalling efficacy to much the same extent as the other cysteine mutants. If however the low affinity site is actually the site responsible for signalling then the signalling efficacy for C98A is much higher and shows no difference

from WT efficacy values. Figure 4.8 below shows that the high affinity site can not be responsible for signalling since the affinity constant of the high affinity site is greater than the pEC_{50}.

4.2.9. TM Domain Mutants-Efficacy

D99A had no effect on ACh stimulated signalling efficacy, whereas F197A and W378A reduced efficacy more significantly by 12 and 13-fold respectively.

Table 4.2. Summary of Functional Data for all Mutants

	R_T	pEC_{50}	pKa	e_A	$\log \frac{e_A mut}{e_A WT}$
Wild Type	20	7.03	5.00	5.31	
E2 Loop Mutants					
W164A	17.5	5.61	4.43	0.81	-0.82
Q165A	12.3	6.53	5.33	1.28	-0.62
G169A	12.3	6.49	4.61	6.17	0.07
E170A	14.4	6.99	5.19	4.31	-0.09
R171A	14.0	6.31	4.17	9.79	0.27
T172A	22.5	6.71	5.13	1.69	-0.50
Q177A	15.4	6.34	5.14	1.00	-0.73
Y179A	18.7	6.39	4.75	2.28	-0.37
I180A	20.8	6.29	4.35	4.14	-0.11
Q181A	28.6	6.86	5.68	0.49	-1.03
F182A	12.6	6.90	5.08	3.75	-0.15
S184A	30.0	5.84	4.87	0.28	-1.23
Cysteine Mutants					
C98A(low)	2.43	3.56	2.43	5.13	-0.01
C98A(high)	2.43	3.56	4.16	0.30*	-1.25*
C178A	3.08	3.51	3.18	0.55	-0.9
C178N	10.3	3.62	2.94	037	-1.15
C98A/C178A	16.7	3.54	3.10	0.11	-1.68
TM Domain Mutants					
D99A	2.5	5.13	3.65	2.25	-0.32
F197A|	11.3	5.54	4.76	0.44	-1.08
W378A	22.2	4.51	3.86	0.40	-1.12

*Calculated using alternative e_A equation. $e_A=(Emax / 1-Emax) \times 1/R_T$

Figure 4.8. Comparison of ACh Binding Curve (2-Site Model) and Dose Response Curve for C98A

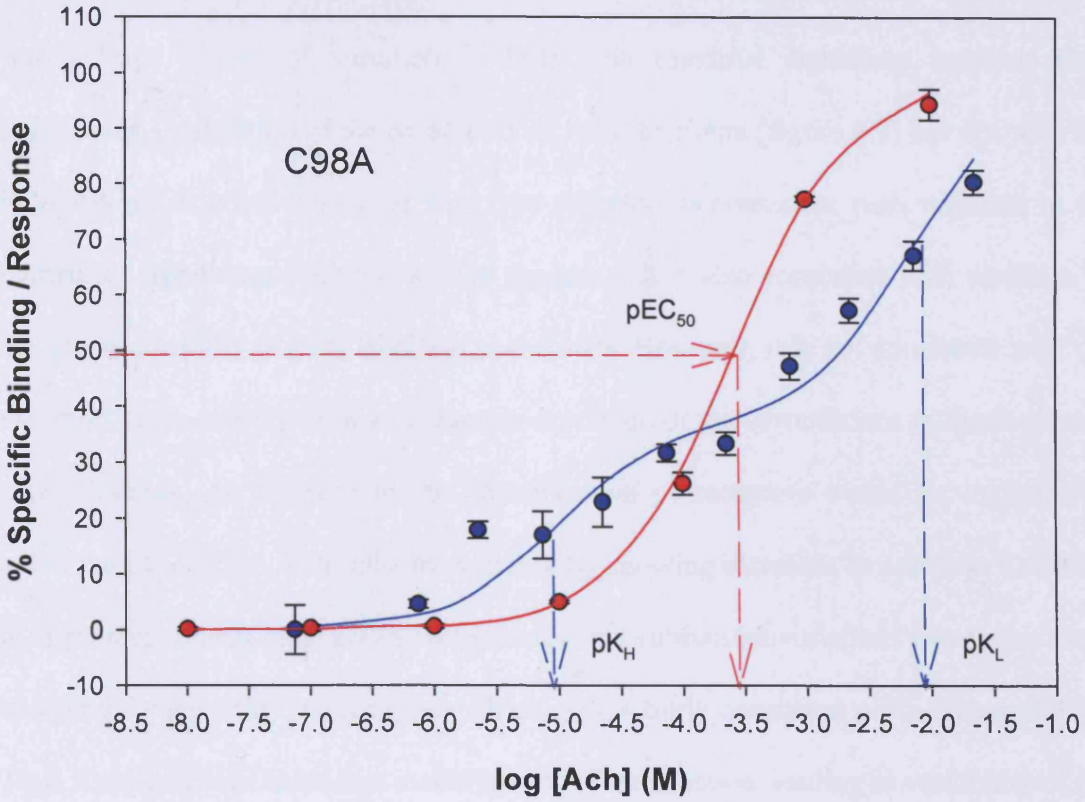

The graph illustrates the 2-site fit ACh binding curve of C98A in comparison to the dose response curve for the same mutant. The figure highlights the fact that it cannot be the high affinity population of C98A receptors responsible for the ACh induced signalling activity since the pK_H is greater than the mean pEC_{50} value. Thus the low affinity (pK_L) site must be responsible for signalling activity. Therefore, an efficacy calculation could not be made for the high affinity population of C98A mutants. pEC_{50} = 3.58±0.05. pK_H = 5.02±0.002, pK_L = 2.13±0.002. Fraction of high affinity sites = 0.46.

4.3 Discussion and Conclusions

One of the problems interpreting the functional data stemmed from the fact that there was a large degree of variation in basal and maximal signalling between each experiment. Correlation of the basal activity with the Emax (figure 4.3) but not with the EC_{50} values (data not shown) of wild type receptors is consistent with variation in the number of responsive cells per well in the assay. It is also consistent with variation in the specific activity of PIP_2 labelling in the cells. However, it is not consistent with the variation in the concentration of receptors expressed or major variations in the G-protein concentrations. An increase in the concentration of receptors would be expected to affect the EC_{50} of the ACh induced response by showing increases in potency. Variation in G-protein content must also affect potency. No substantial variations in potency were observed for the wild type receptors which gave a fairly consistent pEC_{50} value of 7.00. Thus it must be concluded that inefficiencies of transfection, leading to variability of the number of responsive cells or inefficient labelling of PIP_2 were responsible for the variations in basal and maximum wild type signalling.

4.3.1. E2 Loop Mutants

Summary potency and efficacy data for all E2 loop mutants are shown in figure 4.9 (page 171). Three mutations, G169A, E170A and F182 had very little effect (<3-fold) on ACh affinity or signalling efficacy and may be regarded as null mutations. Furthermore, these mutations did not significantly reduce expression, basal and maximal signalling or ACh potency. Therefore, it is the conclusion of this author that the native residues G169, E170 and F182 behave like filler residues that appear to have no particular function in the M_1 mAChR. By analogy, since G169 and F182 but not E170 are conserved in the other 5 mAChR sub-types, the corresponding residues in the other sub types may also be non-functioning filler residues. It may have been better to substitute G169 with a residue other than alanine, since alanine and glycine are both

small amino acids and thus alanine substitution of G169 may not invoke significant differences in phenotype. F182A did have a small effect on NMS affinity but does not appear to be important for the binding of ACh or ligand transduction.

Two E2 loop mutations, R171A and I180A significantly reduced ACh affinity and potency but did not reduce signalling efficacy or seem to have any effect on basal and maximum levels of signalling. These characteristic are consistent with native residues that are important for ligand interaction or ligand anchoring. If I180 is part of the β4 sheet that dives down into the transmembrane binding pocket, analogous to the I184 residue in the D2 dopamine receptor (Shi and Javitch, 2004), it is conceivable that it does play some role in the stabilisation of ACh in the binding pocket via a second shell interaction. The side chain of R171 appears in the homology model of the M_1 mAChR to protrude in to the extracellular space and it is difficult to imagine R171 being able to make contact with ACh in the binding pocket. The data however seems to imply that R171 is in some way involved in the stabilisation of ACh in the binding site. It is possible that the homology model needs some revision, perhaps re-orientating R171 so that it is positioned so as to face into the binding site. The fact that both these residues are highly conserved amongst all mAChR subtypes supports the theory that these residues have a role to play in the binding of ACh, although they are not critical contact residues.

During this study it was observed that the mutations W164A and S184A reduced signalling efficacy more than any reductions in ACh affinity. In fact both mutations had very small (<4-fold) effects on the binding of ACh and yet reduced signalling potency 26 and 15-fold, translating into reductions of signalling efficacy of 7-fold and 17-fold respectively. This was in conjunction with a strong reduction of basal signalling activity compared to WT. W164 and S184 are highly conserved residues in mAChRs. In

rhodopsin, W175 is homologous to W164 at the N-terminal end of the E2 loop and a threonine residue, T193, also with a hydroxyl group in its side chain is analagous to S184 at the C-terminal end of the E2 loop. The characteristics of W164A and S184A are consistent with activator residues. The fact that these mutations cause the loss of basal signalling and reduce potency and efficacy, but do not affect expression levels or ACh affinity, suggests that they are intrinsic in the activation process of the receptor. The fact that the analogous residues in rhodopsin can form a hydrogen bond network with proline residues at the top of TM4 and TM5 suggests that these residues may be involved in the conformational reorganisation of the receptor upon ACh-induced activation. Thus it seems likely that W164 and S184 are also part of a H-bonding network important for the active state of the receptor. It would be interesting to see if mutation of S184 to threonine would re-instate wild type signalling activity. Perhaps to a lesser extent Q165, Q177 and Y179 may also be regarded as activator residues since they share similar characteristics of loss of signalling potency and efficacy, but have less of an affect on basal signalling.

Q181A showed high basal activity. The substitution of Q181 with alanine had the effect of unleashing the receptor from its predominantly inactive state, causing it to signal at >150% of WT basal levels in the absence of any ACh stimulation. However, this effect was observed in only two out of three experiments and so unfortunately, definitive statements about this mutation cannot be made and this accounts for the large standard error in the recorded mean Emax (1.41±0.50) seen in table 4.1. Perhaps poor transfection in one of the assays may account for the inconsistency. Nevertheless, Q181 is also completely conserved amongst the muscarinic receptor sub-types and therefore is likely to be an important residue, in this case, for maintenance of the inactive state. Klco and colleagues (Klco et al. 2005), using random saturation mutagenesis of the E2 loop of the C5a receptor (similar in length to the E2 loop of the M_1 receptor), showed that

~80% of mutants displayed constitutive activity, implicating the E2 loop as a stabiliser of the inactive conformation of the receptor and suggesting that this may be the case for other GPCRs. This theory cannot be corroborated, since the majority of E2 loop mutants analysed in the present study did not show any apparent increase in constitutive activity and this may reflect differences in the structure of the E2 loop of mAChRs and C5a receptors. Furthermore, in the Klco study (Klco et al., 2005) multiple substitutions were of E2 loop residues were made whereas in the present study only point mutants were studied. However, in the case of the Q181 residue there may well be a case for implicating this particular residue as important for the preservation of the inactive ground state of the M_1 receptor. The mechanism by which Q181 is able to do this is open to speculation and may require a revision of the M_1 homology model to determine possible ground state contacts made by Q181. Q181A fulfils two of the three accepted requirements of a constitutively active receptor, it increases agonist affinity (5-fold) and it increases basal activity (300%) but surprisingly the AR complex couples less efficiently to G-protein, as the 5-fold reduction in agonist signalling efficacy indicates. Q181 lies at the C-terminal end of the E2 loop beyond the proposed β-4 sheet close to the top of TM5 where it may serve to constrain a reorganisation of the E2 loop required for activation by forming a hydrogen bonding network with surrounding residues. The raised basal activity seen for Q181A resembles similar increases observed for S120A and L116 (Lu and Hulme, 1999a) and may also indicate a selective destabilisation of the inactive ground state due to this mutation. It may be suggested therefore that the native Q181 residue may act as a constraining residue in the wild type receptor. Further functional analysis of Q181A is required to verify the points made above.

Receptor constitutive activity, whereby a receptor is functionally active in the absence of an agonist, was a component of original receptor theory before modern biochemical and cloning techniques substantiated the premise (Costa and Cotecchia, 2005). It is now

an accepted phenomenon. With relevance to this study, constitutive activity of mutant muscarinic receptors has been described previously by Jakubik et al and Spalding et al (Jakubik et al., 1995; Spalding and Burstein, 2001) showing that M_1-M_4 subtypes were constitutively active in CHO cell lines and that the basal activity could be reversed by atropine binding, which switched the receptor back to an inactive conformation. Similarly, inhibition of WT basal activity was achieved in the present study (see figure 4.3) by binding of increasing concentrations of the antagonist atropine, proving that the constitutive activity seen was a real phenomenon. Spalding and Burstein (Spalding and Burstein, 2001) also showed that mutations in TM 3 and TM6 and the 2nd intracellular loop all increased constitutive activity and that ~ 20-30% of those mutations in the 2nd intracellular loop and TM6 respectively raised constitutive activity up to 30% of the total cellular response. Constitutive activity occurs because receptors can exist in spontaneous equilibrium between the active and inactive conformation in the absence of ligand. Assuming the G-protein preferentially interacts with the active conformation, it can be imagined that an increase in the concentration of G-protein in the cell for whatever reason could lead to an increase in basal activity. This finding was confirmed by Burstein et al (Burstein et al., 1997), where they showed that over expression of the G_q class of G-proteins did indeed raise basal activity, since increasing the G-protein concentration allows more interactions with receptors that spontaneously assume the active conformation. Thus, it can be seen that constitutive basal activity of the M_1 wild type receptor and indeed most other GPCRs, is a well defined and accepted component of receptor function. The subject of GPCR constitutive activity is concisely reviewed by Millligan (Milligan, 2003).

Figure 4.9 Summary of Changes in ACh Signalling Potency and Efficacy for E2 loop Mutants

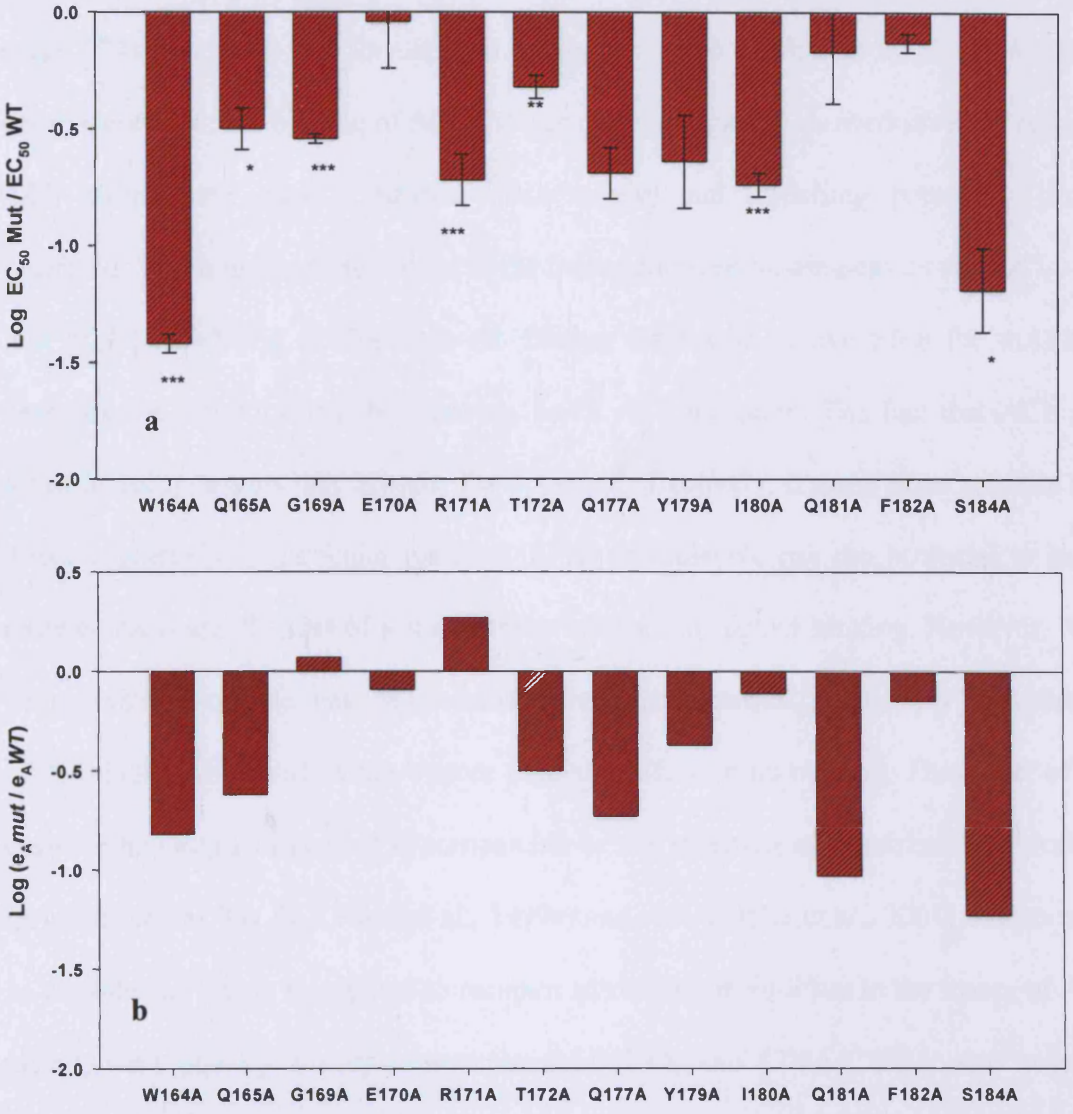

Overview of the effects of E2 loop mutations on ACh signalling potency **(a)** (EC_{50}) and efficacy **(b).** Bars represent the log reduction in potency or efficacy compared to wild type and are given with error bars (where applicable) indicating S.E.M and statistical significance where;* p = <0.05 and ** p = <0.01 ***p<0.001 with respect to WT values.

4.3.2 Cysteine Mutants

Summary data for potency and efficacy for the cysteine residues is shown in figure 4.10 (page 174). It appears that the removal of the conserved disulphide bond has dramatic consequences for the binding of ACh. All the cysteine mutants showed severely reduced ACh affinity and greatly reduced basal activity and signalling potency. This is consistent with a major perturbation of the transmembrane binding cavity caused by the loss of the stabilising disulphide bond. During the course of evolution the mAChRs have been selected to bind the relatively small ACh molecule. The fact that ACh is a small molecule means that in order for it to bind effectively, it must make specific and direct contacts with particular residues. A larger molecule has the potential to make more contacts and the loss of some contacts may not disrupt its binding. However, ACh being a small molecule, has the potential to make less contacts, so that any perturbation of the binding site residues has a more dramatic effect on its binding. The effect of the cysteine mutations in general is comparable to the mutation of important TM domain residues such as Tyr 381(Ward et al., 1999a) and Asn 414(Lu et al., 2001) and so must be regarded as highly significant to receptor activation. In addition to the losses of ACh affinity and potency the cysteine mutants C178A and C98A/C178A also reduced signalling efficacy by 10 and 50-fold respectively. This implies that not only is the disulphide bond important for the integrity of the transmembrane binding site it is also important for the efficient transduction of ACh induced signalling. Thus, C178 may be characterised as a stabiliser residue and as a transducer residue important for the active conformation of the receptor.

As regards efficacy, C98A is a special case and is discussed separately below. The data supports the notion that the maintenance of the E2 loop structure is essential for M_1 mAChR activation and that a disulphide bond between C98 and C178 now seems unambiguous since there appears to be no additative effect of mutating both C98 and

C178 together, as comparded to the point mutants. Baneres et al (Baneres et al., 2005) have now provided direct evidence showing that removal of the S-S bond in the 5-HT4 receptor produced a significantly different CD spectra of the E2 loop to that of the wild type receptor. Perturbation of the E2 loop structure caused by the disruption of the disulphide bond clearly has dramatic effects on the signalling efficiency and potency of the mACh receptor. The inability of the cysteine mutated E2 loop to facilitate the conformation changes required for the active state indicates the importance of the E2 loop to a fully functional receptor. In terms of the ternary complex model mutation of the cysteine residues affects the conformation constant αK i.e. the change from the inactive ground state to the active conformation. It is surprising that the cysteine mutants can actually function at all, albeit at a much reduced level than that of the wild type receptor. It may have been expected that the cysteine mutants would completely abolish signalling as was seen for the D105A mutation (Lu and Hulme, 1999a). This proved not to be the case however with all three cysteine mutants signalling at more or less the same levels (see figure 4.6). Thus, removal of the disulphide bond perturbs the E2 loop structure and severely reduces signalling but does not abolish it, again supporting the idea that the E2 loop plays an important role in allowing the induction of the active conformation of the receptor.

Figure 4.10. Summary of Changes in ACh Signalling Potency and Efficacy for Cysteine Mutants

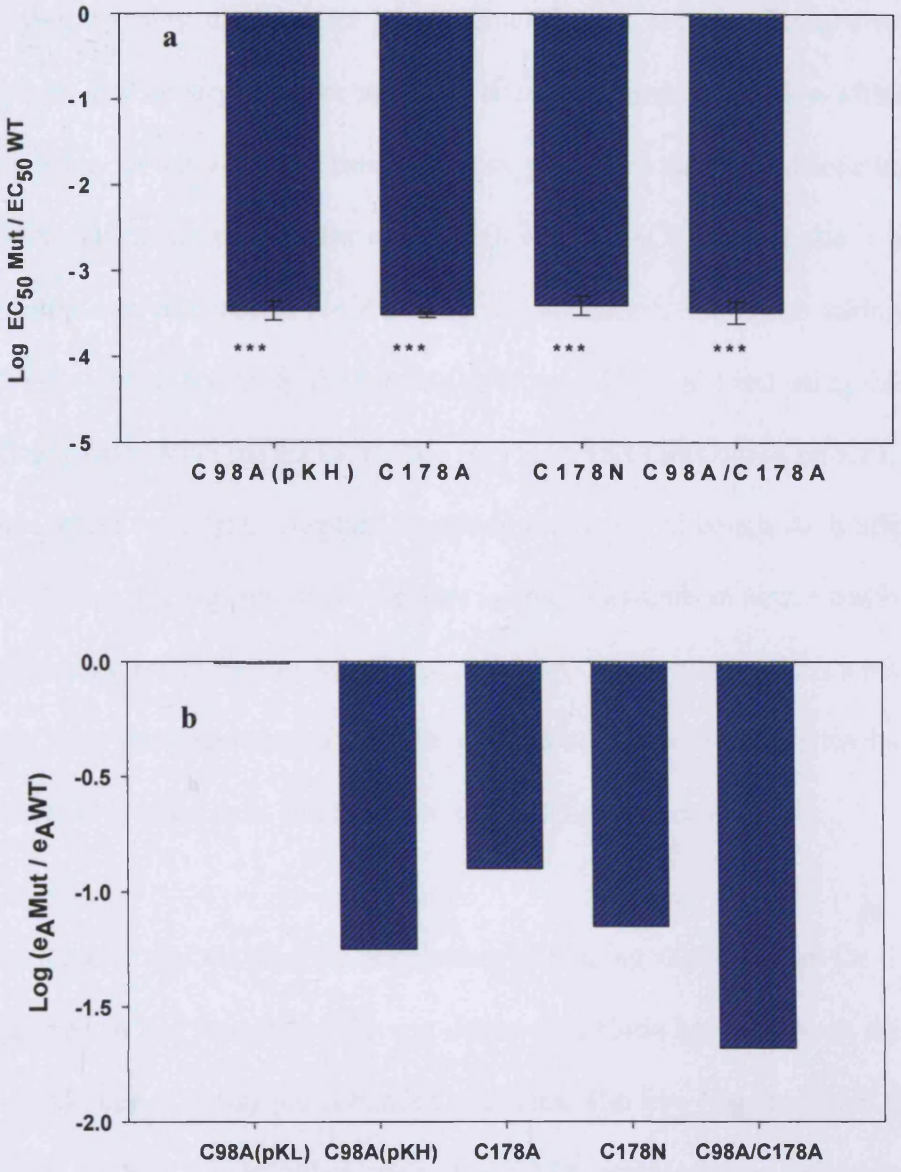

Overview of the effects of cysteine mutations on ACh signalling potency (EC_{50}) **(a)** and efficacy **(b)**. Bars represent the log reduction in potency or efficacy compared to wild type and are given with error bars (where appropriare) indicating S.E.M and statistical significance where *** = $p<0.001$ with respect to wild type.

4.3.3. The C98A Mutant is a Special Case

It has been shown in results Chapter 1 that the ACh binding curve for the C98A mutant is complex, showing the presence of two binding sites, a high affinity site and a low affinity site. The ternary complex model dictates that it must be the low affinity site that is responsible for activation. Figure 4.8 above illustrates the point. Since the pEC_{50} of the C98A mutant lies to the right of the high affinity ACh binding site it must be the low affinity site responsible for the observed activation. Therefore taking the mean value of the low ACh affinity site binding constant (pK = 2.43) and using this figure for the efficacy calculation the efficacy value (e_A) for C98A turns out to be 5.13, practically the same as the wild type receptor. Accepting this logic, although ACh affinity at this site is reduced, this population of receptors is able to assume an active conformation on agonist binding and is able to effectively couple to G-protein and ellicit a response. The problem with this reasoning is that the existence of two binding sites has not been demonstrated in intact cells and therefore requires further investigation.

The existence of the two separate populations of binding sites apparent for C98A, could be explained by the formation of a non-native disulphide bond between the free C178 residue and other non disulphide bonded cysteines. The free cysteine could theoretically participate in S-S bonds either with free C178 residues from adjacent receptors, effectively creating a dimer or a non-native disulphide bond could be created within the same receptor. The third extracellular loop of the M_1 mAChR contains two cysteine residues at C391 and C394. Thus the possibility exists that different combinations of disulphide bonding could be created by the free C178 residue. The existence of alternative S-S bonding is not unprecedented. Noda et al (Noda et al., 1994) performed a systematic mutagenesis study on the β2 adrenergic receptor, which contains three cysteine residues in the E2 loop (C184, C190 and C191) and one at the top of TM3 (C106), analogous to C98. By antagonist binding, DTT reduction and thermal stability

studies they showed it was possible to create either high affinity sites or low affinity sites depending on which cysteine was mutated to alanine. They concluded that in the wild type β_2 adrenergic receptor two S-S bonds are likely to exist, C106-C184 and C106-C191. So, it is possible that the C98A mutant in the M_1 receptor allows the free C178 residue to form disulphide bonds with the cysteine residues of the E3 loop thus creating a hybrid receptor with two binding sites with different agonist affinities. The formation of a dimeric receptor, whereby the free C178 residue of one receptor forms a S-S bond with another free C178 residue or even with the E3 loop cysteines of an adjacent receptor could also allow the creation of two binding sites. This possibility has been suggested by Zeng and Wess (Zeng and Wess, 1999) who were able to show through immunoblotting and systematic mutation of cysteine residues of the M_3 receptor that the receptor is capable of forming disulphide linked dimers and multimers as well as non-covalently linked dimers. It is suggested that these S-S bonds are formed during transit through the ER and Golgi bodies.

Our data suggests that it is the low affinity site that allows coupling to G-protein. Further investigation would be required to reach a more definitive conclusion as to which possible structure is responsible for the creation of a high and a low agonist affinity binding site. The same potential for the creation of two binding sites does not exist for the C178A mutant because it is unlikely that the free C98 residue would be accessible to either the cysteines of the E3 loop or the analogous free C98 of an adjacent receptor, therefore negating the possibility of an anomalous S-S being formed. Similarly, removal of both cysteine residues would also exclude the possibility of extraneous S-S bonds being formed. There is no substantial evidence from the data that two binding sites exist for the C178A mutant, but the possibility that C178A also creates two populations of receptors with different agonist affinities, cannot be excluded.

4.3.4. TM Domain Mutants

In the transmembrane domain, D99 seems to behave like a ligand anchor residue in that the D99A mutation significantly reduces ACh affinity and as a consequence potency, but it has little effect on ACh signalling efficacy or basal activity. This evidence may support the notion that D99 is part of a ligand access channel, anchoring the agonist to the receptor before translocation of the agonist to the transmembrane binding pocket. Once acetylcholine reaches the binding site a full signalling response is seen and the efficacy of signalling is very similar to wild type, only a ~2-fold reduction in e_A. So, it can be imagined that substitution of the D99 residue with alanine hinders the initial contact of ACh with the receptor, thus requiring a higher concentration of ACh to activate the receptor, but once bound ACh is able to induce the conformational change required for activation, despite the loss of the D99 residue. Expression of D99A was also reduced significantly. Taken together these data suggest that D99 may play a dual role, as part of the supporting structure and as a ligand anchor residue.

F197A and W378A both reduced potency, 34-fold and 371-fold respectively and efficacy ~9-fold and ~10-fold (see figures 4.6 and 4.11 and table 4.2). W378 displays good expression but reduced agonist affinity and potency and a reduction in efficacy, the hallmarks of a residue important for activation. Proposed to sit at the base of the binding pocket W378 is positioned towards the cytoplasmic end of TM6, its side chain facing into the core of the receptor. W378 may be involved in an intra-molecular hydrogen bonding network, linking core regions beneath the binding pocket, the re-organisation of which is required for activation. The analogous residue in rhodopsin is W265 which forms a water mediated H-bond with Y301 (Li et al., 2004), the conserved tyrosine residue in the NPXXY motif found in TM7. The outward movement of TM6 and mobilization of TM7 are thought to occur on disruption of the hydrophobic latch structure by the closure of an aromatic cage around the compact tetra-methylammonium

head group of ACh (Hulme. E.C et al, 2003). Both the H-bonding network and the hydrophobic latch structure are required to change for receptor activation. Thus, W378 not only seems to be important for the binding of agonist, since the alanine mutant causes losses in ACh affinity (13-fold) but also crucial to receptor activation, qualifying this residue as a member of the ligand activator category as described in section 1 of this chapter (see figure 4.1). F197A on the other hand did not reduce ACh affinity significantly and is likely not to be a ligand activator. Thus it can be concluded that F197 behaves like an activator residue, probably involved in the re-organisation of the TM helices upon receptor activation. W378 seems to behave like a ligand transducer residue involved in both ACh binding and in receptor activation and its phenotype resembles that of the important binding site residue Y381.

Figure 4.11 Summary of Changes in ACh Signalling Potency for TM Domain Mutants

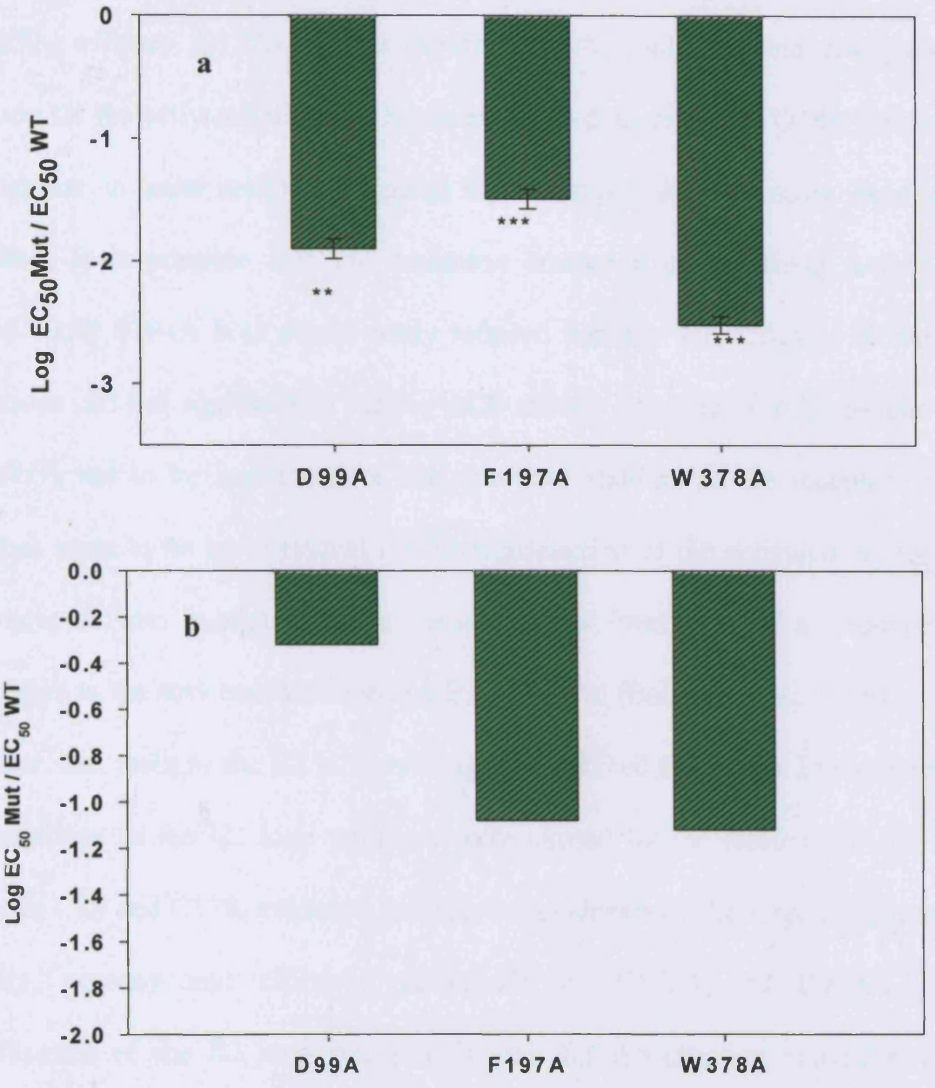

Overview of the effects of TM Domain mutations on ACh signalling potency (EC_{50}) **(a)** and efficacy **(b)**. Bars represent the log reduction in potency or efficacy compared to wild type and are given with error bars (where appropriate) indicating S.E.M and statistical significance where;* p = <0.05 and ** p = <0.01 ***p<0.001 with respect to wild type.

4.3.5. Summary

The majority of the E2 loop mutants had a relatively minor impact on both potency and signalling efficacy. Q177A may be important for the conformational realignment of the E2 loop for the activated receptor. Some evidence does exist that Q181A which showed an increase in basal activity compared to wild type, although more experiments are required. It is possible that this mutation created a constitutively active receptor. W164A and S184A both significantly reduced potency and efficacy. However, these mutations did not significantly reduce ACh affinity or expression levels and therefore are likely not to be important for the structural stability of the receptor. Both these residues seem to be more critical for the transduction of the activated conformation of the receptor into a signal. These residues may form part of a "connecting rod" analogous to the structure described by Baneres et al (Baneres et al., 2005) in the 5-HT_4 receptor, that realigns the E2 loop upon agonist induced activation. Even more dramatic perturbations to the E2 loop structure were caused by the removal of the S-S bond between C98 and C178, evidence for which was shown by the large reductions in ACh affinity, potency and efficacy, particularly by C178A and C98A/C178A. The maintenance of the E2 loop structure is vital for the efficient activation of the M_1 mAChR, because it probably maintains the transmembrane domains in the correct conformation required for consequent activation induced by the binding of ACh. The C98A mutant seems to be a special case in that it displays characteristics of having a high and a low affinity binding site, perhaps because of the non-native creation of S-S bonds either intra-molecular or with adjacent mutant receptors. Evidence provided for D99 is consistent with the theory that this residue is part of a ligand access channel. W378 is important both for ligand binding and activation, suggesting that it can be classified as a ligand activator residue. F197, having little effect on ACh binding or potency but reducing efficacy, may participate in a supporting network of bonds.

Chapter 5

Kinetics of Ligand Binding

5.1 Introduction

In order to fully characterise the mutants discussed in this study and to better understand binding modalities it was decided to conduct experiments examining the kinetics of ^{3}H-NMS and ^{3}H-QNB binding. For each individual mutant of the E2 loop, the TM domain mutants and also a selection of important binding site mutants,Y106A, Y404A, Y408A and N382A a series of measurements were taken to determine differences in dissociation rate constants for ^{3}H-NMS. However, the low ^{3}H-NMS affinity of Y106A, Y404A, Y408A and N382A precluded them from ^{3}H-NMS dissociation experiments. Only a few, although detailed, studies have previously described the dissociation and association kinetics of NMS (Waelbroeck et al., 1989; Waelbroeck et al. 1987) and QNB (Waelbroeck et al., 1991) at muscarinic receptors. Earlier evidence (Fields et al., 1978b; Yamamura and Snyder, 1974) suggested that there is a rate limiting step for antagonist dissociation from muscarinic receptors, involving a two step process and receptor isomerization. Receptor isomerization, the change in receptor conformation induced by binding of a ligand in a two-step binding process, can be detected by biphasic dissociation kinetics. However for ^{3}H-NMS these authors found no evidence of biphasic dissociation from muscarinic receptors, and concluded that ^{3}H-NMS follows a simple monophasic model of dissociation. Walbroek et al (Waelbroeck et al., 1991) explained that the biphasic kinetics seen for ^{3}H-QNB in the earlier experiments by Fields and Yamamura (Fields et al., 1978a), was probably due to the existence of several muscarinic subtypes present in the rat brain tissues used and the use of the (R) and (S) – enantiomers of QNB. However, evidence provided by Galper et al (Galper et al., 1982) using chick embryo hearts (containing only M_2 mACh receptors) showed that the dissociation kinetics of ^{3}H-QNB was indeed biphasic and that receptor isomerization

was the explanation for the biphasic kinetics observed. The binding kinetics of a ligand also depends on the stereoisomer of the ligand used. Since dissociation rate constants depend on the breaking of specific short range interactions between ligand and receptor, stereo-selectivity of the receptor is a key element determining the dissociation kinetics of the receptor. Thus it can easily be imagined that incorrect sub-optimal interactions would increase dissociation rate constants. Walbroek et al demonstrated that the binding kinetics of the (R) and (S) enantiomers of ^{3}H-QNB were in fact different as are the antagonist dissociation kinetics between the muscarinic sub-types (Waelbroeck et al., 1991). The (S) enantiomers of ^{3}H-QNB dissociate faster than (R)-enantiomers this can be explained by the lower affinity of the (S) enantiomer for muscarinic receptors. The experiments described in the present study use the (R) (-) enantiomer of ^{3}H-QNB and the (S)(-) enantiomer of NMS.

The rate constants of ligand binding to a receptor depend on the size, hydrophobicity and the general chemical characteristics of a ligand. The addition of extra chemical groups, such as methyl groups etc, all influence the rate at which the ligand can associate with the receptor. In the case of the M_1 mAChR the maximum association rate constant of a ligand binding to the receptor is determined by the collision or diffusion limited rate constant which turns out to be 10^{7}M sec^{-1}(Abbott and Nelsestuen, 1988). Ligands are not observed to associate with the receptor at rates faster than the diffusion limited rates. This could be consistent with the existence of an evolutionarily tailored entrance channel. The simple model L + R $\leftrightarrow$ LR describes the binding of ligand to a receptor. In order for a receptor ligand complex to form or break down, reactants must acquire sufficient energy to surmount the activation energy barrier. The net formation of specific bonds between residues and the ligand upon binding contribute to the energy required to break the activation barrier for the reverse reaction. The mutation of those specific interacting residues should increase the rate of dissociation, since the removal

of specific interactions reduces the amount of energy required for the reverse reaction. In contrast, mutation of residues that help maintain the structure of an entrance channel, or facilitate the the entry and exit of ligand molecules from the binding site might be expected to raise the activation barrier for both association and dissociation. The rate at which a ligand/drug dissociates from the orhosteric binding site has implications for the functional effectiveness of the receptor.

In recent years there has been considerable research on the effectiveness of allosteric modulators which can have profound effects on the association and more importantly on the dissociation rate constants of ligands from 7-TM receptors. For a full review of allosteric modulators see references (Birdsall and Lazareno, 2005; Christopoulos and Kenakin, 2002). With particular significance to this study, there is evidence from studies of the M_2 mAChR that the EDGE sequence (LAGQ in M_1) of the E2 loop is involved in the binding of the allosteric modulator gallamine (Gnagey et al., 1999; Leppik et al., 1994) and a report by Ellis and Seidenburg also provided evidence that the E2 loop of the M_2 mAChR sub-type was important for binding the allosteric ligand alcuronium. (Ellis and Seidenberg, 2000) Most allosteric modulators for muscarinic receptors, when bound, slow rates of ^{3}H-NMS dissociation to immeasurably low levels, but other modulators have lesser effects. Obidoxime for example only weakly inhibits the dissociation of ^{3}H-NMS from M_2 receptors and furthermore interacts competitively at the same site as gallamine. Similarly, another allosteric modulator, 3,4,5 trimethoxybenzoic acid 8-(dimethylamino) octyl ester (TMB-8) also has a weaker effect on the dissociation of ^{3}H-ACh, also from M_2 receptors (Gnagey and Ellis, 1996).

Allosterism at GPCRs is of growing interest, as the expanding literature on the subject testifies. Increasingly, allosteric modulators are being championed for their potential therapeutic benefit due to their inherent sub-type selectivity, their ability to enhance or

"de-tune" the effectiveness of endogenous ligands, such as ACh and provide further selectivity for optimally active receptors due to local ACh depletion. (Birdsall, 2005). Although interesting, a detailed discussion of allosterism is beyond the scope of this study. However, considering that many allosteric modulators cause inhibition of ligand dissociation, it was considered interesting to try to identify which residues may be involved in the indigenous molecular mechanisms involved in ligand association to and dissociation from the M_1 mAChR. Affinity constants are directly proportional to the ratio of the rates of association and dissociation of ligand and it would be expected therefore that mutations that decrease affinity constants are likely to also increase dissociation rate constants but not necessarily affect association rate constants. Thus dissociation experiments were conducted to try and corroborate and support affinity constant data collected for the mutants in this study.

In this study, dissociation assays were performed (as described in Methods 2.15) and using the resulting data equations as described below were used to evaluate both the k_{on} (association) and k_{off} (dissociation) rate constants, In nearly all cases the k_{on} and k_{off} were calculated using the simplest assumption of a 1-step binding process. The kinetics for radioligand binding have been predicted by the laws of mass action (Motulsky and Mahan, 1984). Using equations derived from the simple binding model (shown below) it is possible to determine dissociation and association rate constants, assuming that the radioligand (L) and the competing ligand (I) bind reversibly to the receptor (R) following the laws of mass action with kinetic constants (k).

$$R + L \underset{k_2}{\overset{k_1}{\rightleftharpoons}} RL \qquad R + I \underset{k_4}{\overset{k_3}{\rightleftharpoons}} RI$$

The symbols k_1 and k_3 relate to the association rate constants, whereas k_2 and k_4 relate to the dissociation rate constants. In the experiments described in Methods 2.15 an excess concentration of competing ligand (10^{-5} M atropine) is added to a mixture of pre-

bound radioligand and receptor negating the forward re-association of R + L, so that only the dissociation reactions are possible. Since the receptor saturating concentration of atropine prevents the forward association of R with L, the reaction is essentially irreversible. Thus, as the atropine replaces radioligand in the receptor binding site over time (t), so [RL] declines exponentially and radioligand dissociates from the receptor (figure 5.1). k_2 (dissociation rate constant) can be determined by the following equation: (omits the terms that describe the forward association of R+L).

$$[RL] = [RL_0].e^{-k_2 t} \quad ....(1a)$$

where $[RL_0]$ is the amount of radioligand associated with receptor at the start of dissociation (addition of atropine),. In our experiments [RL] and $[RL_0]$ are measured as dpm, hence .....

$$dpm = dpm_0.e^{-k_2 t} \quad ..(1b)$$

This is the formula which is used by the fitting program in Sigma Plot to derive a value for k_2, the dissociation constant.The time it takes for 50% of radioligand to dissociate, is given by.....

$$t_{1/2} = 0.693 / k_2 ....(2).$$

Figure 5.1. An Example Graph Representing the Parameters Obtained From Dissociation Experiments.

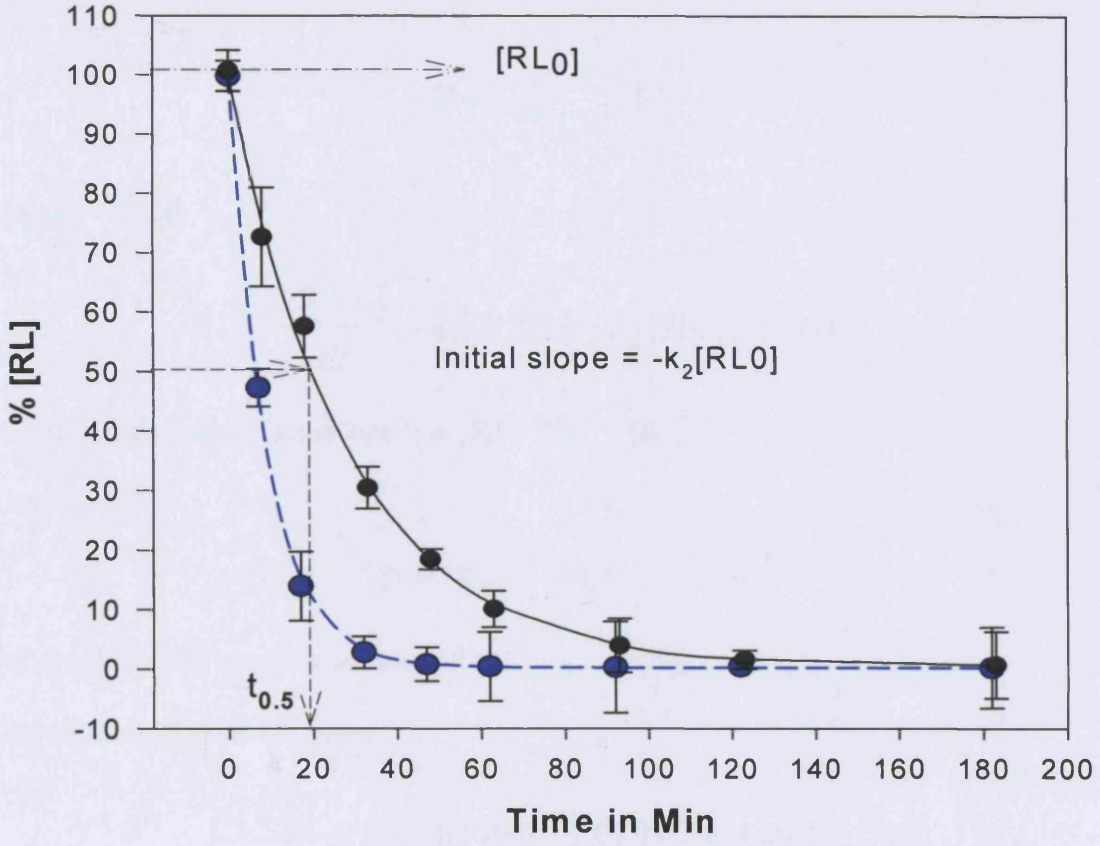

A graph showing radioligand dissociation time curves in the presence of excess competing ligand obtained as described in detail in the text. An increase in the dissociation rate constant causes an increase in the initial slope of the curve. The black symbols represent typical data obtained from experimental data fitted by a curve with k_2 = 0.0347 ($t_{1/2}$ = 20min). The blue symbols represent an increase in the dissociation rate constant fitted by k_2 = 0.0867 ($t_{1/2}$ = 8 min). [RL_0] is the concentration of [^{3}H]-Radioligand bound to receptor at time 0. For presentational purposes the data are normalised by division by RL_0

From the same initial model of ligand binding shown at the beginning of the chapter it is also possible to derive an expression describing the rate of ligand association.

So if

$$R + L \underset{k_2}{\overset{k_1}{\rightleftharpoons}} RL$$

Then

$$\frac{d[RL]}{dt} = k_1[R][L] - k_2[RL] \text{.....(1)}$$

subject to the conservation equation $[R] + [RL] = [R_T]$

And if

$$[R] = [R_T] - [RL] \text{.....(2)}$$

where [R] = free receptor concentration

Substituting (2) into (1) gives...

$$\frac{d[RL]}{dt} = k_1[L]([R_T] - [RL]) - k_2[RL] \text{.....(3)}$$

Solution of this first order differential equation (not shown) yields an expression that describes the rate of formation of the receptor ligand complex .....

$$[RL] = \frac{k_1[L][R_T]}{k_1[L] + k_2}(1 - e^{-(k_1[L] + k_2)t}) \text{....(4)}$$

Thus we arrive at the equation....

$$[RL] = \frac{K_A[L][R_T]}{K_A[L] + 1}(1 - e^{-(k_1[L] + k_2)t}) \text{.....(5)}$$

where K_A is the affinity constant (measured and known) and $1\text{-}e^{-(k1[L]+k2)t}$ is the exponential increase in [RL] over time. Increasing [L] increases the rate of [RL] formation. Association rate constants (k_1) can be determined experimentally by using equation (5) to fit curves derived from experimental data, since K_A, [L], $[R_T]$ and k_2 are

all known quantities. At low concentrations of ligand the rate of equilibration of the ligand is dependant upon the off rate. Effectively, at sub-saturating levels of ligand concentration only dissociation rates can be measured since there is not enough ligand to reach equilibrium quickly and this explains why an increase of ligand concentration increases the association rate. Hence, experimentally, at low ligand concentrations incubation times for saturation binding assays must be extended to ~5 times dissociation half times (~2hrs for NMS) to allow the system to reach equilibrium. From the simple one step model of binding it is shown that the affinity constant K_A (or K_D) is equal to the ratio of the rate of association (k_1) and the rate of dissociation (k_2) of the ligand....

$$K_D = \frac{k_2}{k_1} \ldots.(6)$$

In terms of the rate of association (M^{-1} sec^{-1})

$$k_1 = K_A.k_2 \ldots\ldots(7)$$

Using this equation, estimates of association rate constants for our mutant and wild type receptors can be made, using just the data gained from dissociation assays. Still, it must be assumed that the binding and release of ligand is a monophasic process and that receptor isomerization on binding ligand is not an issue. This assumption may not be appropriate since evidence of a biphasic process has been reported by Walbroeck et al (Waelbroeck et al. 1989) and more recently and comprehensively by Jakubik et al (Jakubik et al., 2000). Nevertheless, a monophasic model of binding was assumed for the calculation of association rates in this study simply because time restrictions did not allow experimental association assays to be performed. Moreover, any significant differences observed for dissociation rate constants should be reflected in the calculated association rate constant values since $k_1 = K_A \times k_2$ despite the reservations noted above. Of particular interest and a further aim of these assays is to provide supporting evidence that D99 is indeed part of an access channel.

5.2 Results of Kinetic Studies

Tables 5.1 and 5.2 summarise the binding kinetic data for NMS and QNB for all mutants. All dissociation assays were performed on membranes from COS-7 cells transfected with the mutant or wild type rat M_1 mAChR gene. Since rates of ligand dissociation are sensitive to changes in temperature all NMS dissociation assays were performed at between 28-30°C, unless otherwise stated, in quadruplicate. All data, without exception, for ^{3}H-NMS dissociation was analysed and fitted to a single exponential model of dissociation. The mean rate of dissociation of ^{3}H-NMS from wild type receptors was k_2 =0.066±0.001 min^{-1} (1.1 x 10^{-5} sec^{-1}), which equates to a mean half time of dissociation of 10.5min from a range of half times between 8min and 14min. The value for ^{3}H-NMS dissociation rate constants from WT M_1 receptors compares favourably with a k_2 value = 0.076±0.003 ($t_{1/2}$ = 9.1min) previously obtained by Lazereno and Birdsall (Lazareno and Birdsall, 1995). For wild type, the association rate constant was calculated as described above where k_1 is equal to 8.02 x 10^6 $M^{-1}sec^{-1}$ (4.81 x 10^8 $M^{-1}min^{-1}$).

For the E2 loop mutants small increases in dissociation rates were noticed compared to wild type. The most notable increases in the dissociation rate constants for NMS were seen for R171A k_2 = 0.1494 min^{-1} ($t_{1/2}$ = 4.6min), I180A k_2 = 0.156 min^{-1} ($t_{1/2}$ 4.3min) and F182A k_2 = 0.156 min^{-1} ($t_{1/2}$ 4.4min). (see figure 5.2) This coincided with small reductions in the calculated association rate constants. For the cysteine mutants C178A and C178N dissociation rate constants were increased k_2 = 0.160 min^{-1} and 0.158 min^{-1} respectively ($t_{1/2}$ = ~4min), but for C98A a more pronounced increase in the dissociation rate was seen with k_2 = 0.313 min^{-1} ($t_{1/2}$ ~2min). These increases in dissociation rate constants were accompanied by ~8-fold reductions in the association rate constants for all the cysteine mutants analysed.

Figure 5.2 Representative ^{3}H-NMS Dissociation Curves for E2 Loop Cysteine and D99A Mutants

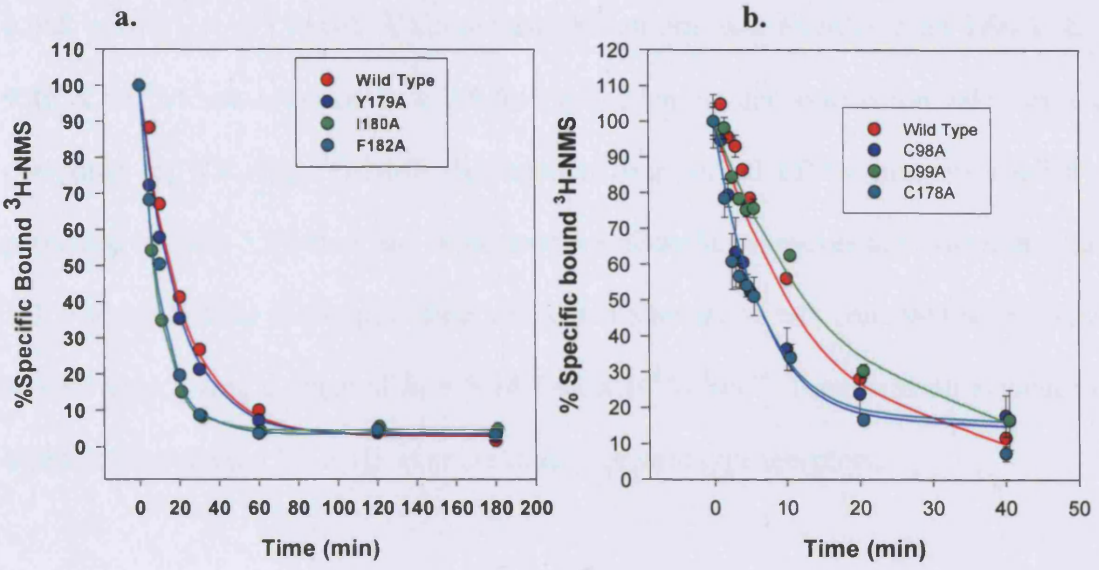

Representative dissociation curves for E2 loop and cysteine mutants. Assays were performed on transfected COS-7 cells membranes and contained ~10µg/mL.of protein [^{3}H-NMS] was 2 x 10^{-9}M. Membranes and were equilibrated at 28°C-30°C with ^{3}H-NMS for a minimum of 20 minutes before addition of 2 x 10^{-6}M atropine dissociation mix.

a.E2 loop mutants. **Wild type** k_2 = 0.0489 min^{-1}, ($t_{1/2}$ = 14min); **Y179A** k_2 = 0.0531 min^{-1}, ($t_{1/2}$ = 13min); **I180A** k_2 = 0.1049 min^{-1}($t_{1/2}$ = 7min). **F182A** k_2 = 0.0942 min-1($t_{1/2}$ = 7min).

b. Cysteine mutants. **Wild type** k_2 = 0.0638 min^{-1}($t_{1/2}$ = 11min). **C98A** k_2 = 0.159 min^{-1}($t_{1/2}$ = 4min); **D99A** k_2 = 0.058 min^{-1}($t_{1/2}$ = 11min); **C178A** k_2 = 0.158 min^{-1}, ($t_{1/2}$ = 4min). Full curves represent the fit to a single exponential model of ligand dissociation.

There was no data recorded for the double cysteine mutant C98A/C178A. The large reduction in NMS affinity caused by the F197A and W378A mutations meant that dissociation experiments were not attempted. D99A gave a dissociation rate constant of 0.088 min^{-1} ($t_{1/2}$ = 7.9min). A slower association rate was calculated for D99A, k_1 = 9.46 x $10^{-5}M^{-1}$sec-1 which is a >8-fold reduction in the association rate constant compared to WT. The ^{3}H-NMS dissociation data for all of the mutants studied is presented in table 5.1 below and representative dissociation curves are shown in figure 5.2. For most of the E2 loop mutants calculated association rate constants were similar to wild type giving a range of k_1 = 3.44-7.64 x $10^6M^{-1}sec^{-1}$. There was no evidence of biphasic dissociation for NMS at either mutant or wild type receptors.

The rate of ^{3}H-QNB dissociation from wild type receptors was substantially slower than that of ^{3}H-NMS. All wild type data was fitted to a mono-exponential model of dissociation and all data for wild type fit the model well, with no evidence of biphasic dissociation. Wild type gave a mean half time of dissociation k_2 = 0.0019 min^{-1} or 3.16 x $10^{-5}sec^{-1}$ ($t_{1/2}$ = 5 hours 51 min), similar to Walbroeks reported value of 5.3 x $10^{-5}sec^{-1}$ (Waelbroeck et al., 1991), with a corresponding association rate constant of 1.40 x $10^6M^{-1}sec^{-1}$, which is also in good agreement with the association rate constant for (R)-QNB reported by Walbroek et al (Waelbroeck et al., 1991) as 1.6 x $10^6M^{-1}sec^{-1}$. The effect of the E2 loop mutations on ^{3}H-QNB dissociation was varied with some mutant showing slow, WT-like dissociation kinetics whereas a few showed faster rates of dissociation (see figure 5.3). All data was fitted to the single exponential model of dissociation, except for C98A which better fitted the double exponential model of dissociation (see figure 5.4). E170A and Q177A had little effect on QNB dissociation with a mean half time of dissociation of k_2 = 0.002min^{-1} ($t_{1/2}$ = ~5-6 hours for both mutants), similar to that of the wild type. This is in direct contrast to the mutated residue R171A which increased the rate of dissociation of QNB with a k_2 value = 0.013min^{-1},

equating to a mean half time of just 54 minutes. Less dramatic than R171A, Y179A, I180A and F182A also increased QNB dissociation rates k_2 = 0.013, 0.006, 0.004 and 0.005 min^{-1} respectively ($t_{1/2}$ = ~1-3 hours).

Initial ^3H QNB dissociation experiments for C98A and C178A using single exponential fits, failed to produce meaningful estimations of dissociation rate constants. This was due to the fact the more than 50% of the radio ligand had dissociated before the first time point (30min) was recorded. Thus it can only be stated that the half time of QNB dissociation for these mutants was less than 30 minutes. Since it was shown in Chapter 3 that C98A had the potential to produce two separate populations of receptor, a more detailed dissociation experiment was performed and analysed using a double exponential fit to account for the possible biphasic nature of QNB dissociation from the cysteine mutants. In the detailed experiment where more time points over a shorter period of time were analysed and assessed using a double exponential model of dissociation, a better fit for the C98A and C178A data was made. The fast component for C98A giving a k_2 = ≥0.40 min^{-1}($t_{1/2}$ < 5 min) and the slow component gave a k_2 value = 0.007 min^{-1}, ($t_{1/2}$ = ~98min) the fast component was 31% of total sites (69% slow). For C178A the fast component was too fast to determine $t_{1/2}$ <5 min and the slow component k_2 = 0.218 min^{-1} ($t_{1/2}$ = ~32 min) the fast component was 83% of total sites (17% slow). Figure 5.4 shows the comparison of mono and double exponential fits for ^3H-QNB dissociation at both C98A and C178A mutant receptors. The calculated association rate of QNB to WT receptors was 1.4 x $10^6 M^{-1}sec^{-1}$ which is ~10-fold slower than the diffusion limited rate constant of 1 x $10^7 M^{-1}sec^{-1}$. Calculated association rates for mutants of the E2 loop were in the range of 1.2 – 6.5 x $10^6 M^{-1}sec^{-1}$. Most interesting is the 6-fold increase in the calculated association rate constant for R171A (k_1 = 6.1 x $10^6 M^{-1}sec^{-1}$) and the 5-fold increase in the association rate constant for F182A (k_1 = 6.49 x $10^6 M^{-1}sec^{-1}$).

Figure 5.3. Representative ^{3}H-QNB Dissociation Curves for E2 Loop Mutants

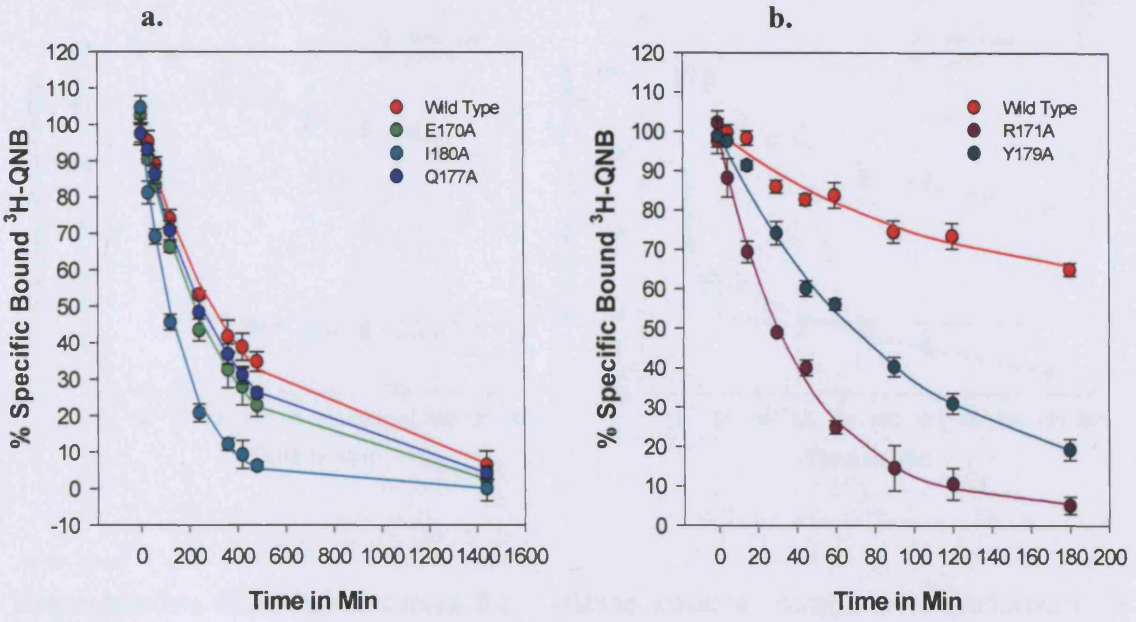

Representative dissociation curves for E2 loop mutants. Assays were performed on transfected COS-7 cells membranes and contained ~10µg/mL protein. [^{3}H-QNB] was 3 x 10^{-10}M. Membranes were equilibrated with ^{3}H-QNB at 28°C-30°C for minimum of 240 minutes before addition of 10^{-5}M unlabelled NMS dissociation mix.

a.E2 loop mutants with slow ^{3}H-QNBdissociation kinetics: **Wild Type** k_2 = 0.0025min^{-1}($t_{1/2}$ = ~5 hours); **E170A** k_2 = 0.003 min^{-1}($t_{1/2}$ = ~4 hours); **I180A** k_2 = 0.006 min^{-1}($t_{1/2}$ = ~2 hours); **Q177A** k_2 = 0.003 min^{-1}($t_{1/2}$ = ~4 hours).

b. E2 loop mutants with fast ^{3}H-QNB dissociation kinetics: **Wild Type** k_2 = ND. **R171A** k_2 = 0.024 min^{-1}($t_{1/2}$ = 30 min); **Y179A** k_2 = 0.011min^{-1}($t_{1/2}$ = ~60 min).Full curves represent the fit to a single exponential model of ligand dissociation.ND= Not determined (<50% dissociation after 180 min(3hrs)

Figure 5.4 Comparison of Single and Double Exponential Models to Fit ^{3}H-QNB Dissociation Curves for C98A and C178A

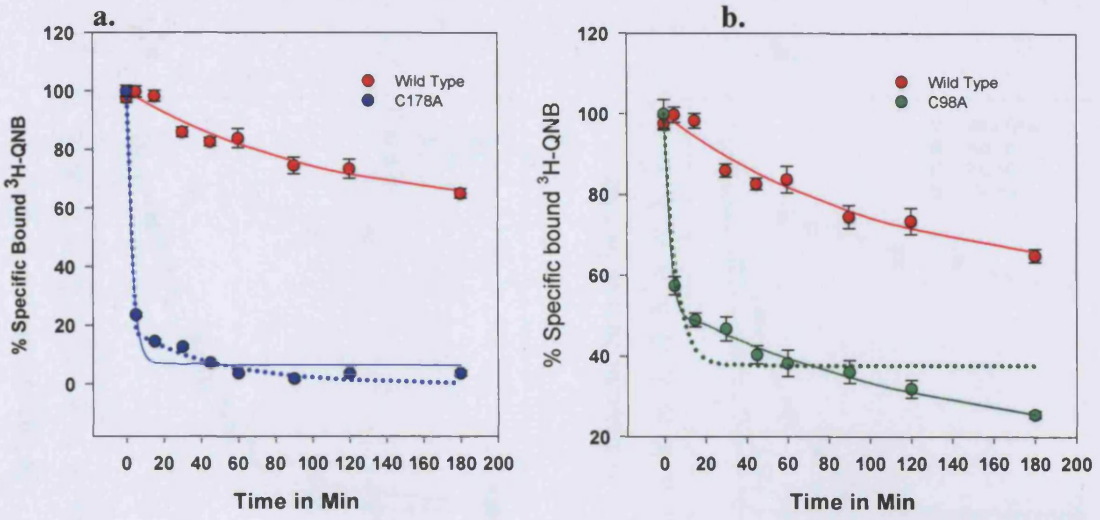

Representative dissociation curves for Cysteine mutants. Assays were performed on transfected COS-7 cells membranes and contained ~10µg protein. [^{3}H-QNB] = 3 x 10^{-10}M. Membranes were equilibrated with ^{3}H-QNB at 28°C-30°C for minimum of 240 minutes before addition of 10^{-5}M unlabelled NMS dissociation mix.

a. Wild type k_2 = ND (<50% dissociation). **C178A** using single exponential fit (solid blue line) k_2 = >0.3 (>50% dissociation after 5 min) $t_{1/2}$ <5 min and double exponential fit (dotted blue line) fast $k2$ = ND(too fast) slow k_2 = 0.0218min^{-1}($t_{1/2}$ = ~32 min) ratio fast to slow = 4:1 (80%). slow component = 17% of total sites Span 1 (fast) = 38.7dpm, Span 2 (slow) = 8.1 dpm plateau = 9.7

b.Wild type (as above). **C98A** single exponential fit (dotted green line) k_2 = 0.184 min^{-1}($t_{1/2}$ = <4 min) and double exponential fit (solid green line) fast k_2 = 0.40 min^{-1}($t_{1/2}$ = 1.7min) and slow k_2 = 0.007 min^{-1}($t_{1/2}$ = 98min) slow component = 69% of total sites Span 1 (fast) = 17.5dpm, Span 2 (slow) = 39.3 dpm plateau = 9.7

Figure 5.5. Representative ^{3}H-QNB Dissociation Curves for TM Domain Mutants.

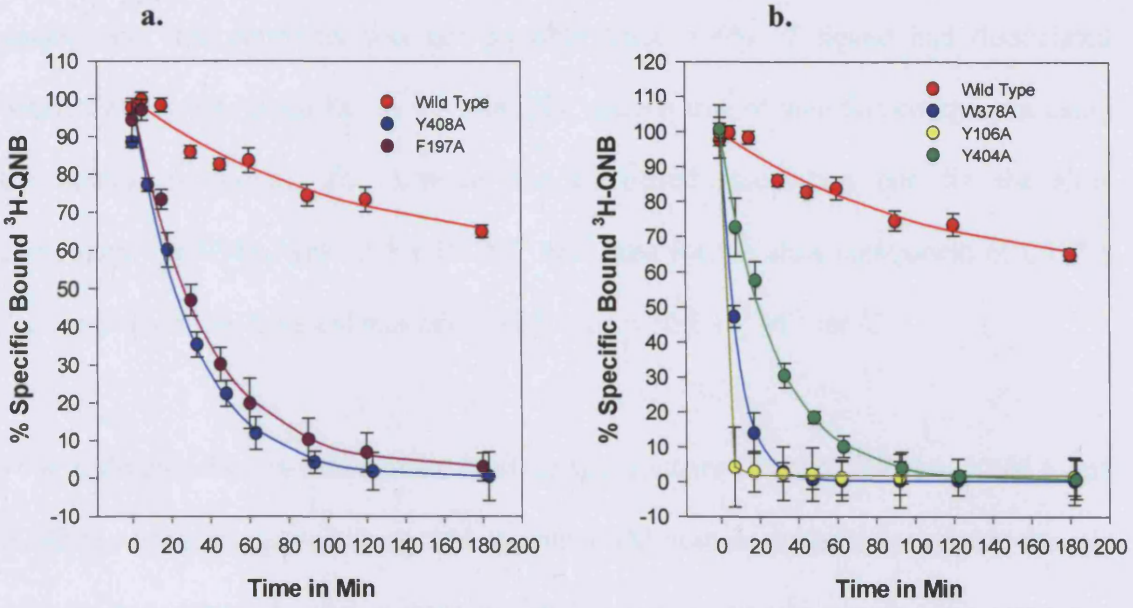

Representative dissociation curves for TM Domain Mutants. Assays were performed on transfected COS-7 cells membranes and contained ~10µg/mL protein. [^{3}H-QNB] was 3 x 10^{-10}M. Membranes were equilibrated with ^{3}H-QNB at 28°C-30°C for minimum of 240 minutes before addition of 10^{-5}M unlabelled NMS dissociation mix

a. TM Domain mutants. **Wild Type** k_2 = ND, **Y408A** k_2 = 0.033 min^{-1}($t_{1/2}$ = 21 min); **F197A** k_2 = 0.028 min^{-1}($t_{1/2}$ = 25 min).

b. TM domain mutants. Wild Type k_2 = ND, **W378A** k_2 = 0.111 min-1($t_{1/2}$ = 6 min); **Y106A** $k_2 \geq 0.525$ min^{-1}($t_{1/2}$ = <2 min). **Y404A** k_2 = 0.036 min^{-1}($t_{1/2}$ = 20 min). Full curves represent the fit to a single exponential model of ligand dissociation. ND = Not Determined (<50% dissociation after 180 min (3hrs).

The other E2 loop mutants gave association rate constants for ^{3}H-QNB at values similar to WT, and between 5-10-fold slower than the rate constantfor ^{3}H-NMS. Calculating association rate constants for C98A and C178A using the single exponential fit the dissociation rate constants was not possible since >50% of ligand had dissociated beforethe first time point i.e $t_{1/2} < 5$ min. The same is true of then fast component using the double exponential fit. However the calculated association rate for the slow component for C98A was 1.68×10^5 M^{-1} sec^{-1}. and for the slow component of C178A the association rate constant was calculated to be 6.70×10^5 M^{-1} sec^{-1}.

Four additional M_1 transmembrane binding site mutants (Y106A, Y404A, Y408A and N382A) were also assayed along with the other TM-domain mutants to evaluate the role of these endogenous transmembrane binding pocket residues in securing the antagonist in the central binding pocket. In fact, all mutations of residues in the TM domain involved in ligand binding drastically accelerated the rate of ^{3}H-QNB dissociation with a range of k_2 values between 0.024 and 0.332 min^{-1} ($t_{1/2}$ between 30 and 2 minutes). The most significant increase in the dissociation rate was effected by Y106A ($k_2 = 0.332min^{-1}$) ~170-fold faster than ^{3}H-QNB dissociation from wild type receptors. W378A also caused a significant increase with a $k_2 = 0.086min^{-1}$ a ~40-fold faster rate of QNB dissociation than from the WT receptor. The other TM domain mutants all increased QNB dissociation rates between 10 and 25-fold ($t_{1/2}$ = between 15-30mins) (see figure 5.5). A 3-fold reduction in calculated ^{3}H-QNB association rates compared to wild type was found for D99A, ($k_1 = 5.1 \times 10^5 M^{-1}sec^{-1}$). By contrast, the rest of the TM domain mutants increased the calculated association rate constants. Y404A ($k_1 = 1.18 \times 10^7 M^{-1}sec^{-1}$), Y408A ($k_1 = 1.6 \times 10^7 M^{-1}sec^{-1}$) and F197A ($k_1 = 7.31 \times 10^6 M^{-1}sec^{-1}$) and W378A ($k_1 = 5.98 \times 10^6 M^{-1}sec^{-1}$) all increased the calculated association rate constants for QNB between 5-11-fold, approaching association rate constants at the diffusion limited rate.

Table 5.1. Summary of Dissociation Rate Constants and Calculated Association Rate Constants for ^{3}H-NMS

^{3}H-NMS					
Mutant	**n**	**Half Time (min)**	**Mean k_2 (min^{-1})**	**Log $k_2$mut/$k_2$wt**	**Calculated k_1 ($M^{-1}sec^{-1}$)**
Wild Type	13	10.5	0.066±0.01	0	8.02E+06
E2 Loop Mutants					
E170A	3	8.8	0.079±0.01	0.078	7.33E+06
R171A	3	4.7	0.149±0.04***	0.35	4.45E+06
Q177A	3	9.9	0.070±0.01	0.024	7.64E+06
Y179A	3	9.2	0.076±0.02	0.06	3.44E+06
I180A	3	4.3	0.161±0.03***	0.39	7.68E+06
F182A	3	4.5	0.156±0.03***	0.37	6.13E+06
Cysteine Mutants					
C98A	3	2.2	0.313±0.11***	0.68	1.00E+06
C178A	3	4.3	0.160±0.01***	0.38	1.77E+06
C178N	3	4.4	0.158±0.04***	0.38	9.61E+05
TM Domain Mutants					
D99A	4	7.9	0.088±0.03	0.12	9.46E+05
W378A	1	37.5	0.019±nd	ND	5.48E+03

Student T-Test (two-tailed equal variance) $p<0.05$*, $p<0.01$** and $p<0.001$, *** with respect to wild type values.
k_2 = dissociation rate constant, k_1 = association rate constant

Table 5.2. Summary of Dissociation Rate Constants and Calculated Association Rate Constants for ^{3}H-QNB

^{3}H-QNB					
Mutant	**n**	**Half Time (min)**	**Mean k_2 ($M^{-1}min^{-1}$)**	**Log $k_2$mut/$k_2$wt**	**Calculated k_1 ($M^{-1}sec^{-1}$)**
Wild Type	4	352	0.002±4.0E-04	0	1.40E+06
E2 Loop Mutants					
E170A	3	288	0.002±6.0E-03	0.08	2.64E+06
R171A	3	54	0.013±0.006	0.82	6.10E+06
Q177A	3	350	0.002±0.0005	-0.02	1.23E+06
Y179A	3	119	0.006±0.002	0.47	2.41E+06
I180A	3	189	0.004±0.001	0.27	2.07E+06
F182A	2	154	0.005±0.001	0.36	6.49E+06
Cysteine Mutants					
C98A‡	3	<30	ND	ND	ND
C178A‡	3	<30	ND	ND	ND
C98A§(f)	1	<5.0	>0.40	2.30	ND
C98A§(s)	1	98	0.007	0.54	1.68E+05
C178A§(f)	1	<5.0	>0.30	ND	ND
C178A§ (s)	1	32	0.0218	1.04	6.70E+05
TM Domain Mutants					
D99A	3	288	0.002±3.0E-03	0.09	5.09E+05
Y106A	2	<5.0	>0.332±0.15*	2.23	7.63E+06
F197A	3	35.4	0.020±0.004**	1.00	7.31E+06
W378A	4	8.1	0.086±0.03*	1.64	5.98E+06
N382A	2	<5.0	0.139±0.09	1.85	1.25E+06
Y404A	2	24.1	0.029±0.006**	1.16	1.18E+07
Y408A	2	29.5	0.024±0.007*	1.08	1.60E+07

Student T-Test (two-tailed equal variance)

‡ Cys muts using single exponential fit

§ Cys muts detailed experiment using double exponential fit.(f) fast component and (s) slow component.

$p<0.05$*, $p<0.01$** and $p<0.001$***

k_2 = dissociation rate constant, k_1 = association rate constant

5.3 Discussion and Conclusions

The dissociation kinetics of N-methylscopolamine have been described previously for wild type M_1-M_4 mAChRs (Lazareno and Birdsall, 1995) where M_1, M_3 and M_4 give dissociation rate constants equal to ~0.08min^{-1} which equals a half time of dissociation of ~10 minutes. However, NMS dissociates more rapidly from M_2 receptors k_2 = ~0.4min^{-1} ($t_{1/2}$ = ~2min) The dissociation rate constant for NMS at wild type receptors, were shown in this study to be in good agreement with previous data (Lazareno and Birdsall, 1995). Perturbations of the E2 loop caused by alanine substitutions had the general effect of accelerating the rate of ^{3}H-NMS dissociation, although the increased acceleration was little more than 2-3-fold from WT rates of NMS dissociation. The increase in dissociation rate constants induced by R171A, I180A and F182A were significant (see table 5.1).

A plot of the changes in the dissociation rate constants compared to the changes in affinity constants (figure 5.6) suggests that the magnitude of the changes are consistent with a decrease in binding energy resulting from these mutations. Q177A, E170A, I180A and F182A follow the k_2 versus K trendline for NMS. E170 and Q177 behave like null residues in terms of kinetic and equilibrium binding. This supports evidence in Chapter 4 that also suggested E170 was a null residue in terms of activation. I180 by contrast shows a phenotype consistent with its being ligand anchor residue for NMS, similar to its role in binding ACh as shown in Chapter 4.

Figure 5.7 shows the correlation between changes in dissociation rate constants and changes in affinity constants for QNB. It can be seen that R171 and F182 in the E2 loop and Y106, F197, W378, Y404 and Y408 all lay well below the 1:1 trendline. In Chapter 3 it was shown that R171A, F182A and F197A did not significantly reduce QNB binding affinity constants. Thus, the acceleration of QNB dissociation seen for these

mutants implies that they cause perturbations in the structure of the receptor, decreasing receptor stability. The same is true for Y404A and Y408A. Y106A and W378A both significantly reduce the binding affinity of QNB, implicating them as ligand binding residues, but the larger effect on the QNB dissociation rate constant suggests that they also contribute to the structural stability of the receptor.

By contrast, C98A, C178A and D99A lie above the 1:1 correlation line for NMS, while for QNB only D99A lies above the trend line. The removal of the disulphide bonded cysteine residues causes an acceleration of ^{3}H-NMS dissociation, approximately a 3-5 fold increase in the rate relative to WT receptors and a ~5-8-fold reduction in the calculated NMS association rate constant. However, the magnitude of the acceleration is much less than might be expected from the decreases in binding affinity. The same applies to D99A which also diminishes the calculated association rate constant for NMS about 10-fold. These observations might be consistent with the presence of an access channel and is also consistent with the calculated reduction in association rate constant derived for D99A. The strong effects of the cysteine mutations could suggest that the disulphide bond is also vital to the preservation of the entrance channel architecture. Smaller effects are seen for R171A and Y179A. These residues may also play a role in the structure of the entrance channel. Recent experiments by Avlani (Avlani, 2005) have shown slowing of the rate of dissociation of ^{3}H-NMS by pinning down the E2 loop of the M_2 mAChR by incorporating an additional disulphide bond between a Cys substituted for Val 171 of the E2 loop and Asp 419 of TM-7. By reducing this S-S bond with dithiothreitol the receptor recovers to wild type rates of ligand dissociation. These authors suggest that not only is the E2 loop important for the binding of allosteric modulators, it is also important for the natural entry and egress of ligands to and from the central binding cavity and that it is the dynamic nature of the E2 loop that allows for this.

Figure 5.6. Plot of Dissociation Rate Constant vs Affinity Constant for NMS Binding to Alanine Substitution Mutants

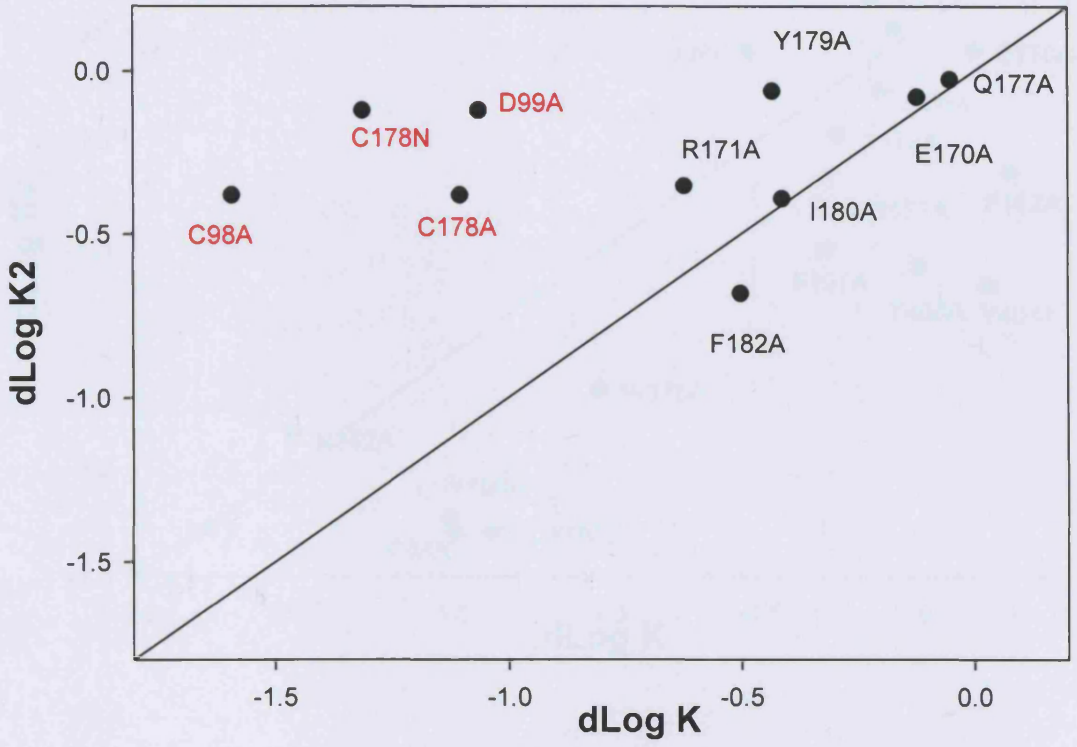

Correlation of the changes in dissociation rate constants and NMS binding affinity constants for mutants tested in this study. The positive correlation trend line represents the 1:1 ratio for change in dissociation and change in affinity. Mutants that lie above the trendline show smaller effects on the dissociation rate constant than would be expected from the change in affinity constant, whereas mutants below the trend line had greater effects on dissociation rate constants. Points close to the trend line are indicative of mutations where an increase in the dissociation rate constant can be accounted for by reduction in NMS affinity.

Figure 5.7 Plot of Dissociation Rate Constant vs Affinity Constant for QNB Binding to Alanine Substitution Mutants

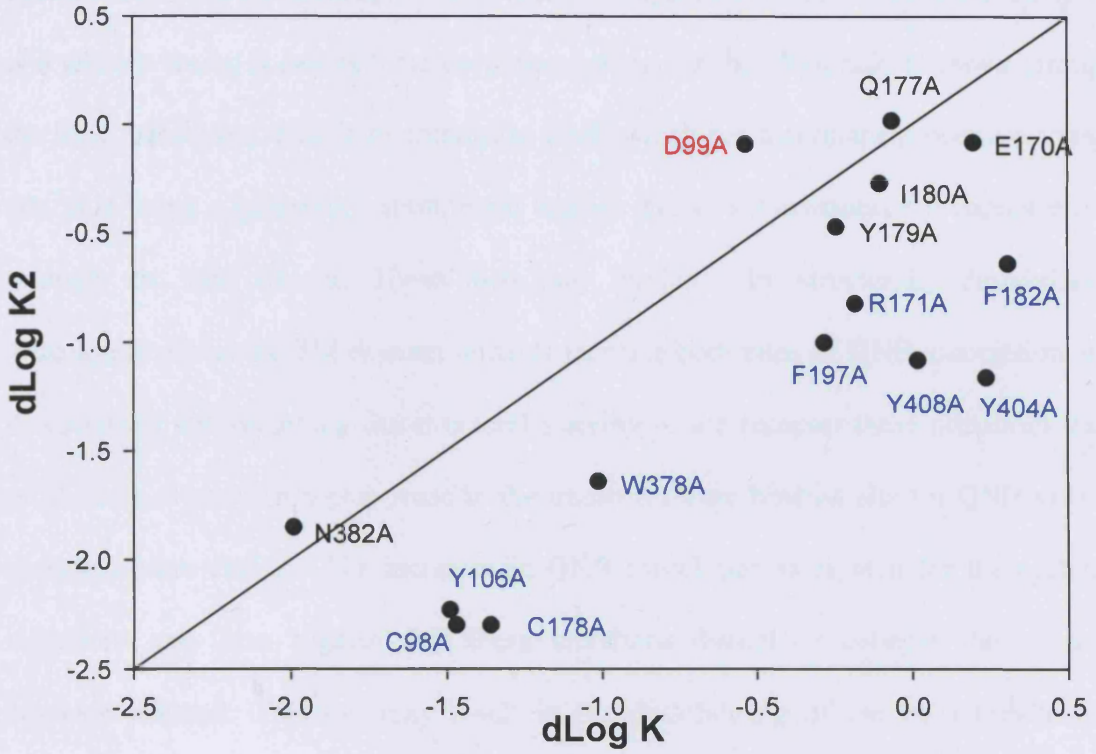

Correlation of the changes in dissociation rate constants and QNB binding affinity constants for mutants tested in this study. The positive correlation trend line represents the 1:1 ratio for change in dissociation and change in affinity. Mutants that lie above the trendline have smaller effects on the dissociation rate constant than would be expected from the change in affinity, whereas mutants below the trend line had greater effects on dissociation rate constants. Points close to the trend line are indicative of mutations where an increase in the dissociation rate constant can be accounted for by a reduction in QNB affinity. Values for QNB affinity: Y106A (Lu and Hulme, 1999a), N382A (Ward et al., 1999a)Y404A and Y408A (Lu et al., 2001).

Does QNB access the receptor via the same entrance channel as ACh and NMS? A reduction in the association rate constant for QNB shown by the D99A mutation suggests that it may. The fact that QNB is a bulky and hydrophobic molecule may account for its slower association rate kinetics compared to NMS. However, since QNB is a tertiary amine it can become de-protonated and is therefore able to move through the lipid membrane. This is in contrast to NMS which has a permanent positive charge due to it being a quaternary ammonium species and as a consequence it cannot move through the lipid bilayer. These facts may explain why structurally destabilising mutations such as the TM domain mutants increase both rates of QNB association and dissociation. By disturbing the structural stability of the receptor these mutations may produce an alternative access route to the transmembrane binding site for QNB via the transmembrane helices. The increases in QNB association rates seen for the cysteine mutations may also suggest that these mutations disrupt or collapse the aqueous entrance channel. This too may result in the destabilising of the helix-bundle and facilitate the entry of a lipophilic molecule such as QNB via the transmembrane helices. Two mutations R171A and F182A both increased the association rate constants of QNB ~6-fold to that of the WT receptor, approaching values close to the diffusion limited rate. Although these two mutations do not significantly reduce the affinity constant of QNB, it is possible that they perturb the structure of the E2 loop sufficiently to allow enhanced random movement of the TM helices. This 'breathing' motion, induced by the mutations in the E2 loop, may allow QNB to enter the binding site at a quicker rate than for the WT receptor, entering more readily through the gaps in the helices caused by a relaxation in the E2 loop structure.

In general the dissociation of antagonists from mutant WT and M_1 receptors was found to be monophasic. The major exception was that of the C98A mutant. The dissociation data for this mutant better fitted the double exponential model (see figure 5.4). There

was a rapid phase of dissociation where approximately 50% of ^{3}H-QNB had dissociated within 2-5 minutes and a slow phase of dissociation whereby 50% of the remaining bound ligand took a further 98 minutes to dissociate. This finding may be explained by the possibility that the creation of the C98A mutation generated two separate populations of receptor. One population with a fast dissociation rate constant and another with a slow dissociation rate constant for ^{3}H-QNB could exist simultaneously. It seems plausible that the putative populations might correspond to the high and low affinity ACh binding sites described in Chapter 4. Equilibrium ^{3}H-QNB binding assays do not differentiate between the two sites. Further experimentation is required to discover which of the two populations of ACh binding sites seen for the C98A mutant receptor may be responsible for the rapid and slow QNB dissociation kinetics. This could be achieved by protecting the sites with a high affinity for ACh with a sufficient concentration of ACh. An ACh concentration of 10^{-3} M would be sufficient to block the high affinity site but allow ^{3}H-QNB to bind to the unoccupied low affinity sites. Measuring the rate of QNB dissociation from the ACh unoccupied sites would provide an indication whether or not the low affinity site was responsible for the fast or slow QNB dissociation kinetics.

The C98A receptor effectively has a highly reactive free cysteine residue at C178. This reactive free cysteine 178 could potentially form a disulphide bond with another free reactive cysteine elsewhere in the receptor. There are two free cysteine residues within the E3 loop of the M_1 receptor at positions 391 and 394 respectively. It is possible that the formation of a disulphide bond with either of these residues could create a structure similar to that imparted by the natural S-S bond between C98 and C178 in the wild type receptor, thus negating rapid dissociation of the antagonist. Again it is evidence provided by Avlani (Avlani, 2005) that may support this proposition. Avlani showed that it was indeed possible to create a non-native disulphide bond between the E2 and

E3 loops. Therefore it may not be unreasonable to think that a free C178 residue could form a similar intramolecular disulphide bond. Alternatively the free cysteine may form an intermolecular disulphide bond with an adjacent receptor, effectively forming a dimer with a high and low affinity antagonist binding site. The same observation is not seen for the C178A mutant, since the free reactive cysteine 98 residue is located at the top of TM3 and is probably out of range of the free cysteine in the E3 loop. However the presence of two populations of binding sites cannot be excluded for the C178A mutant.

In all dissociation experiments conducted with NMS (but not QNB) in this study pre-incubation times were of intermediate length (20-25 minutes) and no evidence of biphasic dissociation was witnessed. Jakubik et al (Jakubik et al., 2000) presented data where longer periods of pre-incubation (60-90min) with ^{3}H-NMS followed by dissociation with varying concentrations of unlabelled NMS led to the observation that the dissociation of NMS from M_1 receptors was significantly slowed. During the short pre-incubations (2-5min) faster rates of dissociation were observed the conclusion being that both ^{3}H-NMS and unlabelled NMS can bind to the receptor simultaneously a finding also noted by Walbroeck using other muscarinic antagonists (Waelbroeck, 1994). Jakubik proposed that his observations were indicative of there being a high and a low affinity site for NMS. Fast dissociation during the short pre-incubations is consistent with a low affinity site and conversely slow dissociation from a high affinity site as seen during longer pre-incubations. This led to the theory that there is an initial binding of antagonist to the receptor via an access channel before the ligand is translocated to the central binding pocket. In the case of M_1 mAChR, D99 is the residue postulated to be involved in the initial binding of antagonist. As has been explained above there is some corroborative evidence that D99 is indeed part of an access channel.

There is a well described access channel or 'gorge' lined with 14 conserved hydrophobic residues in the acetylcholinesterase (AChE) enzyme (Sussman et al. 1991). This hydrophobic gorge is believed to be in part responsible for the fast catalytic activity of this enzyme because it reduces the free energy required for the ACh molecule to reach the active site, effectively forming a slippery channel through which the ACh molecule reaches the catalytically active site deeper in the enzyme The quaternary head group of ACh interacts with AChE via cation –π interactions with two highly conserved tryptophan residues in the anionic site while de-acylation occurs at the esteratic locus (Quinn, 1987) , (Silman and Sussman, 2005) It is reasonable to imagine that there is a similar hydrophobic access channel in the muscarinic receptors that also allows rapid association of ACh with the binding site and that D99 and W157 (both fully conserved in the mAChR family) are the two residues situated at the entrance to that channel. These two residues are analogous to the negatively charged glutamate residue, Glu 292 and an aromatic Tryptophan, Trp 286 which, among other aromatic residues, are located at the entrance to the gorge in AChE (Bourne et al., 1995).

Rhodopsin, which does not bind Ach, does not contain analogous residues at these positions. During the evolutionary process acetylcholine binding receptors and acetylcholinesterase may have developed similar strategies for the translocation of ACh from the hydrophilic milieu to the hydrophobic core of the functioning molecule.The findings of the present study would seem to suggest that the E2 loop of the M_1 receptor fulfils an analogous role to that of the M_2 receptor as described by Avlani et al (Avlani, 2005). Furthermore, the role, structure and flexibility of the E2 loop of the muscarinic receptors probably differ from that of rhodopsin. In rhodopsin the ligand, retinal is covalently bound to the TM domains of the receptor and is not required to diffuse into the transmembrane binding site before activating. It seems reasonable therefore to suggest that the E2 loop of rhodopsin is required to be less dynamic than that of the

muscarinic receptors but that it is more important for the protection of the ligand and providing the environment of the retinylidene Schiff base in the active conformation (Yan et al., 2002). This and other studies (Savarese et al., 1992; Ward et al., 2002; Zeng et al.1999) have shown that once properly folded and at the cell surface the maintenance of the disulphide bond is less critical to the binding of antagonists than the TM domain residues have proved to be so. Nevertheless the E2 loop maintains the conformation of the ligand binding pocket and probably the entrance channel and thus helps to minimise the change in free energy required to surmount the activation barrier necessary to favour ligand interaction with the receptor The cysteine mutations and D99A must increase the activation energy of the association step more than the dissociation step of NMS binding since the reduction in the association rate constants were more pronounced than the dissociation rate constants for these mutants. The~20-fold increase in QNB dissociation rate and 3-5-fold increase in NMS dissociation rates support the idea the removal of the important S-S bonded cysteines do indeed perturb the binding energies of ligands in the transmembrane binding pocket.

Chapter 6

Binding of Other Ligands.

6. 1. Introduction-

Extensive residue substitution experiments have been reviewed (Hulme et al., 2003; Lu et al., 2001; Heitz et al., 1999; Vogel et al., 1997; Wess et al., 1991) These authors have identified the important amino acid side chains that form the central binding cavity of the muscarinic acetylcholine receptors. There is a large degree of overlap of key residues and interactions involved in the binding of the endogenous agonist, acetylcholine and the high affinity classical antagonist N-methylscopolamine, although differences do occur. A critical interaction for both ligands is the stabilizing ionic interaction of the positively charged tetramethylammonium head group of ACh and the quaternery amine head group of NMS with the negatively charged and highly conserved side chain of aspartate 105. The substitution of this residue with alanine reduces both ACh and NMS affinity 100-fold and completely abolishes any ACh induced signalling (Lu and Hulme, 1999b) There is a negatively charged residue at the analogous position in all cationic amine receptors, and this underlines the essential role of this residue for the binding of agonists with positively charged head groups such as ACh (Shi and Javitch, 2002).

The predominant transmembrane binding site residues, Tyr 106, Tyr 381, Tyr 404, and Tyr 408 form a charge-stabilized aromatic cage into which the quarternary ammonium head group of the active S(-) enantiomer of NMS and the gauche conformer of ACh can be docked in the ground state of the M_1 mAChR homology model (Hulme et al., 2003) (see figure 6.1.) Interactions with the docked ligands are further stabilized by a hydrogen bonding network involving residues Ser 109, Thr 182, Thr 192, Asn 382 and Cys 407. The presence of an anionic group and of hydrogen bond donors within the

muscarinic binding site had long been predicted by pharmacophore modelling (Schulman JM. Michael L. Sabio, 1983; Schwarz et al., 1995; Vogel et al., 1999) suggesting that there must be a negative charge in the binding site and that a full muscarinic agonist must have the equivalent of five atoms in its side chain, the classic 5-atoms rule. The specificity of muscarinic agonist binding is comprehensively reviewed by Ringdahl (Ringdahl, 1989a). The interaction of the quaternary ammonium head groups of NMS and ACh is with D105 and the carbonyl or ester oxygens of both NMS and ACh may be hydrogen bonded to the hydroxyl group of the Y381 residue. The side chain oxygens of both ligands may also hydrogen bond to the hydroxyl group of Y106, the mutation of which induces a comparable loss of affinity and function to that of the D105A mutant (Lu and Hulme, 1999a) and the hydroxymethyl group of NMS may hydrogen bond with Asn 382. NMS and ACh bind in a similar manner except that the side chain of NMS possibly binds deeper within the binding cavity than ACh. Confirmatory evidence for this has been provided in this thesis (see Chapter 3), whereby the mutation to alanine of Phe 197 (TM5) and Trp 378 (TM6) at the predicted base of the binding cavity, led to a ~100-fold and ~400-fold reduction in NMS affinity respectively and Trp 378 but not Phe 197 showed a ~10-fold loss of affinity for ACh. Thus it is likely that these two residues also participate in the binding of NMS, but only Trp 378 in the binding of ACh. The binding modality of QNB, which contains a tertiary amine head group, probably differs to that of the quaternary ammonium-containing NMS molecule. Ward et al (Ward et al., 1999a) showed that the mutation of Tyr 381, a critical contact residue for NMS had virtually no effect on the affinity of QNB. A similar observation was made in results Chapter 3 of the present study, where mutation to alanine of Phe 197 severely reduced (~100-fold) the affinity of NMS but reduced the affinity of QNB less than 3-fold. This indicates that different residues may be important contact residues for one ligand but not another and revealing their identity has implications for pharmaceutical design.

Other peripheral residues providing stabilizing polar and Wan der Waals interactions also discriminate between NMS and ACh binding modalities in the M_1 mAChR. For example, the phenyl ring of NMS resembles the β-ionone ring of retinal (the covalently bound agonist of rhodopsin) and is predicted in the homology model to be in close proximity to residues Asn 110, Val 113 (TM3) and Phe 374 (TM6), where it is expected to support the contacts in TM3, TM5 and TM6 required for the preservation of the inactive conformer of the receptor. Additional residues surrounding D105 such as Trp 101, Leu 102 (TM3), and Leu 386 may provide a second shell of interactions that help to position the primary binding site residues and residues Thr 189, Thr 192 and Ala 196 may contribute to a hydrogen bonding network probably including water molecules that complete the muscarinic pharmacophore. The role of the E2 loop in the primary binding site has now been evaluated in this study and it appears that E2 loop residues may also provide a second tier of residues that stabilise the primary binding site without making any critical ligand contact.

The existence of a ligand docking site has been supported by work done in the present study (results Chapter 5), other kinetic studies (Jakubik et al., 2000) and radioligand binding studies where mutation of Trp 157 (W157) to alanine, significantly reduced ACh (~100-fold) and NMS (123-fold) affinity and signalling efficacy (160-fold) (Lu et al., 2001). However, in the homology model of the M_1 mAChR this residue lies too far from the ligand binding site to participate in ligand contact without a conformational change. The other residue postulated to be part of the ligand docking site is Asp 99, a residue under investigation in this thesis. The D99A mutant has shown similar patterns of reduced ACh affinity but in contrast to W157 no significant reductions in efficacy. Although the reduction in ACh affinity is not as large as that seen for Trp 157, D99 also lies too distant from the central binding core to be directly involved in the binding site, according to the homology model (Hulme and Lu, 1998). Ligands need to enter and

leave the central binding core rapidly, unlike the covalently bound retinal of rhodopsin and the idea of an entrance channel, based on this study and others (Heitz et al., 1999) seems highly plausible and may be synonymous with the peripheral ionic site at the entrance channel to the acetylcholinesterase enzyme (Silman and Sussman, 2005).

A previous study in this laboratory (Page et al., 1995) examining the effect of mutating the critical binding site residue Asp 105 to glutamate (preserving the negative charge) on agonist binding affinities showed that although the mutation reduced the affinity of ACh ~20-fold the effect on oxo-M, pilocarpine and McN-A-343 affinity was minimal, although oxo-M-induced signalling was severely disabled by the D105E mutant. This suggests that there are likely to be different modes of binding for different ligands that may or may not involve the critical binding site residues necessary for the binding of the endogenous agonist acetylcholine. However, there is an argument as to whether or not evolution of the cationic amine receptors binding site has allowed for the binding of non-endogenous or non- productive ligands. Have evolutionary forces positioned the side chains of the amino acids so as to minimise the possibility that the receptor can be activated by ligands structurally and chemically heterologous to the endogenous agonist?

The atypical muscarinic agonist 4-(chlorophenyl-carbamoyloxy)-2-butynyl trimethylammonium (McN-A-343) was first shown to stimulate mAChRs in sympathetic ganglia by Roszkowski (Roszkowski, 1961). McN-A-343 is unusual because it has a potent and selective muscarinic receptor mediated effect on sympathetic ganglia but a weaker muscarinic effect on non ganglionic tissues (Ringdahl, 1989b). It was proposed that McN-A-343 mediates these effects through M_1 mAChRs and this was studied in more detail by Birdsall et al (Birdsall et al. 1983) on membrane preparations of the cerebral cortex (M_1) and myocardium (M_2). The conclusion of their

study stated that McN-A-343 "binds to a site distinct from that occupied by NMS" and that McN-A-343 "does not behave as a simple competitive ligand". A study by Hardouin et al. (Hardouin et al., 2002) explains this earlier observation. They showed that although M_1 is not expressed in cardiac tissue, it was the activation of postganglionic cells by McN-A-343 that results in the release of catecholamines that in turn affect cardiac stimulation. Hence the treatment of WT mice with ACh leads to arrhythmia. The residues responsible for the binding of McN-A-343 are still to be identified. It was shown that the primary binding site residue Asp 105 may not be involved. The mutation of Asp 105 to a negatively charged glutamate (D105E) reduced the binding of McN-A-343 less than 3-fold in the M_1 receptor and less than 4-fold in the analogous D103E mutation in M_2 receptors (Page et al., 1995). The mutation of D103 to another negatively charged amino acid may not be the best mutation to make to analyse the contribution of D103 to the binding site, since maintenance of the charge may confer a similar phenotype to the WT receptor. Schwarz et al. (Schwarz et al., 1995) produced a more imfomative mutant in the M_2 mAChR, D103N which also showed very little effect on McN-A-343 binding. This again suggests that mcN-A-343 does not bind in the transmembrane binding site. Therefore, the work presented in this chapter hopes to clarify whether or not McN-A-343 binds to an allosteric site distinct from that of the orthosteric site.

There are many ligands that have been shown to bind to sites other than the principal orthosteric site. Strychnine and brucine are just two examples of many ligands that bind at sites unique from the central or orthosteric binding site. The existence of allosteric sites first came to light during whole tissue studies on muscarinic agonist interactions with hexamethonium analogues on ileum and with gallamine in the heart (Birdsall and Lazereno, 2005). The existence of a second allosteric site was discovered by Lazareno et al., using equilibrium and non-equilibrium radioligand binding studies who showed

that both sites can affect the binding of ACh in a co-operative manner (Lazareno et al., 2000). It is has recently been proposed that there are three distinct binding sites on the M_1 receptor in addition to the central orthosteric site. There are two extracellular allosteric binding sites and another cytoplasmic binding site which have been shown to bind the allosteric modulator staurosporine and chemical derivatives thereof (Espinoza-Fonseca and Trujillo-Ferrara, 2005).

AC-42 is a novel functionally selective M_1 agonist developed by the USA-based company Accadia (Spalding et al., 2002). They discovered the compound using a live cell-based screening assay, receptor selection and amplification technology (R-SAT) (Brauner-Osborne H, 1996) whereby the binding of a selective agonist to cells expressing receptor induces β-galactosidase that can be visualised by a change in colour of receptor transfected cells. The study by Spalding et al (Spalding et al., 2002) has suggested that the M_1 receptor is selectively activated by AC-42 via a binding site different from the orthosteric site, since chimeric mutants of the central binding site domains did not affect the binding affinity of AC-42, whereas extracellular domain mutants did. The specific residues that bind this ligand have yet to be identified, but it is likely that AC-42 binds to an allosteric site, perhaps overlapping with the residues responsible for gallamine or perhaps with the analogous residues involved in the binding of alcuronium-like compounds to the M_2 receptor (Ellis and Seidenberg, 2000). One of the aims of this section of work is to test whether or not mutations of the central binding site affect the binding affinity of AC-42 at M_1 mAChRs or if residues of the E2 loop are involved in the interaction of this ligand.

The questions for consideration in this chapter are: - (i) Do the ligand contact residues of the central binding pocket in the M_1 mAChR, that participate in ACh and NMS binding, also participate in the binding of other agonists and antagonists? (ii) How do

mutations of the E2 loop affect the binding of other ligands, in particular, do they participate in primary ligand contacts with other agonists? (iii) is the proposed ligand docking residue D99 also important for the initial binding of other ligands before their entry into the binding site? (iv) Do residues of the E2 loop provide binding contacts for the novel agonist AC-42 and the partial agonists pilocarpine and McNA-343?

Competitive radioligand binding assays on COS-7 cell membranes using a selection of competing ligands (described below) against either ^{3}H-NMS or ^{3}H-QNB were performed to provide insight in to these questions. A selection of the major binding site residues, mutated to alanine in previous studies, along with the E2 loop and TM domain mutants from this study, were analysed. Differences in affinity compared to wild type, were assessed for a small selection of typical and atypical agonists and antagonists. In addition to the classical antagonists NMS and QNB the NMS analogue scopolamine was analysed along with the acetylcholine homologues, oxotremorine-M (oxo-M), a potent agonist and oxotremorine. The classical partial agonist pilocarpine, the functionally selective M_1 agonist McN-A-343 and the atypical and the novel AC-42 compound were also investigated. Their structures are presented in figure 6.2 and a description is provided in the figure legend

.

Figure 6.1. S(-)-N-Methylscopolamine and Acetylcholine Docked Into the M_1 mAChR Transmembrane Binding Pocket

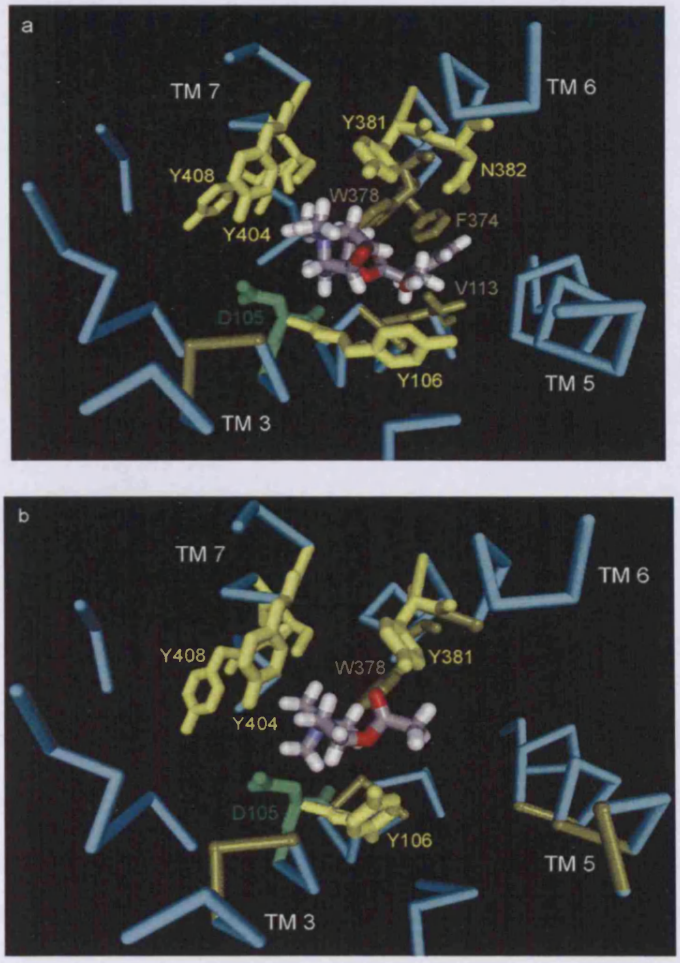

Docking of ligands into the central transmembrane binding pocket of the M_1 mAChR. **a.)** The S(-)-NMS enantiomer docked into the homology model of M_1. In addition to Asp 105 residues highlighted in yellow indicate amino acid side chains that, when mutated to alanine, reduce NMS affinity ≥30-fold (Tyr 105, Tyr106, Tyr 381, Asn 382, Tyr 404 and Tyr 408 [aromatic cage residues]). Residues highlighted dark green, Val113 and Phe 374 reduced NMS affinity (but not ACh) ~10-fold. b.) Acetylcholine in the gauche conformer (as predicted by Furukawa et al. (Furukawa et al., 2002) is positioned with the tetramethylammonium head group anchored to Asp 105 and the acetoxy side chain stabilised by Tyr 381. Mutation of these and other residues highlighted in yellow reduce ACh affinity ≥30-fold (Tyr 106, Tyr 404 and Tyr 408).

Figure 6.2. Structures of Muscarinic Ligands used in This Study

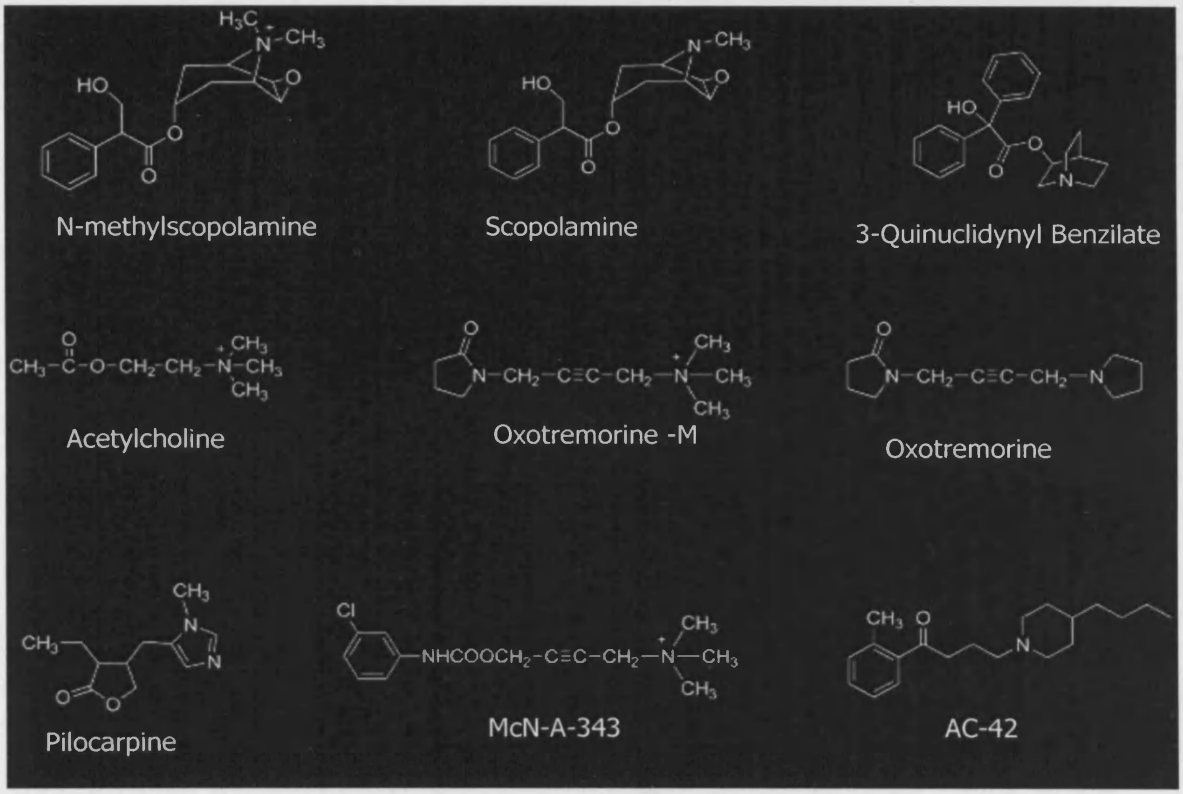

Chemical structure of ligands used in this study. In order from top left to bottom right: N-methylscopolamine (NMS) has a quaternary head group and a bulky scopine side chain with a benzene ring . Scopolamine is the tertiary amine analogue of NMS with reduced potency. Quinuclidinylbenzilate (QNB), a potent antagonist, has a tertiary amine and a two phenyl rings. Acetylcholine (ACh), the endogenous agonist, has a positively charged tetramethylammonium head group and an acetoxy side chain. Oxotremorine-M, a potent agonist with full efficacy is an acetylcholine analogue but contains a pyrrolidone ring. Oxotremorine is a tertiary amine analogue of ACh distinct from oxo-M by the presence of a pyrrolidine head group. Pilocarpine is a partial agonist with an N-methyl imidizole ring. McN-A343, a functionally selective M_1 agonist, is also an ACh analogue but contains a chlorinated benzene ring. AC-42 a novel and functionally selective tertiary amine agonist is distinguished by a benzene and a piperidene ring structure.

6.2. Results of Competitive Binding Assays for Other Ligands.

All competition curves were analysed using a 1-site model of binding assuming a Hill coefficient of 1. None of the data presented varied significantly from this model. Mean wild type M_1 mAChR pK_A values for the agonists Oxotremorine-M, McNA-343 and Pilocarpine at 4.56±0.11, 5.06±0.14 and 5.15±0.041 are slightly lower than values previously reported by this laboratory (Page et al., 1995), which were 5.1±0.04, 5.53±0.02 and 5.69±0.03 respectively. The WT affinity constant for AC-42, 6.10±0.15, determined here, is in good agreement with Spalding et al (Spalding et al., 2002) and Baig (unpublished data). Similarly, the M_1 mAChR WT mean pK value for scopolamine 9.23±0.15 determined in this study is in close agreement with Ward et al (Ward et al., 1999b) who recorded a value of 9.51±0.04. No previous data has been reported for the binding affinity of oxotremorine at WT M_1 mAChRs expressed in COS-7 cells. In this study pK at WT M_1 mAChRs for oxotremorine was found to be 5.6±0.1. All competition binding data generated in this section of work is summarised in tables 6.1, 6.2 and 6.3 shown below.

6.2.1. E2 Loop Mutants

In general, the E2 loop mutants made no significant difference to the binding affinity constants of the agonists pilocarpine, McN-A-343 and AC-42. The exceptions were Q177A and I180A. Q177A reduced the affinity of both pilocarpine and McN-A-343 (figure 6.6) by ~4-5-fold ($p<0.05$) compared to the WT pK value. I180A also slightly reduced the affinity of pilocarpine 3-fold ($p<0.05$) and more significantly reduced the affinity of McN-A-343 by 6-fold ($p<0.01$). Reductions in pilocarpine and McN-A-343 affinity for I180A reflect similar reductions recorded for ACh at this mutant. The I180A mutant also had the effect of increasing the binding affinity of the novel functionally selective AC-42 compound by 6-7-fold compared to wild type. I180A did not

significantly change the affinity of either oxotremorine or oxo-M. Table 6.1 below summarises the binding data for the E2 loop mutants.

Table 6.1 Summary of Data for E2 Loop Mutants

Ligand	WT	E170A		R171A		Q177A		Y179A		I180A		F182A	
	pKd	pKd	fold	pKd	fold	pKd	fold	pKd	fold	pKd	fold	pKd	fold
Scopolamine	9.2±0.2	ND	ND	ND		ND	ND	8.43*		8.7±0.1	3	ND	ND
Pilocarpine	5.2±0.1	5.2±0.1	nsd	4.8±0.2	nsd	4.5±0.1[b]	5	4.7*		4.6±0.2[b]	3	5.0±0.1	nsd
McN-A-343	5.1±0.1	4.8±0.2	nsd	5.0±0.2	nsd	4.5±0.2[a]	4.0	4.5*		4.3±0.3[a]	6	4.9±0.1	nsd
AC-42	6.1±0.2	6.0±0.1	nsd	6.4±0.2	nsd	6.0±0.3	nsd	5.9*		6.9±0.3[b]	7↑	6.3±0.3	nsd
Oxotremorine-M	4.6±0.1	ND	ND	ND	ND	ND	ND	4.0*		4.85±0.2	nsd	ND	ND
Oxotremorine	5.6±0.1	ND	ND	ND	ND	ND	ND	5.3*		6.0±0.1	nsd	ND	ND

[a]$p<0.05$, [b]$p<0.01$ wrt corresponding WT (1 way anova / 2-tailed t-test)
nsd = no significant difference to WT value i.e. fold difference in pKd<3-fold. (↑ Indicates fold Increase)
Values shown are pKd ±S.E.M to 1 significant figures where;
ND = No Data N=≥3 except *

6.2.2. Cysteine Mutants

Mutation of the cysteine residues produced more dramatic effects on affinity for oxotremorine, oxo-M pilocarpine and McN-A-343 than individual mutations of the E2 loop. Comparable losses of affinity were seen for the antagonist scopolamine to those seen for NMS. C98A and C178A reduced both oxotremorine and oxo-M affinities by between 7-13-fold ($p<0.05$). C98A, C178A and C98A/C178A reduced the affinity of pilocarpine by ~15, 6 ($p<0.05$) and ~20-fold ($p<0.01$) respectively. Insufficient data for the double cysteine mutant for these two agonists negates further comparison, although initial data suggests there may be a negative cumulative effect on the affinity of oxo-M for the double cysteine mutant. Interestingly, C178A made no significant difference to the binding affinity of McN-A-343, despite C98A and C98A/C178A reducing the affinity of McN-A-343 by a modest~4-6-fold ($p<0.05$) from the wild type pK value. All three cysteine mutants consistently raised the binding affinity constant of AC-42 from the WT value of pK 6.1±0.1 to a mean pK6.9±0.1 for C178A and a mean pK6.6±0.1 for the C98A mutant. The double mutant also consistently increased the affinity binding constant although the increases were ≤3-fold in most cases (see table 6.2. below). The interesting difference between the reduced affinity of pilocarpine compared to the increased affinity for AC-42 at the cysteine mutants is highlighted in figure 6.3 below. The reduction in affinity of pilocarpine reflects the losses of affinity observed for ACh at the cysteine mutants, although perhaps because pilocarpine is a larger molecule than ACh and a partial agonist, the reductions in pilocarpine affinity are relatively smaller than those seen for ACh in results Chapter 1 of this thesis.

Table 6.2 Summary of Binding Data for Cysteine Mutants

Ligand	WT	C98A		C178A		C98A/C178A	
	pKd	pKd	fold	pKd	fold	pKd	fold
Scopolamine	9.2±0.2	7.83±0.2[a]	25.1	7.9±0.2[b]	22.0	7.78*	
Pilocarpine	5.1±0.1	4.0±0.1[b]	14.5	4.3±0.3[b]	6.3	3.9±0.1[b]	19.5
McN-A-343	5.1±0.1	4.5±0.2[a]	3.8	4.7±0.2	nsd	4.3±0.1[b]	5.8
AC-42	6.1±0.2	6.6±0.1	3.0↑	6.9±0.1[b]	6.3↑	6.4±0.2	nsd
Oxotremorine-M	4.6±0.1	3.68±0.1[b]	7.6	3.7±0.1[a]	7.9	2.76*	
Oxotremorine	5.6±0.1	4.5±0.3[a]	12.9	4.8±0.1[b]	7.8	4.5*	

Values shown are pKd ±S.E.M to 1 significant figures where;
N≥3 except *where N=1
ND = No Data
[a]$p<0.05$, [b]$p<0.01$ wrt corresponding WT (1 way anova / 2-tailed t-test)
nsd = no significant difference to WT value i.e. fold difference in pKd<3-fold.
(↑ Indicates fold Increase)

Figure 6.3 Comparison of Changes in Affinity for Pilocarpine and AC-42 at the Cysteine Mutants.

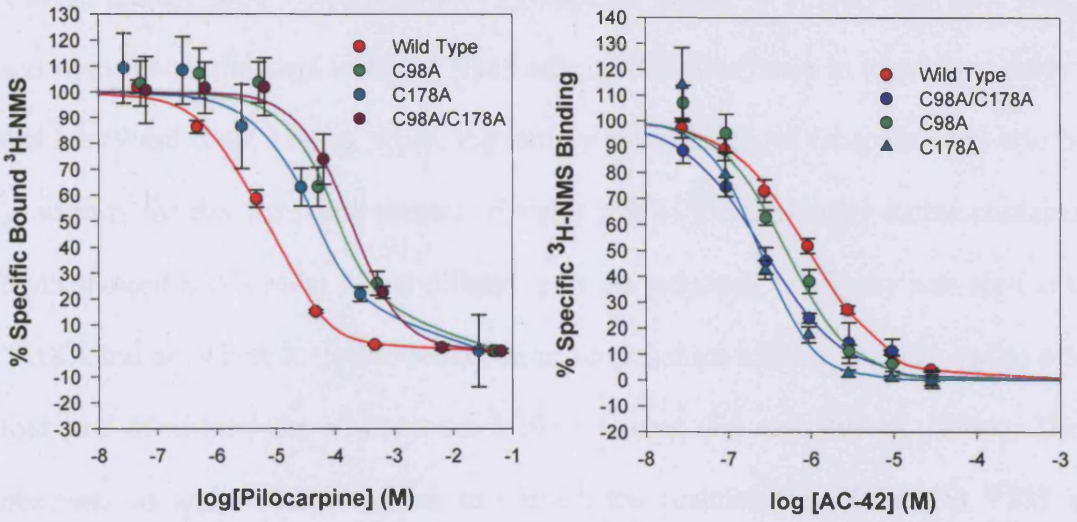

Pilocarpine and AC-42 competition assays were performed on transfected COS-7 cell membranes incubated at 30°C for 2 hours with [^{3}H-NMS] at 10^{-9}M (mutants) or 10^{-10}M (WT) respectively. Plocarpine concentration range = log -8.52 to log -3.00, AC-42 concentration range = log -10.52 to log 4.52. N.S.B was determined using 10^{-6} M atropine (K values are the mean ±S.E.M of at least 3 independent experiments) Data was fitted to a 1-site model of binding and corrected using the Cheng-Prusoff equation.

a. Representative pilocarpine competition curves for; **WT** pK = 5.25±0.04, **C98A** pK = 4.18±0.05, **C178A** pK = 4.92±0.10, **C98A/C178A** pK = 4.24±0.06

b. Representative AC-42 competition curves for; **WT** pK = 6.02±0.04, **C98A** pK = 6.29±0.06, **C178A** pK = 6.69±0.05, **C98A/C178A** pK = 6.56±0.06.

6.2.3. Transmembrane Mutants

As expected, the loss of affinity for the antagonist scopolamine (~125-fold) at the Y381A mutant pK= 7.1±0.1 ($p<0.01$) compared to pK = 9.2±0.1 for WT was in accordance with the huge losses of NMS affinity (630-fold) seen in a previous study in this lab (Ward et al., 1999a), where the tertiary amine analogue (scopolamine) also had an affinity for this particular mutant ~5 times that of the quaternary amine containing NMS molecule. A similar 5-fold difference in the reduction in affinity was seen at the Y106A mutant where a 10-fold reduction in scopolamine affinity is compared to a 50-fold loss of affinity for NMS at the Y106A mutant (Lu and Hulme, 1999a). These observations add further evidence to support the premise that Y106 and Y381 are crucial central binding site residues.

The affinity of oxotremorine-M was reduced by 10-16-fold at the Y106A and Y381A mutants, a change in pK from 4.6±0.1 (WT) to 3.6±0.1 ($p<0.05$) and 3.4±0.1 ($p<0.05$) respectively. The transmembrane binding domain mutants Y106A and Y381A both gave pK values for pilocarpine of 3.91±0.1 ($p<0.05$) a 16-fold reduction in affinity compared to the WT value. However, these two mutations had virtually no effect on the binding affinity constant of McN-A-343 compared to WT (pK= 5.1±0.1, giving pK values = 5.0±0.1 and 4.6±0.5 respectively. Consistent with the majority of the mutants tested in this study the Y381A mutant generated a small but reproducible and significant ($p<0.01$) increase in the affinity of AC-42, giving a mean pK = 6.9±0.1 representing a 6-fold increase over the WT binding affinity constant (see figure 6.4). The Y106A mutant had a substantial and significant effect on the binding affinity of oxotremorine, reducing its affinity 20-fold ($p<0.01$) from the mean WT value to a mean pK = 4.3±0.1 (see figure 6.5). The Y381A mutant reduced oxotremorine affinity less significantly ($p<0.05$), producing a 6-fold loss of binding affinity compared to WT.

The proposed central binding site residues F197 and W378, overall, had minimal effects on the binding of muscarinic agonists. The exception was the ~13-fold loss of affinity seen at the W378A mutant pK = 4.1±0.1($p<0.05$) compared to WT (pK = 5.1±0.1) for pilocarpine. This reflects a similar reduction in affinity (14-fold) seen for acetylcholine at the W378A mutant. The binding site mutants Y404A and Y408A both reduced the affinity of pilocarpine between 5-10-fold ($p<0.05$ and $p<0.01$ respectively) and the antagonist scopolamine by ~8-fold, but had little effect on the other ligands for which a full data set was collected.

In general, none of the TM domain mutations reduced the affinity of McN-A-343 and if they did, it was to reduce affinity between 3-6-fold. Two interesting exceptions were F197A and N382A, where the mutation slightly, but significantly, increased McN-A-343 affinity by 3 and 5 fold respectively ($p<0.01$). Mutation of the proposed access channel residue D99 to alanine did consistently reduce the affinity of all the agonists tested and with the exception of AC-42 and oxotremorine-M, the reductions in affinity although relatively small were significantly different to WT values.

Table 6.3 Summary of Binding Data for Transmembrane Domain Mutants.

Ligand	WT	D99A		Y106A		F197A		Y381A		W378A		N382A		Y404A		Y408A	
	pKd	pKd	fold	pKd	fold	pKd	fold	pKd	fold	pKd	fold	pKd	fold	pKd	fold	pKd	fold
Scopolamine	9.2±0.2	8.7±0.3	3	8.3±0.4[a]	10	8.2±0.4	10.	7.4±0.4[b]	63	8.5*		7.3*		8.3±0.3	8	8.4*	
Pilocarpine	5.2±0.1	4.5±0.1[a]	4	3.9±0.1[b]	16	4.8±0.1	nsd	3.9±0.1[b]	16	4.1±0.1[b]	13	4.8±0.2	nsd	4.3±0.1[b]	6	4.2±0.1[a]	9
McN-A-343	5.1±0.1	4.5±0.1[b]	4	5.0±0.1	nsd	5.6±0.1[a]	3↑	4.6±0.5	nsd	5.2±0.1	nsd	5.8±0.3[a]	5↑	4.7±0.3	nsd	4.5±0.1	4
AC-42	6.1±0.2	5.8±0.1	nsd	6.3±0.1	nsd	6.5±0.3	nsd	6.9±0.1[a]	6↑	6.2±0.3	nsd	6.4±0.3	nsd	6.6±0.3[a]	3↑	6.4±0.3	nsd
Oxo-M	4.6±0.1	4.4±0.2	nsd	3.6±0.1[b]	10	4.9±0.1	nsd	3.4±0.1[b]	16	4.0*		4.1*		4.6±0.1	nsd	4.0*	
Oxo	5.6±0.1	5.2±0.1[a]	nsd	4.3±0.1[a]	20	5.2±0.1	nsd	4.8±0.1[b]	6	4.7*		4.8*		5.6±0.1	nsd	4.7*	

Values shown are pKd ±S.E.M to 1 significant figures where;
N≥3 except *
ND = No Data
[a]$p<0.05$, [b]$p<0.01$ wrt corresponding WT (1 way anova / 2-tailed t-test)
nsd = no significant difference to WT value i.e. fold difference in pKd<3-fold. (↑ Indicates fold Increase)

Figure 6.4 Effect of Y381A Mutation on AC-42 Affinity.

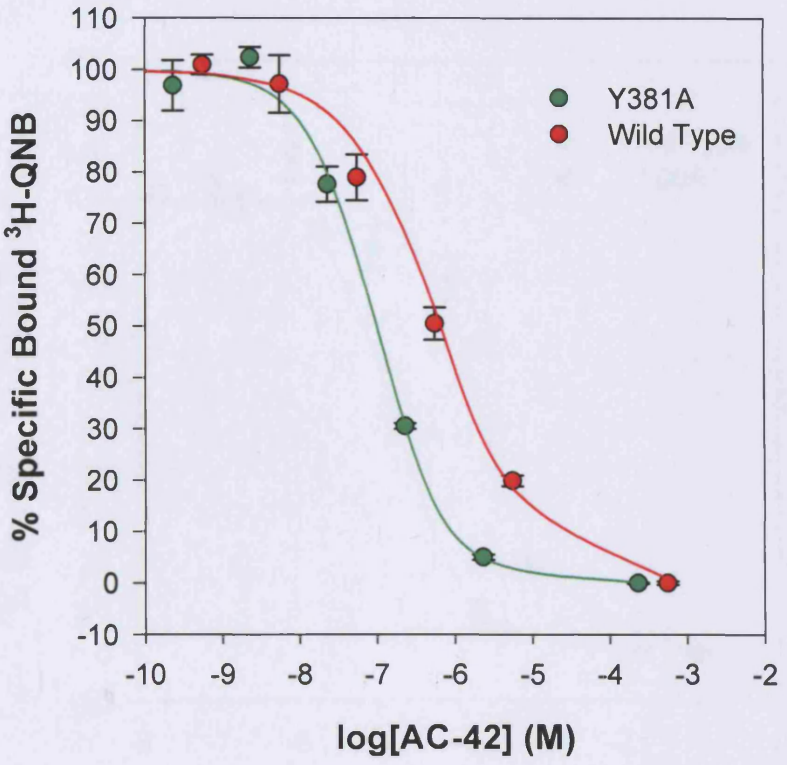

AC-42 Competition assays were performed in quadruplicate on transfected COS-7 cell membranes incubated at 30°C for 2-4 hours with [^{3}H-QNB] at 10^{-9}M (mutant) or 10^{-10}M (WT) respectively. AC-42 concentration range = log -10.52 to log -5.00. N.S.B was measured using 10^{-6} M atropine. Data were fitted to a 1-site model of binding and corrected using the Cheng-Prusoff equation pK values are the mean ±S.E.M of at least 3 independent experiments. **WT** pK = 6.17±0.06, **Y381A** pK = 7.00±0.03.

Figure 6.5 Reduction in Oxotremorine Affinity Caused by the Y106A Mutation

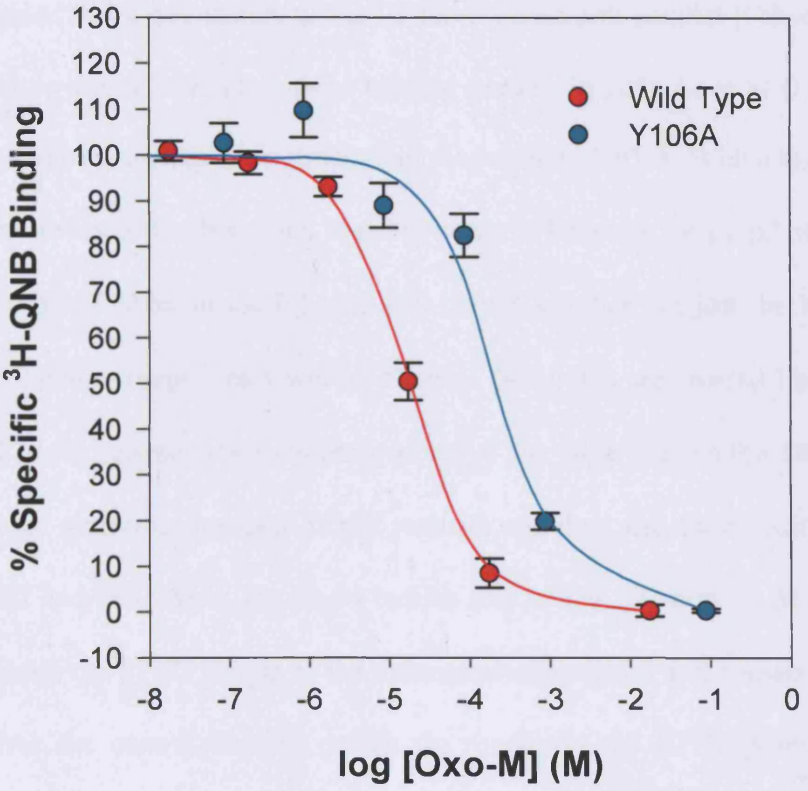

Oxotremorine competition assays were performed on transfected COS-7 cell membranes incubated at 30°C for 2-4 hours with [^{3}H-QNB] at 10^{-10}M Oxotremorine concentration range = log -8.00 to log -3.00. N.S.B was measured using 10^{-6} M atropine.. Data were fitted to a 1-site model of binding and corrected using the Cheng-Prusoff equation. pK values are the mean ±S.E.M of at least 3 independent experiments. Representative oxotremorine competition curve: **WT** pK = 4.73±0.07; **Y106A** pK = 3.63±0.05.

6.3 Discussion and Conclusions

In 2000 the 2.8 Å resolution of rhodopsin, reported by Palczewski et al (Palczewski et al., 2000), indicated that a key feature of the E2 loop was an anti-parallel β-sheet (β3-β4) that formed a lid or a plug over the central binding pocket. In 2004 Li et al (Li et al., 2004) refined the X-ray crystallographic structure of rhodopsin to 2.65 Å. With a higher definition 3D map they revealed the hydrogen bonding network between the β1-β2 sheet in the E1 loop and the β3-β4 sheet in the E2 loop that helped stabilise not just the loop structures themselves, but the receptor as a whole. The two β-hairpins are crossed-linked by water-mediated H-bonds between the main chain atoms of Tyr 10 in β-2 and Pro 180 in β3. There are three water molecules involved in this network and they also form additional H-bonds with Gly 182 and Gln 184 in the β3-β4 hairpin and to Tyr 192 near to β4. This network serves to anchor the β1-β2 hairpin to the transmembrane regions and consequently, secures the plug over the central binding pocket. In rhodopsin the E2 loop residues provide hydrophobic contacts that maintain the covalently bound chromophore 11 cis-retinal in the inactive dark state. In particular Ser 186, Cys 187, Gly 188, Ile 189 and Tyr 191 lie mostly in the β4 sheet within 4 Å of the chromophore and are participating residues of the rhodopsin binding site. The rhodopsin residues are analogous to Q177, C178, Y179, I180 and F182 in the M_1 mAChR.

6.3.1 E2 Loop Mutants

A summary of the binding data for McN-A-343, AC-42 and pilocarpine at E2 loop mutant receptors is shown below in figure 6.6. It has been predicted, using homology modelling that the M_1 mAChR E2 loop residues may also participate in the binding of ligands in the central orthosteric binding pocket and that the β-hairpin and plug-like structures are also

features common to both rhodopsin and the M_1 mAChR. Evidence collected in this study seems to highlight the fact that mutations of the E2 loop in M_1, apart from the highly conserved cysteine residue at position 178, do not have an overtly dramatic effect on the affinity of various ligands. It is likely that residues beyond the conserved cysteine at position 178 do extend towards the orthosteric binding site, where they contribute to a second shell of ligand interaction, stabilising the predominant and critical orthosteric binding site residues. The inference from the reduction of affinity for ACh shown by the I180A mutant is that it may be analogous to ligand contact residues in both rhodopsin (Yan et al., 2002) and the D_2 dopamine receptor (Shi and Javitch, 2004) and similarities between the structure of the E2 loop of rhodopsin and the predicted structure in the M_1 receptor may be made. Menon and colleagues (Menon et al., 2001) argued that the buried nature of the E2 loop in the central binding site was a feature unique to rhodopsin, but the present study and that of Javitch suggest that in the biogenic amine class of receptors at least, this structural feature may be the norm rather than the exception.

Although it appears that residues in the E2 loop of the muscarinic receptors do not participate directly in ligand binding, although they do probably face towards the binding site, evidence exists from several studies that residues in the E2 loop of other aminergic receptors in the rhodopsin family of GPCRs do in fact make important ligand contacts. For example, Javitch et al (Shi and Javitch, 2004) using a substituted cysteine accessibility method (SCAM) highlighted two residues, I184 and N186 in the E2 loop of the dopamine D2 receptor that were very likely to make contact with the antagonist N-methylspiperone. These residues are analogous to I180 and F182 in the M_1 mAChR. Perez and colleagues (Zhao et al., 1996) also identified three consecutive residues (G196, V197 and T198) in the E2 loop, that when substituted changed the ligand specificity profile of the α_{1b} adrenergic

receptor to that of the α_{1a} adrenergic receptor and vica versa. Furthermore, Olah et al. (Olah et al., 1994) identified several important glutamate residues in the E2 loop, using a chimeric substitution approach, that were critical for the binding of the antagonist 1,3-dipropyl-8-cyclopentylxanthine to adenosine receptors.

Considering this evidence it may be a little surprising that mutations in the M_1 mAChR E2 loop did not have more profound effects on the binding of either endogenous or synthetic ligands. Although mutations to Q177, Y179, I180 and F182 which are part of the predicted β3-β4 strand lid structure, did cause minor reductions in ligand affinity, the effects were not significant enough to suggest that they make any critical or direct contact with ligands bound to the central binding pocket. The mutation that most consistently reduced the binding affinity of the majority of ligands was I180A. Interestingly of all the mutations, including the cysteine and the TM domain mutants, I180A caused the biggest reduction (~7-fold) in McN-A-343 affinity. McN-A-343 was originally proposed as an allosteric modulator of M_2 mAChRs (Birdsall et al., 1983.) but a later study (Christopoulos and Mitchelson, 1997) could not distinguish whether this compound interacted with the receptor allosterically with high negative co-operativity or via simple competition with the orthosteric binding site, when tested against carbachol. Contact residues for McN-A-343 have yet to be identified and the loss of affinity effected by I180 (see figure 6.6 below) may provide a clue as to the mode of binding for this mysterious ligand. Mutation of I180 also significantly increased the affinity of AC-42 (~7-fold), probably because this mutation allows better access of AC-42 to its binding epitope.

The I180 residue (apart from C178) is the only E2 loop candidate that one might tentatively suggest makes a contribution to the ligand binding environment other than to provide a

structural role. Possibly I180 contributes to the hydrophobic nature of the central binding cavity as indeed may Q177, Y179 and F182, but I180 being in closer proximity (as suggested by the homology model in figure 6.7) to a bound ligand (ACh for example) may exert a more influential effect. Loss of these residues could be easily compensated for by the other non-polar residues if their role was simply to maintain a hydrophobic environment in the core binding site. This would be consistent with our findings that single point mutations of the E2 loop residues do not perturb the structure or the ligand binding capabilities of the M_1 mAChR enough to warrant their inclusion in a list of binding site residues. Nevertheless, the small reductions in affinity seen for these mutants for various agonists supports the idea that agonists bind closer to the extracellular surface of the central binding pocket and may therefore have a role in stabilizing or restraining agonists in the central binding cavity. This is concordant with the idea of the E2 loop, and in particular the residues C-terminal to the conserved cysteine C178, acting as a "lid" covering the central binding site. Thus, the function of the E2 loop maybe to maintain the structural stability of the central binding cavity without making any direct contact with bound ligands by providing second shell stabilizing interactions. Figure 6.7 below shows the possible orientation of a bound ACh molecule in relation to the E2 loop and I180 in particular and supports the idea that the β4 strand dives down into the central binding pocket.

Figure 6.6 Summary of Differences in the Binding Affinities of Ligands to E2 Loop Mutants Compared to WT.

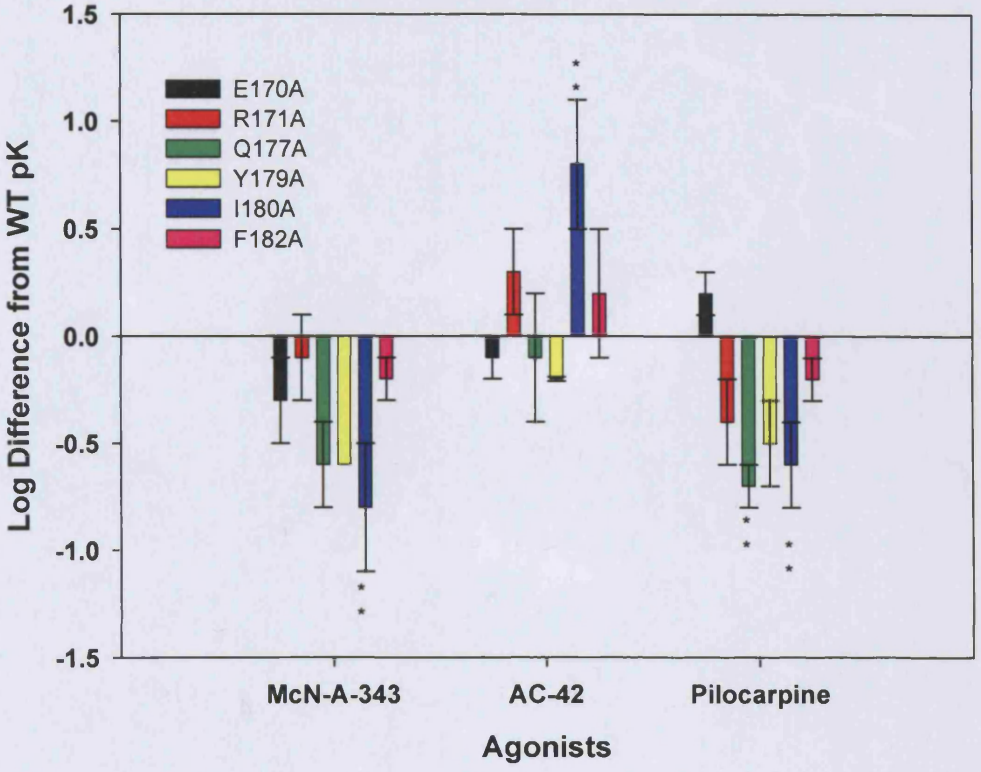

Bars represent the mean log difference of in pK values for E2 loop mutants compared to wild type receptors for the partial agonist pilocarpine and the atypical agonists McN-A-343 and AC-42 and error bars show the S.E.M. N=≥2 unless stated and statistical significance analysed by a 2 tailed T-test where * = $p<0.05$ and **=p,<0.01 with respect to wild type values.

Figure 6.7 Homology Model of the M_1 mAChR Showing Acetylcholine Docked Into the Transmembrane binding Site In Relation to I180

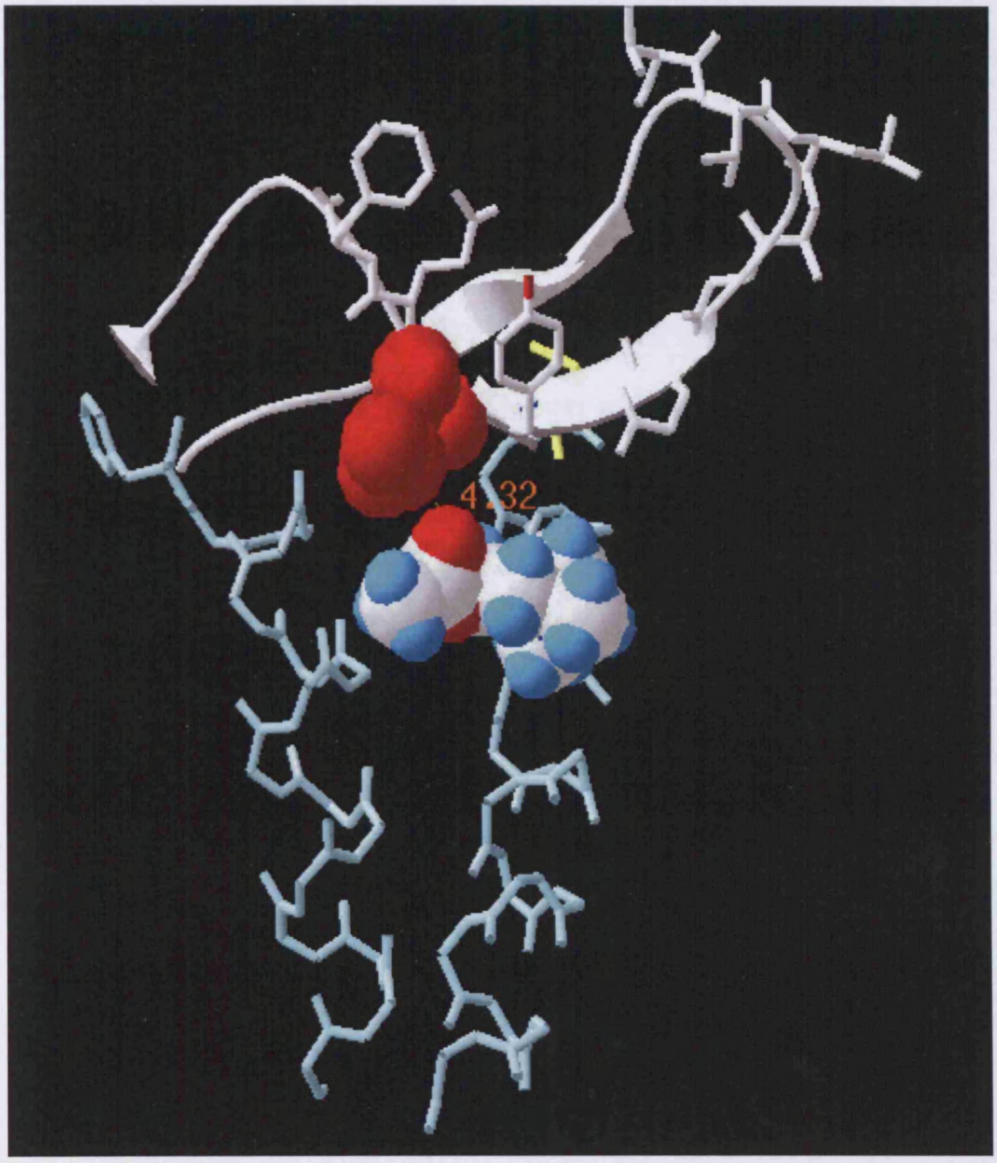

The figure highlights the proximity of the I180 residues (red) of the E2 loop (white) of the M_1 mAChR to a docked acetylcholine molecule (default colour) in the M_1 mAChR homology model. This simple model suggests that acetylcholine is in close enough proximity (4.3Å) to allow second shell interactions with I180 and that analogous to rhodopsin the β4 strand dives down into the transmembrane binding pocket.

6.3.2 Cysteine Mutants

The substitution of the cysteine residues with alanine exerts more pronounced effects on the binding of ligands. There is now a substantial weight of evidence (Davidson et al., 1994; Savarese et al., 1992; Zeng et al., 1999a; Zeng et al., 1999b) stating that the disulphide bond between the two conserved cysteine residues is of major importance to the structural stability of nearly all GPCRs, both in terms of correct folding and expression but also in terms of ligand binding affinity and the stabilization of the central binding site. Without rescuing the expression of the cysteine mutants with an atropine chaperone there would be no cysteine mutants to examine, underlining their importance in the correct folding and compartmentalization of the receptors in the cell membrane. Nevertheless, once cysteine mutants are coerced into correctly expressing and locating their importance in the binding of ligands is secondary to those residues of the TM domains that are critical for ligand binding. There is a modest but significant losses of affinity ($p<0.01$) seen for NMS and QNB. There is a larger effect on ACh affinity and a reduction in ACh signalling efficacy (15 – 20-fold), but this is probably not as large as the loss in efficacy incurred by the mutation of binding site residues D105 or Y381 for example.

Data gathered from analysis of the cysteine mutants C98A, C178A and the double cysteine mutant C98A/C178A suggests a more complex role for these particular residues than just the maintenance of structural stability. The C178A and the C98A/C178A mutants reduced ACh affinity by 66-fold and 79-fold respectively but reduced pilocarpine affinity by only 6-fold and 20-fold respectively ($p<0.01$). Pilocarpine being a partial agonist and a larger molecule than ACh has the potential to make more interactions with the receptor and the loss of one or two contacts may not affect pilocarpine binding as dramatically as ACh, which has fewer possible interactions. The discrepancy between the reductions in affinity

seen between ACh and pilocarpine may reflect this fact. In general the C98A mutant reduced the binding affinity of acetylcholine, (although the presence of 2 populations of binding sites as shown in results Chapter 3 is a complicating factor), pilocarpine, oxotremorine and oxotremorine-M by ~10-15-fold, and there is no conclusive evidence therefore that C178 itself participates directly in the binding of these ligands or ACh. This is because the reduction in affinity of these ligands at the C178A receptor is more consistent with a general perturbation of the binding site rather than removal of a critical contact residue, where reductions in affinity would likely to be >100-fold. Also, there was no evidence that C98A produced two populations of binding sites for the other ligands, as all C98A data fitted a 1-site model of binding for both the partial, full and atypical agonists. The phenomenon seems to be limited just to ACh as far as the evidence provided in this thesis can discern.

The cysteine mutants all had similar effects (~7-13-fold reductions in affinity) on the binding of oxotremorine and oxotremorine-M, probably due to global structural changes rather than any direct disruption of binding contacts. The more interesting results for the cysteine mutants concerned the binding of AC-42 which consistently bound with a higher affinity to the cysteine mutants than to the wild type receptors. In particular AC-42 bound, consistently, with a 6-fold higher affinity to C178A than to WT receptors. A very recent paper by Langmead and colleagues (Langmead et al., 2006) has provided direct pharmacological evidence that AC-42 is in fact an M_1 selective allosteric agonist, but these authors did not identify the regions or residues of the M_1 receptor that impart the selective properties of this ligand. The results presented here concur with the findings of both Langmead and Spalding (Spalding et al., 2002) in that they suggest that AC-42 does not bind within the central binding pocket. The fact that the C178A increases the affinity of AC-42, may indicate the uncovering of a high affinity epitope on the receptors extracellular

surface. Removal of the disulphide bond may increase the dynamic nature of the E2 loop creating a more "relaxed" receptor, allowing AC-42 better access to its high affinity binding epitope. Spalding (Spalding et al., 2002) implied from their study that the binding epitope for AC-42 may actually be located at the N-terminal region and incorporating residues of the E3 loop. As has already been stated only I180 of the E2 loop residues increased the affinity of AC-42, the rest having no effect at all. Thus it seems unlikely that the AC-42 binding epitope resides in the E2 loop, although perturbation of the E2 loop may allow better access of the AC-42 ligand to its binding epitope, elsewhere on the extracellular surface of the receptor. Further mutagenesis based investigations of the N-terminal and E3 loop domains are required to identify a binding epitope for AC-42. A summary of the differences in affinity from WT receptors for the binding of ligands to cysteine mutant receptors is shown below in figure 6.8.

Figure 6.8 Summary of Differences in Binding Affinity of Ligands to Cysteine Mutants Compared to WT.

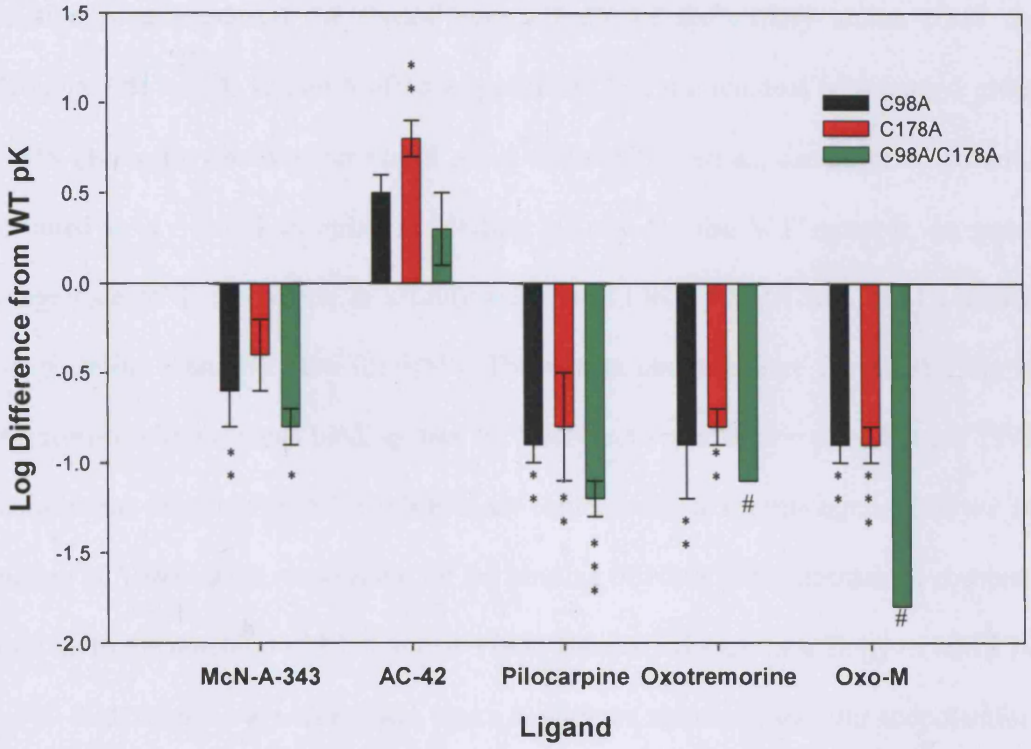

Bars represent the mean log difference of in pK values for cysteine mutants compared to wild type receptors for the partial agonists pilocarpine and oxotremorine and the atypical agonists McN-A-343 and AC-42 and error bars show the S.E.M. N=>3 except # where N <3 and statistical significance was analysed by a 2 tailed T-test. * = $p<0.05$ ** = $p<0.01$ and *** = $p<<0.01$ with respect to wild type values.

6.3.3 Transmembrane Mutants

A summary of ligand binding to TM domain mutants is presented below in figure 6.9. The transmembrane domain binding site mutants, Y106A, F197A and Y381A as might have been expected reduced the ground state affinity of the tertiary amine NMS analogue scopolamine by 10, 10 and 63-fold respectively. It is the removal of a methyl group from NMS (quaternary ammonium) head group to form the tertiary amine of scopolamine that resulted in a ~5-fold decrease in binding affinity for the WT receptor. In general the magnitude of the reduction in affinity seen for Y106A, F197A and Y381A was less for scopolamine than was seen for NMS. The results obtained here for Y381A are in good agreement with previous binding data for NMS and scopolamine (Ward et al., 1999a) and confirm the premise that Y381 is a primary contact residue for this ligand. It is the aromatic nature of Y381 that is responsible for the binding of NMS and scopolamine compounds. In this study the mutation of F197 and W378 to alanine reduced the affinity of NMS 100- and ~500-fold, respectively. There was also a significant reduction seen for scopolamine. It has been proposed in this lab that the benzene ring of the NMS and scopolamine ligands may form a pi-pi stacking bond with the aromatic rings of F197 and W378. This interaction would be possible if a slight re-orientation of the torsion angles in the homology model were made (see figure 6.10). It may also be possible that the loss of NMS and scopolamine binding affinity caused by W378A is due to a disruption of the aromatic cage environment. F197 is too far away from the NMS or scopolamine head group to be a part of the aromatic cage environment of the head group but W378 is close enough. F197, it has been proposed in the present study (Chapters 3 & 5), may make a pi-pi stacking bond with the benzene ring of NMS. This would explain the differences seen in the reductions in affinity for these two mutants. Thus, making critical contact with the head group of NMS or scopolamine

and potentially with ACh, W378 can probably be considered as a key binding site residue, whereas F197 may only be critical to the binding of atropine-like antagonists.

The mutants Y106A and Y381A caused significant losses of affinity for both oxotremorine (20 and 6-fold respectively), oxotremorine-M (10 and 16-fold respectively) and pilocarpine (both 16-fold). This reflects the loss of ground state ACh affinity seen previously for these mutants (Lu and Hulme, 1999b; Ward et al., 1999a). In general, losses of pilocarpine affinity for the majority of TM binding site mutants were similar to losses of ACh affinity. This may suggest that there is an overlap of residues that bind both ACh and pilocarpine despite significant differences in structure. It is likely that the positively charged N-methyl-imidizole head group of pilocarpine forms an ionic bond with the key binding site residue Asp 105 and a hydrogen bond may be formed between Y381 and the internal ester of the γ-lactone ring in a manner analogous to the binding of ACh as described by Ward et al. (Ward et al., 1999a). The fact that the W378A mutation also reduces pilocarpine affinity by ~15-fold as it does ACh, might suggest that W378 contributes significantly to the aromatic cage environment. It was suggested earlier in this work that ACh and probably pilocarpine, bind more towards the extracellular surface of the receptor than the antagonists NMS and scopolamine and the data shown in this chapter seems to corroborate this.

As part of the proposed ligand access channel (Lu et al., 2001) the D99A mutant did significantly reduce the affinity of the agonists pilocarpine and McN-A-343 by 4-fold and the antagonist scopolamine by 3-fold. This loss of affinity was not as pronounced as seen previously for ACh (23-fold reduction) or NMS (11-fold). However, since it can be assumed that the D99A (and W157) residues are positioned extracellular to the central binding core, just above the lipid bilayer, these small but significant losses in agonist and antagonist affinity are consistent with a two step binding process. This is such that a ligand

binds initially to the outer surface of the receptor, perhaps binding to D99 and W157 (TM4) before translocation to the core binding site. Mutation of the analogous residues D97N (Vogel et al., 1999) and W155A (Heitz et al., 1999) in the M_2 mAChR also significantly reduced agonist affinity and agonist mediated signaling responses. It is interesting to note that, affinity constants for oxotremorine and oxotremorine-M were not significantly reduced from WT values when bound to the D99A mutant in the present study. What this implies however may have to be left as an open question.

Thus the results presented here on D99 are in accord with previous analysis and support the theory that D99 and W157 (M_1) may be initial contact residues for only some agonists at the opening of a ligand access channel, leading to the central binding pocket. It would have been interesting to include the W157A mutant in this study on the binding of other atypical agonists to provide further evidence of its involvement in an access channel. However, this oversight means that further investigation into this mutant is still outstanding. Nevertheless, mutation of the W157 to alanine has a much larger effect (100-fold reduction) on both ACh affinity and signaling efficacy (>1000-fold) (Lu et al., 2001), than the D99A mutation, which although it reduces agonist binding and expression, does not severely affect efficacy as seen in Chapter 4 of this thesis. This is consistent with the fact that affinity and efficacy are not related, i.e. the ability of the agonist receptor complex to couple to G-protein is independent of the binding of the ligand to the receptor. So, although the mutation of D99 to alanine may reduce the ability of ACh to bind to the receptor, once bound the receptor can be activated in the usual way since the mutation does not influence the change to the active conformation. Thus, it can be concluded that D99 is not a residue important for receptor activation. It can be imagined, however that an agonist with a positively charged head group can be stabilized at the entrance to the channel via the negative charge of the D99 but that it is the maintenance of the non-polar environment of the channel and the

binding pocket that is the key for ligand access. The non-polar W157 residue may be crucial in this respect and may be analogous to the residue found at the entrance gorge of the acetylcholinesterase enzyme, where ligands bind to the peripheral site by the indole ring of the Trp 279 (Silman and Sussman, 2005). Further investigations are required to elucidate fully the role of W157 and D99 in a possible two-step system of agonist binding in the M_1 mAChR.

Figure 6.9 Summary of the Differences in Binding Affinity of Ligands to TM Domain mutants Compared to WT.

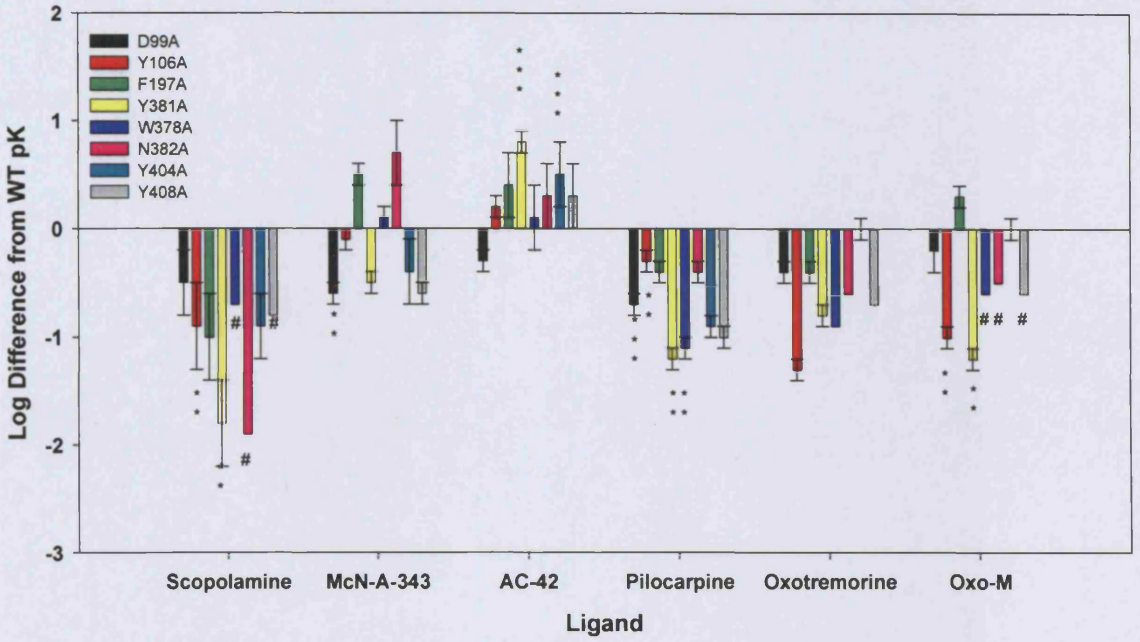

Bars represent the mean log difference of in pK values for transmembrane mutants compared to wild type receptors for the antagonist scopolamine, the partial agonists pilocarpine and oxotremorine and the atypical agonists McN-A-343 and AC-42 and error bars show the S.E.M. N=>3 except # where N=<3 and statistical significance analysed by a 2 tailed T-test where * = $p<0.05$ and ** = $p<0.01$ and *** = $p<<0.01$ with respect to wild type values.

Figure 6.10 Possible pi-pi-Stacking Bond Between Benzene Ring of NMS or Scopolamine and Phe 197 and Trp 378.

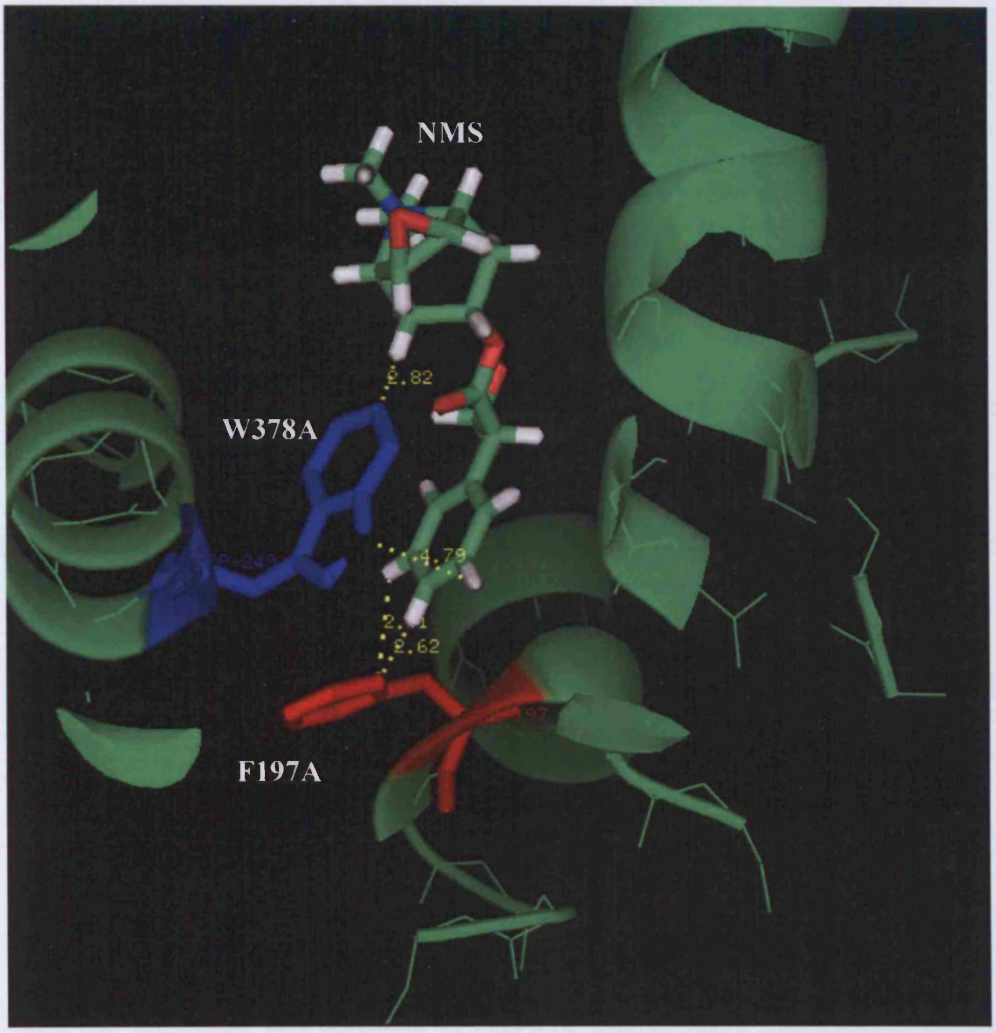

Consistent with binding data collected Phe 197 and Trp 378 are key residues for the binding of both NMS and scopolamine, but not QNB. A slight change in the torsion angles in the homology model may allow for a pi-pi stacking bond between the benzene ring of NMS/scopolamine and the aromatic rings of Phe 197 (red) and Trp 378 (blue). The loss of such a strong bond would severely reduce binding affinity as has been borne out by the data. Alternatively the significant losses of affinity may be due to the disruption of the aromatic cage environment. Relative distances between ligand and residues are indicated in yellow dotted lines and are marked in angstoms.

6.4 Summary

The main findings of the section of work on the effects of mutations on ligand binding are as follows.

1) The classical antagonists, NMS & scopolamine, the agonists ACh and oxo-M, and the partial agonists oxotremorine and pilocarpine showed similar responses to the mutations studied. This is consistent with their binding within the primary ACh binding pocket

2) The E2 loop is likely to function as a stabilising element, constraining the binding site environment, maintaining a conformation conducive to correct ligand orientation in the central binding pocket, without making direct contact with bound ligands

3) The C178A mutation consistently enhanced affinity for AC-42. Relaxation of the receptor due to disruption of the disulphide bond may allow better access of AC-42 to its binding epitope.

4) McN-A-343 and AC-42 showed weak or no interaction with the primary ligand binding residues. There was evidence that Asp 99 participates in the initial binding of some but not all agonists or antagonists

Chapter 7

Final Discussion

7.1 E2 Loop Residues

One of the features of the E2 loop seen in the rhodopsin structure is that residues Ser 186 and Asp 190 of the β4 sheet dive down into the transmembrane region and sit on top of the ligand binding crevice, Glu 181 is positioned ~4 Å from C_{12} of retinal and is part of the linking sequence between the β3 and β4 sheets (Yan et al., 2002). E2 loop residues Glu 181 and Ser 186 also provide important H-bonds with Glu 113 of TM3 via a water molecule and are directly linked to the process of photoisomeration of the ligand from 11-cis retinal to all-trans retinal and subsequent receptor activation. These residues are part of a proton transfer mechanism for switching the protonated Schiff base counterion and are believed to be essential for the photon induced activation of rhodopsin (Yan et al., 2003). Considering the importance of these residues and the E2 loop in rhodopsin function, it is logical to suppose that the functional importance of the E2 loop in other GPCRs is analogous to rhodopsin. The main difference, and it is not a minor difference, is that rhodopsin and its natural retinal ligand are covalently bound and that isomerization of other GPCR ligands may not be an issue. Nevertheless, this study set out to examine the possibility that the E2 loop of the muscarinic receptor family also provided important elements for the efficient functioning of the receptor. Specifically, an attempt was made at identifying residues that may provide a role in ligand binding, structural stability and activation.

The data presented here does not support the idea that any of the E2 loop residues make direct critical contact with NMS, QNB or the endogenous agonist ACh. Mutation of important binding site residues generally leads to very large reductions in binding affinity constants. For example, the mutation to alanine of the highly conserved Arg 3.50 reduces

both agonist and antagonist affinity ~100-fold. Reductions in binding affinity constants of that magnitude were not observed for any of the E2 loop residues. In general however, reductions in ACh affinity were observed, leading to the conclusion that ACh binds more superficially in the binding pocket than NMS. The E170 residue in the M_1 mAChR is analogous to the important E181 in rhodopsin, but its mutation to alanine had very little effect on expression, agonist or antagonist binding or agonist induced activation of the M_1 receptor. It should be noted that E170 is not conserved in M_2, M_3, M_4 or M_5 mAChRs and so it may not be surprising that its mutation produced null effects. More interesting is the I180 residue which is completely conserved in the muscarinic sub family of aminergic receptors. Mutation to alanine of I180 significantly reduced both NMS and ACh affinity. As part of the β4 sheet I180 may be in close proximity to the bound ACh molecule and may provide a second shell of electron density that helps to stabilise the ACh molecule with the transmembrane binding site. Small reductions in affinity were also seen for McN-A-343 and pilocarpine at the I180A mutant. These observation may be in line with the suggestion by Shi & Javitch (Shi and Javitch, 2004) that the conserved analogous residue I184 in the dopamine D_2 receptor lines the binding site crevice and contributes in some way to the binding site environment. This may also be true for R171 (conserved) and Y179 (not conserved) which also reduced NMS and ACh binding. In the homology model of the E2 loop (figure 1.12 in the main introduction) R171 is positioned pointing away from the transmembrane binding site. The significant reductions in both ACh and NMS binding affinity constants seen for the alanine mutant may imply that in fact R171 is orientated into the binding site where its positively charged side chain may provide an important ionic interaction, which again may stabilise the ligand in the binding pocket. However, it is more likely that R171 forms part of a stabilising microdomain since a positively charged residue would negate a possible interaction with the positively charged ACh head group.

The involvement of certain E2 loop residues in the activation of the M_1 mAChR seems to be more important than ligand binding. In particular residues W164, Q177, Q181 and S184 seem to provide important H-bond interactions important for the activated state of the receptor. Using a modelling program (Deep view) the analogous residues in rhodopsin, all appear to make H-bond interactions. So, by comparison it is possible that the M_1 residues may also be involved in a similar set of H-bond interactions. Except for Q177 these residues are conserved in the mAChR family and in particular the W175 residue of rhodopsin receptor is analogous to W164. H-bonds of the highly conserved tryptophan in rhodopsin (W175) are formed with a proline at P190 and a serine at S202. Figure 7.1 shows the analogous residues and the potential H-bond interactions of W164 of the M_1 mAChR. W164 and W175 (rhodopsin) both lie at the N-terminus of the E2 loop just a few residues beyond the top of TM4. A space filling model (figure 7.2) also suggests that W164 and P159 are close enough to form a Van der Waals interaction. The striking feature is that in both models the conserved tryptophan forms a H-bond, via the backbone nitrogen atom to the backbone carbonyl oxygen of a highly conserved proline residue P159 (P170 in rhodopsin) which sits at the top of the fourth transmembrane helix. In the rhodopsin model however there is a H-bond formed between the nitrogen of the pyrrole ring of the tryptophan and a protonated serine (S202), an analogous H-bond does not appear to be possible in the M_1 receptor as the 9.27Å distance between the backbone of the nearest serine residue in the M_1 receptor (S184) is too great. Mutation of the of P159 (Lu et al 2001) to alanine had a somewhat larger effects on ACh affinity (100-fold) and potency (~1000-fold) than W164A. this may be explained by the proximity of P159 to the important W157 residue which is critical for ACh binding and potency. The P159A mutant did however show a similar loss of efficacy (~10-fold) to that of W164A, which may support the claim that the maintenance of W164 is important for receptor activation. Mutation to alanine of W164 reduced ACh potency ~30-fold and signalling efficacy by ~7-fold.

Furthermore, basal signalling was practically abolished compared to wild type basal signalling levels. It is suggested therefore that W164 is an important residue providing interactions necessary for the structural stability of the E2 loop which is required for the conformational rearrangement of the TM helices upon ACh induced activation of the M_1 mAChR receptor.

Figure 7.1 H-Bond Interactions for the Conserved Tryptophan Residue at the N-Terminus of the E2 loop in M_1 mAChR

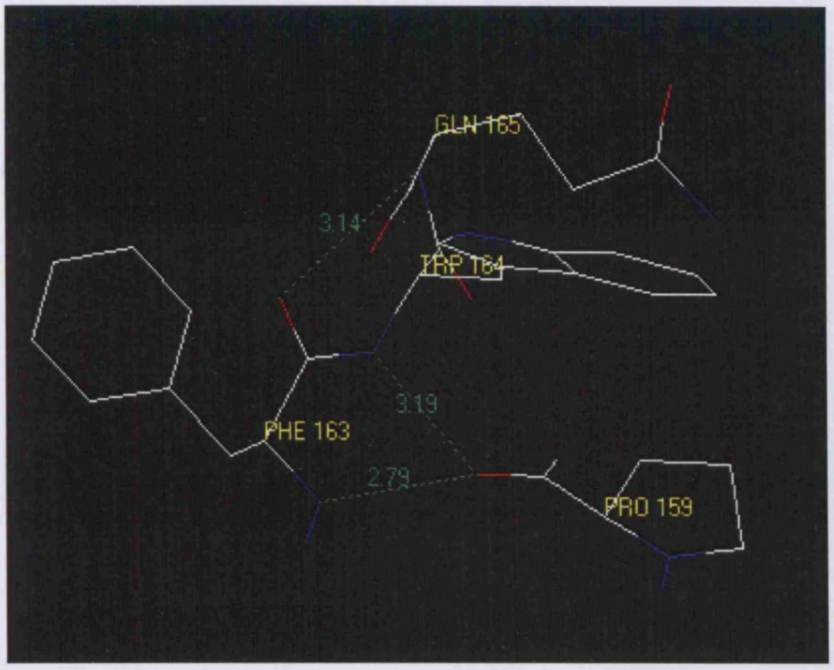

The figure represents the W164 residue at the N-terminal of the E2 loop that potentially may make important hydrogen bonds important for the structural stability of the E2 loop. Dose response data shows that mutation of W164 to alanine significantly reduces the receptors ACh potency and reduces the ability of the receptor to couple effectively with G-protein. The disruption of these bonds may be important for the receptor to attain the active conformation. The figure was adapted from the M_1 mAChR homology model and H-bonds were set a detection threshold with a minimum distance of 2.2 Å and a maximum distance of 3.27 Å using the webviewer lite modelling programme. Nitrogen atoms are shown in blue, hydrogen atoms are shown in red and carbonyl backbones are shown in white.

Figure 7.2 Space Filling Model to Show Possible Interaction Between W164 and P159

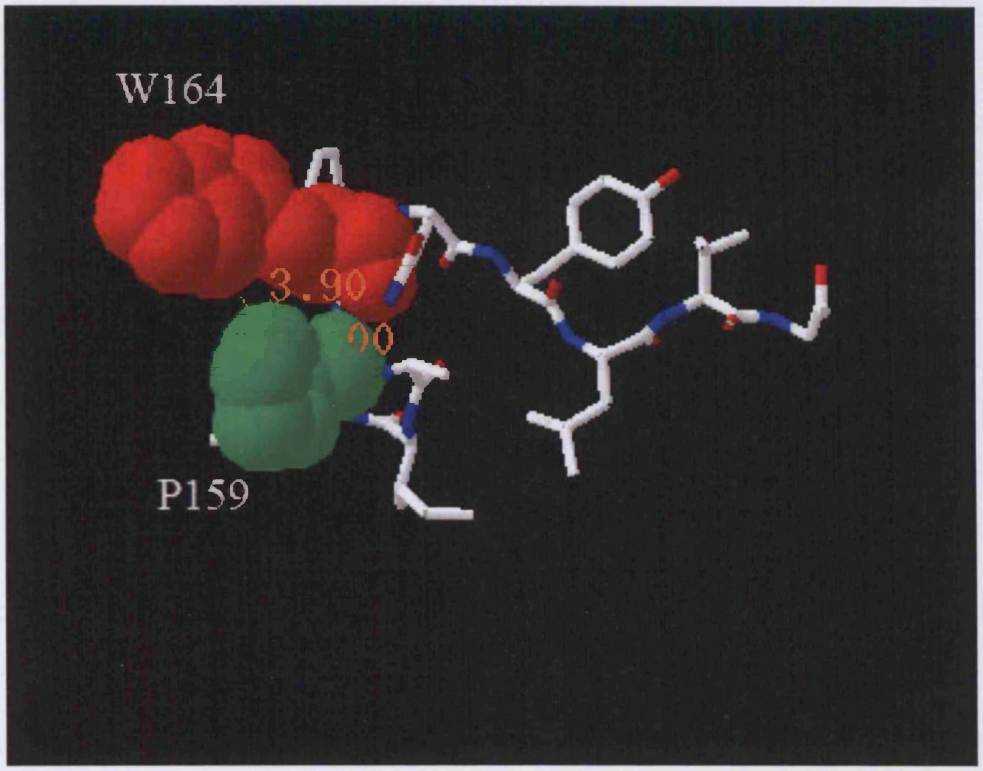

The figure highlights the relative proximity of W164 and P159 at the top of TM4 and the N-terminal of the E2 loop. Both residues appear to be important for signalling of the M_1 mAChR. The approximate distance between these residues is 3.9 Å, close enough to make a Van der Waals intertaction. The mutation of W164 to alanine significantly reduced both ACh potency and efficacy, suggesting that there may be an interaction between W164 and P159 after a conformational change in the E2 loop upon ACh induced receptor activation. This model was adapted from an in-house M_1 mAChR model using the Webviewer Lite modelling programme.

A recent paper by Kota et al. (Kota et al., 2006) has provided good evidence using FRET and cysteine substitution cross-linkig studies that W175 is a key residue in the formation of the rhodopsin dimer. Their study did not address the role of dimerisation and in particular W175 in opsin function. Nevertheless, the rearrangement of the H-bonds between W164 and P159 may be necessary for the conformational change of the M_1 receptor upon ACh induced activation. In light of the Kota et al. (Kota et al., 2006) study W164 may be important for a functional M_1 dimer, although further study is required to explore this possibility. In terms of maintaining the structural stability of the E2 loop, W164 may provide the first of three anchor points, the second being the disulphide bond between C98 and C178 and the third at the C-terminus of the E2 loop via a H-bond interaction between S184 and P186. The conservation of both the tryptophan and the proline in the mAChR family is a good indication of that these residues have been maintained during evolution of the receptor because of their importance in efficient receptor function. It is interesting to note that, although the tryptophan analogous to W164 is not conserved in the dopamine D_2 receptor the proline residue analogous to P159 is.

At the C-terminal end of the E2 loop where the loop meets the top of TM5, the S184 residue also appears to make an important H-bond interaction. In an interaction similar to W164 at the N-terminus of the E2 loop S184 potentially also makes a H-bond interaction with a proline residue (P186) at the top of TM5, and potentially provides a third anchor point for the E2 loop. Figure 7.3 shows the potential H-bond interaction between the side chain oxygen of the S184 and the carbonyl oxygen in the backbone of P186. The fact that mutation to alanine of the S184 residue does not significantly reduce ACh affinity (Matsui et al., 1995) but reduces ACh potency and efficacy more than 15-fold strongly implicates this residue as being important for the active state of the receptor. Again the S184A mutant abolished WT levels of basal activity but had no effect on receptor expression levels.

Furthermore, the S184 residue may make two H-bond contacts with Q181 that are required for the ground state of the receptor since the Q181A may have genuinely raised basal activity compared to wild type.

A serine at the analogous position to S184 is conserved in all 5 mAChR sub types and in rhodopsin there is a similar uncharged polar threonine side chain. The proline at position 159 in the M_1 sub type is conserved in M_3 M_4 and M_5 but not in M_2 which contains an alanine at the analogous position, but a similar H-bond with the protonated backbone of the M_2 alanine residue may also be possible. To use an analogy, W164 and S184 may act like the two ends of a skipping rope, the other end in each case is S-S bond in the approximate centre of the loop. If the person at one end of the skipping rope lets go the entire structure of the rope changes, particular if the rope is required to be activated (rotating). Similarly by removing these important residues the overall conformation of the E2 loop is affected and in turn restricts the proper conformational changes required for the receptor to assume the active conformation.

In the rhodopsin homology model the inner strand of the β-hairpin of the E2 loop forms a "lid" on the retinal binding site (Palczewski et al., 2000). If the E2 loop of the M_1 mAChR functions in an analogous manner, it is easy to imagine that mutations in the E2 loop structure especially in the β-hairpin region would cause the acceleration of ^{3}H-NMS dissociation. The E2 loop mutants that increased ^{3}H-NMS dissociation rate constants, R171A, I180A and F182A are all proximal to or indeed part of the β-hairpin structure. This evidence may support the idea that the E2 loop of the M_1 receptor serves to prevent the premature release of ligand from the central binding pocket. In Chapter 3, evidence was provided to show that NMS binds deep in the central binding pocket and that it is unlikely

that residues of the E2 loop are critical for NMS binding. The dissociation rate constant data supports this since loss of critical binding residues might be expected to accelerate the dissociation of ^{3}H-NMS more than is actually observed. Removal of critical binding site residues would decrease the activation energy of the reverse reaction RL→R+L. The increases in dissociation rates for NMS seen for the E2 loop mutants R171A, I180A and F182A are not of the order to suggest that they are ligand contact residues. However this data may support the idea that these residues are involved as second shell residues helping to stabilise the ligand in the transmembrane binding pocket. Nevertheless this data provides corroborating evidence that E2 loop residues do not make contacts essential for NMS binding. However, perturbing the structure of the E2 loop proximal to the β-hairpin structure does appear to have a deleterious effect on the stability of the ligand in the binding pocket. There were no significant changes in the association rate constants for the E2 loop mutants. Only R171A and Y179A reduced the association rate by a factor of 2-3 relative to the WT and the diffusion limited association rate constant. This may be due to slight changes in the conformation of the region above the TM binding site creating small perturbations in the alignment of specific contact residues, thus slightly increasing the activation energy barrier for the bound ligand.

The wild type residues of the E2 loop probably fulfil the role which has been proposed, that is, they form a plug or lid like structure that helps retain the ligand in the binding cavity. There is the question of whether or not the conformation of the E2 loop is altered along with other structural changes that occur on the binding of ligand. If the E2 loop is a dynamic structure, being able to move into and away from the central binding pocket, it is possible that the binding of ligand invokes movement of the E2 loop in towards the binding cavity to create a conformational change favourable to the retention of ligand. This closing in effect may be a result of movement of the TM-domain helices. Potentially, the effect of

the proximity of the re-aligned E2 loop residues could be to sterically hinder any movement of the ligand as it dissociates from the receptor

Figure 7.3 H-Bond Interactions for the Conserved Serine Residue at the C-Terminus of the E2 loop in M_1 mAChR

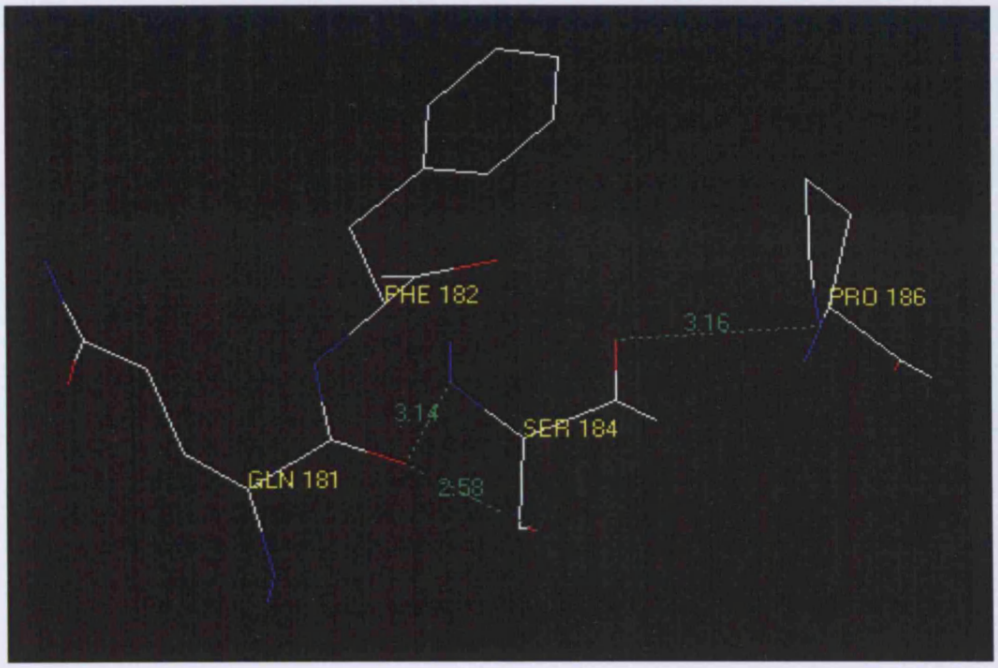

Analagous to the the W164 residue at the N-terminus of the E2 loop, S184 also appears to provide important H-bonds with a proline residue (P186) at the top of TM5. Mutation of S184 also significantly reduced ACh potency and receptor efficacy. The implication is that S184 provides another point of contact with the TM helices that help maintain the structural integrity of the E2 loop which is important for allowing the correct movement of the TM helices upon receptor activation. The figure was adapted from the M_1 mAChR homology model and H-bonds were set a detection threshold with a minimum distance of 2.2 Å and a maximum distance of 3.27 Å using the WEbviewer Lite modelling programme. Nitrogen atoms are shown in blue, hydrogen atoms are shown in red and the carbon backbone is shown in white.

7.2. Cysteine Residues

There now seems little doubt that the most highly conserved pair of cysteine residues in the whole family of GPCRs form a disulphide bond, stabilising the inactive ground state and are important for allowing the correct re-alignment of the helices during activation of the receptor. Evidence provided by this study supports the existence of an S-S bond and show that the bond is important for both expression of the receptor and agonist induced activation. In addition the maintenance of the disulphide bond would appear to also stabilise the transmembrane binding site, especially for the binding of the endogenous agonist acetylcholine. It still remains to be determined however whether or not the C178 residue itself provides a specific contact residue. The model of C178 in relation to ACh in the binding site shown in figure 7.4, implies that the electron fields of the atoms in C178 are too far distant at 6.3 Å from the bound ACh molecule to make direct and specific contact. However, it must be stressed that the model is just a homology model and the real distances may be shorter, allowing for contact. What is clear is that mutating the conserved cysteine residues reduces ACh affinity by ~100-fold. The conclusion of this report, therefore, is that it is the general perturbation of the central binding site cavity caused by the disruption of the stabilising E2 loop structure that decreases the free energy resulting from the binding of ACh to the receptor. As a result of the cysteine mutations ACh potency and signalling efficacy are also dramatically and significantly affected and this highlights the importance of the overall structure of the E2 loop to receptor activity and ground state stability.

One of the most interesting observations during this study was the apparent formation of two populations of receptors caused by the mutation of C98 to alanine, one with a high affinity for ACh and the other with a low affinity. Evidence for this was seen in both the

ACh competition binding experiments and in the QNB dissociation kinetics and it appears to be a real phenomenon. It has been suggested that the two populations may exist as dimers with one population having an inter-molecular S-S bond formed between the two free C178 residues and the other population existing as a monomer with the C178 residue unconnected. Alternatively, the C178 residue could form a S-S bond with one of the free cysteine residues of the E3 loop leaving the second population with no alternative S-S bonds. The relative distance between C178 and the C394 in the E3 loop is 18.3 Å (see figure 7.3) as determined by the homology model and is sufficiently close to propose that an interaction is possible. In the homology model the E2 loop actually crosses double over itself (see main introduction figure 1.5). Removing the anchoring S-S bond would make the loop more dynamic and with a total length of ~50 Å it could be imagined that the free C178 could reach the free C394 in the E3 loop. Obviously a conformational rearrangement of the structure would result from this. It was shown that the high affinity site could not have been responsible for ACh induced signalling since the potency of ACh was less than its affinity for the high affinity site. Certainly this requires further investigation, not least to ascertain which population of binding sites is responsible for the fast dissociation rate constant of QNB and which site is responsible for the slow rate of dissociation. In general the cysteine mutants increased the rates of dissociation for both NMS and more significantly for QNB. The general disruption of the central binding site may reduce the amount of free energy required for NMS and QNB to surmount the activation barrier for the reverse binding reaction and so dissociate more readily from the cysteine mutated receptor than from the wild type receptor.

Another surprising result was the significant increases in AC-42 affinity seen particularly for the C178A mutant. This mutation may uncover an epitope on the exo-facial surface of the receptor that allows AC-42 to bind with higher affinity. In fact, the increase in AC-42

affinity was a feature of the cysteine mutants. Reductions in the affinity of other agonists and antagonists seen for the cysteine mutants was in keeping with a general perturbation of the central binding site caused by disruption of the S-S bond. Since there was an equal effect seen for the double cysteine mutant it could concluded that neither C98 nor C178 makes specific contact with the other ligands tested.

Figure 7.4 Relative Distance Between C178 and ACh and Cysteine 394 of the E3 Loop

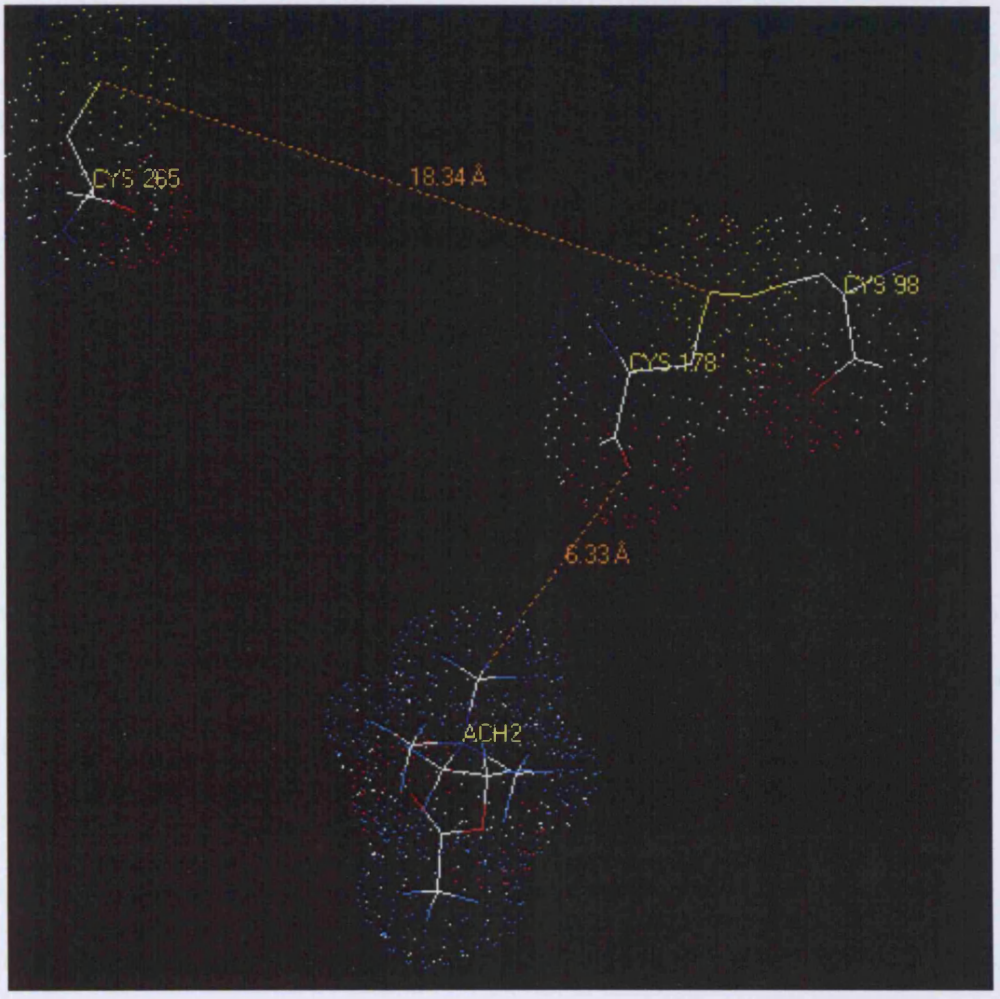

The figure serves to show the relative distance of the disulphide bonded cysteine pair to both the bound ACh molecule and the free cysteine in the E3 loop, shown here as Cys 265 since the image was designed from a homology model of the M_1 mAChR that omitted the large intracellular loop 3 region, hence the unusal numbering.. In fact the this cysteine is at position C394 in the wild type receptor. There is the possibility that the C98A mutant may allow the free C178 to make an alternative S-S bond with C394 in the E3 loop. The homology model also predicts that C178 at 6.33 Å is too far distant to make direct contact with ACh. However, the model may require refinement and radioligand binding studies in this report have shown that the C178A significantly and severely reduces ACh affinity.

7.3. TM Domain Residues

The residues F197 (TM5)and W378 (TM6) were also mutated to alanine in this study to help complete the identification of binding site residues. The potential ligand docking residue D99 was also mutated to further investigate the possibility of there being a ligand access channel in the M_1 mAChR. Evidence from ligand binding studies suggest that both F197 and W378 make critical contacts with the antagonist NMS, as their mutation reduced the affinity constant for NMS greater than 90 and 400-fold respectively. It is possible that the benzene ring of NMS can form pi-pi stacking bond with F197 and the indole ring of the tryptophan may contribute to the aromatic cage environment of the transmembrane binding site by making contact with the head group of the NMS molecule. Interestingly, there was further evidence for a different mode of binding of QNB compared to NMS. This was highlighted by the fact that W378A reduced QNB affinity by ~10-fold whereas F197A did not significantly reduce QNB affinity at all. Also, only W378A significantly reduced ACh affinity by ~13-fold. Thus, W378 which is highly conserved in rhodopsin like and aminergic receptors seems to be another critical transmembrane binding site residue. The mutation D99A severely reduced expression of the receptor and significantly reduced the affinity of NMS 11-fold and ACh 22-fold, but had little effect on the binding of QNB. This may be the best evidence we have that QNB actually enters the central binding cavity via a different route than either NMS or ACh. That is QNB being a hydrophobic molecule may access the central binding cavity through gaps in the TM helices via the lipid membrane. The fact that D99A reduces ACh affinity but not the signalling efficacy of the receptor is circumstantial evidence that D99 potentially in partnership with W157, does indeed act as a docking residue in a two step process of binding analogous to the model described by Jakubik et al (Jakubik et al., 2000). That is, once ACh has found its way to the

transmembrane binding site, the D99A mutation does not affect the activation of the receptor induced by ACh binding.

Both F197A and W378 affected the potency of ACh and both reduced the efficacy of the receptor by 10-fold. It is likely that W378 is part of a H-bond network that is rearranged upon activation of the receptor. Consistent with the conserved nature of this residue, its importance to both, the binding of ligands and to the activation of the receptor have been confirmed by these studies. For example the W378A also reduced the affinity of pilocarpine by more than 10-fold. It may be of little surprise therefore that the mutation of W378 also substantially increased the dissociation rate constant of QNB. This was also true for the other proven binding site residues. Mutation of these residues may disrupt helix-helix interactions, allowing a less impeded egress of QNB from the receptor, reducing the amount of free energy required for the ligand to proceed in both the forward and reverse binding reaction.

Interestingly, the major binding site mutant residues Y106A, Y381A and N382A had little or no effect on the affinity of McN-A-343 or AC-42, the strongest evidence provided by this study that these two atypical agonists bind to a site distinctly different from the transmembrane binding site. In fact N382A significantly ($p<0.05$) increased the affinity of McN-A-343 by 5-fold. It is likely therefore McN-A-343 and AC-42 bind to an allosteric site on the exofacial surface of the receptor and may bind to a site analogous to the gallamine allosteric site. Evidence shown in this study suggests that the E2 loop is not part of this ectopic site for these ligands since the selected mutant E2 loop residues did not significantly reduce affinity.

Chapter 8

Future Work

The following list highlights interesting points that have arisen during this study and require further investigation to provide a more comprehensive understanding of the molecular basis of ligand binding to muscarinic acetylcholine receptors.

1. The Cysteine mutants, in particular, require further study. In particular, more evidence is required that there exist two populations of receptor for the C98A mutant. A more detailed analysis of the dissociation kinetics is needed for this particular mutant. Since the initial off rate is so fast, an experiment needs to be conducted that has more time points to provide data on the initial slope in the rapid phase of QNB dissociation. Furthermore, an experiment needs to be conducted whereby the high affinity binding site is blocked with a single high concentration of unlabelled acetylcholine at ~10^{-3}M concentration. Then a detailed dissociation assay should be performed in the usual way. This experiment would tell us whether or not it was the high or low affinity site that was responsible for the fast rate dissociation kinetics of QNB at the C98A receptor.

2. To ascertain whether or not there is an alternative S-S bond formed between the free C178 residue in the C98A mutant, a reduction experiment using DTT could be performed on purified C98A mutant receptors followed by a gel analysis. The existence of dimers would be evident by comparison of DTT treated receptors with non treated receptors and examining the relative molecular weights of the different bands on a Western blot. The fact that C98A severely reduces receptor expression might be a problem however. Another approach would be to make a double mutant C98A and C394A and analyse the differences in acetylcholine competition assays between the double mutant and the single C98A

mutant. A two site model of binding would not fit the double mutant data if indeed the free C178 residue were forming an alternative S-S bond or a dimer with C394.

This study was unable to confirm or refute whether C178 itself makes direct contact with the bound ACh molecule. One approach to further investigate this question is to try to chemically reduce the S-S with DTT or Tributyl phosphine and then perform standard ACh competition binding assays. An initial attempt at this approach was made during the course of this investigation but an effect was not seen. The buried nature of the conserved S-S bond may render it difficult to access with DTT. A more systematic and comprehensive approach is recommended. In particular, reduced S-S bonds would require treatment with iodoacetamide for example; to prevent re-oxidisation of reduced SH groups. This was not done in the initial attempt.

3. There was tantalising evidence that the Q181A mutant imparted significantly raised basal activity to the receptor. Should this be true it may have important implications for the further study of receptor activation. Unfortunately in one of three experiments the Q181A mutant showed basal levels of activity similar to wild type. It may have been the case that in that particular assay there was a problem with the transfection of plasmid. Therefore, it is necessary to conduct more PI assays on this particular mutant to confirm or deny that this mutant significantly raises basal activity and whether the wild type residue is crucial for the ground state conformation of the receptor.

4. In order to test the theory that W164 and S184 provide important H-bonds and act as anchor points at either end of the E2 loop it would be interesting to see if certain mutations could restore receptor activity. For example, by mutating S184 to another uncharged polar side chain, such as threonine, it may be possible to reinstate H-bonds lost by the mutation

of S184 to alanine. Comparing the S184T mutant to the S184A and WT receptors may provide more insight into the function of this strategically placed residue. Also mutation of the corresponding proline residues would be necessary to gain a full insight as to whether or not the E2 loop is anchored to the TM helices by the H-bond interaction described above. The analogous mutation for W164 would be changing it to a histidine residue and conducting a similar analysis to the S184 mutants.

5. Some evidence was provided in this study that D99 is part of an entrance channel and participates in a two-step binding process. Another approach may be to mutate D99 to a bulkier residue, one that effectively blocks the access channel, leucine or valine or perhaps. Performing NMS binding and dissociation experiments would show whether or not the bulkier residue restricted NMS access and egress to and from the central binding site. It would also be interesting to see the effect of changing the negative charge of D99 for a positively charged lysine residue to assess the importance of the negative charge of D99 in the native receptor. An oversight of this study was not to further characterise W157, for which our laboratory has the alanine mutant. Assessing the binding of other ligands to the W157A mutant would further our understanding of the role played by W157 and D99 in the initial binding of ligands.

6. From this study it was apparent that single point mutations of the E2 loop, apart from a couple of exceptions, did not drastically perturb ligand binding or receptor activity. Also some residues in the E2 loop were not mutated and analysed at all. It may be prudent, before definitive statements about the function of the M_1 mAChR E2 loop can be made, to mutate and examine not only the residues overlooked by this and Leppiks (Leppik et al., 1994) study, but also to perform multiple substitutions on E2 loop residues. Amino acids do not exist in isolation and it is likely that there are several specific interactions between the

E2 loop residues that need to be disrupted before they affect the properties of a functioning receptor. Therefore there is the scope for many more E2 loop mutations to be made, both multiple substitutions and mutating residues to residues other than alanine to alter the physico-chemical properties of the E2 loop. In particular it would be informative to replace the cysteine residues at C98 and C178 with other residues to see if any function could be gained.

7. As a general point, association assays need to be performed on all the mutants tested in this study to compare with the calculated association constants derived from dissociation assays. Also data needs to be acquired for all mutants to fill in the missing affinity constants of the other agonists and antagonists used in this study to better understand the nature of non-endogenous ligand binding.

8. There is a need for a more comprehensive analysis of the residues responsible for the binding of McN-A-343 and AC-42. Evidence indicates that these selective agonists bind to an allosteric site distinct from the orthosteric site. It is proposed that systematic mutations of the N-terminal region, the E1 loop and the E3 loop would reveal the ligand contact residues responsible for the binding of these two unusual agonists.

9. Based on the results of this thesis it is envisaged that further manipulation of the M_1 homology model may be required. The current homology model suggests that the E2 loop is in closer proximity to the central binding site than the data in this thesis may suggest. Molecular dynamic modelling may help to resolve these issues.

References

Abbott A and Nelsestuen G (1988) The collisional limit: an important consideration for membrane- associated enzymes and receptors. *FASEB J.* **2**:2858-2866.

Abdulaev NG and Ridge KD (1998) Light-induced exposure of the cytoplasmic end of transmembrane helix seven in rhodopsin. *PNAS.* **95**:12854-12859.

Agnati LF OS, Rondanini C, Zoli M, Fuxe K (1982) New Vistas on Synaptic Plasticity; the receptor mosaic hypothesis of the engram. *Med. Biol.* **60**:183-190.

Akam EC, Challiss RA and Nahorski SR (2001) G(q/11) and G(i/o) activation profiles in CHO cells expressing human muscarinic acetylcholine receptors: dependence on agonist as well as receptor-subtype. *Br. J. Pharmacol.* **132**(4) 950-8.

Allman K, Page KM, Curtis CA and Hulme EC (2000) Scanning mutagenesis identifies amino acid side chains in transmembrane domain 5 of the M(1) muscarinic receptor that participate in binding the acetyl methyl group of acetylcholine. *Mol. Pharmacol.* **58**:175-84.

Alousi A, Jasper J, Insel P and Motulsky H (1991) Stoichiometry of receptor-Gs-adenylate cyclase interactions. *FASEB J.* **5**:2300-2303.

Altenbach C, Yang K, Farrens DL, Farahbakhsh ZT, Khorana HG and Hubbell WL (1996) Structural Features and Light-Dependent Changes in the Cytoplasmic Interhelical E-F Loop Region of Rhodopsin: A Site-Directed Spin-Labeling Study. *Biochemistry.* **35**:12470-12478.

Amatruda TT, III, Dragas-Graonic S, Holmes R and Perez HD (1995) Signal Transduction by the Formyl Peptide Receptor. *J. Biol. Chem.* **270**:28010-28013.

Angers S, Salahpour A, Joly E, Hilairet S, Chelsky D, Dennis M and Bouvier M (2000) Detection of beta 2-adrenergic receptor dimerization in living cells using bioluminescence resonance energy transfer (BRET). *PNAS.* **97**:3684-3689.

Avlani V (2005) A Dynamic Role of the Second Extracellular Loop in M2 Muscarinic Acetylcholine Receptor Allosteric Modulation, in *ASCEPT*, Melbourne, Australia.

Baldwin JM, Schertler GFX and Unger VM (1997) An alpha-carbon template for the transmembrane helices in the rhodopsin family of G-protein-coupled receptors. *J. Mol. Biol.* **272**:144-164.

Ballesteros JA, Deupi X, Olivella M, Haaksma EEJ and Pardo L (2000) Serine and Threonine Residues Bend alpha-Helices in the chi 1 = g-Conformation. *Biophys. J.* **79**:2754-2760.

Ballesteros JA, Shi L and Javitch JA (2001) Structural Mimicry in G Protein-Coupled Receptors: Implications of the High-Resolution Structure of Rhodopsin for Structure-Function Analysis of Rhodopsin-Like Receptors. *Mol. Pharmacol.* **60**:1-19.

Ballesteros WHJ (1995) Integrated methods for the construction of three dimensional models and computational probing of structure function relations in G-protein coupled receptors. *Methods. Neurosci.* **25**:366-428.

Baneres J-L, Mesnier D, Martin A, Joubert L, Dumuis A and Bockaert J (2005) Molecular Characterization of a Purified 5-HT4 Receptor: A Structural Basis for Drug Efficacy. *J. Biol. Chem.* **280**:20253-20260.

Baneres J-L and Parello J (2003) Structure-based Analysis of GPCR Function: Evidence for a Novel Pentameric Assembly between the Dimeric Leukotriene B4 Receptor BLT1 and the G-protein. *J. Mol. Biol.* **329**:815-829.

Barlow DJ and Thornton JM (1988) Helix geometry in proteins. *J. Mol. Biol.* **201**:601-619.

Basile AS, Fedorova I, Zapata A, Liu X, Shippenberg T, Duttaroy A, Yamada M and Wess J (2002) Deletion of the M5 muscarinic acetylcholine receptor attenuates morphine reinforcement and withdrawal but not morphine analgesia. *PNAS.* **99**:11452-11457.

Berkeley JL, Gomeza J, Wess J, Hamilton SE, Nathanson NM and Levey AI (2001) M_1 Muscarinic Acetylcholine Receptors Activate Extracellular Signal-Regulated Kinase in CA1 Pyramidal Neurons in Mouse Hippocampal Slices. *Mol. Cell. Neurosci.* **18**:512-524.

Bernardini N, Roza C, Sauer SK, Gomeza J, Wess J and Reeh PW (2002) Muscarinic M2 receptors on peripheral nerve endings: a molecular target of antinociception. *J. Neurosci.* **22** (12):RC229.

Bernardini N, Sauer SK, Haberberger R, Fischer MJM and Reeh PW (2001) Excitatory Nicotinic and Desensitizing Muscarinic (M2) Effects on C-Nociceptors in Isolated Rat Skin *J. Neurosci.* **21**:3295-3302.

Bernstein LS, Ramineni S, Hague C, Cladman W, Chidiac P, Levey AI and Hepler JR (2004) RGS2 Binds Directly and Selectively to the M_1 Muscarinic Acetylcholine Receptor Third Intracellular Loop to Modulate Gq/11{alpha} Signaling. *J. Biol. Chem.* **279**:21248-21256.

Berridge MJ, Dawson RM, Downes CP, Heslop JP and Irvine RF (1983). Changes in the levels of inositol phosphates after agonist-dependent hydrolysis of membrane phosphoinositides. *J. Biol. Chem.* **271**:473-82.

Biddlecome GH, Berstein G and Ross EM (1996) Regulation of Phospholipase C-beta1 by G(q) and m1 Muscarinic Cholinergic Receptor. *J. Biol. Chem.* **271**:7999-8007.

Birdsall NJ, Burgen AS, Hulme EC, Stockton JM and Zigmond MJ (1983) The effect of McN-A-343 on muscarinic receptors in the cerebral cortex and heart. *Br. J. Pharmacol.* **78**:257-9,

Birdsall NJM and Lazareno S (2005) Allosterism at Muscarinic receptors: Ligands and Mechanisms. *Mini-Rev. Med. Chem.* **5**:523-543.

Bjarnadottir TK, Fredriksson R, Hoglund PJ, Gloriam DE, Lagerstrom MC and Schioth HB (2004) The human and mouse repertoire of the adhesion family of G-protein-coupled receptors. *Genomics.* **84**:23-33.

Bockaert J and Pin JP (1999) Molecular tinkering of G protein-coupled receptors: an evolutionary success. *EMBO J.* **18**:1723-9.

Bonner TI, Buckley, N.J., Young, A.C. & Brann, M.R. (1987) Identification of a family of Muscarinic Acetylcholine Receptor Genes. *Science.* **237**:527-532.

Bourne Y, Taylor P and Marchot P (1995) Acetylcholinesterase inhibition by fasciculin: Crystal structure of the complex. *Cell.* **83**:503-512.

Brauner-Osborne HEB, Brann MR, Falch E, Krogsgaard-Larsen P. (1996) Functional partial agonism at cloned human muscarinic acetylcholine receptors. *Eur. J. Pharmacol.* **313**:145-50.

Bunemann M, Frank M and Lohse MJ (2003) From The Cover: Gi protein activation in intact cells involves sub-unit rearrangement rather than dissociation. *PNAS.* **100**:16077-16082.

Burstein ES, Spalding TA and Brann MR (1997) Pharmacology of Muscarinic Receptor Subtypes Constitutively Activated by G Proteins. *Mol. Pharmacol.* **51**:312-319.

Burstein ES, Spalding TA and Brann MR (1998) The Second Intracellular Loop of the m5 Muscarinic Receptor Is the Switch Which Enables G-protein Coupling. *J. Biol. Chem.* **273**:24322-24327.

Bymaster FP, Carter PA, Yamada M, Gomeza J, Wess J, Hamilton SE, Nathanson NM, McKinzie DL and Felder CC (2003a) Role of specific muscarinic receptor subtypes in cholinergic parasympathomimetic responses, in vivo phosphoinositide hydrolysis, and pilocarpine-induced seizure activity. *Eur. J. Neurosci.* **17**:1403-1410.

Bymaster FP, McKinzie DL, Felder CC and Wess J (2003b) Use of M_1-M_5 muscarinic receptor knockout mice as novel tools to delineate the physiological roles of the muscarinic cholinergic system. *Neurochem. Res.* **28**:437-42.

Cabrera-Vera TM, Vanhauwe J, Thomas TO, Medkova M, Preininger A, Mazzoni MR and Hamm HE (2003) Insights into G Protein Structure, Function, and Regulation.. *Endocr. Rev.* **24**:765-781.

Carravetta M, Zhao X, Johannessen OG, Lai WC, Verhoeven MA, Bovee-Geurts PHM, Verdegem PJE, Kiihne S, Luthman H, deGroot HJM, deGrip WJ, Lugtenburg J and Levitt MH (2004) Protein-Induced Bonding Perturbation of the Rhodopsin Chromophore Detected by Double-Quantum Solid-State NMR. *J. Am. Chem. Soc.* **126**:3948-3953.

Caulfield MP and Birdsall NJM (1998) International Union of Pharmacology. XVII. Classification of Muscarinic Acetylcholine Receptors. *Pharmacol. Rev.* **50**:279-290.

Chanda P, Minchin M, Davis A, Greenberg L, Reilly Y, McGregor W, Bhat R, Lubeck M, Mizutani S and Hung P (1993) Identification of residues important for ligand binding to the human 5- hydroxytryptamine1A serotonin receptor. *Mol. Pharmacol.* **43**:516-520.

Cheng Y and Prusoff WH (1973) Relationship between the inhibition constant (KI) and the concentration of inhibitor which causes 50 per cent inhibition (IC_{50}) of an enzymatic reaction. *Biochem. Pharmacol.* **22**:3099-108.

Christopoulos A and Kenakin T (2002) G Protein-Coupled Receptor Allosterism and Complexing. *Pharmacol. Rev.* **54**:323-374.

Christopoulos A and Mitchelson F (1997) Pharmacological analysis of the mode of interaction of McN-A-343 at atrial muscarinic M2 receptors. *Eur. J. Pharmacol.* **339**:153-156.

Clapham DE (2001) The TRP Ion Channel Family. *Nat. Rev. Neurosci.* **2**:387-396.

Clapham DE and Neer EJ (1997) G protein {Beta}{Gamma} Subunits. *Annu. Rev. Pharmacol. Toxicol.* **37**:167-203.

Conklin BR, Farfel Z, Lustig KD, Julius D and Bourne HR (1993) Substitution of three amino acids switches receptor specificity of Gq[alpha] to that of Gi[alpha]. *Nature.* **363**:274-276.

Conner AC, Simms J, Howitt SG, Wheatley M and Poyner DR (2006) The Second Intracellular Loop of the Calcitonin Gene-related Peptide Receptor Provides Molecular Determinants for Signal Transduction and Cell Surface Expression. *J. Biol. Chem.* **281**:1644-1651.

Costa T and Cotecchia S (2005) Historical review: Negative efficacy and the constitutive activity of G-protein-coupled receptors. *Trends in Pharm. Sci.* **26**:618-624.

Cotte N, Balestre M-N, Phalipou S, Hibert M, Manning M, Barberis C and Mouillac B (1998) Identification of Residues Responsible for the Selective Binding of Peptide Antagonists and Agonists in the V2 Vasopressin Receptor. *J. Biol. Chem.* **273**:29462-29468.

Dale HH (1914) The Action of Certain esters and ethers of choline and their relation to muscarine. *J. Pharm. Exp. Ther.* **6**:147-190.

Davidson F, Loewen P and Khorana H (1994) Structure and Function in Rhodopsin: Replacement by Alanine of Cysteine Residues 110 and 187, Components of a Conserved Disulfide Bond in Rhodopsin, Affects the Light-Activated Metarhodopsin II State. *PNAS.* **91**:4029-4033.

Diaz J, Levesque D, Lammers CH, Griffon N, Martres M-P, Schwartz J-C and Sokoloff P (1995) Phenotypical characterization of neurons expressing the dopamine D3 receptor in the rat brain. *Neurosci.* **65**:731-745.

Du K, Nicole P, Couvineau A and Laburthe M (1997) Aspartate 196 in the first extracellular loop of the human VIP1 receptor is essential for VIP binding and VIP-stimulated cAMP production. *Biochem. Biophys. Res. Comm.* **230**:289-92

Dunham TD and Farrens DL (1999) Conformational Changes in Rhodopsin. Movement of Helix F Detected by Site-Specific Chemical Labeling and Fluorescence Spectroscopy. *J. Biol. Chem.* **274**:1683-1690.

Hulme EC and Curtis C (1998). Purification of recombinant M_1 muscarinic acetylcholine receptor. *Biochem. Soc. Trans.* **26**(4):S361,

Elling CE, Nielsen SM and Schwartz TW (1995) Conversion of antagonist-binding site to metal-ion site in the tachykinin NK-1 receptor.*Nature.* **374**:74-7

Ellis J and Seidenberg M (2000) Interactions of Alcuronium, TMB-8, and Other Allosteric Ligands with Muscarinic Acetylcholine Receptors: Studies with Chimeric Receptors. *Mol. Pharmacol.* **58**:1451-1460.

Espinoza-Fonseca LM and Trujillo-Ferrara JG (2005) Identification of multiple allosteric sites on the M_1 muscarinic acetylcholine receptor. *FEBS Letters.* **579**:6726-6732.

Farahbakhsh ZT, Hideg K and Hubbell WL (1993) Photoactivated conformational changes in rhodopsin: a time-resolved spin label study.*Science.* **262**:1416-9

Farahbakhsh ZT, Ridge KD, Khorana HG and Hubbell WL (1995) Mapping light-dependent structural changes in the cytoplasmic loop connecting helices C and D in rhodopsin: a site-directed spin labeling study. *Biochemistry.* **34**:8812-9

Fields JZ, Roeske WR, Morkin E and Yamamura HI (1978) Cardiac muscarinic cholinergic receptors. Biochemical identification and characterization. *J. Biol. Chem.* **253**:3251-3258.

Fisahn A, Yamada M, Duttaroy A, Gan J-W, Deng C-X, McBain CJ and Wess J (2002) Muscarinic Induction of Hippocampal Gamma Oscillations Requires Coupling of the M_1 Receptor to Two Mixed Cation Currents. *Neuron.* **33**:615-624.

Fong T, Huang R and Strader C (1992) Localization of agonist and antagonist binding domains of the human neurokinin-1 receptor. *J. Biol. Chem.* **267**:25664-25667.

Foord SM and Marshall FH (1999) RAMPs: accessory proteins for seven transmembrane domain receptors. *Trends. Pharmacol. Sci.* **20**:184-187.

Fraser C, Wang C, Robinson D, Gocayne J and Venter J (1989) Site-directed mutagenesis of m1 muscarinic acetylcholine receptors: conserved aspartic acids play important roles in receptor function. *Mol. Pharmacol.* **36**:840-847.

Fredriksson R, Lagerstrom MC, Lundin L-G and Schioth HB (2003) The G-Protein-Coupled Receptors in the Human Genome Form Five Main Families. Phylogenetic Analysis, Paralogon Groups, and Fingerprints. *Mol. Pharacol.* **63**:1256-1272.

Fu D, Ballesteros JA, Weinstein H, Chen J and Javitch JA (1996) Residues in the Seventh Membrane-Spanning Segment of the Dopamine D2 Receptor Accessible in the Binding-Site Crevice. *Biochemistry.* **35**:11278-11285.

Furukawa H, Hamada T, Hayashi MK, Haga T, Muto Y, Hirota H, Yokoyama S, Nagasawa K and Ishiguro M (2002) Conformation of ligands bound to the muscarinic acetylcholine receptor. *Mol. Pharmacol.* **62**:778-87.

Galper J, Dziekan L, O'Hara D and Smith T (1982) The biphasic response of muscarinic cholinergic receptors in cultured heart cells to agonists. Effects on receptor number and affinity in intact cells and homogenates. *J. Biol. Chem.* **257**:10344-10356.

Garnovskaya MN, Gettys TW, van Biesen T, Prpic V, Chuprun JK and Raymond JR (1997) 5-HT1A Receptor Activates Na+/H+ Exchange in CHO-K1 Cells through Gialpha 2 and Gialpha 3. *J. Biol. Chem.* **272**:7770-7776.

Gerber DJ, Sotnikova TD, Gainetdinov RR, Huang SY, Caron MG and Tonegawa S (2001) Hyperactivity, elevated dopaminergic transmission, and response to amphetamine in M_1 muscarinic acetylcholine receptor-deficient mice. *PNAS* **98**:15312-15317.

Gether U (2000) Uncovering molecular mechanisms involved in activation of G protein-coupled receptors. *Endo. Rev.***21**:90-113.

Gether U, Johansen T and Schwartz T (1993) Chimeric NK1 (substance P)/NK3 (neurokinin B) receptors. Identification of domains determining the binding specificity of tachykinin agonists. *J. Biol. Chem.* **268**:7893-7898.

Gnagey A and Ellis J (1996) Allosteric regulation of the binding of ^{3}H-acetylcholine to m2 muscarinic receptors. *Biochem. Pharmacol.* **52**:1767-1775.

Gnagey AL, Seidenberg M and Ellis J (1999) Site-Directed Mutagenesis Reveals Two Epitopes Involved in the Subtype Selectivity of the Allosteric Interactions of Gallamine at Muscarinic Acetylcholine Receptors. *Mol. Pharmacol.* **56**:1245-1253.

Gomeza J, Shannon H, Kostenis E, Felder C, Zhang L, Brodkin J, Grinberg A, Sheng H and Wess J (1999) Pronounced pharmacologic deficits in M2 muscarinic acetylcholine receptor knockout mice. *PNAS.* **96**:1692-1697.

Govaerts C, Blanpain C, Deupi X, Ballet S, Ballesteros JA, Wodak SJ, Vassart G, Pardo L and Parmentier M (2001) The TXP Motif in the Second Transmembrane Helix of CCR5. A Structural Determinant of Chemokine-Induced Activation.. *J. Biol. Chem.* **276**:13217-13225.

Grace CR, Perrin MH, DiGruccio MR, Miller CL, Rivier JE, Vale WW and Riek R (2004) NMR structure and peptide hormone binding site of the first extracellular domain of a type B1 G protein-coupled receptor.*PNAS.* **101**:12836-41

Guo W, Shi L, Filizola M, Weinstein H and Javitch JA (2005) Crosstalk in G protein-coupled receptors: Changes at the transmembrane homodimer interface determine activation. *PNAS.* **102**:17495-17500.

Hamilton SE, Loose MD, Qi M, Levey AI, Hille B, McKnight GS, Idzerda RL and Nathanson NM (1997) Disruption of the m1 receptor gene ablates muscarinic receptor-dependent M current regulation and seizure activity in mice. *PNAS.* **94**:13311-13316.

Hamilton SE and Nathanson NM (2001) The M_1 Receptor Is Required for Muscarinic Activation of Mitogen-activated Protein (MAP) Kinase in Murine Cerebral Cortical Neurons. *J. Biol. Chem.* **276**:15850-15853.

Hammer RBC, Birdsall NJM, Burgen ASV and Hulme EC (1980) Pirenzepine Distinguishes Between Different Subclasses of Muscarinic Receptors. *Nature.* **283**:90-92.

Han M, Lin SW, Minkova M, Smith SO and Sakmar TP (1996a) Functional Interaction of Transmembrane Helices 3 and 6 in Rhodopsin. Replacement of Phenylalanine 261 by Alanine Causes Reversion of Phenotype of a Glycine 121 Replacement Mutant. *J. Biol. Chem.* **271**:32337-32342.

Han M, Lin SW, Smith SO and Sakmar TP (1996b) The Effects of Amino Acid Replacements of Glycine 121on Transmembrane Helix 3 of Rhodopsin. *J. Biol. Chem.* **271**:32330-32336.

Han S-J, Hamdan FF, Kim S-K, Jacobson KA, Bloodworth LM, Li B and Wess J (2005) Identification of an Agonist-induced Conformational Change Occurring Adjacent to the Ligand-binding Pocket of the M3 Muscarinic Acetylcholine Receptor. *J. Biol. Chem.* **280**:34849-34858.

Hanahan D (1983) Studies on transformation of Escherichia coli with plasmids. *J. Mol. Biol.* **166**:557-80.

Hardouin SN, Richmond KN, Zimmerman A, Hamilton SE, Feigl EO and Nathanson NM (2002) Altered Cardiovascular Responses in Mice Lacking the M_1 Muscarinic Acetylcholine Receptor. *J. Pharmacol. Exp. Ther.* **301**:129-137.

Harmar A (2001) Family-B G-protein-coupled receptors. *Genome Biology.* **2**: reviews3013.1

Hawtin SR, Wesley VJ, Parslow RA, Patel S and Wheatley M (2000) Critical Role of a Subdomain of the N-Terminus of the V1a Vasopressin Receptor for Binding Agonists but Not Antagonists; Functional Rescue by the Oxytocin Receptor N-Terminus. *Biochemistry.* **39**:13524-13533.

Hayashi, Mariko Kato Haga and Tatsuya. (1997) Palmitoylation of Muscarinic Acetylcholine Receptor M2 Subtypes: Reduction in their Ability to Activate G-Proteins by Mutation of a Putative Palmitoylation Site, Cysteine 457, in the Carboxyl-Termional Tail. *Arch. Biochem. Biophys.* **340**:376-382

Hebert TE, Moffett S, Morello J-P, Loisel TP, Bichet DG, Barret C and Bouvier M (1996) A Peptide Derived from a beta 2-Adrenergic Receptor Transmembrane Domain Inhibits Both Receptor Dimerization and Activation. *J. Biol. Chem.* **271**:16384-16392.

Hein Peter FM, Hoffmann Carsten, Lohse Martin J and Bunemann Moritz (2005) Dynamics of Receptor/G-Protein Coupling in Living Cells. *EMBO Journal.* **24**:4106-4114.

Heitz F, Holzwarth JA, Gies J-P, Pruss RM, Trumpp-Kallmeyer S, Hibert MF and Guenet C (1999) Site-directed mutagenesis of the putative human muscarinic M2 receptor binding site. *Eur. J. Pharmacol.* **380**:183-195.

Hibert M, Trumpp-Kallmeyer S, Bruinvels A and Hoflack J (1991) Three-dimensional models of neurotransmitter G-binding protein-coupled receptors. *Mol. Pharmacol.* **40**:8-15.

Hill-Eubanks D, Burstein ES, Spalding TA, Bräuner-Osborne H and Brann MR (1996) Structure of a G-protein-coupling Domain of a Muscarinic Receptor Predicted by Random Saturation Mutagenesis. *J. Biol. Chem.* **271**:3058-3065.

Hjorth S, Schambye H, Greenlee W and Schwartz T (1994) Identification of peptide binding residues in the extracellular domains of the AT1 receptor. *J. Biol. Chem.* **269**:30953-30959.

Högger P, Shockley MS, Lameh J and Sadée W (1995) Activating and Inactivating Mutations in N- and C-terminal i3 Loop Junctions of Muscarinic Acetylcholine Hm1 Receptors. *J. Biol. Chem.* **270**:7405-7410.

Hovius R, Vallotton P, Wohland T and Vogel H (2000) Fluorescence techniques: shedding light on ligand-receptor interactions. *Trends. Pharmacol. Sci.* **21**:266-273.

Hoyer D, Hannon JP and Martin GR (2002) Molecular, pharmacological and functional diversity of 5-HT receptors. *Pharmacol. Biochem. Behav.* **71**:533-554.

Huang X-P, Williams FE, Peseckis SM and Messer WS, Jr. (1999) Differential Modulation of Agonist Potency and Receptor Coupling by Mutations of Ser388Tyr and Thr389Pro at the Junction of Transmembrane Domain VI and the Third Extracellular Loop of Human M_1 Muscarinic Acetylcholine Receptors. *Mol. Pharmacol.* **56**:775-783.

Hulme EC (2005) Systematic Mutagenesis of M_1 Muscarinic Acetylcholine Receptors. in G-Protein Coupled Receptors Structure, Function and Ligand Screening. (Hayn T and Takudai S. Ed.) CRC Press. Pages 137-178.

Hulme EC, Birdsall NJM and Buckley NJ (1990) Muscarinic Receptor Subtypes. *Ann. Rev. Pharmacol. Toxicol.* **30**:633-673.

Hulme EC and Lu ZL (1998) Scanning mutagenesis of transmembrane domain 3 of the M_1 muscarinic acetylcholine receptor. *J. Phys.* **92**:269-74.

Hulme EC, Lu ZL, Bee M, Curtis CA and Saldanha J (2001) The conformational switch in muscarinic acetylcholine receptors. *Life Sci.* **68**:2495-500.

Hulme EC, Lu ZL, Saldanha JW and Bee MS (2003) Structure and activation of muscarinic acetylcholine receptors. *Biochem. Soc. Trans.* **31**:29-34.

Hulme EC, Lu ZL, Ward SD, Allman K and Curtis CA (1999) The conformational switch in 7-transmembrane receptors: the muscarinic receptor paradigm. *Eur. J. Pharmacol.* **375**:247-60.

Hulme. E.C, Lu ZL, Bee. MS (2003) Scanning Mutagenesis Studies of the M_1 Muscarinic Acetylcholine Rceptor. *Receptors & Channels.* **9**:215-228.

Jackson DM and Westlind-Danielsson A (1994) Dopamine receptors: Molecular biology, biochemistry and behavioural aspects. *Pharmacol. Ther.* **64**:291-370.

Jakubik J, Bacakova L, El-Fakahany EE and Tucek S (1995) Constitutive activity of the M_1-M_4 subtypes of muscarinic receptors in transfected CHO cells and of muscarinic receptors in the heart cells revealed by negative antagonists. *FEBS Letters.* **377**:275-279.

Jakubik J, El-Fakahany EE and Tucek S (2000) Evidence for a Tandem Two-site Model of Ligand Binding to Muscarinic Acetylcholine Receptors. *J. Biol. Chem.* **275**:18836-18844.

Jakubik J, Krejci A and Dolezal V (2005) Asparagine, Valine, and Threonine in the Third Extracellular Loop of Muscarinic Receptor Have Essential Roles in the Positive Cooperativity of Strychnine-Like Allosteric Modulators. *J. Pharm. Exp. Ther.* **313**:688-696.

Javitch JA, Fu D and Chen J (1995) Residues in the fifth membrane-spanning segment of the dopamine D2 receptor exposed in the binding-site crevice.*Biochemistry.* **34**:16433-9,

Javitch JA, Li X, Kaback J and Karlin A (1994) A cysteine residue in the third membrane-spanning segment of the human D2 dopamine receptor is exposed in the binding-site crevice.*PNAS.* **91**:10355-9

Javitch JA, Shi L, Simpson MM, Chen J, Chiappa V, Visiers I, Weinstein H and Ballesteros JA (2000) The Fourth Transmembrane Segment of the Dopamine D2 Receptor: Accessibility in the Binding-Site Crevice and Position in the Transmembrane Bundle. *Biochemistry.* **39**:12190-12199.

Jensen AD, Guarnieri F, Rasmussen SGF, Asmar F, Ballesteros JA and Gether U (2001) Agonist-induced Conformational Changes at the Cytoplasmic Side of Transmembrane Segment 6 in the beta 2 Adrenergic Receptor Mapped by Site-selective Fluorescent Labeling. *J. Biol. Chem.* **276**:9279-9290.

Jones PG, Curtis CA and Hulme EC (1995) The function of a highly-conserved arginine residue in activation of the muscarinic M_1 receptor. *Eur. J. Pharmacol.* **288**:251-7.

Kallal L and Kurjan J (1997) Analysis of the receptor binding domain of Gpa1p, the G(alpha) sub-unit involved in the yeast pheromone response pathway. *Mol. Cell. Biol.* **17**:2897-2907.

Klco JM, Wiegand CB, Narzinski K and Baranski TJ (2005) Essential role for the second extracellular loop in C5a receptor activation.[see comment].*Nat. Struct. Mol. Biol. Rev.* **12**:320-6

Klein-Seetharaman J, Hwa J, Cai K, Altenbach C, Hubbell WL and Khorana HG (1999) Single-Cysteine Substitution Mutants at Amino Acid Positions 55-75, the Sequence Connecting the Cytoplasmic Ends of Helices I and II in Rhodopsin: Reactivity of the Sulfhydryl Groups and Their Derivatives Identifies a Tertiary Structure that Changes upon Light-Activation. *Biochemistry.* **38**:7938-7944.

Kostenis E, Conklin BR and Wess J (1997) Molecular Basis of Receptor/G Protein Coupling Selectivity Studied by Coexpression of Wild Type and Mutant m2 Muscarinic Receptors with Mutant Gq Sub-units. *Biochemistry.* **36**:1487-1495.

Kota P, Reeves PJ, RajBhandary UL and Khorana HG (2006) Opsin is present as dimers in COS1 cells: Identification of amino acids at the dimeric interface.. *PNAS.* **103**:3054-3059.

Kubo, T. Fukuda, Kazuhiko, Mikami, AtsushiMaeda, AkitoTakahashi, HideoMishina, MasayoshiHaga, TatsuyaHaga, KazukoIchiyama, AratаKangawa, KenjiKojima, MasayasuMatsuo, HisayukiHirose, Tadaaki Numa, Shosaku (1986) Cloning, sequencing and expression of complementary DNA encoding the muscarinic acetylcholine receptor. *Nature.* **323**:411-6

Kumar S and Bansal M (1998) Geometrical and Sequence Characteristics of alpha -Helices in Globular Proteins. *Biophys. J.* **75**:1935-1944.

Kurtenbach E (1990) The putative Disulphide Bond in Muscasrinc Receptors. *Biochem. Soc. Trans.* **18**:442-443.

Kurtenbach E, Curtis C, Pedder E, Aitken A, Harris A and Hulme E (1990) Muscarinic acetylcholine receptors. Peptide sequencing identifies residues involved in antagonist binding and disulfide bond formation. *J. Biol. Chem.* **265**:13702-13708.

Lambright DG, Sondek J, Bohm A, Skiba NP, Hamm HE and Sigler PB (1996) The 2.0 A crystal structure of a heterotrimeric G protein. *Nature.* **379**:311-319.

Langen, R. Cai, K. Altenbach, C. Khorana, HG. and Hubbell, WL. (1999) Structural Features of the C-Terminal Domain of Bovine Rhodopsin: A site Directed Spin-Labelling Study. *Biochemistry.* **38**:7918-7924

Langmead CJ, Fry VAH, Forbes IT, Branch CL, Christopoulos A, Wood MD and Herdon HJ (2006) Probing the Molecular Mechanism of Interaction between 4-n-Butyl-1-[4-(2-methylphenyl)-4-oxo-1-butyl]-piperidine (AC-42) and the Muscarinic M_1 Receptor: Direct Pharmacological Evidence That AC-42 Is an Allosteric Agonist. *Mol. Pharmacol.* **69**:236-246.

Lazareno S and Birdsall N (1995) Detection, quantitation, and verification of allosteric interactions of agents with labeled and unlabeled ligands at G protein-coupled receptors: interactions of strychnine and acetylcholine at muscarinic receptors. *Mol. Pharmacol.* **48**:362-378.

Lazareno S, Popham A and Birdsall NJM (2000) Allosteric Interactions of Staurosporine and Other Indolocarbazoles with N-[methyl-^{3}H]Scopolamine and Acetylcholine at Muscarinic Receptor Subtypes: Identification of a Second Allosteric Site. *Mol. Pharmacol.* **58**:194-207.

Lee N, Geoghagen N, Cheng E, Cline R and Fraser C (1996) Alanine scanning mutagenesis of conserved arginine/lysine- arginine/lysine-X-X-arginine/lysine G protein-activating motifs on m1 muscarinic acetylcholine receptors. *Mol. Pharmacol.* **50**:140-148.

Leppik. RA, Miller RC, Eck M, and Paquet JM (1994) Role of Acidic Amino Acids in the Allosteric Modulation by Gallamine of Antagonist Binding at the M2 Muscarinic Acetylcholine Receptor. *Mol. Pharmacol.* **45**:983-990.

Levey AI (1993) Immunological localization of m1-m5 muscarinic acetylcholine receptors in peripheral tissues and brain. *Life Sci.* **52**:441-448.

Li H, Malbon CC and Wang H-Y (2004) Gene Profiling of Frizzled-1 and Frizzled-2 Signaling: Expression of G-Protein-Coupled Receptor Chimeras in Mouse F9 Teratocarcinoma Embryonal Cells.. *Mol. Pharmacol.* **65**:45-55.

Li J, Edwards PC, Burghammer M, Villa C and Schertler GF (2004) Structure of bovine rhodopsin in a trigonal crystal form. *J. Mol. Biol.* **343**:1409-38, 2004

Liang Y, Fotiadis D, Filipek S, Saperstein DA, Palczewski K and Engel A (2003) Organization of the G Protein-coupled Receptors Rhodopsin and Opsin in Native Membranes.. *J. Biol. Chem.* **278**:21655-21662.

Liapakis G, Ballesteros JA, Papachristou S, Chan WC, Chen X and Javitch JA (2000) The Forgotten Serine. A Critical Role for Ser-2035.42 in Ligand Binding to And Activation of the beta 2-Adrenergic Receptor. *J. Biol. Chem.* **275**:37779-37788.

Liapakis G, Fitzpatrick D, Hoeger C, Rivier J, Vandlen R and Reisine T (1996) Identification of Ligand Binding Determinants in the Somatostatin Receptor Subtypes 1and 2. *J. Biol. Chem.* **271**:20331-20339.

Livnah O, Stura EA, Middleton SA, Johnson DL, Jolliffe LK and Wilson IA (1999) Crystallographic Evidence for Preformed Dimers of Erythropoietin Receptor Before Ligand Activation. *Science.* **283**:987-990.

Lu ZL, Curtis CA, Jones PG, Pavia J and Hulme EC (1997) The role of the aspartate-arginine-tyrosine triad in the m1 muscarinic receptor: mutations of aspartate 122 and tyrosine 124 decrease receptor expression but do not abolish signaling. *Mol. Pharmacol.* **51**:234-41.

Lu ZL and Hulme EC (1999) The functional topography of transmembrane domain 3 of the M_1 muscarinic acetylcholine receptor, revealed by scanning mutagenesis. *J. Biol Chem.* **274**:7309-15.

Lu ZL and Hulme EC (2000) A network of conserved intramolecular contacts defines the off-state of the transmembrane switch mechanism in a seven-transmembrane receptor. *J. Biol Chem.* **275**:5682-6.

Lu ZL, Saldanha JW and Hulme EC (2001) Transmembrane domains 4 and 7 of the M(1) muscarinic acetylcholine receptor are critical for ligand binding and the receptor activation switch. *J. Biol Chem.* **276**:34098-104.

Lu ZL, Saldanha JW and Hulme EC (2002) Seven-transmembrane receptors: crystals clarify. *Trends. Pharmacol. Sci.* **23**:140-6.
+

Madabushi S, Gross AK, Philippi A, Meng EC, Wensel TG and Lichtarge O (2004) Evolutionary Trace of G Protein-coupled Receptors Reveals Clusters of Residues That Determine Global and Class-specific Functions.. *J. Biol. Chem.* **279**:8126-8132.

Maggio R, Barbier P, Colelli A, Salvadori F, Demontis G and Corsini GU (1999) G Protein-Linked Receptors: Pharmacological Evidence for the Formation of Heterodimers. *J. Pharmacol. Exp. Ther.* **291**:251-257.

Matsui H, Lazareno S and Birdsall N (1995) Probing of the location of the allosteric site on m1 muscarinic receptors by site-directed mutagenesis. *Mol. Pharmacol.* **47**:88-98.

McVey M, Ramsay D, Kellett E, Rees S, Wilson S, Pope AJ and Milligan G (2001) Monitoring Receptor Oligomerization Using Time-resolved Fluorescence Resonance Energy Transfer and Bioluminescence Resonance Energy Transfer. The Human delta - Opioid Receptor Displays Constitutive Oligomerization at the Cell Surface, which is not Regulated by Receptor Occupancy. *J. Biol. Chem.* **276**:14092-14099.

Menon ST, Han M and Sakmar TP (2001) Rhodopsin: Structural Basis of Molecular Physiology. *Physiol. Rev.* **81**:1659-1688.

Mesnier D and Baneres J-L (2004) Cooperative Conformational Changes in a G-protein-coupled Receptor Dimer, the Leukotriene B4 Receptor BLT1. *J. Biol. Chem.* **279**:49664-49670.

Milligan G (2003) Constitutive Activity and Inverse Agonists of G Protein-Coupled Receptors: a Current Perspective. *Mol. Pharmacol.* **64**:1271-1276.

Missale C, Nash SR, Robinson SW, Jaber M and Caron MG (1998) Dopamine Receptors: From Structure to Function. *Physiol. Rev.* **78**:189-225.

Miyakawa T, Yamada M, Duttaroy A and Wess J (2001) Hyperactivity and Intact Hippocampus-Dependent Learning in Mice Lacking the M_1 Muscarinic Acetylcholine Receptor. *J. Neurosci.* **21**:5239-5250.

Moro O, Shockley M, Lameh J and Sadee W (1994) Overlapping multi-site domains of the muscarinic cholinergic Hm1 receptor involved in signal transduction and sequestration *J. Biol. Chem.* **269**:6651-6655.

Motulsky H and Mahan L (1984) The kinetics of competitive radioligand binding predicted by the law of mass action. *Mol. Pharmacol.* **25**:1-9.

Mueller KL, Hoon MA, Erlenbach I, Chandrashekar J, Zuker CS and Ryba NJP (2005) The receptors and coding logic for bitter taste. *Nature.* **434**:225-229.

Nasman J, Kukkonen JP, Holmqvist T and Akerman KEO (2002) Different roles for Gi and Go proteins in modulation of adenylyl cyclase type-2 activity. *J. Neurochem.* **83**:1252-1261.

Nelson G, Chandrashekar J, Hoon MA, Feng L, Zhao G, Ryba NJ, Zuker CS (2002) An amino-acid taste receptor.[see comment]. *Nature.* **416**:199-202.

Ng GYK, O'Dowd BF, Lee SP, Chung HT, Brann MR, Seeman P and George SR (1996) Dopamine D2 Receptor Dimers and Receptor-Blocking Peptides. *Biochem. Biophys. Res. Comm.* **227**:200-204.

Nobles M, Benians A and Tinker A (2005) Heterotrimeric G proteins precouple with G protein-coupled receptors in living cells. *PNAS.* **102**:18706-18711.

Noda K, Saad Y, Graham R and Karnik S (1994) The high affinity state of the beta 2-adrenergic receptor requires unique interaction between conserved and non-conserved extracellular loop cysteines. *J. Biol. Chem.* **269**:6743-6752.

Okada T, Fujiyoshi Y, Silow M, Navarro J, Landau EM and Shichida Y (2002) Functional role of internal water molecules in rhodopsin revealed by x-ray crystallography. *PNAS.* **99**:5982-5987.

Olah M, Jacobson K and Stiles G (1994) Role of the second extracellular loop of adenosine receptors in agonist and antagonist binding. Analysis of chimeric A1/A3 adenosine receptors. *J. Biol. Chem.* **269**:24692-24698.

Onrust R, Herzmark P, Chi P, Garcia PD, Lichtarge O, Kingsley C and Bourne HR (1997) Receptor and beta gamma Binding Sites in the alpha Subunit of the Retinal G Protein Tr ansducin. *Science* **275**:381-384.

Page KM, Curtis CA, Jones PG and Hulme EC (1995) The functional role of the binding site aspartate in muscarinic acetylcholine receptors, probed by site-directed mutagenesis. *Eur. J. Pharmacol.* **289**:429-37.

Palczewski K, Kumasaka T, Hori T, Behnke CA, Motoshima H, Fox BA, Trong IL, Teller DC, Okada T, Stenkamp RE, Yamamoto M and Miyano M (2000) Crystal Structure of Rhodopsin: A G Protein-Coupled Receptor. *Science.* **289**:739-745.

Peralta EG, Ashkenazi A, Winslow JW, Smith DH, Ramachandran J, Capon DJ (1987) Distinct primary structures, ligand-binding properties and tissue-specific expression of four human muscarinic acetylcholine receptors. *EMBO J.* **6**:3293-9

Percherancier Y, Berchiche YA, Slight I, Volkmer-Engert R, Tamamura H, Fujii N, Bouvier M and Heveker N (2005) Bioluminescence Resonance Energy Transfer Reveals Ligand-induced Conformational Changes in CXCR4 Homo- and Heterodimers
J. Biol. Chem. **280**:9895-9903.

Perry SJ and Lefkowitz RJ (2002) Arresting developments in heptahelical receptor signaling and regulation. *Trends. Cell Biol.* **12**:130-138.

Phillips W and Cerione R (1992) Rhodopsin/transducin interactions. I. Characterization of the binding of the transducin-beta gamma sub-unit complex to rhodopsin using fluorescence spectroscopy. *J. Biol. Chem.* **267**:17032-17039.

Phillips W, Wong S and Cerione R (1992) Rhodopsin/transducin interactions. II. Influence of the transducin-beta gamma sub-unit complex on the coupling of the transducin-alpha sub-unit to rhodopsin. *J. Biol. Chem.* **267**:17040-17046.

Pitcher JA, Freedman NJ and Lefkowitz RJ (1998) G Protein-Coupled Receptor Kinases. *Annu. Rev. Biochem.* **67**:653-692.

Postina R, Kojro E and Fahrenholz F (1996) Separate Agonist and Peptide Antagonist Binding Sites of the Oxytocin Receptor Defined by Their Transfer into the V2 Vasopressin Receptor.. *J. Biol. Chem.* **271**:31593-31601.

Prinster SC, Hague C and Hall RA (2005) Heterodimerization of G Protein-Coupled Receptors: Specificity and Functional Significance. *Pharmacol. Rev.* **57**:289-298.

Prossnitz ER, Schreiber RE, Bokoch GM and Ye RD (1995) Binding of Low Affinity N-formyl Peptide Receptors to G Protein. *J. Biol. Chem.* **270**:10686-10694.

Pucadyil TJ, Kalipatnapu S and Chattopadhyay A (2005) The Serotonin 1_AReceptor: A Representative Member of the Serotonin Receptor Family. *Cell. Mol. Neurobio.***25**:553-580.

Quinn DM (1987) Acetylcholinesterase: Enzyme Structure, Reaction Dynamics and Virtual Transition States. *Chem. Rev.* **87**:955-979.

Quinn GP and Keough MJ. (2002) Experimental Design and Data Analysis for Biologists. Chaptern 8.6 p.196-201. Cambridge University Press

Raymond JR, Mukhin YV, Gettys TW and Garnovskaya MN (1999) The recombinant 5-HT1A receptor: G protein coupling and signalling pathways. *Br. J. Pharmacol.* **127**:1751-64.

Reddy PS and Corley RB (1998) Assembly, sorting, and exit of oligomeric proteins from the endoplasmic reticulum. *Bioessays.* 546-54.

Rehn M, Pihlajaniemi T, Hofmann K and Bucher P (1998) The frizzled motif: in how many different protein families does it occur? *Trends. Biochem. Sci.* **23**:415-417.

Remy I, Wilson IA and Michnick SW (1999) Erythropoietin Receptor Activation by a Ligand-Induced Conformation Change. *Science.* **283**:990-993.

Riek RP, Rigoutsos I, Novotny J and Graham RM (2001) Non-[alpha]-helical elements modulate polytopic membrane protein architecture. *J. Mol. Biol.* **306**:349-362.

Ringdahl B (1989a) The Muscarinic Receptors. Chapter 5: Structural Determinants of Muscarinic Agonist Activity(Brown JH ed).151-217.

Ringdahl B (1989b) The Muscarinic Receptors. Chapter 6.1: Atypical muscarinic agonists(Brown JH ed).195-217.

Rocheville M, Lange DC, Kumar U, Sasi R, Patel RC and Patel YC (2000) Subtypes of the Somatostatin Receptor Assemble as Functional Homo- and Heterodimers. *J. Biol. Chem.* **275**:7862-7869.

Romano C, Yang W-L and O'Malley KL (1996) Metabotropic Glutamate Receptor 5 Is a Disulfide-linked Dimer. *J. Biol. Chem.* **271**:28612-28616.

Rosenkilde MM, Kledal TN and Schwartz TW (2005) High Constitutive Activity of a Virus-Encoded Seven Transmembrane Receptor in the Absence of the Conserved DRY Motif (Asp-Arg-Tyr) in Transmembrane Helix 3. *Mol. Pharmacol.* **68**:11-19.

Roszkowski A (1961) An Unusual Type of Sympathetic Ganglionic Stimulant. *J. Pharmacol. Exp. Ther.* **132**:156-170.

Sanger F, Nicklen S and Coulson AR (1977) DNA sequencing with chain-terminating inhibitors. *PNAS.* **74**:5463-7.

Sansom SPM and Weinstein H (2000) Hinges, swivels and switches: the role of prolines in signalling via transmembrane [alpha]-helices. *Trends. Pharmacol. Sci.* **21**:445-451.

Savarese T, Wang C and Fraser C (1992) Site-directed mutagenesis of the rat m1 muscarinic acetylcholine receptor. Role of conserved cysteines in receptor function. *J. Biol. Chem.* **267**:11439-11448.

Scheer A, Fanelli F, Costa T, De Benedetti PG and Cotecchia S (1996) Constitutively active mutants of the alpha 1B-adrenergic receptor: role of highly conserved polar amino acids in receptor activation. *EMBO J.* **15**:3566-78.

Schmidt C, Li B, Bloodworth L, Erlenbach I, Zeng FY and Wess J (2003) Random mutagenesis of the M3 muscarinic acetylcholine receptor expressed in yeast. Identification of point mutations that "silence" a constitutively active mutant M3 receptor and greatly impair receptor/G protein coupling. *J. Biol. Chem.* **278**:30248-60.

Schoepp DD (2001) Unveiling the Functions of Presynaptic Metabotropic Glutamate Receptors in the Central Nervous System. *J. Pharmacol. Exp. Ther.* **299**:12-20.

Schulman JM. Michael L. Sabio RLD (1983) Recognition of cholinergic agonists by the muscarinic receptor. 1. Acetylcholine and other agonists with the NCCOCC backbone. *J. Med. Chem.* **26**:817-823.

Schwarz RD, Spencer CJ, Jaen JC, Mirzadegan T, Moreland D, Tecle H and Thomas AJ (1995) Mutations of aspartate 103 in the Hm2 receptor and alterations in receptor binding properties of muscarinic agonists. *Life Sciences Proceedings of the Sixth International Symposium on Subtypes of Muscarinic Receptors.* **56**:923-929.

Sealfon SC, Chi L, Ebersole BJ, Rodic V, Zhang D, Ballesteros JA and Weinstein H (1995) Related Contribution of Specific Helix 2 and 7 Residues to Conformational Activation of the Serotonin 5-HT Receptor. *J. Biol. Chem.* **270**:16683-16688.

Self DW, Barnhart WJ, Lehman DA and Nestler EJ (1996) Opposite Modulation of Cocaine-Seeking Behavior by D1- and D2-Like Dopamine Receptor Agonists.bv *Science.* **271**:1586-1589.

Sheikh SP, Zvyaga TA, Lichtarge O, Sakmar TP and Bourne HR (1996) Rhodopsin activation blocked by metal-ion-binding sites linking transmembrane helices C and F. *Nature.* **383**:347-50

Shi L and Javitch JA (2002) The Binding Site of Aminergic G Protein-Coupled Receptors: The Transmembrane Segments and Second Extracellular Loop. *Ann. Rev. Pharmacol. Toxicol.* **42**:437-467.

Shi L and Javitch JA (2004) The second extracellular loop of the dopamine D2 receptor lines the binding-site crevice. *PNAS.* **101**:440-445.

Silman I and Sussman JL (2005) Acetylcholinesterase: 'classical' and 'non-classical' functions and pharmacology. *Curr. Op. Pharmacol. Resp. / Muscu.* **5**:293-302.

Sinnokrot MO and Sherrill CD (2004) Substituent Effects in pi-pi Interactions: Sandwich and T-Shaped Configurations. *J. Am. Chem. Soc.* **126**:7690-7697.

Slusarski DC, Corces VG and Moon RT (1997) Interaction of Wnt and a Frizzled homologue triggers G-protein-linked phosphatidylinositol signalling. *Nature.* **390**:410-413.

Smith PK, Krohn RI, Hermanson GT, Mallia AK, Gartner FH, Provenzano MD, Fujimoto EK, Goeke NM, Olson BJ and Klenk DC (1985) Measurement of protein using bicinchoninic acid. *Anal. Biochem.* **150**:76-85.

Spalding TA and Burstein ES (2001) Constitutively active muscarinic receptors. *Life Sci.* **68**:2511-2516.

Spalding TA, Trotter C, Skjarbak N, Messier TL, Currier EA, Burstein ES, Li D, Hacksell U and Brann MR (2002) Discovery of an Ectopic Activation Site on the M_1 Muscarinic Receptor. *Mol. Pharmacol.* **61**:1297-1302.

Stacey M, Lin H-H, Gordon S and McKnight AJ (2000) LNB-TM7, a group of seven-transmembrane proteins related to family-B G-protein-coupled receptors. *Trends. Biochem. Sci.* **25**:284-289.

Stenkamp RE, Teller DC and Palczewski K (2005) Rhodopsin: a structural primer for G-protein coupled receptors. *Arch. Pharm. (Weinheim)* **338**:209-16.

Sussman JL, Harel M, Frolow F, Oefner C, Goldman A, Toker L and Silman I (1991) Atomic structure of acetylcholinesterase from Torpedo californica: a prototypic acetylcholine-binding protein. *Science.* **253**:872-9

Takeuchi J, Fulton J, Jia Z-p, Abramov-Newerly W, Jamot L, Sud M, Coward D, Ralph M, Roder J and Yeomans J (2002) Increased drinking in mutant mice with truncated M5 muscarinic receptor genes. *Pharm. Biochem. Behaviour.* **72**:117-123.

Teller DC, Okada T, Behnke CA, Palczewski K and Stenkamp RE (2001) Advances in determination of a high-resolution three-dimensional structure of rhodopsin, a model of G-protein-coupled receptors (GPCRs). *Biochemistry.* **40**:7761-72.

Thirstrup K, Elling CE, Hjorth SA and Schwartz TW (1996) Construction of a High Affinity Zinc Switch in the kappa-Opioid Receptor. *J. Biol. Chem.* **271**:7875-7878.

Trumpp-Kallmeyer S, Hoflack J, Bruinvels A and Hibert M (1992) Modeling of G-protein-coupled receptors: application to dopamine, adrenaline, serotonin, acetylcholine, and mammalian opsin receptors. *J. Med. Chem.* **35**:3448-62.

Vassilatis DK, Hohmann JG, Zeng H, Li F, Ranchalis JE, Mortrud MT, Brown A, Rodriguez SS, Weller JR, Wright AC, Bergmann JE and Gaitanaris GA (2003) The G protein-coupled receptor repertoires of human and mouse. *PNAS.* **100**:4903-4908.

Vogel WK, Peterson GL, Broderick DJ, Mosser VA and Schimerlik MI (1999) Double Mutant Cycle Analysis of Aspartate 69, 97, and 103 to Asparagine Mutants in the m2 Muscarinic Acetylcholine Receptor . *Arch. Biochem. Biophys.* **361**:283-294.

Vogel WK, Sheehan DM and Schimerlik MI (1997) Site-Directed Mutagenesis on the m2 Muscarinic Acetylcholine Receptor: The Significance of Tyr 403 in the Binding of Agonists and Functional Coupling. *Mol. Pharmacol.* **52**:1087-1094.

Waelbroeck M (1994) Identification of drugs competing with d-tubocurarine for an allosteric site on cardiac muscarinic receptors. *Mol. Pharmacol.* **46**:685-692.

Waelbroeck M, Camus J and Christophe J (1989) Determination of the association and dissociation rate constants of muscarinic antagonists on rat pancreas: rank order of potency varies with time. *Mol. Pharmacol.* **36**:405-411.

Waelbroeck M, Camus J, Winand J and Christophe J (1987) Different antagonist binding properties of rat pancreatic and cardiac muscarinic receptors. *Life Sci.* **41**:2235-40

Waelbroeck M, Tastenoy M, Camus J and Christophe J (1991) Binding kinetics of quinuclidinyl benzilate and methyl-quinuclidinyl benzilate enantiomers at neuronal (M_1), cardiac (M2), and pancreatic (M3) muscarinic receptors. *Mol. Pharmacol.* **40**:413-420.

Wang W, Shahrestanifar M, Jin J and Howells R (1995) Studies on {micro} and {delta} Opioid Receptor Selectivity Utilizing Chimeric and Site-Mutagenized Receptors. *PNAS.* **92**:12436-12440.

Ward SD, Curtis CA and Hulme EC (1999a) Alanine-scanning mutagenesis of transmembrane domain 6 of the M(1) muscarinic acetylcholine receptor suggests that Tyr 381 plays key roles in receptor function. *Mol. Pharmacol.* **56**:1031-41.

Ward SD, Curtis CA and Hulme EC (1999b) Alanine-scanning mutagenesis of transmembrane domain 6 of the M(1) muscarinic acetylcholine receptor suggests that Tyr 381 plays key roles in receptor function. *Mol. Pharmacol.* **56**:1031-41.

Ward SDC, Hamdan FF, Bloodworth LM and Wess J (2002) Conformational Changes That Occur during M3 Muscarinic Acetylcholine Receptor Activation Probed by the Use of an in Situ Disulfide Cross-linking Strategy. *J. Biol. Chem.* **277**:2247-2257.

Wells JW (1992) Analysis aqnd Interpretation of Binding at Equilibrium. In Hulme E.C. (Ed.) Receptor Ligand Interactions- a Practical Approach.(IRL Press at Oxford University Press) 289-395.

Wess J (1996) Molecular biology of muscarinic acetylcholine receptors. *Crit. Rev. Neurobiol.* **10**:69-99.

Wess J (1998) Molecular Basis of Receptor/G-protein-Coupling Selectivity. *Pharmacol. Ther.* **80**:231-264.

Wess J, Gdula D and Brann M (1991) Site-directed mutagenesis of the m3 muscarinic receptor: identification of a series of threonine and tyrosine residues involved in agonist but not antagonist binding. *EMBO J.* **10**:3729-3734.

Wess J, Nanavati S, Vogel Z and Maggio R (1993) Functional role of proline and tryptophan residues highly conserved among G protein-coupled receptors studied by mutational analysis of the m3 muscarinic receptor. *EMBO J.* **12**:331-338.

Willets JM, Challiss RAJ and Nahorski SR (2003) Non-visual GRKs: are we seeing the whole picture? *Trends. Pharmacol. Sci.* **24**:626-633.

Wise A, Gearing K and Rees S (2002) Target validation of G-protein coupled receptors. *Drug Discov. Today.* 7:235-246.

Wurch T, Colpaert FC and Pauwels PJ (1998) Chimeric Receptor Analysis of the Ketanserin Binding Site in the Human 5-Hydroxytryptamine1D Receptor: Importance of the Second Extracellular Loop and Fifth Transmembrane Domain in Antagonist Binding. *Mol. Pharmacol.* **54**:1088-1096.

Yamada M, Lamping KG, Duttaroy A, Zhang W, Cui Y, Bymaster FP, McKinzie DL, Felder CC, Deng C-X, Faraci FM and Wess J (2001a) Cholinergic dilation of cerebral blood vessels is abolished in M5 muscarinic acetylcholine receptor knockout mice. *PNAS.* **98**:14096-14101.

Yamada M, Miyakawa T, Duttaroy A, Yamanaka A, Moriguchi T, Makita R, Ogawa M, Chou CJ, Xia B, Crawley JN, Felder CC, Deng C-X and Wess J (2001b) Mice lacking the M3 muscarinic acetylcholine receptor are hypophagic and lean. *Nature.* **410**:207-212.

Yamamura HI and Snyder SH (1974) Muscarinic Cholinergic Binding in Rat Brain. *PNAS.* **71**:1725-1729.

Yan EC, Kazmi MA, De S, Chang BS, Seibert C, Marin EP, Mathies RA and Sakmar TP (2002) Function of extracellular loop 2 in rhodopsin: glutamic acid 181 modulates stability and absorption wavelength of metarhodopsin II. *Biochemistry.* **41**:3620-7.

Yan ECY, Kazmi MA, Ganim Z, Hou J-M, Pan D, Chang BSW, Sakmar TP and Mathies RA (2003) Retinal counterion switch in the photoactivation of the G protein-coupled receptor rhodopsin. 1. *PNAS.* **100**:9262-9267.

Zeng FY, Soldner A, Schoneberg T and Wess J (1999) Conserved extracellular cysteine pair in the M3 muscarinic acetylcholine receptor is essential for proper receptor cell surface localization but not for G protein coupling. *J. Neurochem.* **72**:2404-14

Zeng F-Y, Soldner A, Schoneberg T and Wess J (1999) Conserved Extracellular Cysteine Pair in the M3 Muscarinic Acetylcholine Receptor Is Essential for Proper Receptor Cell Surface Localization but Not for G Protein Coupling. *J. Neurochem.* **72**:2404-2414.

Zeng F-Y and Wess J (1999) Identification and Molecular Characterization of M_3 Muscarinic Receptor Dimers. *J. Biol. Chem.* **274**:19487-19497.

Zeng F-Y and Wess J (2000) Molecular Aspects of Muscarinic Receptor Dimerization. *Neuropsychopharmacol.* **23**:S19-S31.

Zhang W, Basile AS, Gomeza J, Volpicelli LA, Levey AI and Wess J (2002a) Characterization of Central Inhibitory Muscarinic Autoreceptors by the Use of Muscarinic Acetylcholine Receptor Knock-Out Mice. *J. Neurosci.* **22**:1709-1717.

Zhang W, Yamada M, Gomeza J, Basile AS and Wess J (2002b) Multiple muscarinic acetylcholine receptor subtypes modulate striatal dopamine release, as studied with M_1-M_5 muscarinic receptor knock-out mice. *J. Neurosci.* **22**:6347-52.

Zhao M, Hwa J and Perez D (1996) Identification of critical extracellular loop residues involved in alpha 1-adrenergic receptor subtype-selective antagonist binding. *Mol. Pharmacol.* **50**:1118-1126.

Acknowledgements

I would like to thank Dr. Ed Hulme for giving me the opportunity to better myself by allowing me to enter into this PhD study. With immense knowledge, wisdom and patience he has guided my study and taught me the value of considered thought, carefully planned experimentation and paying close attention to the details. Ed has given me the skills to approach my next project with confidence. Thank you Ed aswell, for the endless proof reading, which was probably more than most could bear, where you found the time I will never know!!. Thanks Ed for everything and the very best of luck with the current project.

I also wish to thank Carol Curtis, whose practical knowhow and humour have made this study a real pleasure. Always there with great ideas and practical measures, Carol has enbled me to overcome the inherrant frustrations of molecular biology and has given excellent first hand intstruction of various procedures used in this study. Furthermore, I would like to thank Carol for providing glowing references to prospective employers. Carol, many thanks.

The expert advice of Dr. Nigel Birdsall has also proved both practical and insightful. Dr. Birdsall has helped me to understand some of the complexities of molecular pharmacology and organic chemistry. Always on hand to offer assistance and advice Dr. Birdsall has also made this project an enjoyable experience. Thank you Nigel and all the best for the future

.I would also like to thank Dr. Jonny Hern who has helped me in the lab and with my computer problems on countless occasions. Great to have around and while away a long experiment by talking about the state of British football, Jonny has also helped to make this project a pleasure. Hope to see Aberdeen top the SPL sometime soon !! (In your Dreams).

Thanks Jonny and I wish you every success in your post doc at Nottingham. Also a big thank you to Dr. Asma Baig for her friendly and kind support during my thesis writing. Look forward to reading your paper soon Asma. All the best for the future and I hope you move on to even greater things.

To everyone mentioned above – Its been a real pleasure and I'll miss you all.

I could not have even started my first degree if it was not for the support of my fantastic wife Elise. Elise supported me both financially and emotionally through my first degree and only because of her was I able to reach the place I am now. Thanks again Elise with all my love. Thanks also to my wonderful children Ronan and Rhian who put everything into its true perspective and providing me with no end of joy to help me approach the difficult times with a smile.